

# Pioneering function of Isl1 in epigenetic regulation during second heart field development

Dissertation

zur Erlangung des Doktorgrades der Naturwissenschaften

- Doctor rerum naturalium -

(Dr. rer. nat.)

eingereicht am Fachbereich Biologie und Chemie der

Justus-Liebig-Universität Gießen

von

Rui Gao

Aus Shandong, China

2019

angefertigt am Max-Planck-Institut für Herz- und Lungenforschung, Bad Nauheim

und Medizinische Fakultät Mannheim - Universität Heidelberg, Mannheim

**1. Gutachter: Prof. Dr. Katja Sträßer**

Institut für Biochemie, Justus-Liebig-Universität Gießen  
35392 Gießen/ Germany

**2. Gutachter: Prof. Dr. Gergana Dobрева**

Medizinische Fakultät Mannheim, Universität Heidelberg  
68167 Mannheim/ Germany

Disputation am 31.10.2019

## EIDESSTATTLICHE ERKLÄRUNG

„Ich erkläre: Ich habe die vorgelegte Dissertation selbständig und ohne unerlaubte fremde Hilfe und nur mit den Hilfen angefertigt, die ich in der Dissertation angegeben habe. Alle Textstellen, die wörtlich oder sinngemäß aus veröffentlichten Schriften entnommen sind, und alle Angaben, die auf mündlichen Auskünften beruhen, sind als solche kenntlich gemacht. Bei den von mir durchgeführten und in der Dissertation erwähnten Untersuchungen habe ich die Grundsätze guter wissenschaftlicher Praxis, wie sie in der „Satzung der Justus-Liebig-Universität Gießen zur Sicherung guter wissenschaftlicher Praxis“ niedergelegt sind, eingehalten.“

Mannheim, den

Rui Gao

# Table of Contents

<b>List of Figures</b> .....	<b>5</b>
<b>List of Tables</b> .....	<b>7</b>
<b>Zusammenfassung</b> .....	<b>8</b>
<b>Abstract</b> .....	<b>9</b>
<b>1. Introduction</b> .....	<b>10</b>
<b>1.1 Heart development</b> .....	<b>10</b>
1.1.1 Mouse heart development .....	10
1.1.2 Congenital heart disease.....	14
1.1.3 Cell types and cardiac lineages in mammalian heart .....	17
1.1.4 Signaling pathways in cardiac development.....	19
1.1.5 Transcriptional factors involved in heart development .....	25
<b>1.2 Isl1</b> .....	<b>31</b>
1.2.1 Protein structure of ISL1 .....	31
1.2.2 Expression and function of Isl1 during development .....	32
1.2.3 Expression and function of Isl1 during heart development .....	33
1.2.4 ISL1 and CHD .....	36
<b>1.3 Pioneer transcription factors</b> .....	<b>36</b>
<b>1.4 Epigenetic regulation</b> .....	<b>40</b>
1.4.1 Chromatin structure.....	40
1.4.2 Epigenetic control mechanisms .....	41
<b>2. Objectives</b> .....	<b>51</b>
<b>3. Results</b> .....	<b>52</b>
<b>3.1 Isl1 regulates cardiogenesis in CPCs by directly targeting a large group of downstream targets</b> .....	<b>52</b>
3.1.1 Generation of <i>Isl1</i> KO ESC line .....	52
3.1.2 Establishing <i>in vitro</i> mESC-based cardiac differentiation protocol .....	53
3.1.3 <i>Isl1</i> KO ESC lines can differentiate into CPCs .....	54
3.1.4 <i>Isl1</i> loss-of-function results in downregulation of a large number of genes critical for cardiogenesis in CPCs .....	55
3.1.5 <i>Isl1</i> directly regulates a large amount of genes in CPCs .....	57

<b>3.2 <i>Isl1</i> is essential in regulating second heart field development in mouse embryos....</b>	<b>58</b>
3.2.1 <i>Isl1</i> knockout leads to significant gene expression changes at early stage of mouse embryonic development.....	58
3.2.2 Reduced level of <i>Isl1</i> results in cardiac defects and deregulation of target genes in E10.5 <i>Isl1</i> hypomorphic embryos.....	60
3.2.3 ChIP-Seq analysis identified <i>Isl1</i> primary downstream targets <i>in vivo</i> .....	62
<b>3.3 <i>Isl1</i> orchestrates a regulatory network driving cardiogenesis.....</b>	<b>63</b>
<b>3.4 <i>Baf60c</i> is a key <i>Isl1</i> downstream target.....</b>	<b>66</b>
3.4.1 <i>Baf60c</i> is directly regulated by <i>Isl1</i> .....	66
3.4.2 RNA-Seq analysis identified <i>Baf60c</i> regulated genes in CPCs.....	67
3.4.3 <i>Isl1</i> and <i>Baf60c</i> share common targets.....	69
<b>3.5 <i>Isl1</i> works in concert with the Brg1-based SWI/SNF complex to regulate its target genes .....</b>	<b>70</b>
3.5.1 <i>Isl1</i> interacts with Brg1 and <i>Baf60c</i> .....	70
3.5.2 The interaction of <i>Isl1</i> with Brg1 does not depend on <i>Baf60c</i> .....	71
3.5.3 Co-occupancy of <i>Isl1</i> and Brg1 in CPCs .....	72
3.5.4 <i>Isl1</i> works cooperatively with Brg1 to regulate its target gene expression .....	74
3.5.5 <i>Isl1</i> recruits the Brg1 complex to its target sequences.....	75
<b>3.6 <i>Isl1</i> acts as a pioneer factor in cardiogenesis .....</b>	<b>76</b>
3.6.1 <i>Isl1</i> binding correlates with sites of open chromatin .....	76
3.6.2 <i>Isl1</i> and Brg1/ <i>Baf60c</i> complex work synergistically to open the chromatin during SHF development.....	77
3.6.3 <i>Isl1</i> plays a pioneering function in all three cardiovascular lineages .....	80
3.6.4 <i>Isl1</i> acts as a pioneer factor independently of <i>Gata4</i> .....	81
<b>3.7 Working model .....</b>	<b>83</b>
<b>4. Discussion .....</b>	<b>84</b>
<b>4.1 <i>Isl1</i> is critical for SHF development and depletion of <i>Isl1</i> leads to cardiac defects as seen in human CHD patients.....</b>	<b>85</b>
<b>4.2 <i>Isl1</i> organizes a regulatory gene network driving second heart field development ..</b>	<b>87</b>
<b>4.3 <i>Baf60c</i> is a key downstream target of <i>Isl1</i>.....</b>	<b>89</b>
<b>4.4 <i>Isl1</i> works together with Brg1-<i>Baf60c</i>-based SWI/SNF complex to regulate gene expression program during cardiogenesis .....</b>	<b>90</b>
<b>4.5 <i>Isl1</i> functions as a pioneer factor during cardiogenesis .....</b>	<b>91</b>

4.6 <i>Isl1</i> plays a pioneering function independently of <i>Gata4</i> .....	93
4.7 Conclusions and perspectives.....	95
<b>5. Materials and Methods .....</b>	<b>97</b>
5.1 Chemicals used in this study .....	97
5.2 Kits used in this study .....	98
5.3 Cell culture medium and supplements .....	99
5.4 Further materials.....	100
5.5 Equipment used in this study .....	101
5.6 RNA extraction, cDNA synthesis and qPCR .....	102
5.6.1 RNA extraction .....	102
5.6.2 cDNA synthesis.....	104
5.6.3 Quantitative real-time polymerase chain reaction (qPCR).....	105
5.7 Mouse lines .....	106
5.8 Genomic DNA extraction.....	106
5.9 Genotyping.....	107
5.10 Protein extraction and co-immunoprecipitation (Co-IP).....	108
5.11 SDS-PAGE and Western Blot.....	108
5.12 Culturing of primary cells and cell lines .....	111
5.12.1 Mouse embryonic fibroblasts (MEFs) .....	111
5.12.2 Mouse embryonic stem cell lines (mESCs) .....	112
5.12.3 HEK293T cell line.....	112
5.13 Generation of stable ES cell lines.....	113
5.14 Generating <i>Isl1</i> KO mESC lines by CRISPR-Cas9 technique .....	114
5.15 Cardiac differentiation .....	114
5.16 Chromatin immunoprecipitation (ChIP).....	116
5.17 Bioinformatic analysis.....	117
5.17.1 RNA-Seq .....	117
5.17.2 ChIP-Seq .....	118
5.17.3 ATAC-Seq.....	119
5.17.4 Others.....	120
5.18 Primers used in this study .....	121
5.18.1 qPCR primers.....	121

5.18.2 CHIP-qPCR primers .....	123
<b>6. References .....</b>	<b>125</b>
<b>7. Acknowledgements .....</b>	<b>150</b>
<b>8. Appendix.....</b>	<b>Error! Bookmark not defined.</b>

# List of Figures

Introduction part
Figure 1 Overview of heart development
Figure 2 Common types of congenital heart disease
Figure 3 Origins and lineage relationships of cardiac cell types
Figure 4 Cellular hierarchy of cardiac progenitors and their lineage specification
Figure 5 Illustration showing the core features of Wnt, FGF, BMP, Hh, and Notch signaling pathways
Figure 6 Cardiac gene regulatory networks
Figure 7 Schematic diagram of ISL1 domains and the intermolecular and intramolecular interactions
Figure 8 Isl1 expression profile in mouse heart
Figure 9 Chromatin binding by pioneer factors
Figure 10 Activities of pioneer factors
Figure 11 Schematic representation shows the organization and packaging of genetic materials
Figure 12 Domain structure of the core ATPase subunits and functional classification of the chromatin remodeling complexes
Figure 13 Tissue/cell-type-specific assemblies of BAF complexes
Figure 14 Roles of BAF chromatin remodeling complex in heart development
Results part
Figure 15 Generating <i>Isl1</i> KO ESC lines by CRISPR-Cas9 technique
Figure 16 Characterization of directed cardiac differentiation of mouse ESCs



Figure 17 Marker gene expression analyses at different stages of cardiac differentiation
Figure 18 Analysis of CPCs differentiated from control and <i>Isl1</i> KO lines
Figure 19 RNA-Seq data analysis in control and <i>Isl1</i> KO CPCs
Figure 20 Genome tracks of some representative <i>Isl1</i> targets in CPCs
Figure 21 <i>Isl1</i> regulates a large group of genes associating with cardiogenesis in CPCs
Figure 22 Analysis of RNA-Seq data from E8.5 <i>Isl1</i> KO embryos
Figure 23 Reduced <i>Isl1</i> expression leads to defects in cardiac morphogenesis
Figure 24 Analysis of RNA-Seq data from E10.5 <i>Isl1</i> hypomorphic embryos
Figure 25 Intersection of RNA-Seq and <i>Isl1</i> ChIP-Seq data in mouse embryos
Figure 26 Venn diagram showing <i>Isl1</i> targets from different datasets
Figure 27 <i>Isl1</i> -regulatory gene network
Figure 28 GO terms enriched in <i>Isl1</i> target genes
Figure 29 <i>Baf60c</i> is a key <i>Isl1</i> downstream target
Figure 30 Analysis of CPCs differentiated from control and <i>Baf60c</i> KD mESC lines
Figure 31 Analysis of RNA-Seq data in control and <i>Baf60c</i> KD CPCs
Figure 32 <i>Isl1</i> and <i>Baf60c</i> share common target genes in CPCs
Figure 33 <i>Isl1</i> interacts with <i>Brg1</i> / <i>Baf60c</i> complex
Figure 34 <i>Baf60c</i> doesn't mediate the interaction between <i>Isl1</i> and <i>Brg1</i> in CPCs and <i>vice versa</i>
Figure 35 <i>Isl1</i> co-occupied with <i>Brg1</i> on its target genes in CPCs
Figure 36 A large subset of genes differentially regulated in <i>Isl1</i> KO CPCs are co-bound by <i>Isl1</i> and <i>Brg1</i>
Figure 37 <i>Isl1</i> works unitedly with <i>Brg1</i> to regulate its target gene expression
Figure 38 <i>Brg1</i> binding at <i>Isl1</i> - bound targets is decreased by <i>Isl1</i> depletion in CPCs
Figure 39 <i>Isl1</i> binding correlates with sites of open chromatin

Figure 40 Isl1 and Brg1-Baf60c-based SWI/SNF complex shape the chromatin landscape at Isl1 target sites in cardiac progenitors

Figure 41 Isl1 and Brg1-Baf60c-based SWI/SNF complex induces chromatin reorganization in cardiac progenitors

Figure 42 Isl1 and Brg1-Baf60c complex promote chromatin accessibility in all three cardiovascular lineages

Figure 43 Isl1 acts as a pioneer factor like Gata4

Figure 44 Isl1 acts as a pioneer factor independently of Gata4

Figure 45 Gata4 occupancy at Isl1- bound sequences is decreased in *Isl1* deficient CPCs

Figure 46 Model of the role of Isl1 in cardiogenesis by controlling epigenetic mechanisms and memory

## List of Tables

### Materials and methods part

5.1 Chemicals used in this study

5.2 Kit used in this study

5.3 Cell culture medium and supplements

5.4 Further materials

5.5 Equipment used in this study

5.18 Primers used in this study

# Zusammenfassung

Während der Embryogenese, bestimmen koordinierte Abfolgen weitreichender transkriptioneller Änderungen und die Reorganisation des Chromatins die Zelltyp-Spezifizierung. Pioneertranskriptionsfaktoren stellen in diesem Prozess eine entscheidende Rolle, bei der Programmierung des Epigenoms und der Rekrutierung weiterer regulatorischer Faktoren, dar. Der LIM-homeodomain Transkriptionsfaktor Isl1 ist entscheidend für die frühe Entwicklung des Herzens und fungiert als Marker der kardialen Vorläuferzellen des sogenannten „*second heart field*“. Allerdings sind, durch die frühe embryonale Letalität von Isl1-Knockout Mäusen, Studien zur Rolle von Isl1 in späteren Phasen der Herzentwicklung unmöglich. Dadurch bleiben die Funktion von Isl1 in der epigenetischen Regulation der *second heart field* Entwicklung und die zugrundeliegenden Mechanismen weitgehendst ungeklärt.

Im Zuge unserer Studie konnten wir, mittels eines Isl1-hypomorphen Mausmodells, Isl1 als kritischen Faktor für die kardiale Entwicklung während der späten embryonalen Entwicklung identifizieren. Mittels high-throughput sequencing und unter Verwendung eines Isl1-Knockout Mausmodells und des Isl1-hypomorphen Mausmodells in Kombination mit einem gerichteten kardialen Differenzierungssystem, konnten wir ein regulatorisches Netzwerk in kardialen Vorläuferzellen identifizieren, deren Derivate durch Isl1 organisiert sind. Mit Hilfe von Analysen des genomweiten Profilings von Isl1-Bindestellen und von ATAC-Sequenzierungsdaten konnten wir Isl1 als entscheidenden Faktor der frühen Kardiogenese identifizieren. Weiterhin konnten wir zeigen, dass Isl1 mit Brg1 und Baf60c interagiert. Isl1 induziert zusammen mit dem Brg1-Baf60c-basiertem SWI/SNF Komplex Genexpressionsprogramme in kardialen Vorläuferzellen und unterstützt die Zell-Spezifizierung durch die Organisation des Genome.

Abschließend konnten wir Isl1 als entscheidenden Pioneertranskriptionsfaktor in der kardialen Zelldifferenzierung charakterisieren. Diese Erkenntnisse gewähren Einblicke in die molekularen Mechanismen der Kardiogenese und eröffnen somit neue Möglichkeiten für ein besseres Verständnis der kardialen Entwicklung.

## Abstract

Coordinated series of large-scale transcriptional changes and chromatin reorganization drive cell type specification and differentiation during embryogenesis. In this process, pioneer transcription factors play key roles in programming the epigenome and facilitating recruitment of additional regulatory factors. *Isl1*, a LIM-homeodomain transcription factor, marks the second heart field and plays a key role in early cardiac development. However, the early embryonic lethality of *Isl1* knockout mouse makes it impossible to study the role of *Isl1* at later stages of mouse heart development. The role of *Isl1* in epigenetic regulation during second heart field development and the mechanisms behind are still not clear.

In this study, using an *Isl1* hypomorphic mouse model, we found *Isl1* is critical for cardiac development even at the later stages of embryonic development. To search for the downstream targets of *Isl1* during cardiogenesis, we performed RNA-Sequencing with an *Isl1* knockout mouse model and the *Isl1* hypomorphic mouse model, together with a mESC-based directed cardiac differentiation system. In combination with CHIP in mESC-derived cardiac progenitor cells and in mouse embryos followed by high-throughput sequencing, we identified a regulatory gene network in cardiac progenitor cells and their derivatives organizing by *Isl1*.

To investigate the molecular mechanism underlying the role of *Isl1* in second heart field development, we firstly revealed that *Isl1* interacts with Brg1 and Baf60c in cardiac progenitor cells by co-immunoprecipitation. We further performed ATAC-sequencing in mESC-derived cardiac progenitor cells and in mouse embryos. Analysis of ATAC-sequencing data, combined with genome-wide profiling of *Isl1* binding in mESC-derived cardiac progenitor cells and in mouse embryos, we identified that *Isl1* acts as a pioneer factor during cardiogenesis. Moreover, we found *Isl1* might recruit Brg1 to its target sites and works cooperatively with the Brg1-Baf60c-based SWI/SNF complex to reorganize the chromatin landscape of target genes with critical functions in cardiac development, thus inducing gene expression programs in cardiac progenitors and promoting cardiac cell fate specification.

In conclusion, our study highlights a pioneering function of *Isl1* in cardiac lineage commitment and provides exciting novel insights into the molecular machinery orchestrating cardiogenesis.

# 1. Introduction

## 1.1 Heart development

In vertebrates, the heart is the first organ to form and is crucial to supply the embryo with nutrients and oxygen while removing metabolic waste. Therefore, the normal formation and function of the heart are essential for fetal life (Bruneau 2013). So far, numerous studies have defined the process of heart morphogenesis. Mouse heart development resembles that of the human, and thus has been supplied as a good model for understanding human cardiogenesis and congenital heart disease (CHD). A better understanding of heart development might in the long run have an impact on clinical management of CHD and help to generate efficient therapies.

### 1.1.1 Mouse heart development

In mouse embryos, myocardial cells are derivatives of the mesoderm, which emerges from the primitive streak during gastrulation (Buckingham, Meilhac et al. 2005). At around embryonic day 6.5 (E6.5), cardiac progenitor cells leave the primitive streak and migrate in an anterior-lateral direction to positions under the head folds, forming two groups of cells on either side of the midline (Figure 1A) (Buckingham, Meilhac et al. 2005). The cells then extend across the midline to form the cardiac crescent where differentiated myocardial cells are now observed (E7.5) (Figure 1B) (Buckingham, Meilhac et al. 2005). The region of the crescent, which fuses at the midline to form the primitive cardiac tube, is termed the first heart field (FHF, shown in red in Figure 1) (Vincent and Buckingham 2010). The second population of cells, which resides medially and posteriorly to the first heart field at E7.5, and later locates behind the heart tube, is referred to as the second heart field (SHF, shown in green in Figure 1) (Vincent and Buckingham 2010, Xin, Olson et al. 2013). The FHF is the source of the early left ventricle (LV) whereas the SHF gives rise to the outflow tract (OFT) and the right ventricle (RV), and both populations contribute to the atria (Dyer and Kirby 2009, Vincent and Buckingham 2010, Buckingham 2016).

One of the key steps in this refinement was the identification of Islet 1 (*Isl1*) as a SHF marker (Schoenwolf 2000, Waldo, Kumiski et al. 2001, Cai, Liang et al. 2003, Vincent and Buckingham 2010). According to marker gene expression and their contribution to the heart, the SHF is further divided into two main subdomains: anterior SHF (aSHF, shown in dark

green in Figure 1C) and posterior SHF (pSHF, shown in light green in Figure 1C) (Vincent and Buckingham 2010). The aSHF is marked by expression of *Fgf8*, *Fgf10*, and *Tbx1* and mainly contributes to the right ventricle and outflow tract myocardium progenitors (Robert G.Kelly 2001, Xu, Morishima et al. 2004). In contrast, the pSHF cells contribute to the atria at the venous pole of the heart, expressing *Is11*, but not the aSHF marker genes (Galli, Dominguez et al. 2008, Vincent and Buckingham 2010).

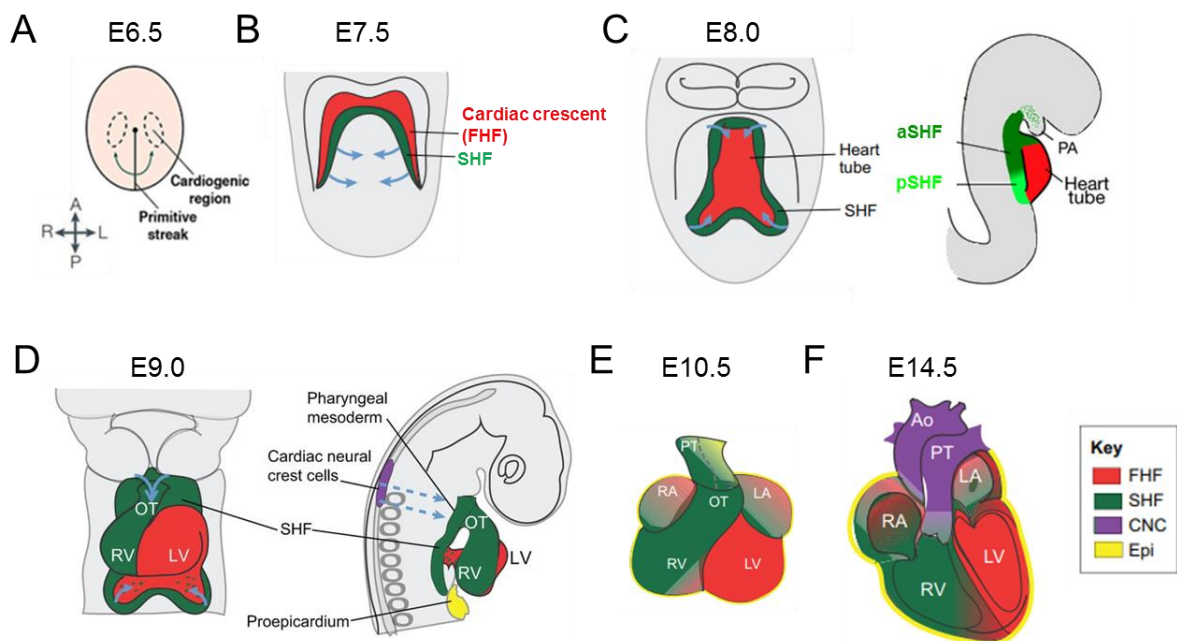


**Figure 1 Overview of mouse heart development (modified from (Buckingham, Meilhac et al. 2005, Meilhac, Lescroart et al. 2014, Zaffran, Robrini et al. 2014, Santini, Forte et al. 2016))**

Different stages in cardiac morphogenesis. FHF and SHF cells and their descendants are shown in red and green, respectively. Solid arrows indicate ongoing rearrangement of FHF and SHF cells. **(A)** Myocardial progenitor cells originate in the primitive streak (PS), from where they migrate to the anterior of the embryo at about E6.5. **(B)** Formation of the cardiac crescent (CC), with the second heart field (SHF) lying medial to it. **(C)** FHF cells form the primary heart tube, with SHF cells being added to the poles of the primary heart tube. At E8.0, frontal and lateral views showing the heart tube and subdomains of the SHF, including aSHF (anterior second heart field, in dark green) and pSHF (posterior SHF, in light green). **(D)** At E9.0, frontal and lateral views of the heart region showing looped heart tube. Dashed arrows indicate migration of cardiac neural crest cells to the heart. **(E and F)** The chambered hearts at E10.5 (E) and E14.5 (F) are shown, with lineage contributions to the heart from the FHF (first heart field), SHF (second heart field), cardiac neural crest (CNC) and proepicardium (PE). PA: pharyngeal arch; OT: outflow tract; RA: right atrium; RV: right ventricle; LA: left atrium; LV: left ventricle; Ao: aorta; PT: pulmonary trunk; Epi: epicardium.

The early FHF-derived cardiac tube provides a scaffold for subsequent growth. The primary heart tube grows by division of existing cardiomyocytes and by addition of the SHF myocardial progenitors to the arterial pole, where blood is pumped out the heart, and to the venous pole, where blood enters the heart. As the heart tube elongates, it undergoes a rightward looping and subsequently ballooning, result in formation of the four-chambered heart (Buckingham, Meilhac et al. 2005, Xin, Olson et al. 2013). During later stages, the mature shape of the heart is generated by differentiation of cardiac cell populations and extensive remodeling of the heart, resulting in a well-developed heart with distinct in- and outflow tracts, cardiac valves separating the different compartments, and a mature conduction system (Scheuermann and Boyer 2013) (Figure 1).

#### **1.1.1.1 Proepicardium**

During heart development, in addition to the cells of FHF and SHF, there are other two cell populations also contribute to the formation of the heart: proepicardium (PE) and the cardiac neural crest (CNC) (Laugwitz, Moretti et al. 2008, Vincent and Buckingham 2010, Santini, Forte et al. 2016). Proepicardium (shown in yellow in Figure 1D) is a transitory structure, which arises from the lateral plate mesoderm (LPM) and forms at the posterior end of the heart tube between E8.5 and E9.5. Proepicardial cells subsequently undergo an epithelial-to-mesenchymal transition (EMT) and invade the myocardium (Rickert-Sperling, Kelly et al. 2015, Meilhac and Buckingham 2018). Proepicardium gives rise to the epicardium which covers the external surface of the heart, smooth muscle cells associated with coronary arteries and cardiac fibroblasts (Maya-Ramos, Cleland et al. 2013, Rickert-Sperling, Kelly et al. 2015) (Figure 3B). *Wt1* (Wilms Tumor 1), *Tbx18* (T-Box 18) and *Tcf21* (Transcription Factor 21) are usually used as PE markers, even though they are also expressed in other tissues (Maya-Ramos, Cleland et al. 2013, Meilhac and Buckingham 2018). Another two PE markers, *Scx* (Scleraxis BHLH Transcription Factor) and *Sema3D* (Semaphorin 3D) are more specifically expressed in the PE and epicardium (Maya-Ramos, Cleland et al. 2013).

#### **1.1.1.2 Cardiac neural crest**

Cardiac neural crest (CNC) (shown in purple in Figure 1D) originate from the neural tube. CNC cells migrate to the pharyngeal arches and a subset continues to migrate through the anterior SHF into the outflow tract, playing a critical role in the remodeling of the outflow tract region. Interactions between neural crest cells and the anterior SHF affect the behavior

of both cell populations and their contributions to the heart (Vincent and Buckingham 2010). Fate mapping studies in both quail/chick chimeras and mouse embryos showed that CNC contributes to the aortopulmonary septum and valve formation which leads to the separation of the distal OFT into aorta and pulmonary trunk (Karen Waldo 1998, Xiaobing Jiang 2000). Moreover, the CNC plays a key role in the development of pharyngeal arch arteries and also gives rise to the cardiac ganglia (Kirby and Hutson 2010). Pax3 is a vital regulator of CNC and serves as a marker of CNC cells in mouse embryos (S.J. Conway 1997, Jun Li 2000).

### **1.1.1.3 Chamber septation and valves formation**

In mouse embryos, the first anatomic features of septation are seen at E10.5, when a distinct ridge appears in the atrial roof (the primary atrial septum) (Anderson, Spicer et al. 2014). During E11.5, this muscular septum extends through the cavity of the initially common atrial chamber, carrying on its leading edge a mesenchymal cap (MC), which arises through epithelial-to-mesenchymal transition (EMT) from the endocardium overlying the cap. With continuing growth of the muscular primary atrial septum, this mesenchymal cap approaches, and then fuses with, the superior endocardial cushion of the atrioventricular (AV) canal (Robert H Anderson 2003, Anderson, Spicer et al. 2014). The endocardial cushions contain mesenchymal cells that are derived from the endocardium through EMT. This primary atrial septum partially septates the atrial chamber and leaves a gap (the ostium primum) between the mesenchymal cap (MC) and the AV canal. The MC then merges anteriorly with the AV cushions and posteriorly with the dorsal mesenchymal protrusion (DMP) to fill the ostium primum. The DMP comes from the SHF and bulges into the atrial chamber as a mesenchymal protrusion. These mesenchymal tissues are later muscularised to form sturdy septum. While the ostium primum is closing, the upper margin of the primary atrial septum dissolves, creating a second opening (the ostium secundum) between the right and left atria. The ostium secundum is later sealed by a muscular septum (the secondary atrial septum), which is formed by part of the atrial roof that folds inward. The primary and secondary atrial septum then fuses to complete the septation of atrial chamber (Robert H Anderson 2003, Lin, Lin et al. 2012). Along with the atrial septum formation, an interventricular muscular septum emerges within the ventricular chamber (Robert H Anderson 2003). The interventricular septum (IVS) forms by outgrowth of two adjacent cell



populations in a small segment of the left and right ventricles (Bruneau 2013). It fuses with atrioventricular cushions, dividing the ventricular chamber into left and right ventricles (Lin, Lin et al. 2012). In addition, a subset of endocardial cushion cells in the atrioventricular canal (AVC) develops into atrioventricular (mitral and tricuspid) valves, whereas the OFT endocardial cushions give rise to semilunar (aortic and pulmonic) valves. The formation of heart valves ensures the blood flows in one direction from the atria to ventricles and then to the arteries (Lin, Lin et al. 2012).

#### **1.1.1.4 Trabeculation**

During vertebrate cardiac chamber maturation, ventricular myocardium undergoes trabeculation which is a process forming highly organized sheet-like muscular structures, termed trabeculae, in the inner surface of the ventricular wall. This is a result of the extrusion and expansion of differentiated cardiomyocytes into the lumen of the ventricular chambers (Liu, Bressan et al. 2010, Samsa, Yang et al. 2013). In mouse, the trabeculation occurs at approximately E9.5 and forms a mature trabeculated network at around E14.5 (Liu, Bressan et al. 2010, Samsa, Yang et al. 2013), increasing the myocardial surface area to facilitate the uptake of oxygen and nutrients (Meilhac and Buckingham 2018). Trabeculae are no longer required when the coronary vascular system develops, so they undergo compaction at the later stages (Meilhac and Buckingham 2018).

#### **1.1.2 Congenital heart disease**

Congenital heart disease (CHD) is the most common cause of major congenital anomalies, representing a major global health problem (Denise van der Linde, Konings et al. 2011). In man, CHD occurs in 0.5%-1% of live births, with similar prevalence all over the world (Harris 2011, Kernell, Sydsjö et al. 2014, Tiedman and Newburger 2016). CHD is usually referred to as abnormality in cardiac structures or associated vessels which are of functional significance (van der Bom, Zomer et al. 2011). It is classified into two main groups: acyanotic and cyanotic CHD (Figure 2). Infants with cyanotic CHD appear a bluish color of the skin and mucous membranes, due to the mixing of large amount of oxygenated and deoxygenated blood, while infants with acyanotic CHD initially do not (Bruneau 2008, Abramzon, Bosaleh et al. 2019). Acyanotic CHD includes ventricular septal defect (VSD), atrial septal defect (ASD), and patent ductus arteriosus (PDA), and so on. Like acyanotic CHD, cyanotic CHD also contains many different types of CHD, such as Tetralogy of Fallot (ToF), Persistent truncus

arteriosus (PTA) and Transposition of the great arteries (TGA). Here I summarized some of the common types of CHD.

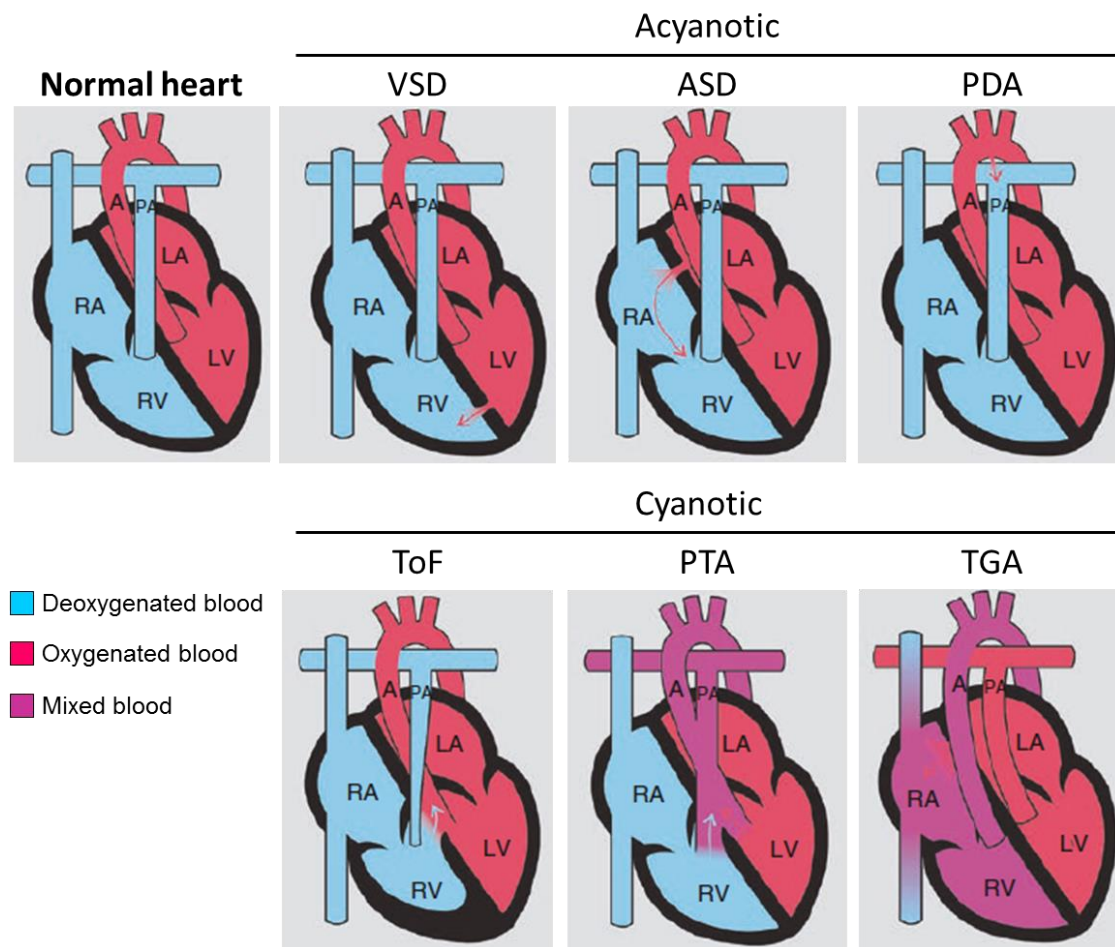


**Figure 2 Common types of congenital heart disease (adapted from (Abramzon, Bosaleh et al. 2019))**

Graphical representation shows the characteristics of some of the main defects with acyanotic and cyanotic CHD. RA: Right atrium; LA: Left atrium; RV: Right ventricle; LV: Left ventricle; A: Aorta; PA: Pulmonary artery; VSD: ventricular septal defect; ASD: atrial septal defect; PDA: Patent ductus arteriosus; ToF: Tetralogy of Fallot; PTA: Persistent truncus arteriosus; TGA: Transposition of the great arteries.

### 1.1.2.1 Ventricular septal defect and atrial septal defect (VSD and ASD)

VSD and ASD are the most common CHD in newborns. They are result from incomplete cardiac chamber septation during heart development. The hole in the atrial or ventricular septum leads to communications between the left and right atria or ventricles, respectively (Garg 2006, Midgett and Rugonyi 2014). The presence of a VSD can result in pulmonary hypertension as more blood needs to be pumped to the pulmonary vessels and can force the

left ventricle to work harder to pump the needed blood to the body (Garg 2006, Midgett and Rugonyi 2014). Moreover, VSDs are commonly associated with other types of CHD, such as Patent ductus arteriosus (PDA) (Abramzon, Bosaleh et al. 2019). In addition, VSDs sometimes undergo spontaneous closure shortly after birth. In contrast, ASD is generally the most frequent CHD found in adults, especially in women (Hoffman and Kaplan 2002, Abramzon, Bosaleh et al. 2019).

#### **1.1.2.2 Patent ductus arteriosus (PDA)**

Patent ductus arteriosus (PDA) is one of the common CHDs, which occurs when the ductus arteriosus that supposed to close after birth does not close (Midgett and Rugonyi 2014). Ductus arteriosus (DA) is a normal connection between the aorta and the pulmonary artery when babies are developing in the uterus. During pregnancy, it is not necessary for blood to circulate through the fetus's lungs because oxygen is provided through the placenta. However, when the baby is born, the blood must receive oxygen from the lungs and this hole is supposed to close. When it fails to close, the oxygenated blood from the aorta will mix with deoxygenated blood from the pulmonary artery. PDA can increase blood pressure in the pulmonary arteries causing pulmonary hypertension (Midgett and Rugonyi 2014).

#### **1.1.2.3 Tetralogy of Fallot (ToF)**

Tetralogy of Fallot (ToF) is the most common cyanotic CHD. It is a combination of four congenital abnormalities, including (1) right ventricular outflow tract obstruction, such as pulmonary stenosis, narrowing of the pulmonary valve opening; (2) VSD; (3) overriding aorta (OA), an OFT alignment defect, in which the aorta is shifted slightly to the right and lies directly above the VSD; and (4) RV hypertrophy, in which muscular wall of the RV is thicken due to the overworking (Abramzon, Bosaleh et al. 2019). Frequent associated defects can be found in ToF patients such as ASD, right aortic arch, and coronary artery anomalies (Abramzon, Bosaleh et al. 2019).

#### **1.1.2.4 Persistent truncus arteriosus (PTA)**

Persistent truncus arteriosus (PTA) is another kind of cyanotic CHD. It results from the failed division of the pulmonary artery and the aorta during fetal development, in which the single common arterial trunk usually overrides the interventricular septum (Mavroudis 2015). In most cases, it is associated with other CHD defects, especially VSD. The deoxygenated blood

from the RV and the oxygenated blood from the LV mix together when they are ejected out into the common trunk, going to both the body and the lungs. Therefore, it makes the heart to work harder and is risky of pulmonary hypertension (Midgett and Rugonyi 2014).

#### **1.1.2.5 Transposition of the great arteries (TGA)**

Transposition of the great arteries (TGA) is one of the most common and severe cyanotic CHD in neonates (Abramzon, Bosaleh et al. 2019). It is principally a result of failed OFT rotation (Neeb, Lajiness et al. 2013). In TGA, The aorta and pulmonary artery are fully septated but the positioning of them is reversed, with the aorta arising from the RV and the pulmonary trunk arising from the left ventricle (LV) (Neeb, Lajiness et al. 2013). It leads to the heart pumps the deoxygenated blood in RV from the body again to the body through the aorta; while pumps the oxygenated blood in LV from the lungs to the lungs again through the pulmonary artery. TGA is often associated with other CHDs, such as ASD, VSD and PDA (Martins and Castela 2008). In this case, the mixing of oxygenated blood and deoxygenated blood by other defects is beneficial, since they provide at least some oxygen to the body. TGA causes high mortality rate without treatment, thus surgical treatment is usually needed (Abramzon, Bosaleh et al. 2019).

#### **1.1.3 Cell types and cardiac lineages in mammalian heart**

The heart is predominantly made up of epicardium, endocardium, and myocardium, as well as cardiac fibroblasts (Doetschman and Azhar 2012). Epicardium is the outermost layer of the heart, whereas endocardium is the innermost layer. In the middle is the myocardium, which forms the muscular walls of the heart (Lin, Lin et al. 2012). The epicardial cells are derived from the proepicardium, some of which subsequently undergo epithelial-to-mesenchymal transition (EMT) and give rise to cardiac fibroblasts and smooth muscle cells in coronary arteries (Ramón Muñoz-Chápuli 2002). The endocardium contains a large group of endothelial cells, which are mainly derived from the cardiogenic mesoderm. Moreover, the endothelial cells also form the interior lining of blood vessels and surround the cardiac valves (Xin, Olson et al. 2013). The myocardium is primarily constituted with cardiomyocytes, which originate from the cardiogenic mesoderm (Doetschman and Azhar 2012). The cardiac conduction cells mainly consist of Purkinje fiber and pacemaker cells (Doetschman and Azhar 2012). They are specialized cardiomyocytes that generate and conduct electrical impulses (Xin, Olson et al. 2013). In addition, cardiac neural crest cells mostly contribute to the aortic

smooth muscle cells in distal outflow tract region, to the septum between the aortic and pulmonary trunks and valves, and autonomic nervous system cells in the heart (Meilhac 2012, Kloesel, DiNardo et al. 2016). These types of cells all work together to form the functional heart.

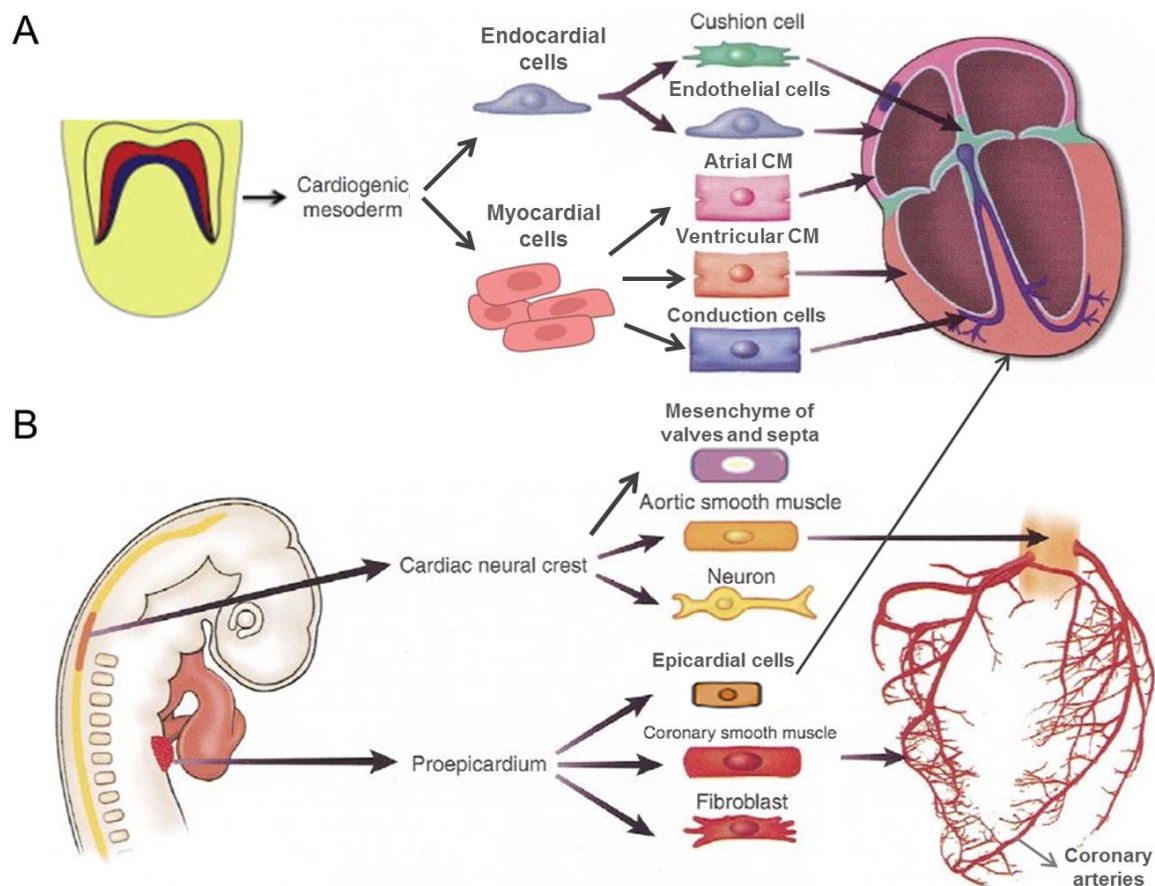


**Figure 3 Origins and lineage relationships of cardiac cell types (adapted from (Mikawa and Takashi 1999, Meilhac 2012, Chong, Forte et al. 2014))**

Schematic diagram summarizes the lineage tree of cardiac cell types, which derive from three origins: cardiogenic mesoderm, cardiac neural crest and the proepicardium. **(A)** Cells from the cardiogenic mesoderm, containing precursors of the endocardium and myocardium. Conduction cells are specialized cardiomyocytes (CM), including the pacemaker cells and Purkinje fibres. **(B)** Cells from cardiac neural crest and the proepicardium. Cardiac neural crest cells mainly contribute to the smooth muscle of the aortic and pulmonary trunks, and the pharyngeal arch arteries, to the septum between the aortic and pulmonary trunks and valves, and to the ganglia of the developing heart. Proepicardium gives rise to the epicardium. A subset of these cells, termed epicardial-derived cells (EPDCs), mainly differentiates into the coronary smooth muscle cells, as well as cardiac fibroblasts.

Interestingly, studies from different labs suggest that, with respect to lineage diversification, different cardiac cell types arise from a common progenitor (Kattman, Huber et al. 2006, Moretti, Caron et al. 2006, Wu, Fujiwara et al. 2006, Bu, Jiang et al. 2009). Moreover, the

work from Moretti et al. revealed the existence of multipotent *Isl1*<sup>+</sup> cardiovascular progenitors (Moretti, Caron et al. 2006), which can generate the three major cell types of the heart: cardiomyocytes, smooth muscle and endothelial cells (Moretti, Caron et al. 2006, Wu, Fujiwara et al. 2006, Laugwitz, Moretti et al. 2008, Bu, Jiang et al. 2009) (Figure 4).

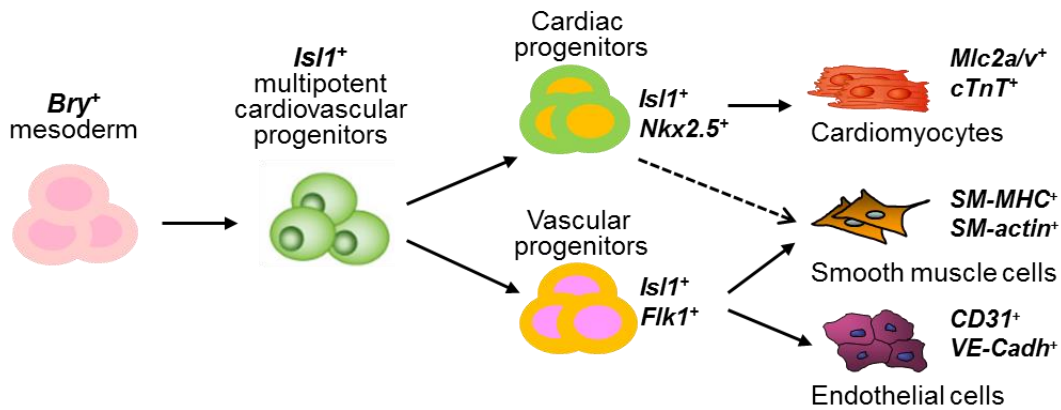


**Figure 4 Cellular hierarchy of cardiac progenitors and their lineage specification (adapted from (Moretti, Caron et al. 2006, Wu, Fujiwara et al. 2006, Laugwitz, Moretti et al. 2008))**

*Isl1*<sup>+</sup> cardiovascular progenitors are multipotent which can give rise to all three major cell types in the heart (Moretti, Caron et al. 2006). *Nkx2.5*<sup>+</sup> progenitor cells are reported to be bipotent (Wu, Fujiwara et al. 2006) or multipotent (Ma, Zhou et al. 2008). However, lineage reconstruction from single cell analysis shows that *Nkx2.5*<sup>+</sup> cells are primed to cardiomyocyte lineage (DeLaughter, Bick et al. 2016, Jia, Preussner et al. 2018).

#### 1.1.4 Signaling pathways in cardiac development

Signaling pathways and networks orchestrated by signaling molecules play key roles in regulating cardiac morphogenesis. Perturbation of signaling molecules during cardiogenesis leads to congenital heart defects. Over the past years, a number of studies have identified key signaling pathways controlling cardiogenesis, such as Wnt, Bmp, FGF, Hedgehog and Notch signaling pathways (Figure 5).

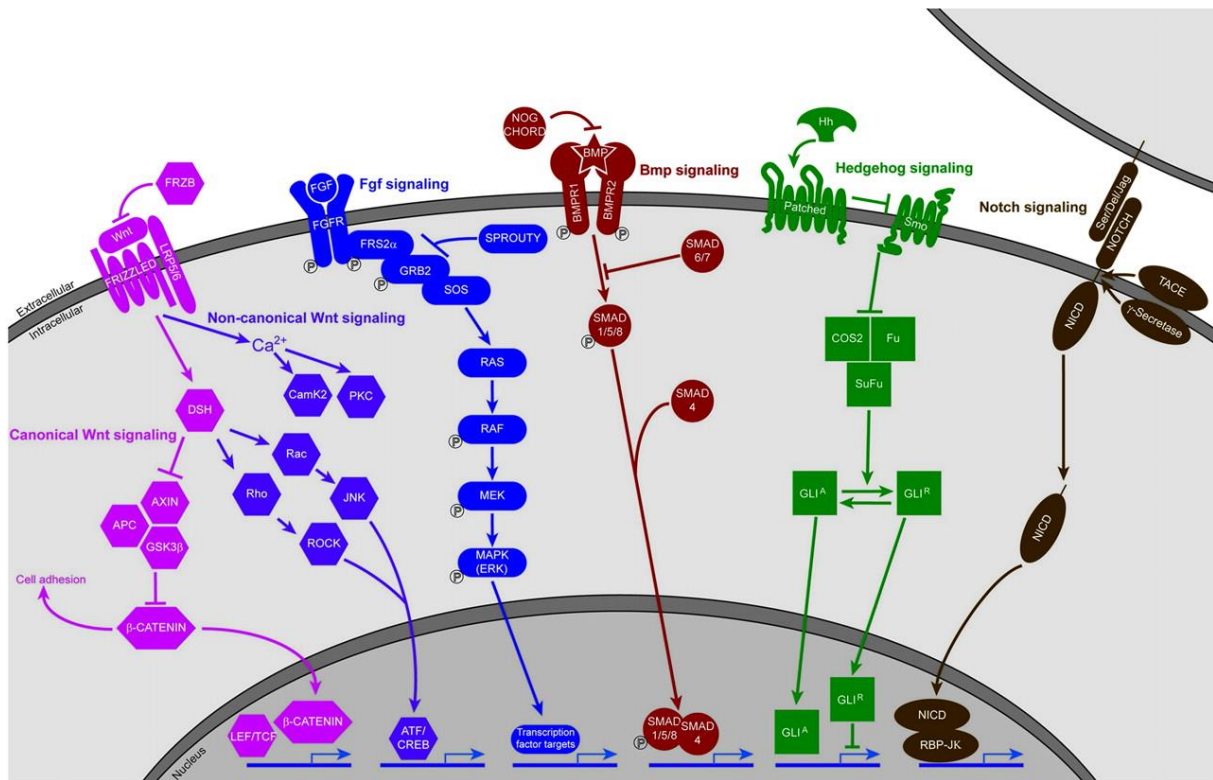


**Figure 5 Illustration showing the core features of Wnt, FGF, BMP, Hh, and Notch signaling pathways (Rochais, Mesbah et al. 2009)**

This simplified schema summarizes the key steps from ligand binding to target gene transcription for each signaling pathway (Rochais, Mesbah et al. 2009). Details are described in the context in sub-sections of each pathway.

### 1.1.4.1 Wnt signaling pathway

Wnt signaling pathway is a key pathway during development and it plays multiple roles in regulating cellular behavior including proliferation, differentiation, cell migration, and cell polarity (Tian, Cohen et al. 2010). It consists of canonical Wnt signaling pathway and noncanonical Wnt signaling pathway.

In canonical Wnt signaling pathway (also called, Wnt/ $\beta$ -catenin signaling pathway), binding of Wnt ligands to the Fzd (Frizzled)-LRP5/6 receptor complex allows the activation of the intracellular effector DSH (Disheveled), which results in the uncoupling of  $\beta$ -catenin from a multiprotein degradation complex composed of APC (adenomatous polyposis coli), Axin, and GSK3 $\beta$  (glycogen synthase kinase 3 $\beta$ ).  $\beta$ -catenin then translocates to the nucleus and, in association with LEF/TCF, activates target gene transcription. Binding of Wnt ligand to receptors can be blocked by its binding to secreted FRZB (frizzled-related molecules).

Canonical Wnt pathway has been reported to play diverse roles during heart development which will lead to different effects depending on the time of action (Gessert and Kuhl 2010, Buikema, Zwetsloot et al. 2014). Canonical Wnt signaling initially promotes cardiogenesis, but later is inhibitory as progenitors begin to differentiate into various cardiac derivatives (Naito, Shiojima et al. 2006, Kwon, Arnold et al. 2007, Bruneau 2013). Cell culture studies of cardiac differentiation revealed that canonical Wnt activation induces nascent mesoderm from pluripotent stem cells, but once mesoderm is induced, inhibition of canonical Wnt signaling is necessary for cardiac specification and prolonged Wnt/ $\beta$ -catenin activation inhibits cardiac differentiation and instead, induces other lineages (Kattman, Witty et al. 2011, Xiaojun Lian 2012, BurrIDGE, Matsa et al. 2014, Loh, Chen et al. 2016, Sadahiro, Isomi et al. 2018). Consistently, inhibition of Wnt/ $\beta$ -catenin signaling results in failure of ESCs to generate *Flk1*<sup>+</sup> mesodermal precursors and subsequent mature mesodermal lineages (Lindsley, Gill et al. 2006).

In addition to playing earlier roles in mesoderm development, canonical Wnt signaling also promotes cardiac progenitor cell proliferation and plays an inhibitory role in later cardiomyocyte differentiation (Cohen, Tian et al. 2008). *In vivo* activation of  $\beta$ -catenin signaling in *Isl1*<sup>+</sup> progenitors of the SHF leads to their massive accumulation, inhibition of differentiation, and outflow tract (OFT) morphogenic defects (Qyang, Martin-Puig et al. 2007). Wnt2 was also shown to regulate the expansion of cardiac progenitor cells in the posterior SHF through canonical Wnt pathway (Tian, Yuan et al. 2010). In contrast, the expression of secreted Wnt antagonists Crescent, which competes with Fzd for Wnt binding via its homology to the Fzd extracellular domain, and Dkk1, which inhibits canonical Wnt signaling by causing Lrp5/6 receptor internalization, induces cardiac gene expression and the appearance of beating cardiomyocytes in noncardiogenic mesoderm in chick and *Xenopus* embryos (Marvin MJ 2001, Valerie A. Schneider 2002). Moreover, tissue-specific deletion of  $\beta$ -catenin in the SHF with *Isl1-Cre* results in nearly complete loss of the right ventricle, suggesting  $\beta$ -catenin is required for right ventricle formation (Kwon, Arnold et al. 2007, Kwon, Cordes et al. 2008).

Noncanonical Wnt signaling pathway consists of two signaling pathways. One is downstream of DSH and the other one is independent of DSH. In the first pathway, activated DSH promotes small G protein (Rac and Rho) activation, leading to the activation of JNK (c-Jun N-



terminal kinase) and ROCK (Rho-associated kinase). Ultimately, the ATF/CREB complex is activated and results in target gene transcription. The second pathway, called Wnt/Ca<sup>2+</sup> pathway, results in intracellular Ca<sup>2+</sup> release and activation of the Ca<sup>2+</sup>/CamK2 (calmodulin-dependent kinase 2) and the PKC (protein kinase C) pathways.

Two noncanonical Wnt ligands, Wnt5a and Wnt11, are expressed at the arterial pole of the heart as SHF cells migrate through on their way to the right ventricle, and mice with homozygous mutations of Wnt5a or Wnt11 have outflow tract defects consistent with those caused by disruption of the SHF (Tian, Cohen et al. 2010, Sinha, Li et al. 2015, van Vliet, Lin et al. 2017). Wnt5a and Wnt11 were reported to promote cardiac differentiation and inhibit the proliferation of SHF progenitor cells (Terami, Hidaka et al. 2004, Koyanagi, Haendeler et al. 2005, Koyanagi, Iwasaki et al. 2009, Abdul-Ghani, Dufort et al. 2011, Cohen, Miller et al. 2012, Bisson, Mills et al. 2015). They are co-required for repressing canonical Wnt signaling in SHF progenitors and promote SHF progenitor development cooperatively (Cohen, Miller et al. 2012, Bisson, Mills et al. 2015). In addition, Wnt2 is strongly expressed in the early developing murine heart, and was reported to be essential for efficient cardiomyocyte differentiation from ES cells through JNK/AP-1 pathway (Onizuka, Yuasa et al. 2012).

#### **1.1.4.2 FGF signaling pathway**

In FGF (Fibroblast Growth Factors) signaling pathway, binding of FGF ligands leads to the autophosphorylation of the FGF receptor tyrosine kinase, allowing interaction of the FRS2 $\alpha$  docking protein and subsequent activation of the GRB2/SOS (growth factor receptor-bound protein 2/Son of sevenless) complex. Activated SOS, a guanine nucleotide exchange factor, in turn, activates the small G protein RAS, triggering a cascade of phosphorylation leading to the successive activation of RAF, MEK, and mitogen-activated protein kinase (ERK) kinases. p-ERK phosphorylates target transcription factors (including Ets family members) to activate gene expression. Sprouty blocks the phosphorylation cascade by interacting with the FRS2 $\alpha$ /GRB2/SOS complex.

FGFs are among the critical signals controlling communications within and between developing cardiac progenitors (Urness, Bleyl et al. 2011). The human/mouse FGF family comprises 22 members (Itoh, Ohta et al. 2016). Among them, FGF ligands implicated in second heart field development include Fgf3, Fgf8, Fgf10 and Fgf15 (Francou, Saint-Michel et al. 2013). Fgf8 is the best understood one among these FGFs regulating cardiovascular

development. Fgf8 signaling was shown to promote SHF proliferation and inhibit myocardial differentiation in chick SHF explants (Hutson, Zeng et al. 2010). Studies from two independent groups showed that *Fgf8* deletion in the SHF leads to severe truncations of the right ventricle and the outflow tract (Ilagan, Abu-Issa et al. 2006, Park, Ogden et al. 2006), indicating the critical role of Fgf8 in SHF development. It was later reported that the role of mesodermal Fgf8 and Fgf10 overlaps during SHF and pharyngeal arch arteries (PAA) development, highlighting the sensitivity of cardiovascular development to FGF dosage (Watanabe, Miyagawa-Tomita et al. 2010). Moreover, Fgf3 and Fgf10 also function redundantly and are dosage sensitively required during cardiovascular development (Urness, Bleyl et al. 2011). In addition, targeted disruption of *Fgf15* in mouse embryos leads to OFT alignment defects and reduced cell proliferation within the OFT myocardium, indicating that Fgf15 is required for proper morphogenesis of cardiac outflow tract (Vincentz, McWhirter et al. 2005).

#### **1.1.4.3 BMP signaling pathway**

In the BMP (Bone Morphogenetic Proteins) signaling pathway, BMP ligands bind to a receptor complex composed of type 1 and type 2 BMP receptors. Upon receptor activation, Smad proteins (Smad1/5/8) are phosphorylated and associate with a coactivator Smad (Smad 4). The resulting Smad complex enters the nucleus and activates target gene expression. BMP signaling can be inhibited by the secreted proteins NOG (Noggin), CHORD (Chordin) and intracellular Smad proteins (Smad 6/7).

BMPs are a group of signaling molecules that belongs to the Transforming Growth Factor- $\beta$  (TGF $\beta$ ) superfamily of proteins (Wang, Green et al. 2014). A lot of studies implicate the role of BMP signaling in regulating cardiogenesis of different species, such as chicken (Birgit Andre'e 1998), mouse (Liu, Selever et al. 2004, Wang, Greene et al. 2010), zebrafish (Emma de Pater 2012) and *Xenopus* (Shi, Katsev et al. 2000). Bmp2 acts as a cardiac specification factor that elicits ectopic expression of the early cardiac markers *Nkx2.5* and *Gata4*, when it is ectopically expressed in chicken (Birgit Andre'e 1998). In SHF explants from chick embryos, Bmp2 decreases SHF proliferation and promotes myocardial differentiation (Hutson, Zeng et al. 2010). Bmp4 was shown to be required for outflow tract septation and branchial arch artery remodeling in mouse embryos (Liu, Selever et al. 2004). Bmp2 and Bmp4 were reported to control the timing of progenitor gene silencing in OFT myocardium by regulating

the expression of miRNAs in mouse embryos (Wang, Greene et al. 2010). Bmp10 is another Bmp member, shown to be essential in regulating cardiac growth and chamber maturation in mouse embryos (Chen, Shi et al. 2004). Bmp10 is also required for maintaining normal expression levels of several key cardiogenic factors (including Nkx2.5 and Mef2c) in the developing myocardium at mid-gestation (Chen, Shi et al. 2004) and works in axis with myocardin (Myocd) in this process (Huang, Elicker et al. 2012). In *Xenopus*, BMP signaling is also required for heart formation as well as maintenance of *Nkx2.5* expression (Shi, Katsev et al. 2000). In zebrafish, Pater et al. reported that Bmp signaling activity is strictly controlled during cardiomyocyte differentiation, since it is required to induce cardiac differentiation of cardiac progenitors but dispensable and even deleterious once differentiation is initiated (Emma de Pater 2012). They further illustrated that *smad6a* is expressed in the cardiac fields and linear heart tube to inhibit Bmp signaling (Emma de Pater 2012).

#### **1.1.4.4 Hedgehog signaling pathway**

The Hh (Hedgehog) signaling pathway is one of the key regulators of metazoan development. In this pathway, the Patched receptor inhibits activity of the transmembrane protein Smo (Smoothened) in the absence of Hh ligand. The Cos2/Fu/SuFu (Costal-2/Fused/Suppressor of fused) complex is thus able to convert the transcription factor GLI into a repressor form (GLI<sup>R</sup>). In the presence of Hh ligand, Hh binds to Patched and thereby releases the inhibition of SMO. SMO blocks the Cos2/Fu/SuFu complex, leading to the generation of the activator form of GLI (GLI<sup>A</sup>) that translocates to the nucleus to drive target gene transcription.

Three different Hedgehog proteins-SHH (Sonic hedgehog), IHH (Indian hedgehog), and DHH (Desert hedgehog), exist in vertebrates. Among them, SHH is the most understood one in heart development. In mouse embryos, loss of *Shh* causes several cardiac abnormalities, including ventricular hypoplasia, septation defects and outflow tract shortening (Tsukui T 1999, Washington Smoak, Byrd et al. 2005). Mice ablated of *Smo* using *Is1-Cre* exhibit cardiovascular defects similar to those observed in *Shh* null mice, defining a spatial requirement for hedgehog signaling within *Is1* expression domains for aortic arch and outflow tract formation (Lin, Bu et al. 2006). In chick embryos, inhibition of *Shh* leads to reduced SHF proliferation and pulmonary atresia, suggesting that *Shh* maintains proliferation in SHF progenitors and is required for normal arterial pole formation (Dyer and Kirby 2009).

#### **1.1.4.5 Notch signaling pathway**

In Notch signaling pathway, interaction of Notch receptor with transmembrane ligand proteins (Ser, Serrate; Del, Delta; Jag, Jagged) in a neighboring cell triggers the proteolytic cleavage of Notch by TACE (tumor necrosis factor (TNF)  $\alpha$ -converting enzyme) and  $\gamma$ -secretase. This cleavage releases the Notch intracellular domain (NICD) and allows its translocation to the nucleus. NICD forms a transcriptional complex with RBPJk (recombination signal binding protein Jk) to activate target genes.

The Notch signaling pathway is an ancient and highly conserved signaling pathway that plays important roles in development. It is also involved in multiple processes during vertebrate cardiogenesis. Analysis of standard and endothelial-specific *Notch1* and *RBPJk* mutants shows that trabeculation is severely impaired and only primitive, poorly organized trabeculae can be observed in these mutants (Grego-Bessa, Luna-Zurita et al. 2007). Functional analysis reveals the requirement of the transcription factor Hey2 (Hes related family BHLH transcription factor with YRPW motif 2) (Kokubo, Miyagawa-Tomita et al. 2004) or the synergistic functions of Hey1 and Hey2 (Kokubo, Miyagawa-Tomita et al. 2005) or Heyl (Hey1 and Hey-like protein) in valve development (Fischer, Steidl et al. 2007). Endothelial-specific deletion of *Jag1* (Jagged1) in mice results in cardiovascular defects, displaying right ventricular hypertrophy, overriding aorta, ventricular septal defects, coronary vessel abnormalities and valve defects and loss of *Jag1* disrupts EMT during endocardial cushion formation (Hofmann, Briot et al. 2012). Moreover, conditional inactivation of *Jag1* in second heart field tissues results in OFT and aortic artery defects resembling those seen in patients with congenital heart disease (CHD), indicating that *Jag1* is an essential Notch ligand in the SHF (High, Jain et al. 2009, MacGrogan, Nus et al. 2010).

#### **1.1.5 Transcriptional factors involved in heart development**

The expression of *Mesp1* is one of the known earliest sign toward cardiovascular development (Yumiko Saga 2000). *Mesp1* promotes the expression of cardiac transcription factors while repressing genes that maintain pluripotency (Bondue 2008). As cardiac precursors migrate away from the primitive streak to form the cardiac crescent, *Mesp1* is downregulated while genes encoding cardiac transcription factors are activated (Y. Saga 1996, Paige, Plonowska et al. 2015). Here I summarized some of the representative transcriptional factors involved in heart development.

### 1.1.5.1 GATA binding factors

Among the six GATA family transcription factors, Gata1, Gata2 and Gata3 are sub-classified as “hematopoietic GATA factors”, while Gata4, Gata5 and Gata6 are “cardiac GATA factors”, due to their priming roles in different systems (Tremblay, Sanchez-Ferras et al. 2018).

*Gata4* is one of the earliest transcription factors expressed in mouse cardiac cells. It can be detected in the precardiac mesoderm as early as primitive streak stage (around E7.0) in mouse embryos and expands subsequently to more structures such as myocardium, endocardium, endocardial cushion and septum tissues, and persists in myocardium even after birth (Heikinheimo, Scandrett et al. 1994). Homozygous *Gata4*-deficient mice arrest in development between E7.0 and E9.5 and die short after, because of severe defects including the loss of a ventral heart tube resulting from a failure in lateral to ventral folding. In detail, in the absence of *Gata4*, the failed migrating of cardiac precursors to the ventral midline leads to forming of cardiac structures in bilateral side of the embryo, which is called cardia bifida (Kuo, Morrisey et al. 1997, Molkentin, Lin et al. 1997). However, studies from chimera mice suggest that the cardiac defects are secondary due to ventral patterning defects, resulting from lacking of *Gata4* in the visceral endoderm, rather than the mesoderm (Narita, Bielinska et al. 1997, Watt, Battle et al. 2004). Analysis of mouse embryos with *Gata4* deficiency in different tissues reveals important activities of Gata4 in proepicardium development, chamber formation, generation of the endocardial cushions, and septation of the OFT (Watt, Battle et al. 2004, Zeisberg, Ma et al. 2005, Rivera-Feliciano, Lee et al. 2006). Moreover, Gata4 was reported to act as a pioneer factor which can bind its target DNA sequences within condensed chromatin (Cirillo, Lin et al. 2002). In mouse heart, Gata4 shapes the chromatin environment and regulates gene expression by recruiting the histone acetyltransferase P300, which deposits H3K27ac deposition at cardiac enhancers to stimulate transcription (He, Gu et al. 2014).

In addition, data from *Gata5*<sup>-/-</sup> mice suggest a role of Gata5 in endocardial cell differentiation and cardiac valve formation (Laforest, Andelfinger et al. 2011). *Gata6* inactivation in vascular smooth muscle cells (VSMCs) leads to perinatal lethality and cardiovascular defects, including interrupted aortic arch and persistent truncus arteriosus, suggesting a role of Gata6 in regulating morphogenetic patterning of the cardiac outflow tract and aortic arch (Lepore, Mericko et al. 2006). Gata4, Gata5 and Gata6 interact with each other (Laforest and

Nemer 2011) and have partially redundant roles in the regulation of heart development (Holtzinger and Evans 2007, Peterkin, Gibson et al. 2007). They also work cooperatively with other cardiac transcription factors in regulation of cardiac gene expression in the developing heart, such as *Nkx2.5*, *Tbx5*, *Tbx20*, *Mef2c*, *Srf* and so on (Durocher, Charron et al. 1997, Stennard, Costa et al. 2003, He, Kong et al. 2011, Schlesinger, Schueler et al. 2011). Mutations of *GATA4*, *GATA5* or *GATA6* in human all lead to CHD, including cardiac septal defects and OFT defects, which are consistent with the phenotypes observed in the mouse models (Garg, Kathiriyala et al. 2003, Kodo, Nishizawa et al. 2009, Wei, Bao et al. 2013).

#### **1.1.5.2 T-box transcription factors**

Among T-box gene family members, *Tbx1*, *Tbx2*, *Tbx3*, *Tbx5*, *Tbx18*, and *Tbx20* are expressed and have functions in the developing heart.

*Tbx1* is expressed in the mesoderm and endoderm of the pharyngeal arches, and OFT in mouse (Xu, Morishima et al. 2004, Maeda, Yamagishi et al. 2006). Lineage tracing experiments have demonstrated that these *Tbx1*-positive cells contribute extensively to myocardial wall and endothelium of the OFT, and some contribute to the myocardium of the right ventricle, suggesting that *Tbx1* expressed mainly in the SHF (Xu, Morishima et al. 2004). *Tbx1* is required for normal development of the pharyngeal arch arteries in a gene dosage-dependent manner. Deletion of one copy of *Tbx1* affects the development of the fourth pharyngeal arch arteries, whereas homozygous mutation severely disrupts the pharyngeal arch artery system, which phenocopies the cardiac defects observed in DiGeorge syndrome in human (Elizabeth A. Lindsay 2001). *Tbx1* was later reported to be required for posterior SHF cells to contribute to the arterial and venous poles of the heart tube (Rana, Theveniau-Ruissy et al. 2014), providing an explanation for the occurrence of venous pole defects seen in DiGeorge syndrome. In addition, *Fgf8* and *Fgf10* act downstream of *Tbx1* in the SHF, while *Foxc1* and *Foxc2* act upstream of the *Tbx1*-FGF cascade (Hu, Yamagishi et al. 2004, Xu, Morishima et al. 2004, Seo and Kume 2006) (Figure 5). Moreover, *Tbx1* regulates the balance between myocardial proliferation and differentiation in the SHF through *Isl1*, *Hod* and *Nkx2.6* (Liao, Aggarwal et al. 2008).

*Tbx2* and *Tbx3* are expressed in the non-chamber myocardium of the atrioventricular canal (AVC) and are redundantly required for AVC patterning by repressing chamber myocardial genes (Christoffels, Burch et al. 2004, Harrelson, Kelly et al. 2004, Christoffels 2012). *Tbx2* is

expressed in the OFT as well, and misexpression of *Tbx2* impairs deployment of SHF derived progenitor cells to the OFT and also leads to defects in OFT remodeling in mouse embryonic heart (Harrelson, Kelly et al. 2004, Dupays, Kotecha et al. 2009). Whereas, *Tbx3* is expressed in the cardiac conduction system as well, and is required for its specification (Bakker, Boukens et al. 2008). Interestingly, *Tbx3* is reported to be required for mouse OFT development, even though it is supposed not to express in the OFT, through an indirect way, by regulation of intercellular signaling pathways coordinating proliferation and deployment of the SHF (Mesbah, Harrelson et al. 2008).

Both *Tbx5* and *Tbx20* play roles in the cardiac chamber formation. *Tbx5* is expressed in the inflow tract, atria, AV cushion, and left ventricle, appearing to be restricted to the FHF-derived region (Benoit G. Bruneau, Malcolm Logan et al. 1999). By contrast, *Tbx20* is primarily expressed in the outflow tract and the right ventricle during heart chamber formation, which are derived from the SHF (Koshiba-Takeuchi, Morita et al. 2016). Mice with *Tbx20* complete knockdown showed defects in heart formation, including hypoplasia of the outflow tract and right ventricle (Takeuchi, Mileikovskaia et al. 2005, Koshiba-Takeuchi, Morita et al. 2016). In the developing heart, *Tbx5* and *Tbx20* are complementarily expressed in the left and right ventricle, respectively (Takeuchi 2003, Plageman and Yutzey 2004). In humans, mutations in *TBX5* are related to Holt-Oram syndrome (Basson, Bachinsky et al. 1997, Li, Newbury-Ecob et al. 1997, Benoit G. Bruneau, Malcolm Logan et al. 1999), while mutations in *TBX20* result in ASD, ToF, PTA and so on (Kirk 2007, Posch 2010, Pan, Geng et al. 2015, Huang, Wang et al. 2017). Moreover, *Tbx5* and *Tbx20* act in combination with *Nkx2.5* and *Gata4* to promote the specification of chamber myocardium (Paige, Plonowska et al. 2015). In mice, *Tbx5* and *Gata4* regulate the expression of *connexin 30.2*, which is required for slow conduction in the atrioventricular node (Munshi, McAnally et al. 2009).

*Tbx18* is expressed in the proepicardium (PE), in the epicardium, and sinus venosus region in mouse (Florian Kraus 2001). Expression domains of *Tbx18* are adjacent but distinct from *Nkx2.5* and *Isl1* expression domains. It is required for the venous pole formation in the heart (Christoffels, Mommersteeg et al. 2006).

### **1.1.5.3 Hand1 and Hand2**

In mice, *Hand1* (eHand) and *Hand2* (dHand) are involved in ventricular chamber formation. After cardiac looping, they are preferentially expressed in the left ventricle and right

ventricle, derivatives of the first and second heart fields, respectively (Tiffani Thomas 1998). Mice that lack *Hand2* die at E10.5 from right ventricular hypoplasia and vascular defects (Deepak Srivastava 1997, Yamagishi, Olson et al. 2000, Tsuchihashi, Maeda et al. 2011). In contrast, embryos homozygous for *Hand1* deletion displayed defects in the left ventricle and endocardial cushions, and exhibited dysregulated ventricular gene expression (McFadden, Barbosa et al. 2005). Moreover, *Hand1* acts downstream of *Nkx2.5* during cardiac morphogenesis (Harvey 1997, McFadden, Barbosa et al. 2005), whereas *Hand2* is a direct downstream target of *Gata4* and *Isl1* (D.G. McFadden 2000, Caputo, Witzel et al. 2015) (Figure 5).

#### **1.1.5.4 Nkx2.5**

The homeobox gene *Nkx2.5* (also called *Csx*), a homolog of *Drosophila tinman*, is one of the earliest known markers of vertebrate heart development (R.J. Schwartz 1999). *Nkx2.5* can be detected in the early cardiac crescent at E7.5. As development proceeds, *Nkx2.5* is expressed in almost all the cardiac regions derived from both first and second heart fields, including left ventricle, outflow tract and right ventricle, as well as atria and sinus venosus. *Nkx2.5* is also detected in the pharyngeal region. However, *Nkx2.5* deletion in the pharyngeal endoderm does not affect heart formation, which may be result from the compensation of endodermal expression of *Nkx2.3* and *Nkx2.6*. In contrast, mesodermal deletion of *Nkx2.5* showed a hypoplastic outflow tract and right ventricle and an arrested looping heart tube, as seen in *Nkx2.5* null mouse embryos, leading to embryonic lethality at around E10.5 (I Lyons 1995, M. Tanaka 1999, Zhang, Nomura-Kitabayashi et al. 2014). These studies indicate that *Nkx2.5* is pivotal for early heart formation in mouse embryos.

*Nkx2.5* acts genetically upstream of multiple genes essential for heart development, including some cardiac transcription factors, such as *Mef2c*, *Hand1* and *Myocd* (M. Tanaka 1999, Ueyama, Kasahara et al. 2003). *Isl1* is also reported to be a downstream target of *Nkx2.5* but is negatively regulated (Dorn, Goedel et al. 2015, Colombo, de Sena-Tomas et al. 2018) (Figure 5).

#### **1.1.5.5 Mef2c**

Among the four *Mef2* transcription factor family members (*Mef2a*, -b, -c, and -d), *Mef2c* is the most extensively studied in heart development. Studies in mouse embryos showed that



Mef2c is required for looping of the cardiac tube, development of the right ventricle, and expression of a subset of cardiac genes, such as *Hand2*, *Mlc1a* and cardiac  $\alpha$ -actin (Qing Lin 1997). Moreover, deletion of *Mef2c* causes embryonic lethal in mouse at around E10.5 (Lin, Schwarz et al. 1997). Mice with *Mef2c* deleted in the anterior second heart field (aSHF) display cardiac defects similar with the ones observed in human CHD (Qiao, Wang et al. 2017, Lu, Wang et al. 2018), such as tetralogy of Fallot (ToF), great arteries (d-TGA) with VSD; or double-outlet right ventricle (DORV), indicating an essential role of Mef2c in OFT alignment (Barnes, Harris et al. 2016). Interestingly, a recent publication further demonstrated that cardiovascular development and survival in mouse require Mef2c function in the myocardial but not the endothelial lineage (Materna, Sinha et al. 2019).

Mef2c works cooperatively with other cardiac transcription factors in regulating cardiac gene expression, such as *Gata4*, *Nkx2.5* and *Tbx5* (Nemer 2000, Vincentz, Barnes et al. 2008, Ghosh, Song et al. 2009). Moreover, *Mef2c* is a direct downstream target of *Isl1*, *Gata4* and *Nkx2.5* (M. Tanaka 1999, Dodou, Verzi et al. 2004, Wang, Li et al. 2016) (Figure 6).

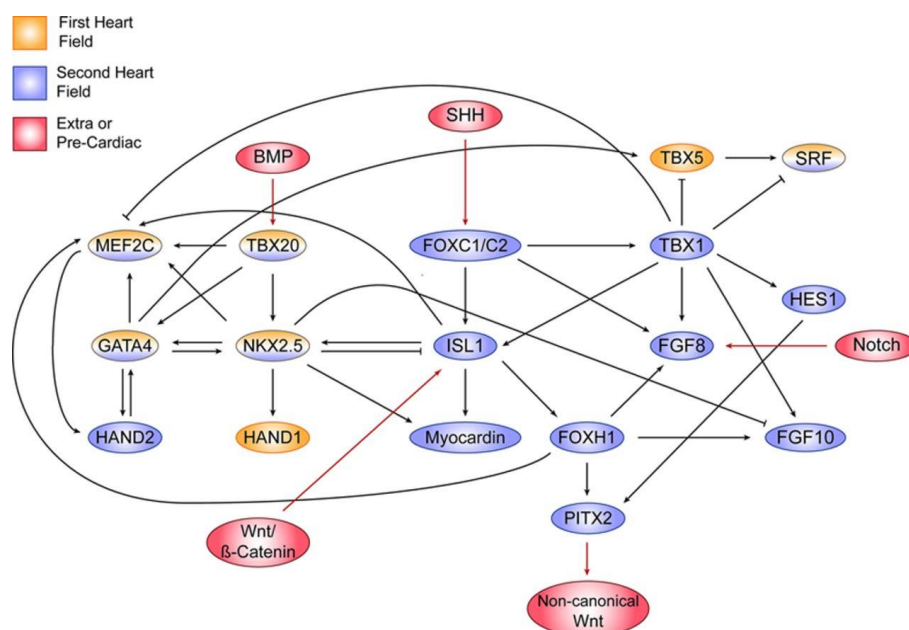


**Figure 6 Cardiac gene regulatory networks (Paige, Plonowska et al. 2015)**

The diagram shown is a brief overview of a subset of known transcription factor interactions and signaling pathways that drive the differentiation of first heart field (FHF; orange) and second heart field (SHF; blue) cardiac progenitor cells (CPCs) during development. Factors colored by both orange and blue represent regulators of both FHF and SHF. Arrows indicate increased expression of one transcription factor or signaling molecule because of activity of another transcription factor. Signaling pathways that activate expression of certain transcription factors are shown in red.

Spatiotemporal and quantitative regulation of cardiac transcription factors must occur in a precise manner to ensure fine regulation of downstream targets (Bruneau 2002). Although networks of interacting transcription factors are being defined (Figure 6), the full complement of their target genes is still not clear, nor is how these factors are integrated at the level of chromatin to activate transcriptional programs (Bruneau 2013).

## 1.2 Isl1

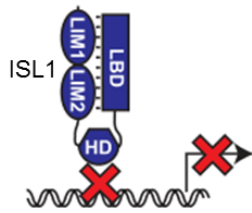
### 1.2.1 Protein structure of ISL1

Islet1 (Isl1) is a LIM-homeodomain transcription factor. The gene encoding Isl1 contains six exons, and is located on chromosome 13 in mouse and chromosome 5 in human (Karlsson, Thor et al. 1990). Like other members in the LIM-homeodomain transcription factor family, ISL1 contains a pair of closely spaced N-terminal LIM domains followed by a central homeodomain (HD); in addition, ISL1 also contains a LBD domain (Figure 7) (Bhati, Lee et al. 2012). ISL1 binds DNA through its homeodomain while its LIM domains usually act as a protein-protein interaction motif (Karlsson, Thor et al. 1990, Bach 2000). LBD domain mediates the interaction of ISL1 with LIM-Homeodomain (LHX) proteins. For example, ISL1 interacts with LDB1 through its LIM domains and with LHX3 through its LBD domain, in the regulation of motor neurons specification (Gadd, Bhati et al. 2011). Although the LIM interaction domain of LDB1 (LDB1<sub>LID</sub>) and the LIM binding domain of ISL1 (ISL1<sub>LBD</sub>) share low levels of sequence homology, they bind LHX3 in an identical manner (Mugdha Bhati 2008). In addition, ISL1 LBD domain can also mediate an intramolecular interaction with LIM domains of ISL1 (ISL1<sub>LIM1+2</sub>), even though in a low affinity, to inhibit DNA binding, with inhibition being relieved by interaction of the LIM domains with another binding partner, such as LDB1<sub>LID</sub> (Figure 7) (Gadd, Jacques et al. 2013).

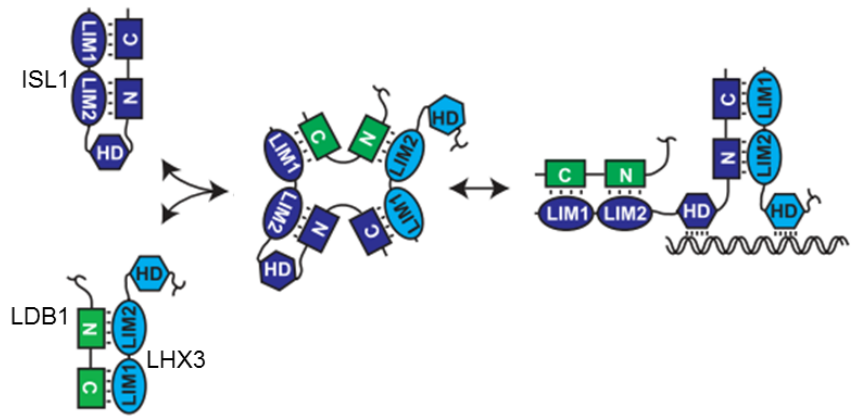
A



B



D



C

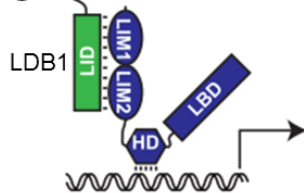


**Figure 7 Schematic diagram of ISL1 domains and the intermolecular and intramolecular interactions (adapted from (Bhati, Lee et al. 2012, Gadd, Jacques et al. 2013))**

(A) Diagram shows domains of mouse ISL1 protein. Numbers refer to the mouse proteins with the domain boundaries as defined in SWISS-PROT (Bhati, Lee et al. 2012). (B) The intramolecular interaction between ISL1<sub>LIM1+2</sub> and ISL1<sub>LBD</sub> could impose steric effects on the homeodomain, impacting DNA binding. (C) When LDB1<sub>LID</sub> binds ISL1, the intramolecular interaction is displaced, and this inhibition would be released. (D) Cofactor exchange mechanism. When ISL1 approaches the binary LDB1/LHX3 complex the intramolecular interaction between ISL1<sub>LIM1+2</sub> and ISL1<sub>LBD</sub> may facilitate the formation of an intermediate ternary complex in which the N- and C-terminal halves of ISL1<sub>LBD</sub> and LDB1<sub>LID</sub> contact different molecules to enable ISL1 to efficiently displace LDB1<sub>LID</sub>/LHX3<sub>LIM1+2</sub> and generate the ternary complex in a stepwise manner (Gadd, Jacques et al. 2013). HD: homeodomain; LBD: LIM binding domain; LID: LIM interaction domain; N and C: the N- and C-terminal halves of ISL1<sub>LBD</sub> and LDB1<sub>LID</sub> domains.

## 1.2.2 Expression and function of *Isl1* during development

Genetic studies have demonstrated that *Isl1* plays essential roles during embryogenesis. A better visualization of *Isl1* expression profile provides further insight into its potential roles during development. Previous studies have revealed expression of *Isl1* in multiple tissues and cell types, including normal adult islet cells (Karlsson, Thor et al. 1990), pancreas (Ahlgren, Pfaff et al. 1997), heart progenitor cells (Schoenwolf 2000, Cai, Liang et al. 2003, Sun, Liang et al. 2007), hindlimb (Yang, Cai et al. 2006), cochlear epithelium of the inner ear (Radde-Gallwitz, Pan et al. 2004), retina (Elshatory, Everhart et al. 2007), nervous system

(Samuel L. Pfaff 1996, Sun, Dykes et al. 2008), thyroid gland (Westerlund, Andersson et al. 2008) and so on.

Isl1 regulates gene expression by binding through its homeodomain to AT-rich consensus elements containing a core TAAT motif (YTAATGR) (Karlsson, Thor et al. 1990, Drucker 1995, Golzio, Havis et al. 2012). ISL1 is originally identified as a protein that binds to an insulin gene enhancer and regulates its expression (Karlsson, Thor et al. 1990). Initial experiments localized Isl1 to the islet cells, suggesting a possible role for this protein in the regulation of insulin gene expression and/or islet cell development (Karlsson, Thor et al. 1990, M Wang 1994). In pancreas, Isl1 is also expressed in the mesenchymal cells surrounding the dorsal lobe, and plays an important role in pancreas development (Ahlgren, Pfaff et al. 1997). Isl1 also functions as a positive regulator of proglucagon gene transcription in the endocrine pancreas (Drucker 1995). Later people found that Isl1 is also expressed in the central and peripheral nervous system (M Wang 1994, Zhuang, Zhang et al. 2013). It is required for the generation of motor neurons (Pfaff, Mendelsohn et al. 1996) and has essential roles in multiple aspects of motor neuron development, including motor neuron cell body localization, motor column formation and axon growth (Liang, Song et al. 2011). A recent study revealed a temporal requirement for Isl1 in multiple aspects of sympathetic neuron development (Zhang, Huang et al. 2018). In addition, Isl1 is also involved in the regulation of other cell types and organs, such as dentition (Mitsiadis 2003) and external genitalia (Ching, Infante et al. 2018). Importantly, more and more studies have determined that Isl1 is critical in heart development.

### **1.2.3 Expression and function of Isl1 during heart development**

With an Isl1-nlacZ mouse line and co-immunostaining for Isl1 and lineage markers, Sun et al. reported the detailed expression pattern of Isl1 in mouse heart (Sun, Liang et al. 2007) (Figure 8). They showed that Isl1 is expressed in distinct subdomains of the heart and in diverse cardiovascular lineages although Isl1 expression is downregulated in most cardiac progenitors as they differentiate (Sun, Liang et al. 2007), which is consistent with the earlier studies (Schoenwolf 2000, Cai, Liang et al. 2003). Cai et al. showed that Isl1 is detectable in the cardiac progenitor cells at the early cardiogenic crescent stages (around E7.0) (Cai, Liang et al. 2003). At this stage, *Isl1*-expressing cells are contiguous with, but medial and dorsal to, *Mlc2a*-expressing cells, which is one of the earliest markers for differentiated

cardiomyocytes (Cai, Liang et al. 2003) (Figure 8A). Studies demonstrate that *Isl1* expressing progenitors migrate into the heart shortly following fusion of cardiac primordia (Park, Ogden et al. 2006, Sun, Liang et al. 2007). At E8.5, *Isl1* is actively expressed in outflow tract and partially in the right atria and right ventricle, but not in the remaining myocardium (Figure 8B). By E9.0, most *Isl1* progenitors have migrated into the heart. *Isl1* is asymmetrically expressed in the right atria, and becomes progressively confined to a subdomain within the right atria, in the region of the cardiac pacemaker (Figure 8C-G). At E11.5 and E13.5, *Isl1* is observed in outflow tract and in the region of the sinoatrial (SA) and atrioventricular (AV) nodes. At E14.5, *Isl1*-nlacZ expression is still detected in subdomains within the outflow tract, aorta, pulmonary artery, venous valves, atrial septum, and in regions corresponding to those of the sinoatrial and atrioventricular nodes, and in clusters of cells in the region of cardiac ganglia (Figure 8G). At postnatal day 3, *Isl1*-nlacZ expression is observed in the region of the sinoatrial node (SAN) and at the base of the aorta/pulmonary artery, but less extensively, with the exception of cardiac ganglia which still exhibits strong expression (Sun, Liang et al. 2007). Moreover, they also showed that *Isl1* expressing cells not only contribute to myocardial lineages, but also contribute to endothelial and vascular smooth muscle lineages including smooth muscle of the coronary vessels by co-immunostaining of *ISL1* with MF20 (myosin heavy chain 1E, MYH1E), CD31 (also called platelet endothelial cell adhesion molecule, PECAM1) and  $\alpha$ -smooth muscle actin ( $\alpha$ -SMA) (Sun, Liang et al. 2007).

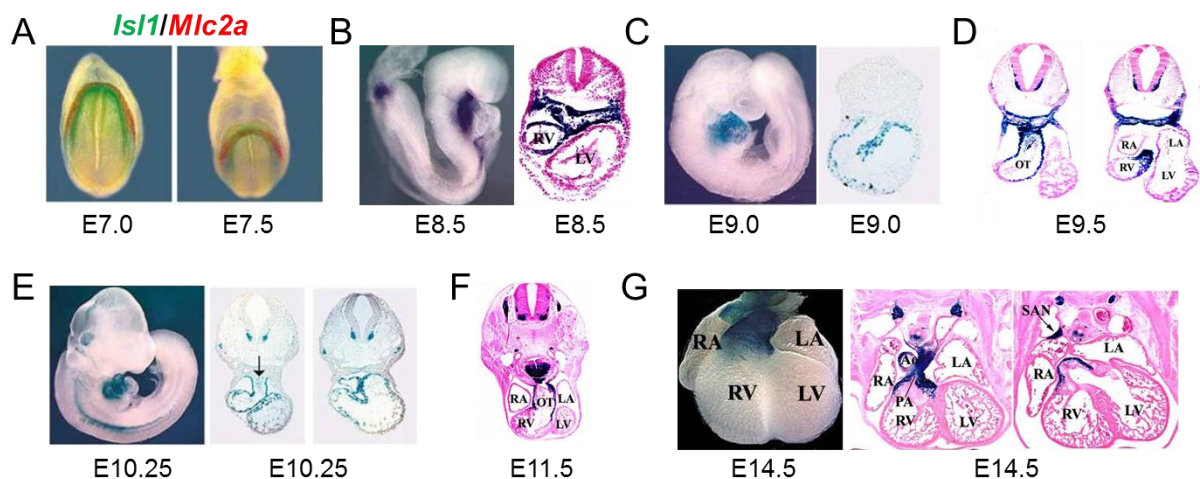


**Figure 8 *Isl1* expression profile in mouse heart (adapted from (Cai, Liang et al. 2003, Sun, Liang et al. 2007))**

**(A)** Embryos were stained with double whole-mount *in situ* hybridization, utilizing probes for *Isl1* (green) and *Mlc2a* (red) mRNAs at E7.0 and E7.5 (Cai, Liang et al. 2003). **(B-G)** Analysis of  $\beta$ -galactosidase expression in *Isl1*-nlacZ knock-in embryos using X-gal staining at E8.5-E14.5 and

representative corresponding sections. The arrow in (E) indicates X-gal-positive cells within the endocardium of the outflow tract (Cai, Liang et al. 2003, Sun, Liang et al. 2007). LA: left atria; LV: left ventricle; OT: outflow tract; RA: right atria; RV: right ventricle; PA: pulmonary artery; Ao: aorta; SAN: sinoatrial node.

In the course of cardiogenesis, *Isl1* marks the second heart field progenitors (Cai, Liang et al. 2003). The key role of *Isl1* in SHF development is evident from genetic studies in mice, showing that *Isl1*-deficient mouse embryos are embryonic lethal due to lacking of all structures derived from the SHF including the right ventricle, the outflow tract and large portions of the atria, since *Isl1* is required for proliferation, survival, migration of SHF CPCs and their differentiation into different cardiac lineages (Cai, Liang et al. 2003, Moretti, Caron et al. 2006, Kwon, Qian et al. 2009). *Isl1* was later shown to play a key role in survival, proliferation, and function of pacemaker cells as well (Liang, Zhang et al. 2015). In *Xenopus*, *Isl1* was reported to be necessary for heart morphogenesis, cardiac marker gene expression, and vasculogenesis (Brade, Gessert et al. 2007), whereas in zebrafish *isl1* is required to complete the cardiomyocyte differentiation process at the venous pole (de Pater, Clijsters et al. 2009).

*Isl1* is known to cooperate with other transcriptional factors such as *Gata4* and *Tbx20*, to regulate a cascade of transcriptional events involving its downstream target genes, such as *Mef2c*, *Myocd*, *Shh*, *Fgf10* and *Bmp4* that collectively control lineage specification of the cardiac progenitors (Dodou, Verzi et al. 2004, Vincent and Buckingham 2010, Golzio, Havis et al. 2012, Watanabe, Zaffran et al. 2012). In addition, *Isl1* also works in concert with other cofactors, such as epigenetic regulators and signaling molecules, in regulating cardiac development and cardiac lineage differentiation. For example, *Isl1* and *Ldb1* works together to orchestrate a network for transcriptional regulation and coordination in three dimensional space, driving cardiac progenitor cell differentiation and heart development (Caputo, Witzel et al. 2015). In addition, the LIM protein *Ajuba* binds *Isl1* and represses its transcriptional activity, which is required to downregulate the expression of key transcription factors in the SHF such as *Mef2c*, and to enable *Isl1* to suppress its own expression (Witzel, Jungblut et al. 2012). Pacheco-Leyva et al. reported that *Cited2* and *Isl1* interact physically and cooperate to promote embryonic stem cell (ESC) differentiation toward cardiomyocytes (Pacheco-Leyva, Matias et al. 2016). *Jmjd3* (Jumonji domain-containing protein 3) also physically interacts with *Isl1* to alter the cardiac epigenome,

instructing gene expression changes that drive cardiac differentiation (Wang, Li et al. 2016). These cofactors act together with Isl1 in a coordinated manner to keep the proper spatiotemporal regulation during cardiac differentiation and heart development. Despite the critical role of Isl1 in cardiac development and disease, detailed insights into its molecular mode of action are critically missing.

#### **1.2.4 ISL1 and CHD**

As a key transcription factor in regulating cardiac development, ISL1 is involved in congenital heart disease (CHD). Genetic variation in ISL1 is associated with risk of non-syndromic CHD has been revealed through a 2-stage case-control study in white and black/African American populations (Stevens, Hakonarson et al. 2010). This study identified eight genic and flanking ISL1 single nucleotide polymorphisms (SNPs) (rs6867206, rs4865656, rs6869844, rs2115322, rs6449600, IVS1+17C>T, rs1017, rs6449612) that are significantly associated with complex CHD (Stevens, Hakonarson et al. 2010). Later the same conclusion was shown and different ISL1 variants were found to be associated with CHD in a Chinese cohorts (Lang, Tian et al. 2013, Luo, Sun et al. 2014). The rs3762977 and IVS1+17C>T variants of ISL1 were identified to be closely associated with the risk of developing ventricular septal defects (VSD) through a study enrolled with 512 congenital VSD patients and 612 healthy controls (Lang, Tian et al. 2013). Another SNP (rs1017) in ISL1 contributes to the risk of CHD in Chinese Han people (Luo, Sun et al. 2014). In addition, a study among 389 infants born with tetralogy of Fallot (ToF) or d-transposition of the great arteries (d-TGA) found that ISL1 haploinsufficiency is associated with d-TGA (Osoegawa, Schultz et al. 2014). A recent study revealed a novel heterozygous ISL1 mutation (c.409G > T or p.E137X) that contributes to congenital heart defects, by analyzing a cohort of CHD patients and healthy controls (Ma, Wang et al. 2018).

### **1.3 Pioneer transcription factors**

A transcription factor (TF) is a protein that controls the rate of transcription of genetic information from DNA to messenger RNA, by binding to a specific DNA sequence (Karin 1990, Latchman 1997). The function of transcription factors is to regulate “turn on and off”-genes in order to make sure that they are expressed in the right cell at the right time and in the right amount throughout the life of the cell and the organism. Therefore, transcription

factors are responsible for the spatial and temporal fine-tuning of transcriptional programs. Although they recognize and bind to specific DNA sequences, the recruitment of transcription factors is also dependent on the chromatin landscape (Tanaka, Tawaramoto-Sasanuma et al. 2004). In eukaryotes, genomic DNA is tightly packaged into a higher order chromatin structure. Thus, chromatin structure becomes a general obstacle for eukaryotic transcription by blocking the access of the basic RNA polymerase machinery, as well as most transcription factors (Iwafuchi-Doi 2019). In the context of embryonic development and cell differentiation, many TFs initiate the assembly of transcriptional complexes at specific enhancers, which in turn trigger nucleosome repositioning so as to increase accessibility for other factors (Spitz and Furlong 2012). Biochemical and genomic studies indicate that such a group of factors can be considered “pioneers” by virtue of their ability to engage target DNA sites in closed chromatin prior to the apparent engagement, opening, or modification of the site by other factors (Iwafuchi-Doi and Zaret 2014). This “pioneer” function was first identified in yeast (Almer, Rudolph et al. 1986) and subsequently at the mouse albumin enhancer during endoderm development (Gualdi, Bossard et al. 1996, Bossard and Zaret 1998). And this subset transcription factors are called “pioneer transcription factors” or “pioneer factors” (Iwafuchi-Doi 2019) (Figure 9).

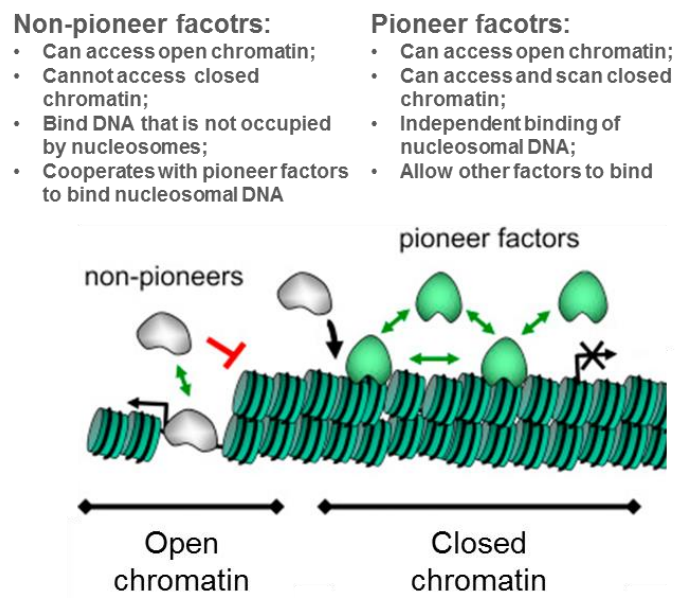


**Figure 9 Chromatin binding by pioneer factors (adapted from (Iwafuchi-Doi and Zaret 2016, Zaret, Lerner et al. 2016))**

Chromatin is depicted as consisting of open domains and closed domains. Pioneer factors (green blobs) are able to target the closed domains, whereas non-pioneer factors (gray blobs) are typically dependent upon pioneers for binding there (black arrow). The green arrows depict transient, on-and-



off association with chromatin as the factors scan the different domains; the red bars indicate the factors being impeded from scanning certain domains.

In recent years, more key transcription factors have been identified as pioneer transcription factors, such as FOXA (Forkhead box A), GATA1/2/3/4, OCT3/4 (Octamer-binding transcription factor 3/4), SOX2 (SRY (sex determining region Y)-box 2), KLF4 (Kruppel like factor 4), PAX7 (Paired box 7), ASCL1 (Achaete-scute family BHLH transcription factor 1), P53 (Tumor protein p53), and so on (Cirillo, Lin et al. 2002, Nili, Field et al. 2010, May, Soneji et al. 2013, Soufi, Garcia et al. 2015, Park, Guilhamon et al. 2017, Mayran, Khetchoumian et al. 2018). Although these pioneer factors belong to diverse structural classes of transcription factors and show different binding repertoires in different cell types, for example, SOX2 binds different target subsets in mouse cortex and spinal cord (Hagey, Zaouter et al. 2016), they have the common activities (Figure 10). Firstly, they scan the nucleosomal DNA in closed chromatin for their target sequences and then bind to their recognition sites (Iwafuchi-Doi and Zaret 2014, Iwafuchi-Doi and Zaret 2016, Iwafuchi-Doi 2019). The ability to target closed chromatin is based on the inherent capacity of pioneer factors to recognize their target DNA sequences on the nucleosome, either by full or partial motif recognition (Cirillo, McPherson et al. 1998, Iwafuchi-Doi and Zaret 2016).

The FOXA family of transcription factors has been most extensively studied in mechanistic depth by biochemical, genetic, and genomic studies. The binding domains of FOXA transcription factors possess a “winged helix” structure, which binds to one side of a DNA helix and leaves the other side of DNA to bind a nucleosome core particle (Clark, Halay et al. 1993, Cirillo, McPherson et al. 1998, Zaret, Caravaca et al. 2010). This structural similarity to linker histones H1/H5 allows FOXA transcription factors to access closed chromatin (Clark, Halay et al. 1993, Zaret, Caravaca et al. 2010). As the second step of pioneering activity, pioneer factors locally open chromatin structure and create a permissive state for gene regulation. In contrast to the chromatin binding step, the molecular mechanisms underlying the chromatin opening step remain to be determined for most pioneer factors. FOXA pioneer factors have the intrinsic ability to open chromatin by themselves as the C-terminal domain of FOXA can bind directly to core histone proteins and is required for opening chromatin (Cirillo, Lin et al. 2002). However, for some pioneer factors, they can recruit chromatin remodelers and achieve chromatin opening. For example, OCT4 recruits the

chromatin remodeler BRG1 and establishes accessible chromatin structure in pluripotent stem cells (King and Klose 2017). Once chromatin is open, pioneer factors can recruit cofactors (for example, transcription factors, chromatin modifiers, histone variants, and repressors) and allow their access to the site for gene and epigenetic regulation (Iwafuchi-Doi and Zaret 2014, Zaret and Mango 2016, Iwafuchi-Doi 2019).

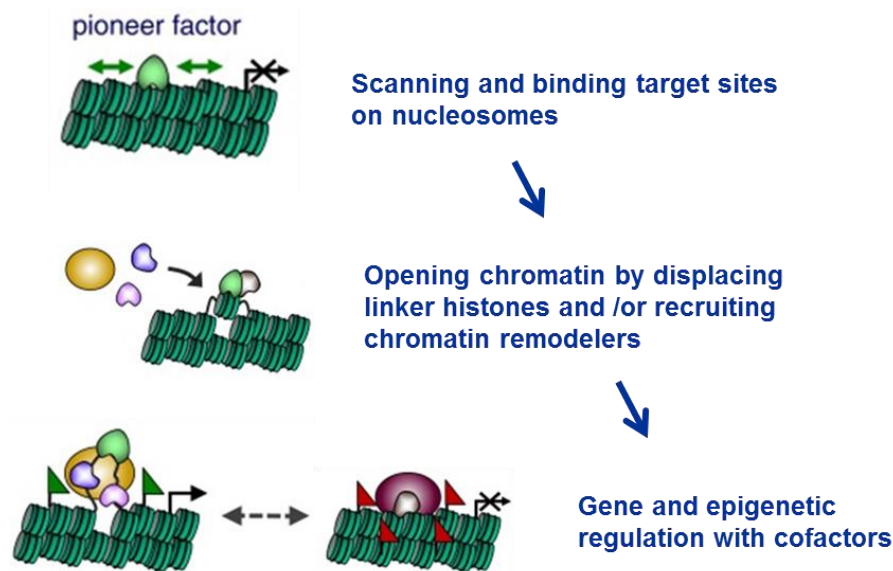


**Figure 10 Activities of pioneer factors (adapted from (Zaret and Mango 2016, Iwafuchi-Doi 2019))**

Pioneer factors can scan nucleosomal DNA for their target sites in closed chromatin (top). Opening chromatin and increased residence time at targeted sites allow for cooperative interactions with chromatin remodelers and more stable binding (middle). Binding of pioneer factors and cofactors can lead to activated sequences (bottom left) with open chromatin features (green flags) and a state of competence to be expressed or direct transcriptional activity, or repressed sequences (bottom right) with closed chromatin features (red flags).

In the context of embryonic development, pioneer factors start being expressed in the early stages and play a role in establishing competence for specific cell fates (Iwafuchi-Doi and Zaret 2014, Zaret and Mango 2016, Iwafuchi-Doi 2019). Genetics and genomics studies demonstrate the role of pioneer factors in cell programming and reprogramming. FOXA pioneer factors have the ability to specify liver fate by altering chromatin organization after binding nucleosomal target-DNA sequences (Cirillo, Lin et al. 2002). PAX7 specifies intermediate pituitary melanotrope cell identity through pioneer activity (Budry, Balsalobre et al. 2012). NeuroD1 (Neurogenic differentiation factor 1) and ASCL1 (also known as MASH1), have also been suggested to have pioneer activity during neural development (Wapinski, Vierbuchen et al. 2013, Pataskar, Jung et al. 2016). The three pluripotency factors

OCT4, KLF4 and SOX2 have pioneer activity on a global scale by widely affecting the epigenome beyond their initial binding sites (Soufi, Donahue et al. 2012, Soufi, Garcia et al. 2015). In addition, the aberrant activation or inhibition of pioneer factors can compromise large-scale chromatin structure and ultimately human health (Iwafuchi-Doi 2019). In many forms of cancer, pioneer factors are misregulated, mutated, or their genomic locus amplified; alternatively, the binding sites of pioneer factors are mutated (Jozwik and Carroll 2012). Although more key transcription factors have been identified as pioneer transcription factors, the molecular mechanisms behind their special properties are only beginning to be revealed (Iwafuchi-Doi 2019). Understanding the pioneering mechanisms will help us to precisely control cell fate for research and therapeutic purposes.

## **1.4 Epigenetic regulation**

### **1.4.1 Chromatin structure**

In the nucleus of eukaryotes, DNA is packaged as chromatin. The nucleosome is the fundamental unit of chromatin and it is composed of an octamer of the four core histones (H2A, H2B, H3 and H4,) around which 147 base pairs of DNA are wrapped (Kouzarides 2007). Each of the histone proteins consists of a structured core and an unstructured tail domain. These histone tails are the most common sites of post-translational modifications (Biswas, Voltz et al. 2011). H1 histone associates with the linker DNA located between the nucleosomes. Nucleosome spacing determines chromatin structure, which can be broadly divided into “closed chromatin” and “open chromatin” (Figure 11). “Closed chromatin” is condensed and usually associated with relative transcriptional repression. In contrast, “open chromatin” is a state which allows proteins governing transcription to access the DNA and effect RNA synthesis (Gillette and Hill 2015). Chromatin structure and gene accessibility to transcriptional machinery are regulated by modifications to both DNA and histone tails (Handy, Castro et al. 2011).

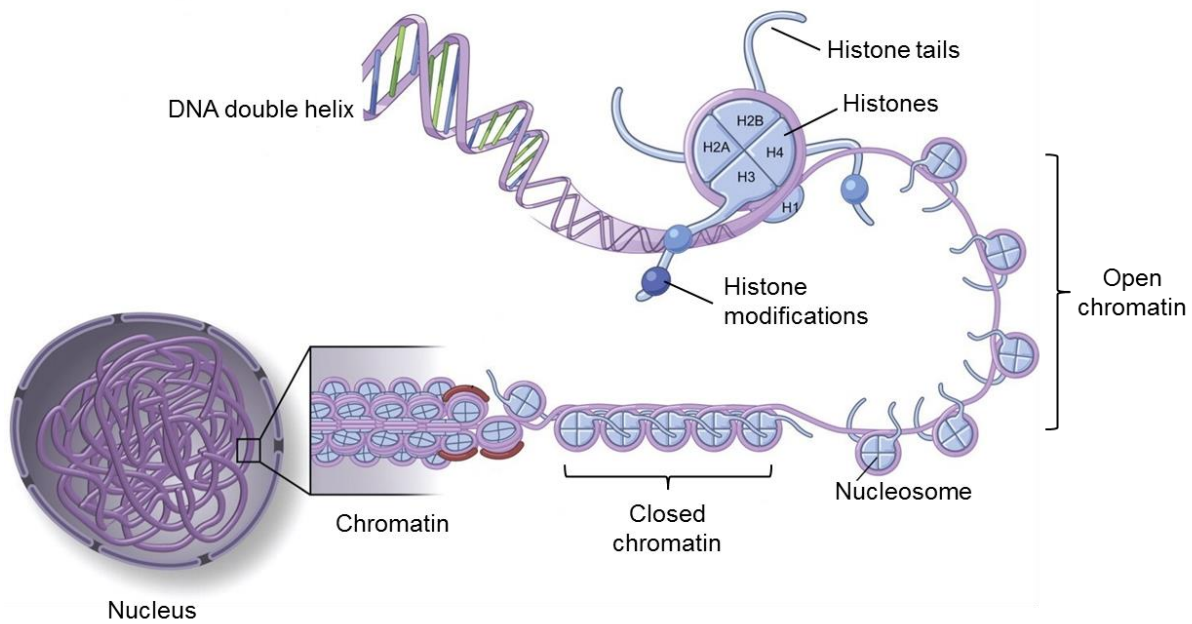


**Figure 11 Schematic representation shows the organization and packaging of genetic materials (adapted from (Yan, Matouk et al. 2010))**

Schematic diagram shows different levels of chromatin compaction. DNA is wrapped around a cluster of histone proteins to form nucleosomes. Nucleosome is represented by DNA wrapped around eight histone proteins, H2A, H2B, H3, and H4. H1 serves as a linker protein. Histone tails are shown protruding from histone proteins and histone modifications are shown with round balls. Nucleosomes are further organized to create open and closed regions of chromatin, which in turn create three-dimensional structures that encompass different levels of gene organization in the chromosomes packed into a cell nucleus.

### 1.4.2 Epigenetic control mechanisms

In 1940s, Waddington first proposed the term “epigenetics” by combining the words “epigenesis” and “genetics”, which was defined as the study of heritable changes in gene expression, that are not a result of changes in the DNA sequence, but rather due to alterations related to the packaging (thereby altering DNA accessibility) and/or translation of genetic information (Morris 2001, Bird 2007, Goldberg, Allis et al. 2007, Lorenzen, Martino et al. 2012, Vallaster, Vallaster et al. 2012). Over the past decade, epigenetics has become an important and rapidly expanding field of research in Biology (Portela and Esteller 2010, Ponchel and Burska 2016). Chromatin structure can be dynamically regulated by three classes of chromatin regulators: DNA methylation (Me) by DNA modifiers, histone modification by histone modifiers, and chromatin organization by chromatin remodelers (Chang 2012). They are reported in a lot of publications to play a central role in various biological processes, including stem cell fate decision (Lunyak and Rosenfeld 2008), cell

proliferation and differentiation (Srinageshwar, Maiti et al. 2016, Marroncelli, Bianchi et al. 2018), embryonic development (Hemberger, Dean et al. 2009) and diseases (Portela and Esteller 2010). Here I only focus on the chromatin organization by chromatin remodelers.

#### **1.4.2.1 Chromatin remodelers**

Chromatin remodeling is widely used to describe changes in chromatin structure that occur during regulatory processes (Aalfs and Kingston 2000). It can occur independently or in concert with other events, such as transcription (Aalfs and Kingston 2000). The complexes that relocate nucleosomes or alter the structure of nucleosomes are called “chromatin remodelers” or “chromatin remodeling complexes”.

The chromatin remodeling complexes are primarily made up of a single ATPase and multiple associated subunits (Hota and Bruneau 2016). The core catalytic subunit is the ATPase subunit. On the basis of the sequence and structure of the core ATPase subunit, the ATP-dependent chromatin remodeling complexes are divided into four major subfamilies (Figure 12A): ISWI (imitation switch), CHD (chromo domain helicase DNA-binding), INO80 (inositol requiring 80)/SWR (SWI2/SNF2 related), and SWI/SNF (switch/sucrose non-fermentable) subfamilies (Ho and Crabtree 2010, Mazina and Vorobyeva 2016, Clapier, Iwasa et al. 2017). With energy derived from ATP hydrolysis, these complexes work on chromatin remodeling in a variety of ways (Figure 12B): (A) nucleosome assembly: factors, especially those belonging to the ISWI and CHD subfamily remodelers, participate in the random distribution of newly formed nucleosomes, as well as their maturation and arrangement into regularly-spaced chromatin structures; (B) Chromatin access: factors that mainly belong to the SWI/SNF family mediate DNA accessibility by repositioning nucleosomes, ejecting octamers or evicting histone dimers; (C) Nucleosome editing: factors of the INO80 subfamily change nucleosome composition by exchanging canonical and variant histones (like H2AZ).

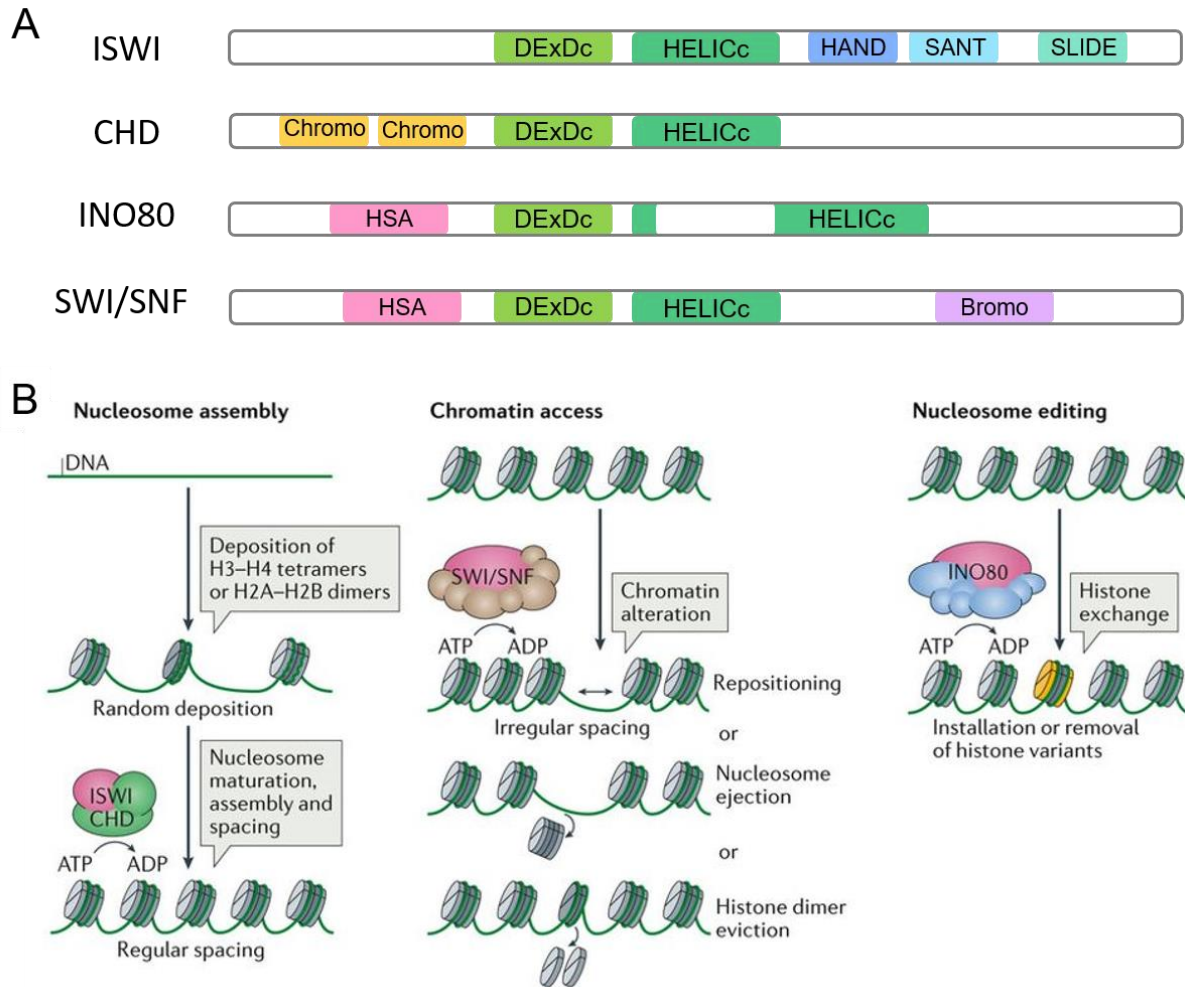


**Figure 12 Domain structure of the core ATPase subunits and functional classification of the chromatin remodeling complexes (adapted from (Manelyte and Langst 2013, Hota and Bruneau 2016, Clapier, Iwasa et al. 2017, Sokpor, Castro-Hernandez et al. 2018))**

**(A)** Diagram shows the domain organization of the catalytic subunits of ISWI, CHD, INO80/SWR and SWI/SNF subfamilies of chromatin remodelers. All of these subunits are SNF2 family proteins. They all contain an ATPase domain, which consists of DEXDc and HELICc domains, with each subfamily possessing additional domains. For example, ISWI proteins harbor a C-terminal SANT domain as well as SANT-like ISWI (SLIDE) and HAND domains. CHD proteins are defined by the presence of tandem N-terminal chromo domains, with some family members containing N-terminal plant homeodomain (PHD) domains. INO80R/SWR proteins notably contain a split ATPase domain, with a spacer between the DEXDc and HELICc domains. By contrast, SWI/SNF proteins are defined by the presence of an N-terminal helicase-SANT (HSA) domain and a C-terminal bromo domain. Image is adapted from (Manelyte and Langst 2013, Hota and Bruneau 2016). **(B)** Summary of the ways of actions of chromatin remodelers. The core ATPase subunits are depicted in pink; additional subunits in different complexes are depicted in green, brown and blue, respectively. Image is adapted from (Clapier, Iwasa et al. 2017, Sokpor, Castro-Hernandez et al. 2018). In addition, to avoid of confusion, “CHD” represents “chromo domain helicase DNA-binding” only in 1.4.2.1 part, whereas in the other parts of this thesis, “CHD” refers to “congenital heart disease”.

### **1. The ISWI subfamily remodeling complex**

The ISWI subfamily of remodeling complexes contains one catalytic subunit and one or more accessory subunits. In mammals, the core ATPase subunit of this complex is SNF2H or SNF2L. They are functionally distinct and are found in different complexes, as distinguished by their accessory subunits. SNF2L is present in the NURF (nucleosome remodeling factor) and CERF (CECR2-containing remodeling factor) complexes, whereas SNF2H is present in the NoRC (nucleolar remodeling complex), WICH (WSTF ISWI chromatin remodeling complex), ACF (chromatin-assembly factor), RSF (remodeling and spacing factor) and CHRAC (chromatin accessibility complex) complexes (Hota and Bruneau 2016, Sokpor, Castro-Hernandez et al. 2018). NURF complexes and NoRC are involved in transcriptional activation and repression. By contrast, ACF, CHRAC and WICH complexes are required for the regulation of chromatin structure (including nucleosome assembly and spacing), the replication of DNA through heterochromatin and the segregation of chromosomes (Dirscherl and Krebs 2004, Ho and Crabtree 2010).

### **2. The CHD subfamily remodeling complex**

The CHD subfamily of chromatin remodeling complexes contains core ATPase subunits of CHD proteins, which comprises nine chromo domain containing members (Figure 12). These CHD proteins are subdivided into 3 groups according to their structural properties. Group I of CHD proteins contain CHD1 and CHD2. They can act as monomeric units to directly regulate chromatin and transcription (Sokpor, Castro-Hernandez et al. 2018). CHD3 and CHD4 are members of Group II of CHD proteins. They are core catalytic components (ATPases) of the nucleosome remodeling deacetylase NuRD complex, which contain histone deacetylases (HDACs) and function as transcriptional repressors (Ho and Crabtree 2010). Group III CHD proteins contain CHD5-9, in which CHD7 is the most extensively studied one. Mutations in *CHD7* result in CHARGE syndrome in humans, which is characterized by coloboma of the eyes, heart defects, choanal atresia, severe retardation of growth and development, and genital and ear abnormalities (Vissers, van Ravenswaaij et al. 2004).

### **3. The INO80 remodeling complex**

The INO80/SWR complexes are characterized by the presence of a conserved split ATPase domain (Figure 12). Similar with the other remodeling complexes, they also contain core

ATPase subunits and some associated subunits. In mammals, the core catalytic subunits include INO80, P400 and SRCAP (homologues of yeast SWR1). They work together with other subunits to play a role in different biological processes, such as transcriptional regulation and DNA damage repair (Ho and Crabtree 2010).

#### **4. The SWI/SNF remodeling complex**

The SWI/SNF subfamily is one of the most-studied subfamilies of chromatin remodeling complexes. It is conserved from yeast to mammals. In mammals, SWI/SNF complexes are known as brahma-associated factor (BAF) complexes. The ATPase subunit of BAF complex is encoded by two homologs, BRM (Brahma) and BRG1 (brahma-related gene 1), and only one of them is present in each complex, which gives rise to a diversity of stable assemblies that differ between cell types and that have distinct functions (Wang, Xue et al. 1996, Lessard, Wu et al. 2007). BRG1 and BRM are associated with different promoters during cellular proliferation and differentiation, and in response to specific signaling pathways by preferential interaction with certain classes of transcription factors. They may direct distinct cellular processes by recruitment to specific promoters through protein-protein interactions that are unique to each ATPase (Kadam and Emerson 2003).

In addition to the core ATPase unit BRG1/BRM, BAF complex contains a lot of associated subunits. The BAF complex composition undergoes progressive changes during the process of development and in different cell types (Wang, Xue et al. 1996, Lessard, Wu et al. 2007) (Figure 13). For example, the BAF complex in mouse embryonic stem cell (ESC), called esBAF, is defined by the presence of BRG1 but not BRM, and BAF155 but not BAF170 (Ho, Ronan et al. 2009). It is essential for ESC self-renewal and pluripotency, and is a critical component and regulator of the core transcriptional network of ES cells (Ho, Jothi et al. 2009, Ho, Ronan et al. 2009). When ESCs differentiate into neuronal progenitors, the esBAF complex undergoes several subunit exchanges: it incorporates BRM and excludes BAF60B, which is now called npBAF, to differentiate it from the BAF complexes in other cell types. As neural progenitors exit the cell cycle, the BAF45a/53a subunits, which are necessary and sufficient for neural progenitor proliferation, are replaced by the homologous BAF45b, BAF45c, and BAF53b. Preventing the subunit switch impairs neuronal differentiation, indicating that this



molecular event is essential for the transition from neural stem/progenitors to postmitotic neurons (Lessard, Wu et al. 2007).

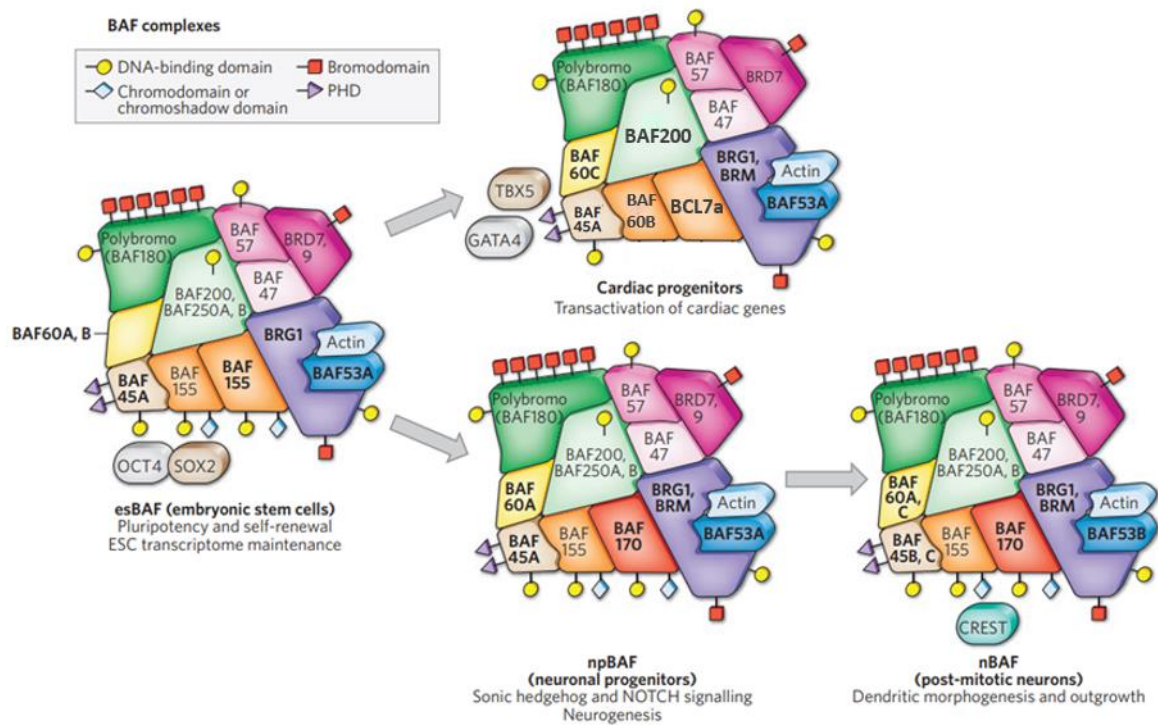


**Figure 13 Tissue/cell-type-specific assemblies of BAF complexes (adapted from (Ho and Crabtree 2010))**

Schematic diagram shows the tissue/cell-type specific subunits of BAF complexes. All of the subunits form the whole complex by occupying specific positions, as in a jigsaw puzzle. The domains that enable the subunits to interact with DNA are depicted at the surface of each protein. The BAF complex in embryonic stem cells (ESCs) is called esBAF; in neuronal progenitors, npBAF; and in neurons, nBAF. In cardiac progenitors, the composition of the BAF complex is also distinct and recently is characterized by proteomic analysis (Hota, Johnson et al. 2019), unlike the other BAF complexes shown. In some cases, key transcription factors that work in cooperation with BAF complexes (such as OCT4 and SOX2 in ESCs, CREST in neurons and GATA4 and TBX5 in cardiac progenitors) are depicted.

Recently, using immunoprecipitation with mass spectrometry, Hota et al. determined the dynamic composition of BAF complexes during mammalian cardiac differentiation, identifying several cell-type specific subunits. For example, ESC-derived BRG1 complexes were enriched for BRD9, GLTSCR1L, BCL7B/C, BAF155 and BAF60A, consistent with previous reports (Kidder, Palmer et al. 2009, Ho and Crabtree 2010, Kadoch and Crabtree 2013), while BRG1 partners in mesoderm (PDE4D, CRABP2, ARID1B), cardiac progenitor cells (BAF60B/C, POLYBROMO-1, BAF200, BAF47, BCL7A, BRD7, and BAF45A) and cardiomyocytes stages (BAF170, BAF60C, BAF57, SS181, BAF45C, WDR5, and CC2D1B) were also identified (Hota,

Johnson et al. 2019). There is a fine balance in the composition of the BAF complex, and perturbation of one subunit extends to the association of other subunits in the complex, and different subunits or isoforms substitute for the absence of one or more subunits, for example, both BAF60A and BAF60B substitute for the lack of BAF60C, and depletion of BAF45C is balanced by enrichment of BAF45A, which indicating that subunit switching and substitution in BAF complex composition could be an important mechanism in cardiac lineage specification (Hota, Johnson et al. 2019).

Tissue-specific BAF complexes have been reported to interact with a variety of transcription factors in different cell types, allowing the complexes to take on context-dependent functions arising from their different interaction partners (Ho and Crabtree 2010). For example, ectopic expression of Baf60c but not Baf60a, in coordination with the transcription factors Gata4 and Tbx5, is sufficient to induce the development of beating cardiomyocytes from non-cardiogenic mesoderm in the developing embryos (Takeuchi and Bruneau 2009). BAF complexes can function as both transcriptional activators and repressors and can even switch between these two modes of action at the same gene (Chi, Wan et al. 2003, Ho and Crabtree 2010).

#### 1.4.2.2 Roles of BAF complex in cardiac development and diseases

BAF complex components are essential for multiple stages of cell differentiation during heart development, for heart formation and postnatal heart function (Figure 14) (Hota and Bruneau 2016). Among all the subunits in BAF complex, BRG1 and BAF60C, in particular, have crucial roles in multiple transcriptional regulatory pathways.

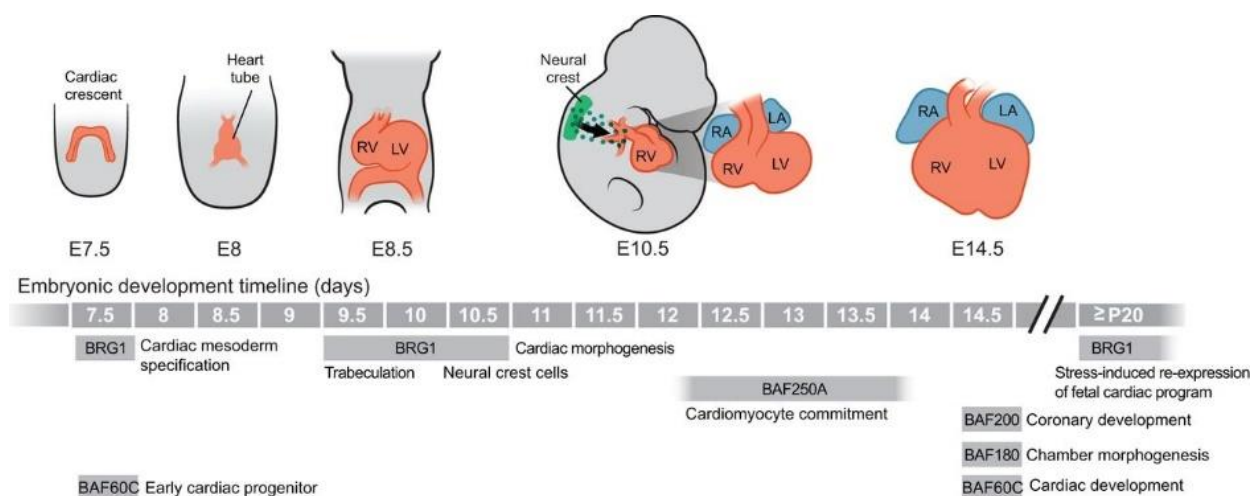


**Figure 14 Roles of BAF chromatin remodeling complex in heart development (adapted from (Hota and Bruneau 2016))**

Stages of mammalian heart development are pictured, with mouse embryonic day (E) indicated below. Key demonstrated roles for specific chromatin-remodeling factors are positioned at relevant stages below the developmental timeline. LA, left atrium; LV, left ventricle; RA, right atrium; RV, right ventricle.

*Brg1*, also known as *Smarca4*, is ubiquitously expressed in the developing mouse embryos from unfertilized egg, two-cell, four-cell, morula, and blastocyst stages (Bultman, Gebuhr et al. 2000, Singh, Foley et al. 2017). *Brg1* is highly expressed in mouse embryos and is downregulated in adult cardiomyocytes (Chang 2012). *Brg1* homozygous (*Brg1*<sup>-/-</sup>) mouse die during the peri-implantation stage of development (Bultman, Gebuhr et al. 2000). In contrast, heterozygous loss of *Brg1* in mouse results in dilated and disorganized ventricles, ventricular septal defects (VSDs) and a double outlet right ventricle, anomalies that resemble human congenital heart defects, indicating that *Brg1* is haploinsufficient in mouse heart (Takeuchi, Lou et al. 2011).

In the developing mouse heart, *Brg1* is critical for cardiac morphogenesis and regulation of cardiac gene expression programs. During cardiac differentiation, *Brg1* is essential for modulating active and repressive chromatin states during mesoderm lineage commitment, in particular the activation of developmentally important enhancers (Alexander, Hota et al. 2015). *Brg1* is also a crucial regulator of cardiomyocyte gene expression and differentiation, and its dosage is critical during mouse and zebrafish heart development (Takeuchi, Lou et al. 2011, Hota, Johnson et al. 2019). In mouse embryos, *Brg1* represses the expression of *Adamts1* in the endocardium and endocardial specific loss of *Brg1* leads to trabeculation defects (Stankunas, Hang et al. 2008). Moreover, *Brg1* deletion in the myocardium leads to thin compact myocardium and fails to form an interventricular septum (Hang, Yang et al. 2010). It was further shown that *Brg1* promotes myocardial cell proliferation by maintaining *Bmp10* and suppressing *p57<sup>kip2</sup>* expression in mouse embryos (Hang, Yang et al. 2010). In addition, *Brg1* is required for the formation and differentiation of neural crest cells (NCCs), which are essential for the formation of pharyngeal arch arteries and the cardiac outflow tract. *Brg1* maintains a NCC progenitor pool by promoting proliferation and inhibiting apoptosis, facilitates NCC maturation to vascular smooth muscle cells and regulates neural crest cell migration to the outflow tract (Wei Li, Yiqin Xiong et al. 2012).

Baf60c, also called Smarcd3, is a subunit of BAF complex. *Baf60c* is initially restricted to the developing heart, as early as E7.5. In the looping heart tube (E8.5-E9.0), *Baf60c* expression is more pronounced at the poles of the heart, which will give rise to the outflow tract anteriorly and to the atria posteriorly. *Baf60c* is also expressed in myotome of somites, dorsal neural tube, and limb bud mesenchyme from E9.5 onwards (Lickert, Takeuchi et al. 2004). *Baf60c* is highly expressed in the heart at the early stages of embryonic development but gradually downregulated at the postnatal stages (Nakamura, Koshiba-Takeuchi et al. 2016). Mouse embryos with reduced levels of *Baf60c* showed defective cardiac differentiation and severe heart defects including outflow tract defects, impaired trabecular formation and hypoplastic atrium and right ventricle (Lickert, Takeuchi et al. 2004). Conditional deletion of *Baf60c* in cardiomyocytes resulted in postnatal dilated cardiomyopathy with impaired contractile function (Sun, Hota et al. 2017).

BAF complexes orchestrate many aspects of heart development, and genetically interact with cardiac transcription factors to finely modulate cardiac gene expression (Hang, Yang et al. 2010, Takeuchi, Lou et al. 2011). Congenital heart defects in humans can result from haploinsufficiency of transcription factors such as TBX5, NKX2.5, and GATA4 (Bruneau 2008). Brg1 interacts with these factors to regulate cardiac gene expression and Baf60c can enhance interactions between transcription factors and Brg1, at least when overexpressed in cell culture, suggesting that Baf60c may function as a bridge between the BAF complex and select cardiac transcription factors (Lickert, Takeuchi et al. 2004, Wang 2012). Genetically, Brg1 interacts with cardiac transcription factors in a dose-dependent manner to regulate heart development in mice and disrupting the balance between Brg1 and disease-causing cardiac transcription factors, including Tbx5, Tbx20 and Nkx2.5, causes severe cardiac anomalies (Takeuchi, Lou et al. 2011). Baf60c, together with the cardiac transcription factors Tbx5, Nkx2.5 and Gata4, can induce non-cardiac mesoderm to differentiate into cardiomyocytes, suggesting that Baf60c may have a central function in the specification of cardiac fate in addition to its later role in cardiac morphogenesis (Takeuchi and Bruneau 2009, Wang 2012).

Targeting subunits and domains of chromatin remodelers is currently being evaluated as a therapeutic strategy in the prevention and treatment of human diseases. Chromatin remodelers harbor epigenetic reader domains that may serve as novel drug targets (Längst

and Manelyte 2015). JQ1 molecule, inhibiting BRD4 protein through its bromo domain, was the first discovered inhibitor, which is already in clinical trials (Delmore, Issa et al. 2011, Längst and Manelyte 2015). Brm and Brg1 bromo domains are also potentially drugable with specific Pfi-3 inhibitor (<http://www.thesgc.org>) (Längst and Manelyte 2015). Moreover, HDACs and PARP1, which interact with Brg1, are therapeutic targets for cardiac hypertrophy, as pharmacological inhibition of their activities or genetic mutations of class I HDACs and PARP1 in mice reduce hypertrophy. Upregulation of Brg1 is observed in heart tissues obtained from patients with hypertrophic cardiomyopathy, and the level of Brg1 upregulation correlates strongly with the severity of hypertrophy and MHC switch (Hang, Yang et al. 2010). Deletion of Brg1 in adult hearts which prevents stress-induced Brg1 reactivation, reduces cardiac hypertrophy, abolishes cardiac fibrosis, and reverses the pathological MHC switch (Chang 2012), indicating that Brg1-based BAF complex may act as a target for treating cardiac hypertrophy and failure.

## 2. Objectives

The work on *Isl1* described in the introduction has demonstrated that *Isl1* is crucial for early heart development. However, still many questions remain. In this study, we want to address the following questions regarding the role of *Isl1* in second heart field (SHF) development:

### **1. What is the genome wide binding profile of *Isl1* during cardiogenesis? What are *Isl1* primary downstream targets in a genome-wide view during SHF development?**

To elucidate the role of *Isl1* in greater details during SHF development, we firstly want to investigate the downstream targets of *Isl1*. To achieve this aim, we selected the mESC-based *in vitro* cardiac differentiation approach and *Isl1* knockout mouse as model systems. mESC-based *in vitro* cardiac differentiation strategy offers a powerful tool to generate large amount of cardiac progenitor cells with high homogeneity and makes it easier to observe cardiac differentiation at different time points. Moreover, *Isl1* knockout mouse lines help us to explore the regulatory network of *Isl1* *in vivo*. Furthermore, ChIP-Seq can help us to identify the genome wide binding profile of *Isl1* during cardiogenesis. In combination of RNA-Seq and ChIP-Seq techniques, we hope to identify *Isl1* directly regulated downstream targets during cardiogenesis in a genome-wide view.

### **2. What is the role of *Isl1* in epigenetic regulation during SHF development?**

After identifying the transcriptional regulatory network of *Isl1*, our next aim is to investigate how these genes are regulated? Transcriptional regulation is associated with chromatin landscape. Pioneer transcription factors are capable of reorganizing the chromatin state and play critical roles in cell fate control during embryonic development (Zaret and Mango 2016). As a transcription factor, we hypothesize that *Isl1* could function as a pioneer factor in regulating SHF development. To investigate whether *Isl1* acts as a pioneer factor and the role of *Isl1* in epigenetic regulation during SHF development, we plan to use biochemical and molecular approaches in this study. Co-immunoprecipitations can help to identify *Isl1* working partners in this process. ATAC-Seq combined with ChIP-Seq analysis in both mESC-derived CPCs and embryonic tissues should be possible to clarify the role of *Isl1* in organizing chromatin landscape at its target sites.

Altogether, we hypothesize that *Isl1* could work as a pioneer factor to reshape the chromatin landscape in regulating a transcriptional gene network during SHF development.

### 3. Results

#### 3.1 *Isl1* regulates cardiogenesis in CPCs by directly targeting a large group of downstream targets

##### 3.1.1 Generation of *Isl1* KO ESC line

To investigate the role of *Isl1* during cardiogenesis using the cell culture system, we generated a mouse embryonic stem cell (mESC) line with *Isl1* deletion using CRISPR-Cas9 technique. Gene editing was done in *Nkx2.5*-GFP mESC line (Wu, Fujiwara et al. 2006, Hsiao, Yoshinaga et al. 2008) which expresses GFP specifically in cardiac progenitor cells and later in cardiomyocytes, driven by a cardiac-specific enhancer together with a *Nkx2.5* base promoter (Figure 15A-B). This allows us to check cardiac differentiation efficiency and sort cardiac progenitor cells and cardiomyocytes by flow cytometry. Exons 1-4 of *Isl1* were deleted, covering the LIM1, LIM2 and Homeodomain (HD) of ISL1 protein. The knockout (KO) efficiency was checked by Western blot which showed *Isl1* is efficiently deleted (Figure 15C).

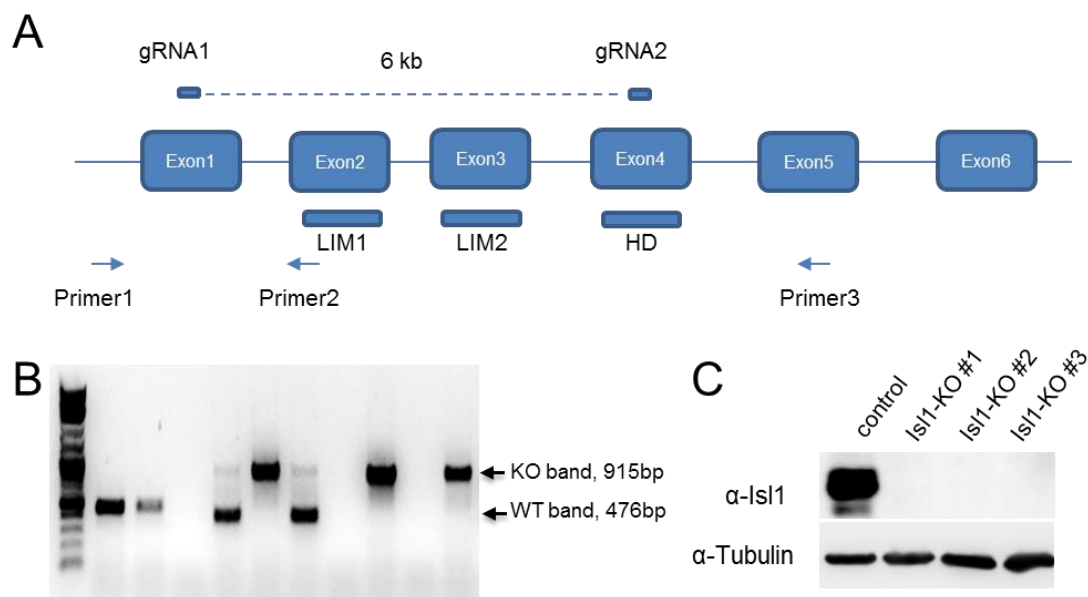


**Figure 15 Generating *Isl1* KO ESC lines by CRISPR-Cas9 technique**

(A) Strategy for generating *Isl1* KO ESC lines by CRISPR-Cas9 technique. Exons 1-4 were deleted by guide1 and guide2 and primers 1-3 were used for genotyping. (B) Genotyping of *Isl1* KO lines by PCR. KO band is 915bp amplified by primers1 and 3 and WT band is 476bp amplified by primers1 and 2. (C) Western Blot to check *Isl1* knockout efficiency in CPCs.  $\alpha$ -Tubulin was used as loading control.

### 3.1.2 Establishing *in vitro* mESC-based cardiac differentiation protocol

Embryonic stem cells (ESCs) are pluripotent which can undergo differentiation *in vitro* to generate derivatives of the three primary germ layers and hence potentially all the cell types present in the body. In most cases, the *in vitro* differentiation recapitulates the stepwise stages of embryological development for the cell types of interest. To explore the role of *Isl1* during cardiac differentiation, we used a directed differentiation method of mESCs into cardiomyocytes in which the mesoderm (MES), cardiac progenitor cells (CPCs), and cardiomyocytes (CMs) were sequentially induced (Figure 16A) (Kattman, Witty et al. 2011, Wamstad, Alexander et al. 2012) as a model system. In this protocol, ESCs were aggregated in petri dishes and cultured for 2 days in the absence of exogenous factors (days 0-2), subsequently treated with Activin A, BMP4, and VEGF for 40 hours to induce mesoderm under serum-free conditions (days 2-3.7), and then dissociated to a monolayer culture to differentiate into CPCs and CMs (days 3.7-10) under the induction of VEGF, bFGF and FGF10 (Figure 16A). This directed cardiac differentiation protocol efficiently specified ESCs into mesoderm, CPCs and CMs at specific stages. By this system we can get roughly 75% cardiac progenitors at day5 (GFP positive cells; Figure 16B-C) and cardiomyocytes at day10 (Wamstad, Alexander et al. 2012).

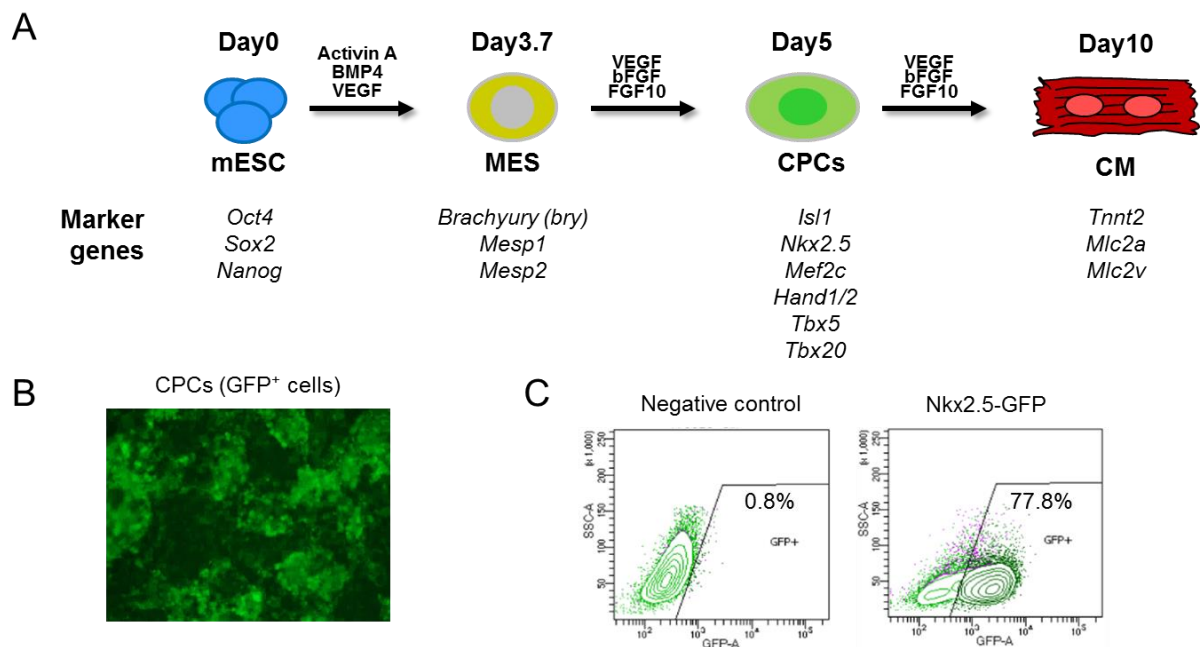


**Figure 16 Characterization of directed cardiac differentiation of mouse ESCs**

**(A)** Schematic representation of the differentiation process and timeline of directed CM differentiation protocol and stage collection. **(B)** Fluorescent images of day5 cultures for Nkx2.5-GFP reporter line. **(C)** Flow cytometry analysis of GFP positive cells in negative control (E14 line) and



Nkx2.5-GFP lines (GFP transgenic line with E14 background) at day5. mESCs: mouse embryonic stem cells; MES: mesoderm cells; CPCs: cardiac progenitor cells; CM: cardiomyocytes.

Based on marker gene expression analysis (Figure 17A-D), we picked four stages of differentiation that represent key cell types in the transition from pluripotent cells to cardiomyocytes: undifferentiated embryonic stem cells (ESCs) expressing pluripotency genes (*Oct4*, *Sox2* and *Nanog*), cells expressing mesodermal markers (*Brachyury*, *Mesp1* and *Mesp2*) (MES), cells expressing cardiac transcription factors (*Nkx2.5*, *Isl1*, *Mef2c*, *Hand1/2* and *Tbx5/20*) but not yet beating (CPCs), and functional cardiomyocytes (CMs) with CM-specific gene expression (*Tnnt2*, *Mlc2a* and *Mlc2v*).

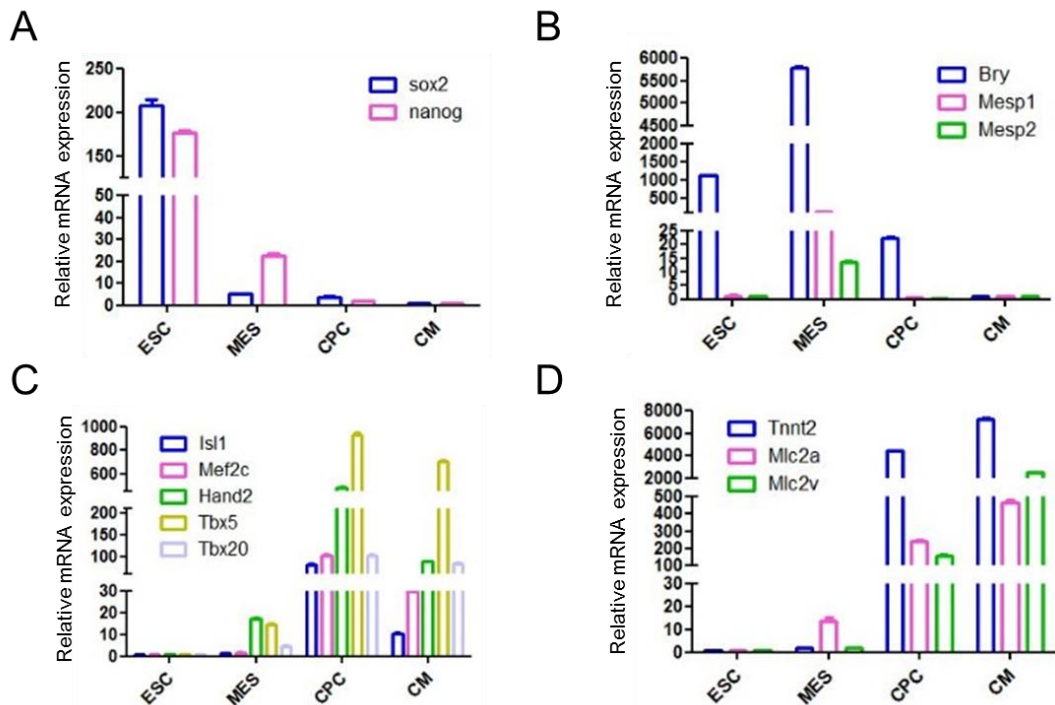


**Figure 17 Marker gene expression analyses at different stages of cardiac differentiation**

Marker genes expression measured by qPCR throughout directed cardiac differentiation protocol: (A) ESC markers; (B) MES markers; (C) CPC markers; and (D) CM marker genes.

### 3.1.3 *Isl1* KO ESC lines can differentiate into CPCs

To check whether our *Isl1* KO (*Isl1*<sup>-/-</sup>) lines generated with CRISPR-Cas9 technique can differentiate properly, we performed the directed cardiac differentiation and harvested cells at cardiac progenitor stage for fluorescence-activated cell sorting (FACS) and qPCR analysis (Figure 18). We can get around 60% GFP positive cells at day5 and *Isl1* depletion did not

change the number of CPCs (Figure 18B). As expected, loss of *Isl1* led to downregulation of known *Isl1* target genes (Figure 18C). These results suggest that our *Isl1* KO ESC lines are successfully generated and they can differentiate into cardiac progenitors by *in vitro* cardiac differentiation.

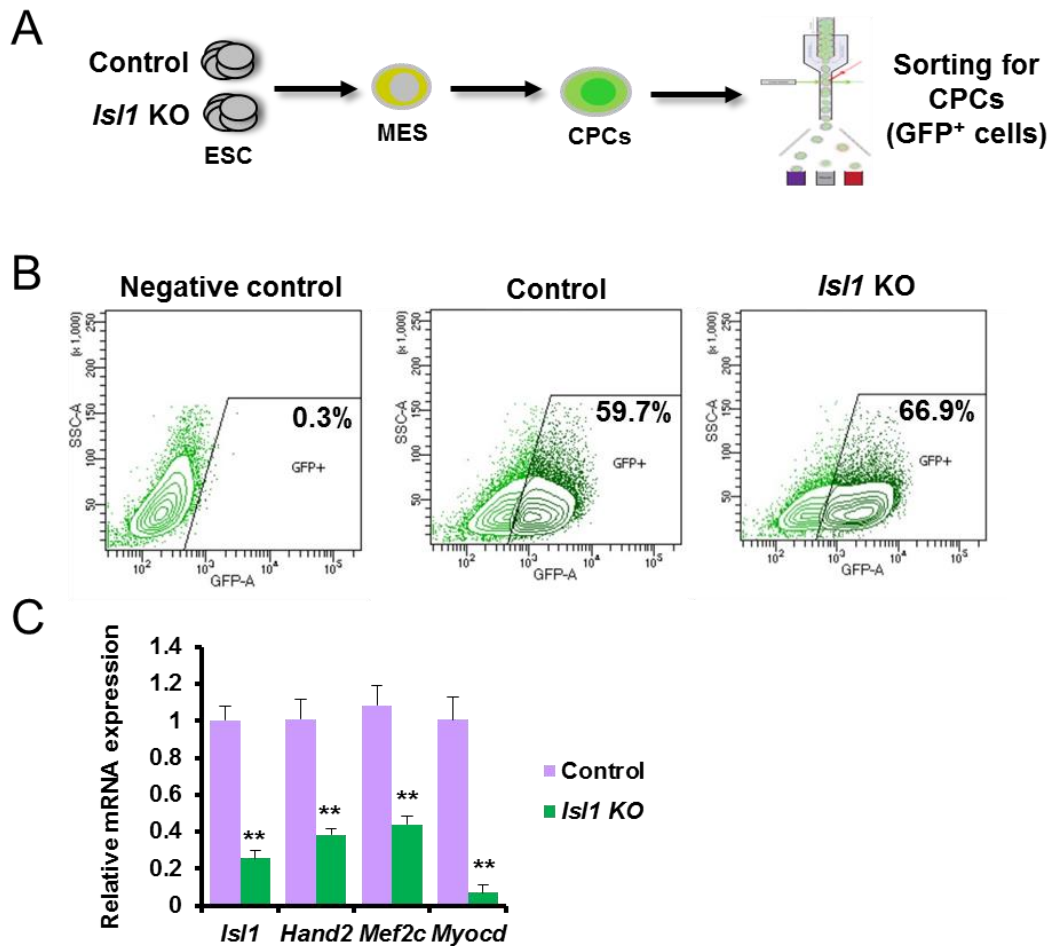


**Figure 18 Analysis of CPCs differentiated from control and *Isl1* KO lines**

(A) Schematic diagram shows cardiac differentiation of control and *Isl1* KO lines and FACS analysis at cardiac progenitor stage. (B) FACS results of CPCs from control and *Isl1* KO lines. CPCs from E14 line are used as negative control. (C) qPCR to check some *Isl1* known targets and some CPC marker genes. Data represent mean±SEM, n=3.

### 3.1.4 *Isl1* loss-of-function results in downregulation of a large number of genes critical for cardiogenesis in CPCs

To identify downstream targets of *Isl1* in CPCs, we performed RNA-Seq of sorted Nkx2.5-GFP<sup>+</sup> CPCs derived by differentiation of control or *Isl1*<sup>-/-</sup> Nkx2.5-GFP mESCs (Figure 19). We observed strong correlation between replicates for control and *Isl1* KO samples,

demonstrating high reproducibility across experiments (Figure 19A). From the results, we identified 1014 differentially expressed genes (fold change > 1.5; log2 fold change < -0.58, > 0.58; p value < 0.05) (Figure 19B). GO analysis of genes downregulated in the *Isl1* KO CPCs revealed over-representation of GO terms linked to heart development, cardiac muscle contraction, sarcomere organization and outflow tract morphogenesis while upregulated genes are highly associated with regulation of transcription and multicellular organism development (Figure 19C).

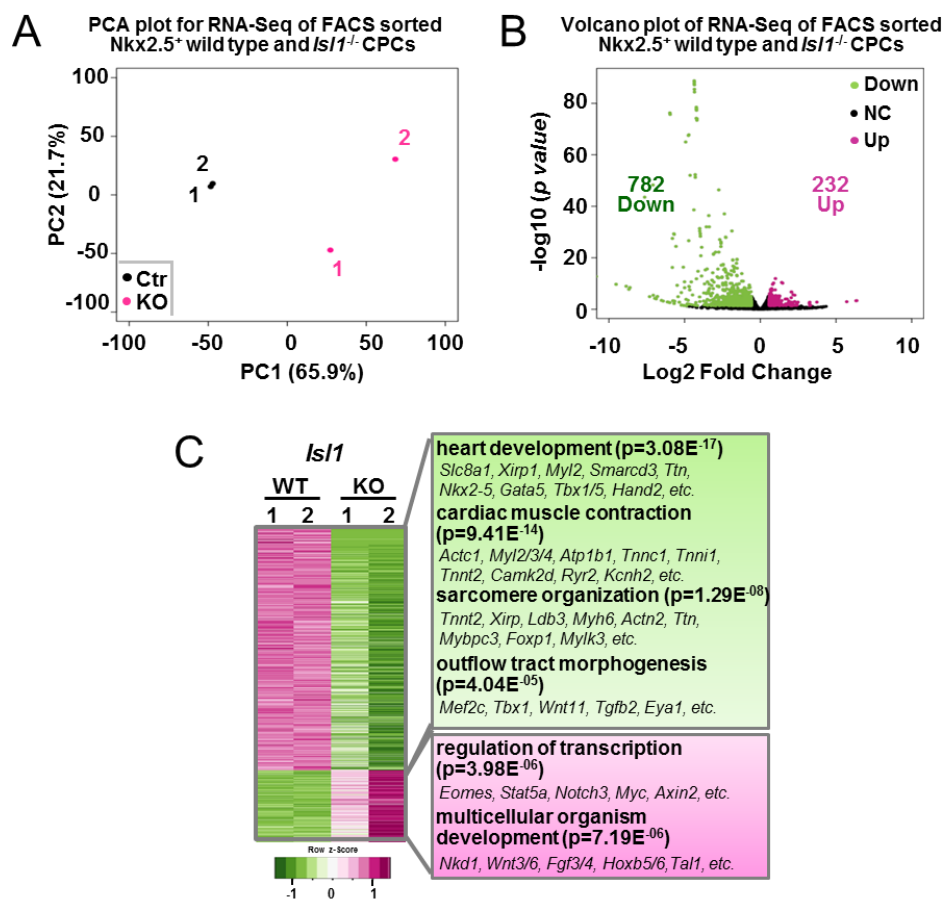


**Figure 19 RNA-Seq data analysis in control and *Isl1* KO CPCs**

(A) Principal component analysis (PCA) of RNA-Seq data from control and *Isl1* KO CPCs (n=2), providing insights into the association between samples. (B) Volcano plot of RNA-Seq data from control and *Isl1* KO CPCs (n=2). Each point represents an individual gene and all genes differentially expressed with fold change >1.5; log2 fold change < -0.58 and p value < 0.05 are highlighted in green (downregulated genes) and red (upregulated genes). (C) Heatmap of differentially regulated genes (782 downregulated and 232 upregulated genes with fold change > 1.5; log2 fold change < -0.58, > 0.58 and p value < 0.05) in CPCs caused by *Isl1* KO (n=2). Representative genes and enriched GO terms are presented on the right side.

### 3.1.5 *Isl1* directly regulates a large amount of genes in CPCs

To investigate whether *Isl1* directly regulates these target genes, we harvested cardiac progenitor cells derived from mESCs through cardiac differentiation and performed chromatin immunoprecipitation followed by high-throughput sequencing (ChIP-Seq) to map the genome-wide binding of *Isl1* in CPCs. ChIP-Seq analysis identified a lot of target genes directly regulated by *Isl1* (Figure 20). Some are its known targets, such as *Mef2c*, *Hand2*, *Myocd*, as we expected. Interestingly, there are also a lot of new targets which have not been reported, such as signaling molecules *Jag1* and *Wnt2*, cardiac transcription factor *Gata4*, and cardiomyocytes structural/contraction associated gene *Mybpc3*, *Tnni1*, *Ryr2* (Figure 20).

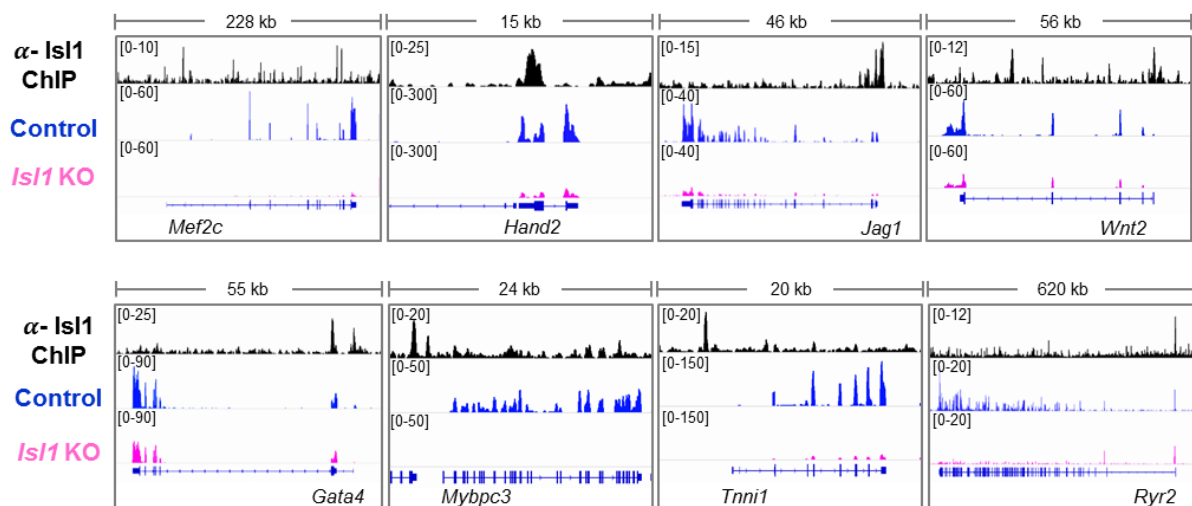


**Figure 20 Genome tracks of some representative *Isl1* targets in CPCs**

Screenshots of RNA-Seq and ChIP-Seq data in CPCs showing genome tracks of some representative *Isl1* target genes.

Intersection of the RNA-Seq data to the ChIP-Seq data revealed more than 60% downregulated genes that were bound by *Isl1* in CPCs and 56% upregulated genes with *Isl1* occupancy (Figure 21A and 21B). GO analysis of genes downregulated in the *Isl1* KO CPCs that were bound by *Isl1* revealed over-representation of GO terms linked to positive regulation of transcription and heart development while hemopoiesis and embryonic hindlimb morphogenesis for the common upregulated genes (Figure 21C and 21D).

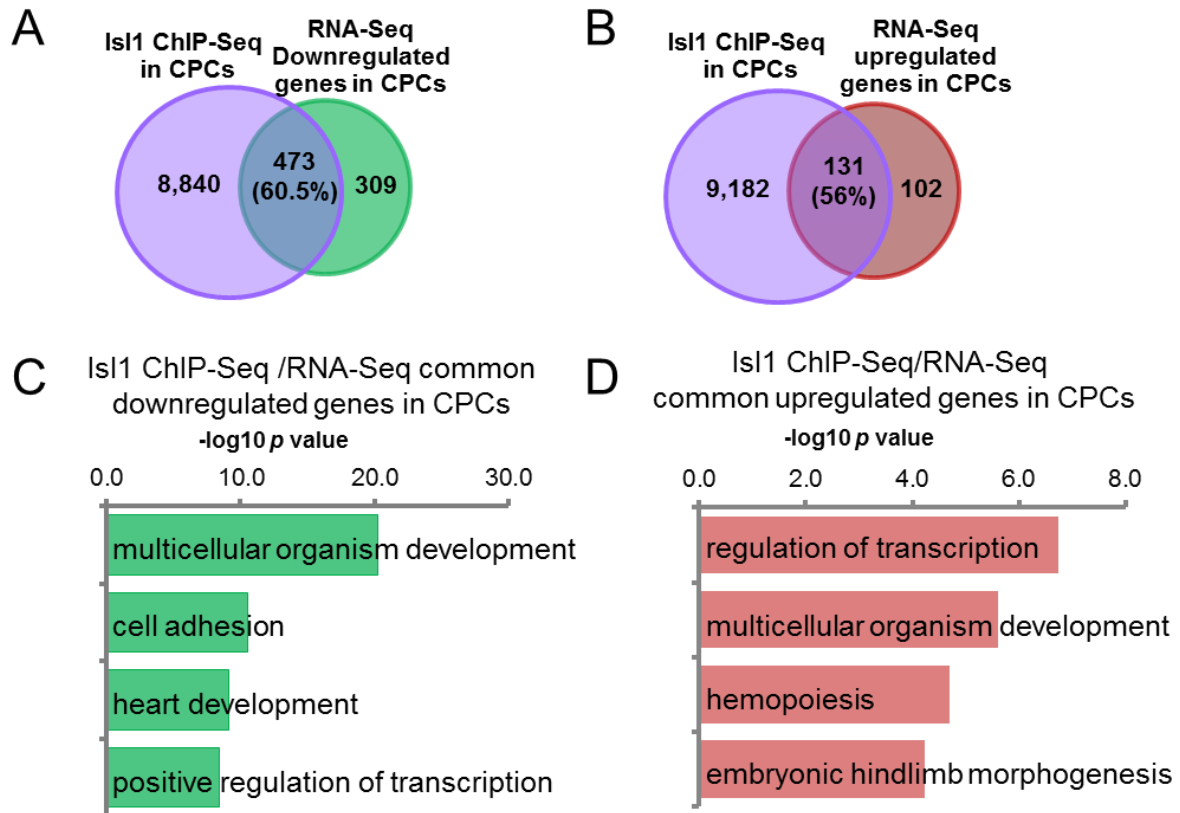


**Figure 21** *Isl1* regulates a large group of genes associating with cardiogenesis in CPCs

(A-B) Common genes of *Isl1* bound genes and downregulated (A) or upregulated genes (B) caused by *Isl1* loss-of-function in CPCs respectively. (C-D) Representative GO items for downregulated genes (C) and upregulated genes (D) with *Isl1* binding in CPCs analyzed using DAVID 6.8.

## 3.2 *Isl1* is essential in regulating second heart field development in mouse embryos

### 3.2.1 *Isl1* knockout leads to significant gene expression changes at early stage of mouse embryonic development

To gain insight into the molecular mechanisms underlying *Isl1* function in cardiogenesis *in vivo*, we performed RNA-Seq (Figure 22) from dissected pharyngeal mesoderm/hearts of E8.5 *Isl1* knockout embryos at which stage the *Isl1*<sup>+</sup> cells are restricted in the cardiogenic region (Figure 8).

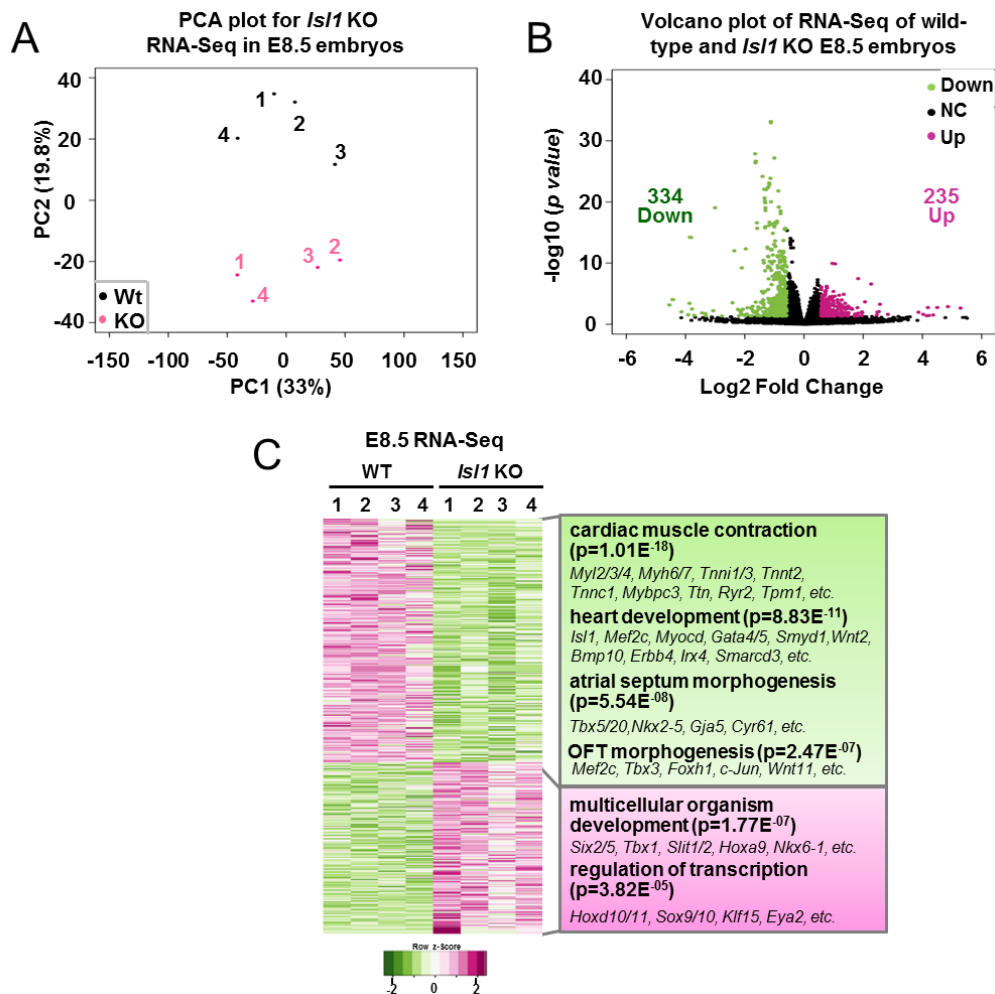


**Figure 22 Analysis of RNA-Seq data from E8.5 *Is11* KO embryos**

(A) PCA plot of RNA-Seq data from E8.5 *Is11* KO and control embryos (n=4). (B) Volcano plot of RNA-Seq data from E8.5 *Is11* KO embryos versus control (n=4). Each point represents an individual gene and all genes differentially expressed with fold change > 1.5; log2 fold change < -0.58 and p value < 0.05 are highlighted in green (downregulated genes) and red (upregulated genes). (C) Heatmap of differentially regulated genes (334 downregulated and 235 upregulated genes with fold change >1.5; log2 fold change < -0.58, > 0.58 and p value < 0.05) in the cardiogenic region of *Is11* KO E8.5 embryos versus control (n=4). Representative genes and enriched GO terms are presented on the right side.

The RNA-Seq results showed four replicates of control and four *Is11* KO samples clustered together very well and showed consistent results (Figure 22A). From the RNA-Seq data, we identified 569 differentially expressed genes in E8.5 *Is11* knockout embryos (fold change > 1.5; log2 fold change < -0.58, > 0.58; p value < 0.05) (Figure 22B). Gene Ontology (GO) analysis revealed over-representation for GO terms linked to cardiac muscle contraction, heart development, atrial septum and OFT morphogenesis in genes downregulated in E8.5 *Is11* knockout embryos, whereas genes involved in multicellular organism development and

transcription regulation were overrepresented in upregulated genes (Figure 22C). This is consistent with our results from *Isl1* KO mESC-derived cardiac progenitor cells.

### 3.2.2 Reduced level of *Isl1* results in cardiac defects and deregulation of target genes in E10.5 *Isl1* hypomorphic embryos

The critical role of *Isl1* in heart development has been demonstrated using an *Isl1* KO mouse line. *Isl1* KO embryos show early embryonic lethality (at around E10.5) (Cai, Liang et al. 2003, Yang, Cai et al. 2006). This severe phenotype makes it impossible to analyze the role of *Isl1* in heart development at later stages during development. For this purpose, we utilized an *Isl1* hypomorphic mouse line (Liang, Song et al. 2011) which survives until birth.

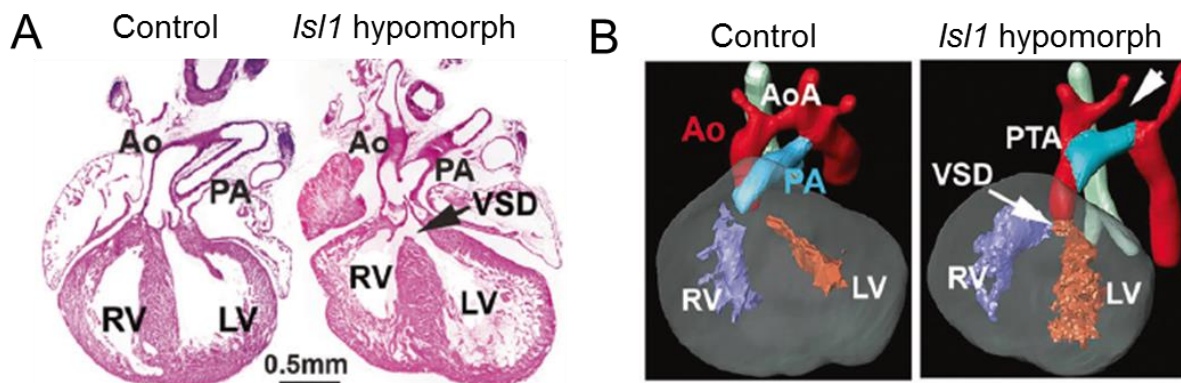


**Figure 23 Reduced *Isl1* expression leads to defects in cardiac morphogenesis**

*Isl1* hypomorphic mice presented various degrees of cardiac outflow tract (OFT) defects with ASDs and VSDs. Here only representative images are shown (Thanks for our collaborators to provide this figure). **(A)** Histological analysis of *Isl1* hypomorphic hearts at E17.5 showing ventricular septal defect (VSD, arrow) and PTA compared to control hearts. **(B)** 3D reconstruction of control and *Isl1* hypomorphic hearts showing PTA and VSD. Ao: Aorta; AoA: aortic arch; PA: pulmonary artery; LV: left ventricle; RV: right ventricle; VSD: ventricular septal defect; PTA: persistent truncus arteriosus.

Histological analyses of *Isl1* hypomorphic embryos at E17.5 revealed various degrees of cardiac outflow tract (OFT) septation abnormalities, including partial OFT septal defects with aortic stenosis and misalignment and persistent truncus arteriosus (PTA). Nearly all *Isl1* hypomorphic mice presented ventricular septal defects (VSDs) and atrial septal defects (ASDs) (Figure 23A). MRI and 3D reconstructions confirmed the presence of various cardiac outflow tract (OFT) abnormalities, VSDs and ASDs (Figure 23B). To conclude, reduced level of *Isl1* in *Isl1* hypomorphic mice led to cardiac defects as seen in human CHD patients,

suggesting *Isl1* is also crucial for heart development at the later stages of embryonic development.

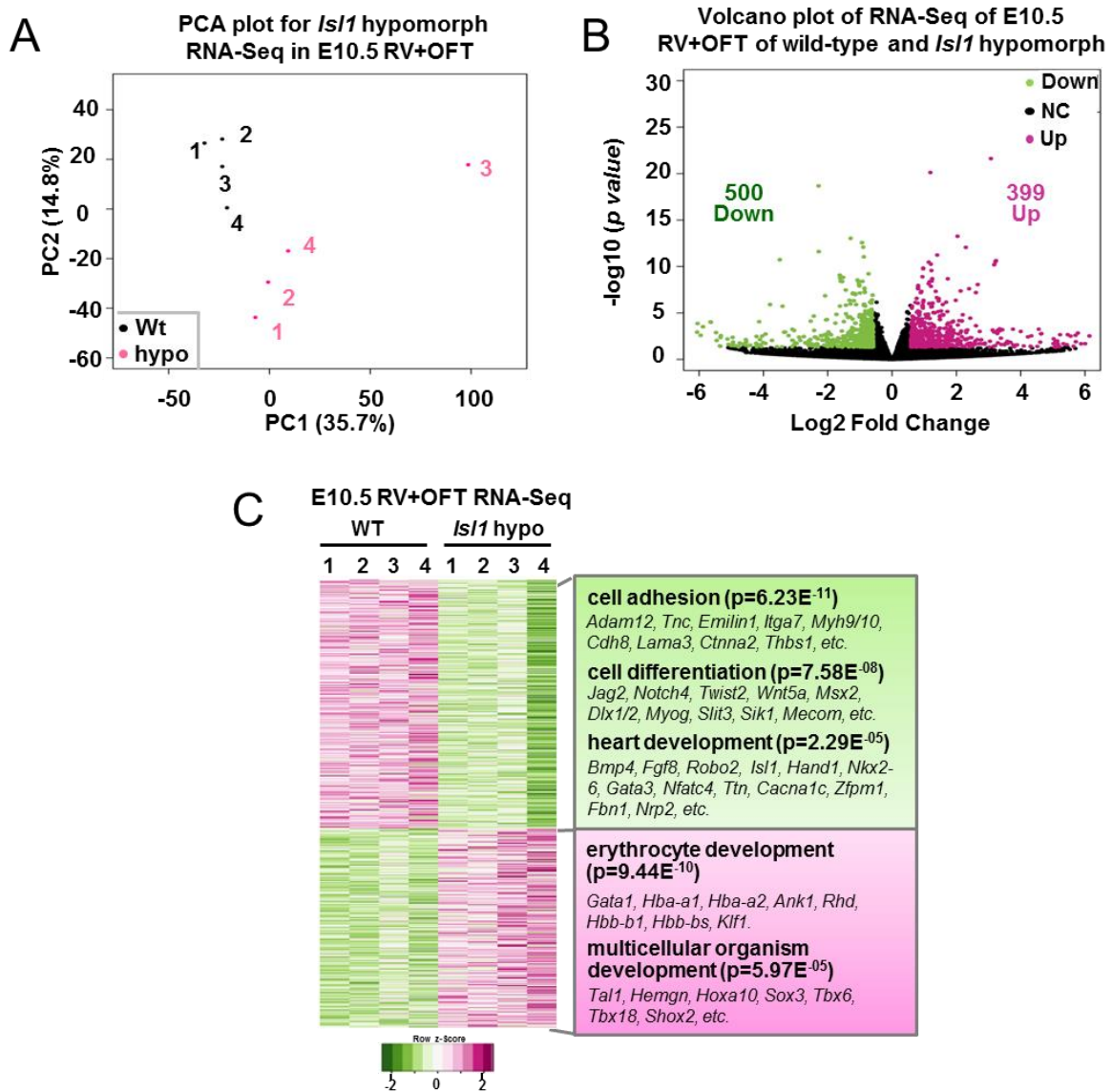


**Figure 24 Analysis of RNA-Seq data from E10.5 *Isl1* hypomorphic embryos**

(A) PCA plot of RNA-Seq data from E10.5 *Isl1* hypomorphic and control embryos (n=4). (B) Volcano plot of RNA-Seq data from E10.5 *Isl1* hypomorphic embryos versus control (n=4). Each point represents an individual gene and all genes differentially expressed with fold change > 1.5; log2 fold change < -0.58 and p value < 0.05 are highlighted in green (downregulated genes) and red (upregulated genes). (C) Heatmap of differentially regulated genes (500 downregulated and 399 upregulated genes with fold change > 1.5; log2 fold change < -0.58, > 0.58 and p value < 0.05) in the SHF of E10.5 embryos caused by reduced *Isl1* expression (n=4). Representative genes and enriched GO terms are presented on the right side.

To explore the molecular mechanisms responsible for the cardiac defects observed at later stages of heart development in *Isl1* hypomorphic embryos, we isolated the OFT and RV of



E10.5 *Isl1* hypomorphic embryos, structures derived from the *Isl1*<sup>+</sup> SHF CPCs, still expressing *Isl1*, and when the phenotype is not so severe yet, to avoid secondary effect on gene expression changes. We performed RNA-Seq with 4 replicates for control and *Isl1* hypomorphic embryos, respectively. The RNA-Seq data showed consistent results of all the replicates (Figure 24A). From the results, we identified 899 deregulated genes caused by reduced level of *Isl1* (fold change > 1.5; log<sub>2</sub> fold change < -0.58, > 0.58; p value < 0.05) (Figure 24B). In addition to many transcriptional regulators of cardiac morphogenesis, we found significant overrepresentation of genes involved in cell adhesion and differentiation that have been shown to play key role in cardiac looping morphogenesis, cushion formation, neural crest addition, ventricular and OFT septation in the downregulated genes (Figure 24C). Interestingly, we identified genes involved in erythroid development and hemogenic lineage specification in genes upregulated upon *Isl1* loss (Figure 24C). Given the antagonistic relationship between hemangiogenic and cardiogenic mesoderm specification (Van Handel, Montel-Hagen et al. 2012), this might suggest that *Isl1* is important for establishing cardiac fate and prevents the acquisition of hemogenic fate.

### **3.2.3 ChIP-Seq analysis identified *Isl1* primary downstream targets *in vivo***

To investigate whether *Isl1* directly regulates these downstream targets *in vivo*, we performed chromatin immunoprecipitation followed by high-throughput sequencing (ChIP-Seq) to map the genome-wide binding of *Isl1* in dissected cardiogenic regions of E8.25-E9.0 embryos. The ChIP-Seq data identified 12,968 *Isl1* direct targets. Intersection of our RNA-Seq data from E8.5 *Isl1* KO embryos to this ChIP-Seq data revealed up to 60% downregulated genes that were bound by *Isl1* in mouse cardiogenic region at E8.5 and more than 53% upregulated genes with *Isl1* occupancy (Figure 25A and 25B). GO analysis of genes downregulated in the *Isl1* KO embryos that were bound by *Isl1* revealed over-representation of GO terms linked to heart development, cardiac muscle contraction, atrial septum and OFT morphogenesis, while multicellular organism development and cellular response to hypoxia for the common upregulated genes (Figure 25C and 25D).

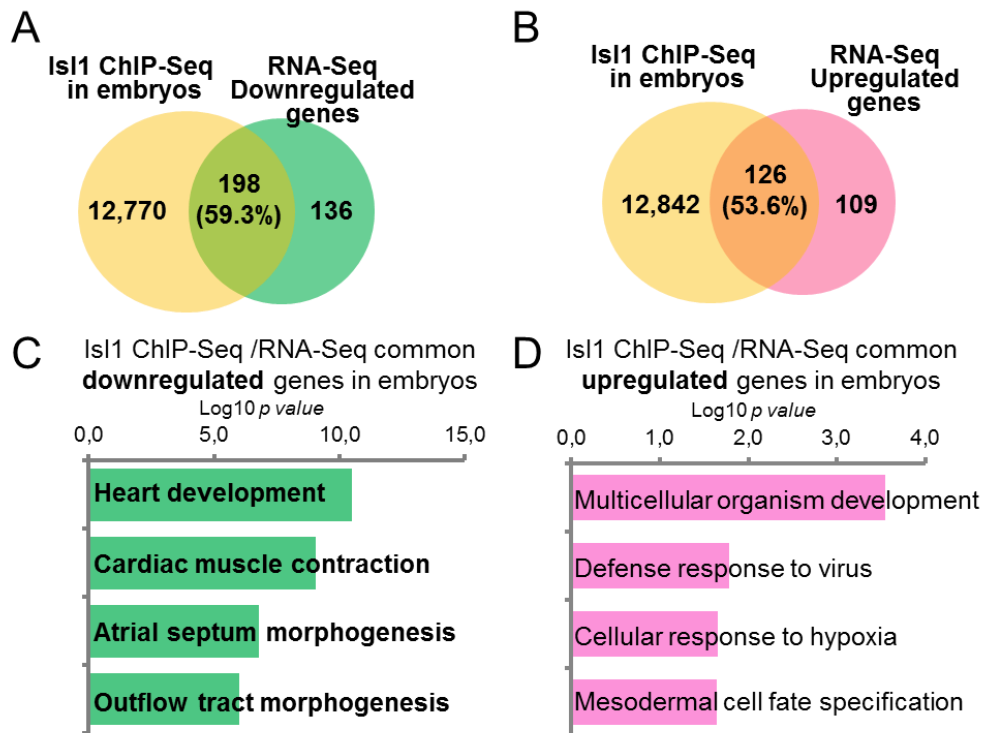


**Figure 25 Intersection of RNA-Seq and Isl1 ChIP-Seq data in mouse embryos**

(A-B) Common genes with Isl1 binding and downregulated (A) or upregulated (B) caused by *Isl1* loss-of-function in cardiogenic region of mouse embryos, respectively. (C-D) Representative GO items for downregulated genes (C) and upregulated genes (D) with Isl1 binding in mouse embryos analyzed using DAVID 6.8.

### 3.3 *Isl1* orchestrates a regulatory network driving cardiogenesis

To get a better view of *Isl1* regulatory network during cardiogenesis, we compared our *in vivo* RNA-Seq and *Isl1* ChIP-Seq datasets with the ones in mESC-derived CPCs (Figure 26). Analysis showed 71% of genes bound by *Isl1* in ESC-derived CPCs were also bound in E8.25-E9.0 embryos. Importantly, 75% of genes deregulated in E8.5 *Isl1* knockout embryos were bound by *Isl1*, whereas 67% of genes deregulated in OFT and RV of E10.5 *Isl1* hypomorphic embryos were bound by *Isl1* (Figure 26).

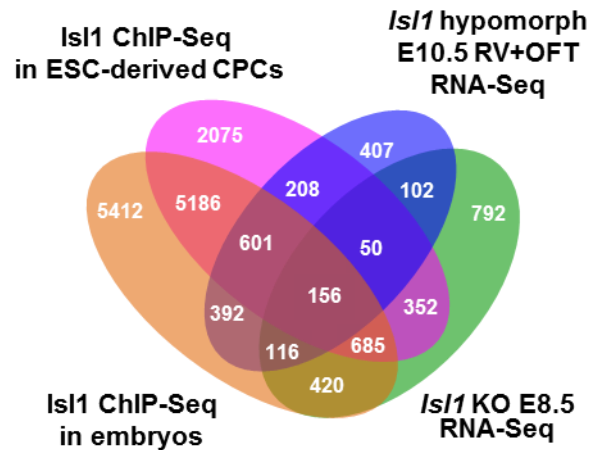


**Figure 26 Venn diagram showing *Isl1* targets from different datasets**

Venn diagram representing the overlap of genes bound by *Isl1* in E8.25-E9.0 embryos or ESC-derived CPCs (n=2) and differentially expressed in dissected pharyngeal mesoderm/hearts of E8.5 *Isl1* knockout embryos as well as OFT and RV of E10.5 *Isl1* hypomorphic embryos (p value < 0.05) compared to control embryos (n=4).

Gene network analysis uncovered distinct groups of *Isl1* primary downstream targets (Figure 27), e.g. (i) transcription factors, such as *Mef2c* and *Myocd*, known *Isl1* downstream targets (Dodou, Verzi et al. 2004, Kwon, Qian et al. 2009), and other key regulators of SHF development, such as *Tbx3*, *Tbx20*, *Eya1*, *Foxc1* (Vincent and Buckingham 2010); (ii) signaling molecules, such as *Fgf10* (Golzio, Havis et al. 2012, Watanabe, Zaffran et al. 2012), and other key components of the Wnt, BMP and FGF signaling pathways; (iii) cardiomyocyte structural genes and genes involved in cardiac contraction, such as *Myl2*, *Myl3*, *Ttn*, *Ryr2*, *Cacna1c*, *Tpm1*, *Tmod1* and *Mybpc3*. The observation that *Isl1* binds to cardiomyocyte structural genes is consistent with the disrupted sarcomerogenesis in *Isl1* hypomorphic embryos, but is somewhat surprising because cardiac structural genes are only highly expressed when *Isl1* transcription is turned off.

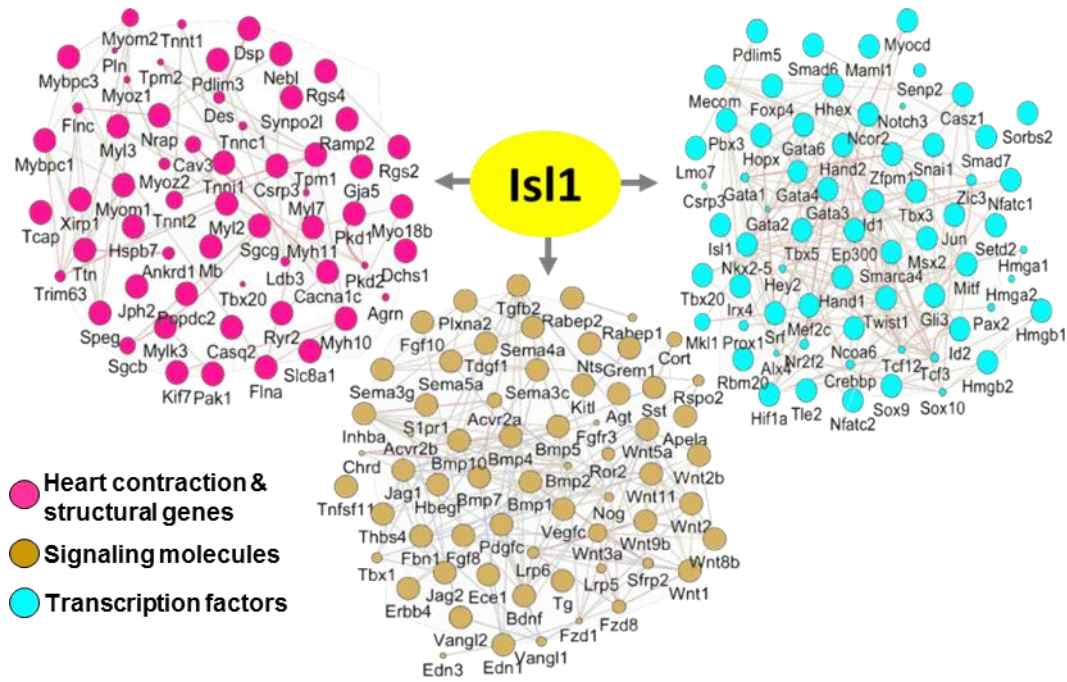


**Figure 27** *Isl1*-regulatory gene network

Gene regulatory networks orchestrated by *Isl1* in mouse embryos identified in heart development associated genes using GeneMANIA and Cytoscape.

GO analysis after intersection of the RNA-Seq data with ChIP-Seq data revealed overrepresentation of GO terms linked to heart development, cell adhesion and differentiation, atrial septum and outflow tract morphogenesis, as well as cardiac muscle fiber development and cardiac conduction (Figure 28A-C), consistent with the defects observed in *Isl1* hypomorphic embryos. Importantly, we observed enrichment of GO terms involved in response to hypoxia in E8.5 embryos (Figure 28A), consistent with the critical role of *Isl1* in regulating SHF progenitor cell function in response of spatial differences in oxygenation during cardiogenesis (Yuan, Qi et al. 2017).

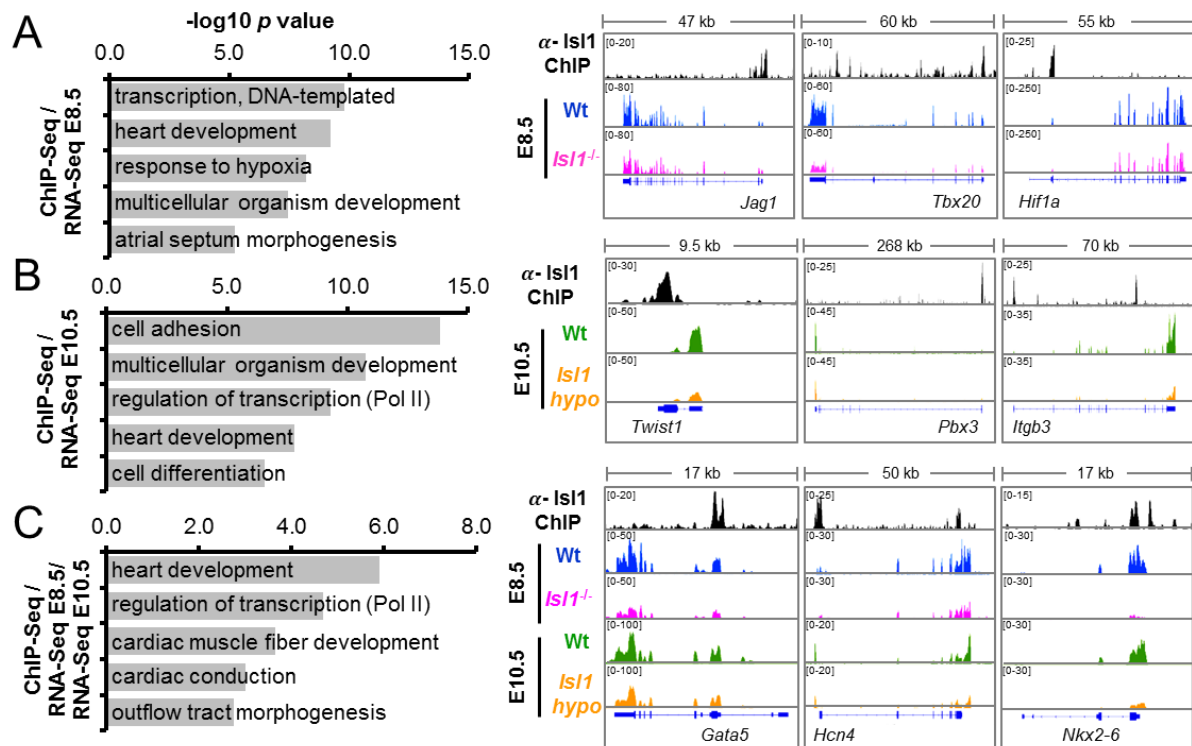


**Figure 28 GO terms enriched in *Isl1* target genes**

(A-C) GO terms enriched in genes bound by *Isl1* deregulated in E8.5 *Isl1* knockout embryos (A), in E10.5 OFT+RV of *Isl1* hypomorphic embryos (B), or in both E8.5 *Isl1* knockout embryos and E10.5 OFT+RV of *Isl1* hypomorphic embryos (C). Examples of genes regulated and bound by *Isl1* in (A), (B), (C), showing genome tracks of *Isl1* ChIP-Seq and RNA-Seq reads, are presented on the right side of the panel.

### 3.4 Baf60c is a key *Isl1* downstream target

#### 3.4.1 Baf60c is directly regulated by *Isl1*

We next want to clarify the subset of *Isl1* primary downstream targets differentially regulated both *in vitro* and *in vivo*, so we further analyzed our RNA-Seq and ChIP-Seq datasets from both mESC-derived CPCs and the ones generated from embryonic tissues. We identified a group of genes directly regulated by *Isl1* and deregulated in both systems (Figure 29A). Among them, in addition to known *Isl1* targets, such as *Hand2* and *Mef2c* (Dodou, Verzi et al. 2004, Caputo, Witzel et al. 2015), we found many novel primary downstream targets with a role in cardiogenesis (Figure 29A). One of the targets, *Baf60c* (*Smarcd3*) (Figure 29A-B), a cardiac-specific component of the Brg1-based SWI/SNF chromatin remodeling complex, plays a crucial role in heart development (Lickert, Takeuchi et al. 2004, Sun, Hota et al. 2017, Hota, Johnson et al. 2019). *Baf60c* level was significantly decreased in

both *Isl1* KO mESC-derived CPCs and in embryos (Figure 29A), confirming Baf60c as a primary downstream target of *Isl1*. In addition, Baf60c downregulation is further validated by qPCR results in *Isl1* KO and control CPCs (Figure 29C).

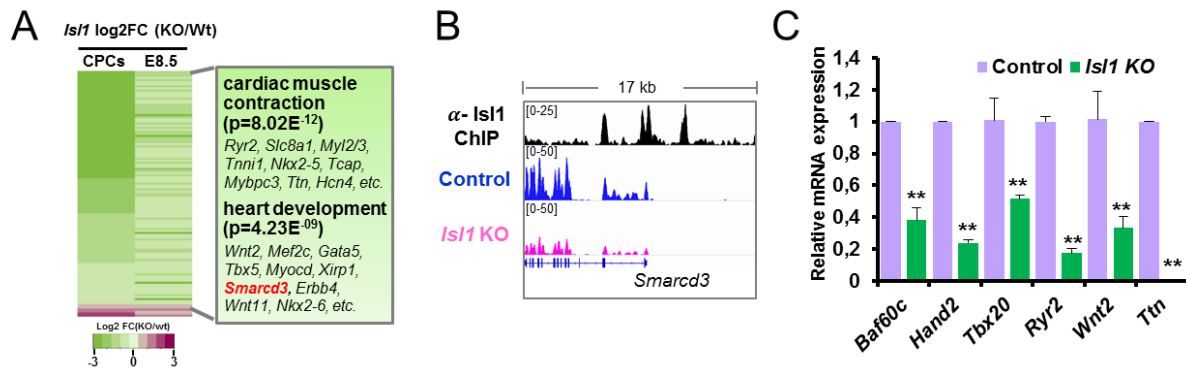


**Figure 29 Baf60c is a key *Isl1* downstream target**

(A) Heatmap of genes bound by *Isl1* and deregulated in both RNA-Seq analysis of dissected pharyngeal mesoderm/hearts of wild-type and E8.5 *Isl1* knockout embryos, and of control and *Isl1* KO *Nkx2.5*<sup>+</sup> CPCs (log2 fold change < -0.58, > 0.58, p value < 0.05). Representative genes and enriched GO terms are presented on the right side. (B) Genome tracks of *Isl1* ChIP-Seq and RNA-Seq on *Baf60c* in control and *Isl1* knockout CPCs. (C) Relative mRNA expression of *Isl1* direct targets in sorted CPCs of control and *Isl1* KO lines. Data are mean $\pm$ SEM, n=3.

### 3.4.2 RNA-Seq analysis identified *Baf60c* regulated genes in CPCs

To investigate the role of *Baf60c* in cardiac progenitor cells, we decided to generate mESC lines with *Baf60c* knockdown (KD). To establish *Baf60c* KD stable mESC lines, we packaged *Baf60c* shRNA into lentivirus and infected WT mESC lines following with puromycin selection. To check the differentiation and *Baf60c* KD efficiency of these cell lines, we performed cardiac differentiation and collected the cells at day5 for sorting of GFP<sup>+</sup> CPCs by flow cytometry (Figure 30A). *Baf60c* is efficiently knocked down, as shown in qPCR results (Figure 30B). Knockdown of *Baf60c* did not affect the differentiation of mESCs to CPCs, as seen by FACS analysis for *Nkx2.5*-GFP<sup>+</sup> cells (Figure 30C).

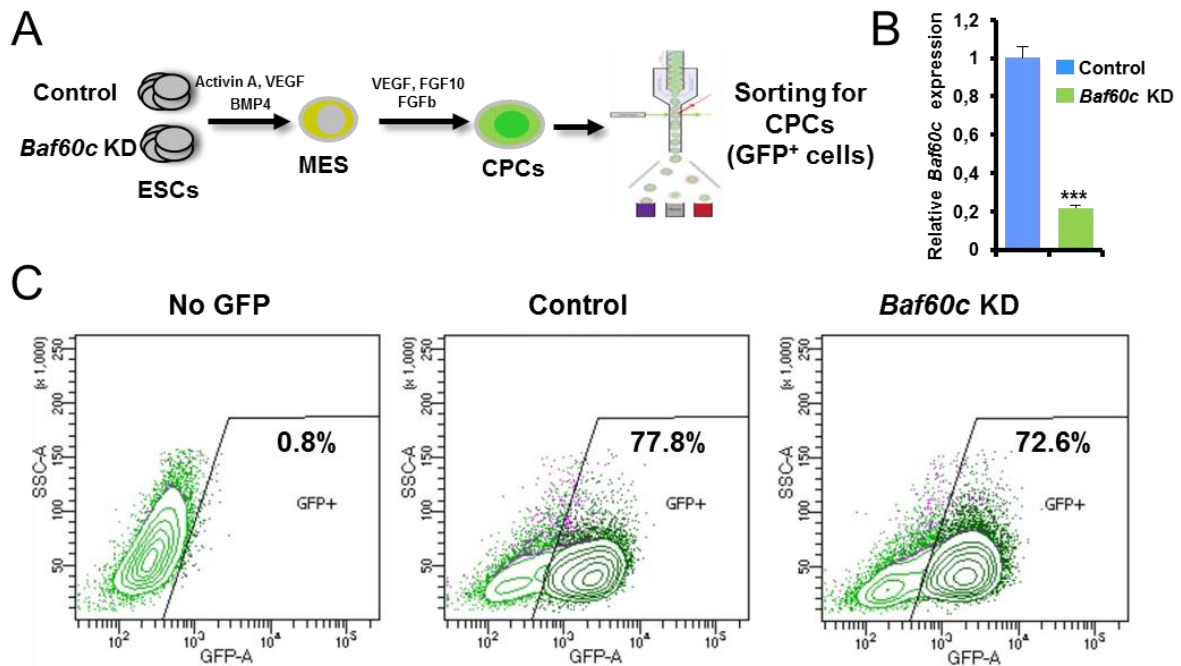


**Figure 30 Analysis of CPCs differentiated from control and *Baf60c* KD mESC lines**

(A) Scheme depicting directed cardiac differentiation and sample harvesting strategy. (B) qPCR for *Baf60c* to check the KD efficiency in sorted control and *Baf60c* KD CPCs. (C) Flow cytometry analysis of control and *Baf60c* KD CPCs.

To address whether *Baf60c* plays a role in mediating *Isl1* function in cardiogenesis, we performed RNA-Seq of sorted *Nkx2.5*-GFP<sup>+</sup> CPCs derived by directed cardiac differentiation of control or *Baf60c* knockdown *Nkx2.5*-GFP mESCs (Figure 31). Principal component analysis (PCA) of the duplicates showed consistent results (Figure 31A). The RNA-Seq data identified 878 downregulated genes and 893 upregulated genes following *Baf60c* depletion (fold change >1.5; log<sub>2</sub> fold change < -0.58, > 0.58 and p value < 0.05) (Figure 31B). GO analysis of downregulated genes showed that *Baf60c* activates genes involved in cardiac muscle contraction, sarcomere organization and ion transport, while repressing genes involved in multicellular organism development and anterior/posterior pattern specification (Figure 31C).

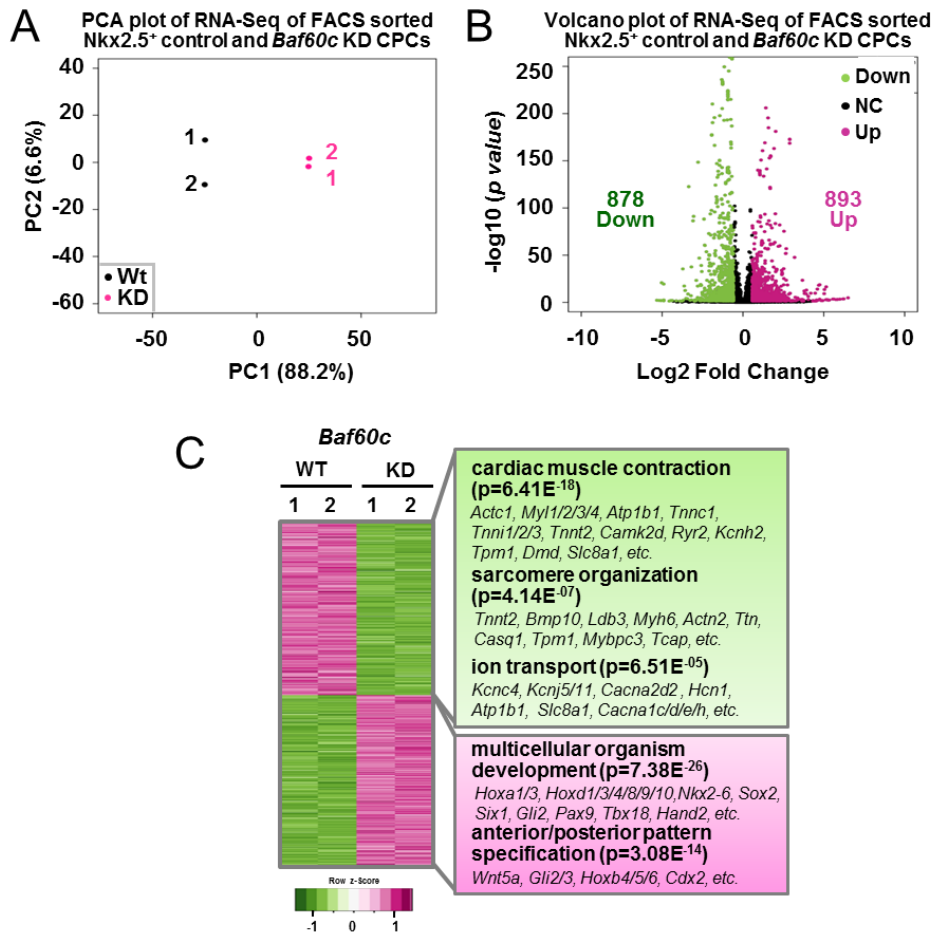


**Figure 31 Analysis of RNA-Seq data in control and *Baf60c* KD CPCs**

(A) PCA plot of RNA-Seq data from control and *Isl1* KO CPCs (n=2). (B) Volcano plot of RNA-Seq data from control and *Baf60c* KD CPCs (n=2). Each point represents an individual gene and all genes differentially expressed with fold change > 1.5; log<sub>2</sub> fold change < -0.58 and p value < 0.05 are highlighted in green (downregulated genes) and red (upregulated genes). (C) Heatmap of differentially regulated genes (878 downregulated and 893 upregulated genes with fold change >1.5; log<sub>2</sub> fold change < -0.58, > 0.58 and p value < 0.05) in CPCs caused by *Baf60c* KD (n=2). Representative genes and enriched GO terms are presented on the right side.

### 3.4.3 *Isl1* and *Baf60c* share common targets

Next, to test whether *Isl1* and *Baf60c* regulate common genes in CPCs, we compared the RNA-Seq data from controls, *Baf60c* KD CPCs and *Isl1*<sup>-/-</sup> CPCs. We found there are 432 common genes differentially expressed following *Isl1* or *Baf60c* depletion (Figure 32A, fold change > 1.5; log<sub>2</sub> fold change < -0.58, > 0.58 and p value < 0.05). GO analysis of common deregulated genes showed that *Isl1* and *Baf60c* activate genes involved in cardiac muscle contraction, sarcomere organization and heart development, while repressing genes involved in immune system process and cellular response to interferon-gamma (Figure 32B).



These results indicate that Baf60c may work in axis with Isl1 to promote chromatin reorganization at cardiomyocyte structural genes and cardiac contraction associated genes in CPCs.

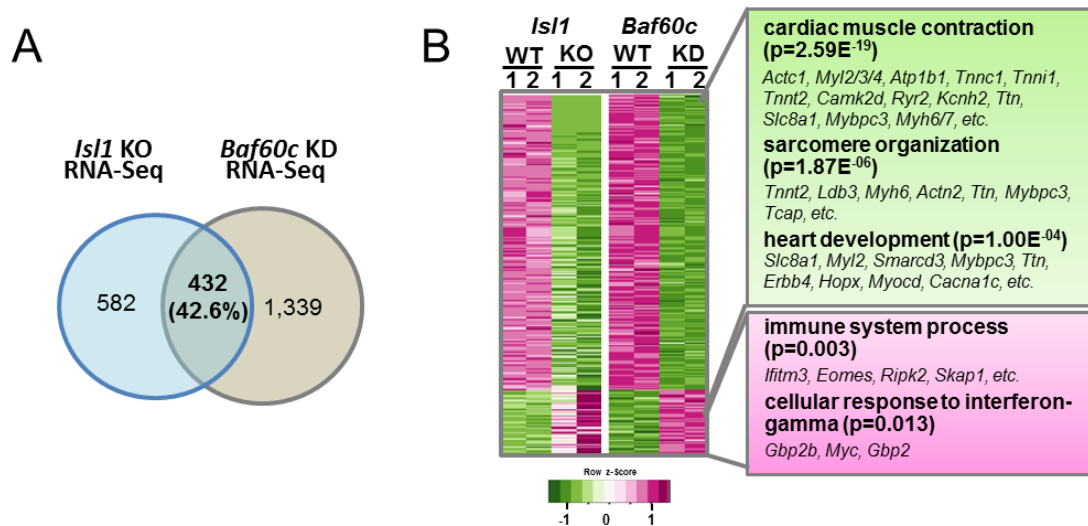


**Figure 32** *Isl1* and *Baf60c* share common target genes in CPCs

**(A)** Venn diagram showing overlap of differentially regulated genes in sorted *Isl1* knockout and *Baf60c* knockdown CPCs (fold change > 1.5; log<sub>2</sub> fold change < -0.58, > 0.58 and p value < 0.05; n=2). **(B)** Heatmap of genes downregulated or upregulated in both *Isl1* knockout and *Baf60c* knockdown versus control CPCs (fold change > 1.5; log<sub>2</sub> fold change < -0.58, > 0.58 and p value < 0.05; n=2). Representative genes and enriched GO terms are presented on the right side.

### 3.5 *Isl1* works in concert with the Brg1-based SWI/SNF complex to regulate its target genes

#### 3.5.1 *Isl1* interacts with Brg1 and Baf60c

As mentioned above, Baf60c is a cardiac-specific subunit of the Brg1-based SWI/SNF complex, which plays an important role in heart development (Lickert, Takeuchi et al. 2004). To analyze whether *Isl1* may also work unitedly with the Brg1-based SWI/SNF complex, we first analyzed whether *Isl1* and Brg1 interact with each other. Co-immunoprecipitation experiments in ESC-derived CPCs revealed that *Isl1* binds to both Brg1 and Baf60c (Figure 33A). The binding of *Isl1* to Brg1 was further validated in E8.25-E9.0 embryos (Figure 33B). The interaction of *Isl1* and Brg1 in mESC-derived CPCs and in mouse embryos suggests *Isl1* may work together with Brg1/Baf60c complex in regulating cardiogenesis.

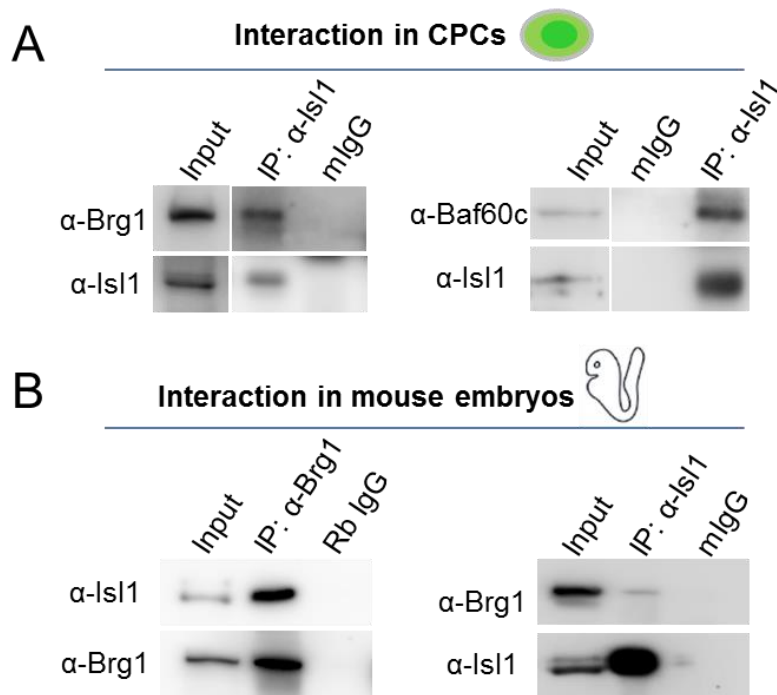


**Figure 33 Isl1 interacts with Brg1/Baf60c complex**

(A) Co-IP showing interaction between Isl1 and Brg1/Baf60c in mESC-derived CPCs. (B) Co-IP showing interaction between Isl1 and Brg1 in mouse embryos. 30 embryos at E8.25-E9.0 were used for each IP. And immunoprecipitation was done by both Brg1 and Isl1 antibodies.

### 3.5.2 The interaction of Isl1 with Brg1 does not depend on Baf60c

Baf60c was reported to mediate interactions between cardiac transcription factors such as Tbx5, Nkx2.5, Gata4 and the Brg1 complex to drive cardiac specific gene expression (Lickert, Takeuchi et al. 2004, Takeuchi and Bruneau 2009). To test whether Baf60c promotes the binding of Isl1 to the Brg1 complex, we performed co-immunoprecipitation in control and *Baf60* KD ESC-derived CPCs using Isl1 antibody, suggesting that, in contrast to Tbx5, Nkx2.5 and Gata4, Baf60c does not mediate the association of Isl1 with the Brg1 complex in CPCs (Figure 34A), and *vice versa* (Figure 34B). Taken together, these results suggested that Isl1 not only plays a role in regulating Baf60c but also works together with the Brg1-Baf60c complex during cardiogenesis.

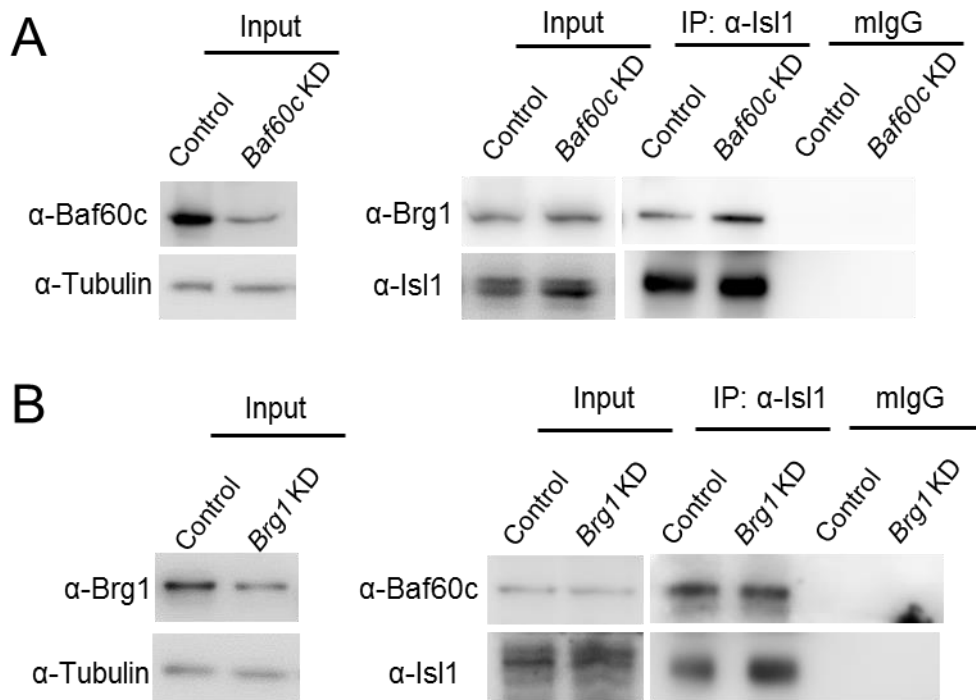


**Figure 34 Baf60c doesn't mediate the interaction between Isl1 and Brg1 in CPCs and vice versa**

**(A)** Co-immunoprecipitation with anti-Isl1 antibody and Western blot analysis for Brg1 in control or *Baf60c* KD CPCs, showing that the interaction between Isl1 and Brg1 does not depend on Baf60c. **(B)** Co-immunoprecipitation with anti-Isl1 antibody and Western blot analysis for Baf60c in control or *Brg1* KD CPCs, showing that the interaction between Isl1 and Baf60c does not depend on Brg1.  $\alpha$ -Tubulin was used as loading control.

### 3.5.3 Co-occupancy of Isl1 and Brg1 in CPCs

To further investigate how Isl1 and Brg1 work together in regulating cardiogenesis, we compared the ChIP-Seq data for Brg1 (Hota, Johnson et al. 2019) and Isl1 in CPCs. Analysis showed high co-occupancy of Brg1 and Isl1 at Isl1 binding sites, especially near the transcription start sites (TSS) of target genes (Figure 35A-C), such as *Smarcd3*, *Tbx20*, *Wnt2* and *Ryr2*, confirming our hypothesis that Isl1 works cooperatively with Brg1 in regulating its target genes during cardiogenesis.

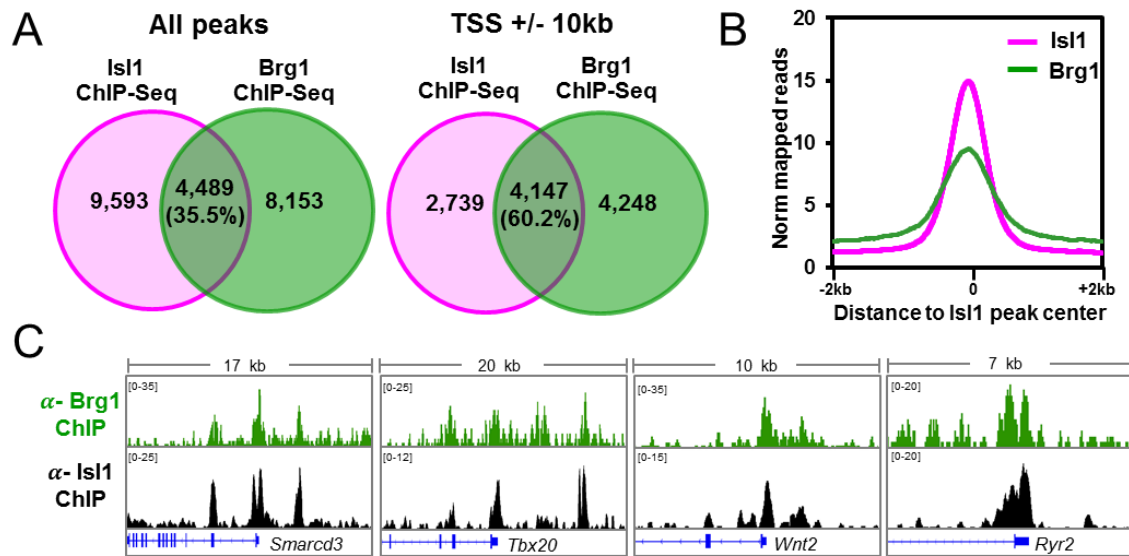


**Figure 35 Is1 co-occupied with Brg1 on its target genes in CPCs**

(A) Venn diagram representing the overlap of Is1 and Brg1 ChIP-Seq peaks (All peaks: left panel; peaks near TSS: right panel). (B) Average ChIP-Seq tag intensities at Is1 peaks. (C) Examples of IGVSnapshots showing co-occupancy of Is1 and Brg1 on the target genes in CPCs.

Furthermore, by analyzing the ChIP-Seq data with our RNA-Seq data in *Is1* KO CPCs, we found that 59.3% of the genes bound by Is1 were bound by Brg1, while 44% of the genes deregulated by *Is1* loss-of-function were concomitantly bound by Is1 and Brg1 (Figure 36). As Brg1/Baf60c complex is chromatin remodeler, these results led us to think that Is1 may work together with the Brg1-Baf60c complex to regulate nucleosomal structure and expression of its target genes.

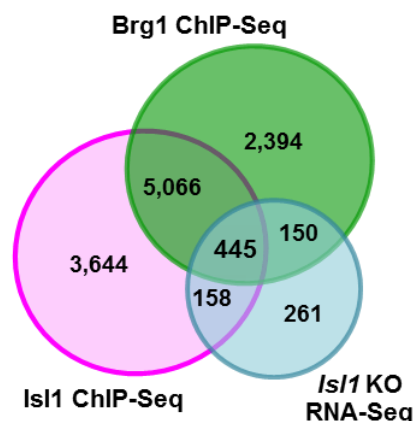


**Figure 36 A large subset of genes differentially regulated in *Is1* KO CPCs are co-bound by Is1 and Brg1**

Venn diagram representing the overlap of genes bound by Is1 and Brg1 (n=2) and differentially expressed in *Is1* KO CPCs (n=2).

### 3.5.4 *Isl1* works cooperatively with *Brg1* to regulate its target gene expression

To investigate our hypothesis *in vivo*, we inactivated *Brg1* (Bultman, Gebuhr et al. 2000) in SHF progenitor cells using an *Isl1-Cre* driver mouse line. We dissected the outflow tract and right ventricle, which are derived from the *Isl1*<sup>+</sup> SHF progenitors, and analyzed the expression of *Isl1* target genes. qPCR expression analysis of dissected OFT and RV of E10.5 wild-type, *Isl1-Cre*<sup>+/-</sup>, *Isl1-Cre*<sup>+/-</sup>/*Brg1*<sup>fl/+</sup> and *Isl1-Cre*<sup>+/-</sup>/*Brg1*<sup>fl/fl</sup> embryos revealed significant downregulation of *Isl1* primary targets in *Isl1-Cre*<sup>+/-</sup>/*Brg1*<sup>fl/+</sup> embryos and further decrease in *Brg1*-deficient embryos (Figure 37A). These results suggested that *Brg1* regulates a common group of target genes with *Isl1* during SHF development, and demonstrated a dosage requirement for *Brg1* in regulating gene expression programs associating with SHF development, similar with the report that allelic balance between *Brg1* and cardiac transcription factors *Tbx5*, *Tbx20* and *Nkx2.5* is essential for cardiogenesis (Takeuchi, Lou et al. 2011).

Furthermore, to check whether *Brg1* loss-of-function in the SHF derivatives affects gene expression in the tissue arisen from the FHF, we dissected the left ventricle and analyzed the expression of *Isl1* target genes. As we expected, no major changes were observed in the left ventricle of these embryos (Figure 37B), suggesting *Brg1* regulates *Isl1* target genes specifically in the SHF derived tissue. Moreover, to test whether *Brg1* generally regulates gene expression in OFT and RV, we analyzed the expression of some example genes that are not *Isl1* targets (Figure 37C). The expression of these genes is not changed with *Brg1* depletion, suggesting that the role of *Brg1* in the SHF development is specific (Figure 37C).

Taken together, the dosage-sensitive interdependence of *Isl1* and *Brg1*, in combination with the interactions and co-occupancy of *Isl1* and BAF complex members, supports the hypothesis that the *Brg1*-*Baf60c* complex might regulate gene expression coordinated with *Isl1* in SHF development.

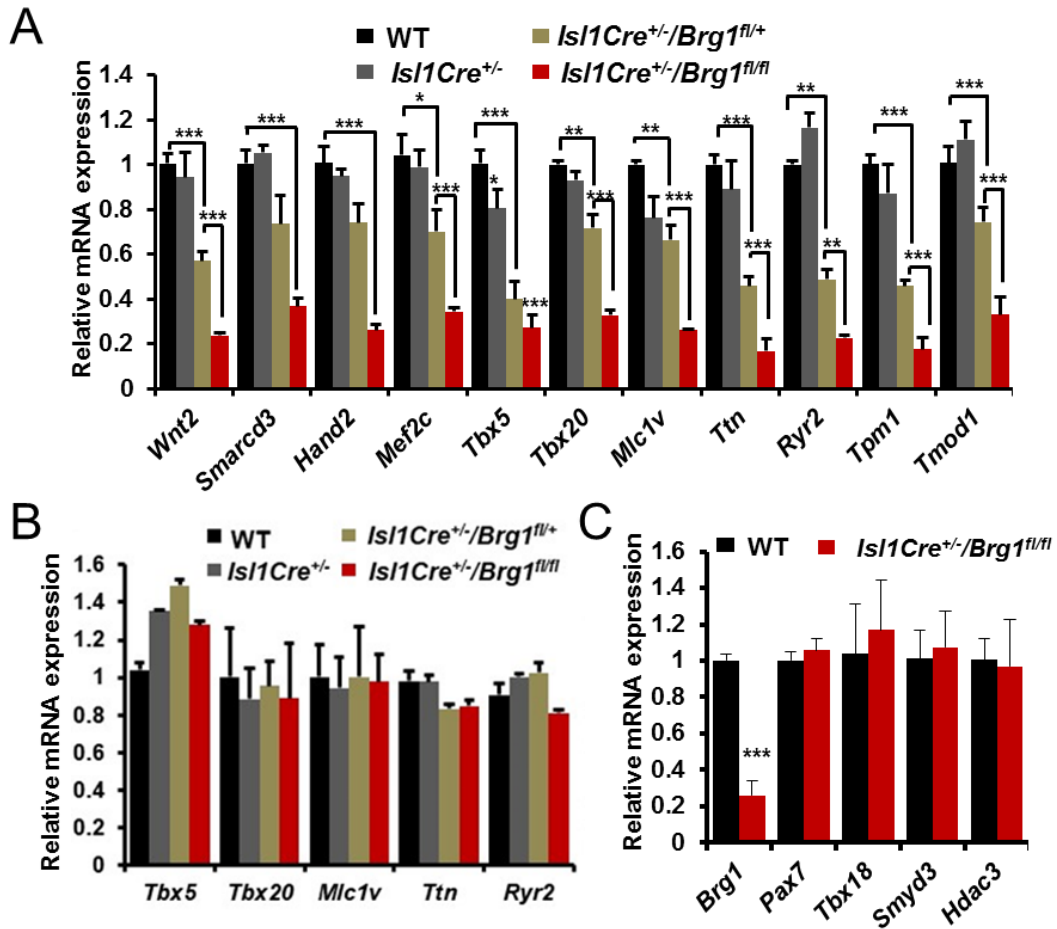


**Figure 37** *Isl1* works unitedly with *Brg1* to regulate its target gene expression

(A) Relative mRNA expression levels of *Isl1/Brg1-Baf60c* common targets in dissected OFT and RV of wild-type, *Isl1-Cre<sup>+/-</sup>*, *Isl1-Cre<sup>+/-</sup>/Brg1<sup>fl/+</sup>* and *Isl1-Cre<sup>+/-</sup>/Brg1<sup>fl/fl</sup>* embryos. Data are mean±SEM, n=4. (B) Relative mRNA expression levels of *Isl1/Brg1-Baf60c* common targets in dissected left ventricle of wild-type, *Isl1-Cre<sup>+/-</sup>*, *Isl1-Cre<sup>+/-</sup>/Brg1<sup>fl/+</sup>* and *Isl1-Cre<sup>+/-</sup>/Brg1<sup>fl/fl</sup>* embryos. Data are mean±SEM, n=3. (C) Relative mRNA expression levels of genes not bound by *Isl1* in dissected OFT and RV of wild-type, *Isl1-Cre<sup>+/-</sup>*, *Isl1-Cre<sup>+/-</sup>/Brg1<sup>fl/+</sup>* and *Isl1-Cre<sup>+/-</sup>/Brg1<sup>fl/fl</sup>* E10.5 embryos. Data are mean±SEM, n=3.

### 3.5.5 *Isl1* recruits the *Brg1* complex to its target sequences

To examine whether *Brg1* was directed to *Isl1* target sequences via *Isl1*, we performed *Brg1* ChIP in control and *Isl1* KD CPCs followed by qPCR analysis. Knockdown of *Isl1* led to a significant reduction of *Brg1* occupancy at *Isl1* targets (Figure 38), suggesting that *Isl1* might recruit the *Brg1* complex to promote chromatin reorganization at its target genes.

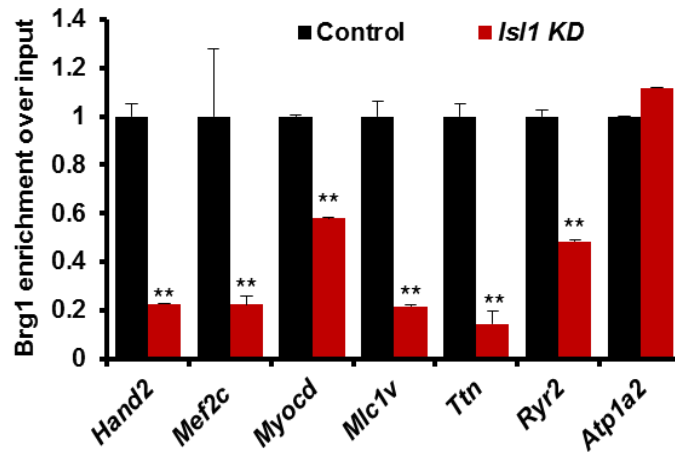


**Figure 38 Brg1 binding at *Isl1*- bound targets is decreased by *Isl1* depletion in CPCs**

ChIP followed with qPCR analysis with *Isl1* antibody was done in control and *Isl1* KD mESC-derived CPCs. *Atp1a2* was used as a negative control (n=2).

## 3.6 *Isl1* acts as a pioneer factor in cardiogenesis

### 3.6.1 *Isl1* binding correlates with sites of open chromatin

Pioneer transcription factors play critical roles in programming the epigenome and instructing lineage specification and differentiation (Zaret and Carroll 2011, Spitz and Furlong 2012, Soufi, Garcia et al. 2015). To initiate cell programming, pioneer transcription factors engage “closed” chromatin covered by nucleosomes and impart competence for transcription by chromatin opening. To test whether *Isl1* acts as a pioneer factor, we analyzed whether *Isl1* binding might induce the formation of accessible chromatin in CPCs by performing genome-wide analysis of open chromatin landscapes using ATAC (“assay for transposase-accessible chromatin”) sequencing (ATAC-Seq) (Buenrostro, Giresi et al. 2013) in mESC-derived CPCs. In ATAC-Seq, Tn5 transposase integrates sequencing adapters into regions of accessible chromatin, whereas steric hindrance in less accessible chromatin makes such transposition less probable (Buenrostro, Giresi et al. 2013). Therefore, amplifiable DNA fragments suitable for high-throughput sequencing are preferentially generated at locations of open chromatin (Buenrostro, Giresi et al. 2013).

Comparison of ATAC-Seq data and *Isl1* binding profiles revealed a 42% overlap of *Isl1* ChIP-Seq and ATAC-Seq peaks in CPCs. At the promoter proximal regions (TSS +/-10kb) more than 76% of *Isl1* binding sites showed open chromatin (Figure 39A). GO analysis of genes characterized by open chromatin at *Isl1* binding sites showed enrichment of genes involved

in transcriptional regulation, covalent chromatin modification and heart morphogenesis (Figure 39B-C), suggesting a role of *Isl1* binding in the formation of accessible chromatin required for cardiogenesis, similar to other “pioneer factors”.

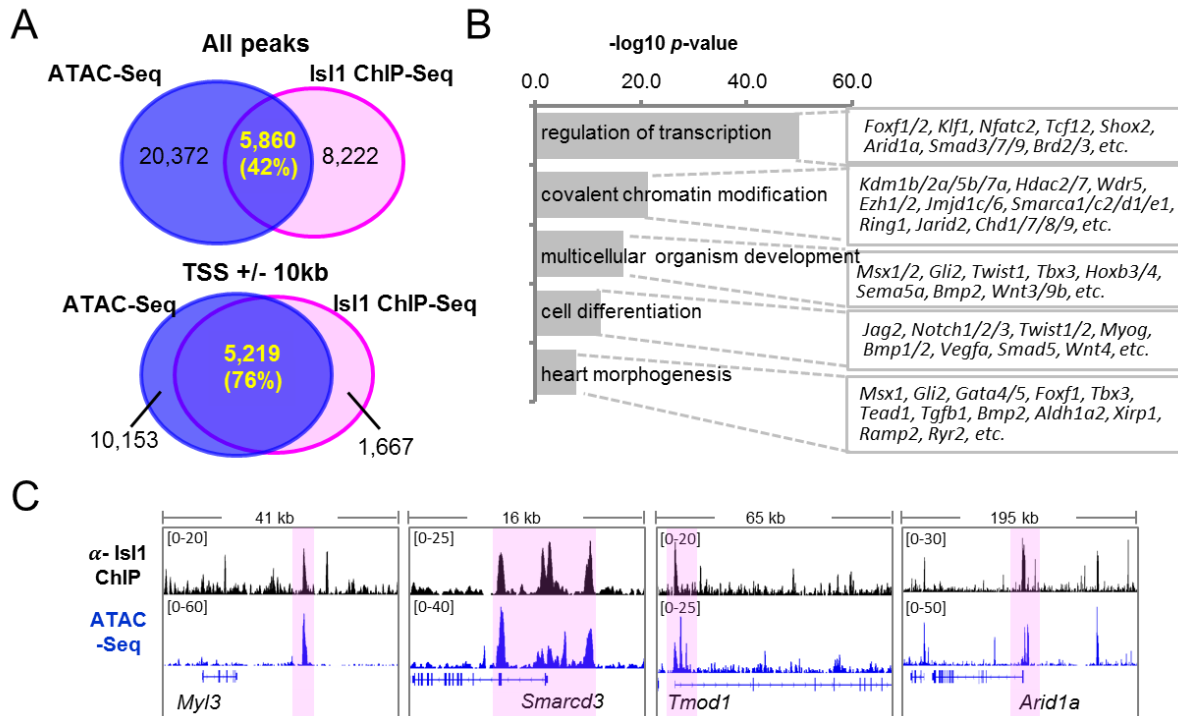


**Figure 39** *Isl1* binding correlates with sites of open chromatin

(A) Overlap of all *Isl1* ChIP-Seq and ATAC-Seq peaks (top) or peaks at Transcription Start Sites (TSS) +/- 10kb (down) in mESC-derived CPCs. (B) Representative genes and GO terms enriched in genes showing open chromatin configuration at *Isl1* binding sites in CPCs. (C) Examples of genes bound by *Isl1*, showing open chromatin configuration at *Isl1* binding sites in mESC-derived CPCs. Genome tracks of *Isl1* ChIP-Seq and ATAC-Seq reads of mESC-derived CPCs.

### 3.6.2 *Isl1* and Brg1/Baf60c complex work synergistically to open the chromatin during SHF development

As described in the introduction, the typical activity of a pioneer factor is to bind to the closed chromatin; then recruit chromatin remodelers to the binding sites and they work cooperatively to open the chromatin. To further investigate how *Isl1* opens the closed chromatin during cardiogenesis, we hypothesized that *Isl1* works together with Brg1/Baf60c remodeling complex to reorganize the chromatin landscape at its target genes. To confirm our hypothesis, we analyzed whether loss of *Isl1* or *Brg1* might affect chromatin opening by performing ATAC-Seq in E8.5 (6 somites) wild-type, *Isl1*<sup>-/-</sup> or *Isl1*-Cre<sup>+/-</sup>/*Brg1*<sup>fl/fl</sup> embryos. We observed 73% overlap of all ATAC-Seq peaks in E8.5 embryos compared to ESC-derived CPCs,



while up to 93% overlap at promoter proximal regions (Figure 40A), showing high similarity between the open chromatin of *in vitro* differentiated CPCs to CPCs in early embryos. Importantly, we observed significant reduction of chromatin accessibility in *Isl1* and *Brg1* knockout embryos at *Isl1*-ATAC (IA) peaks (Figure 40B-C), whereas chromatin accessibility was not affected at ATAC only (A) sites in *Isl1* knockout embryos (Figure 40C). In addition, the high average ATAC signal at *Isl1*-ATAC (IA) sites compared to ATAC only (A) sites further supports a role of *Isl1* in chromatin opening in CPCs (Figure 40C).

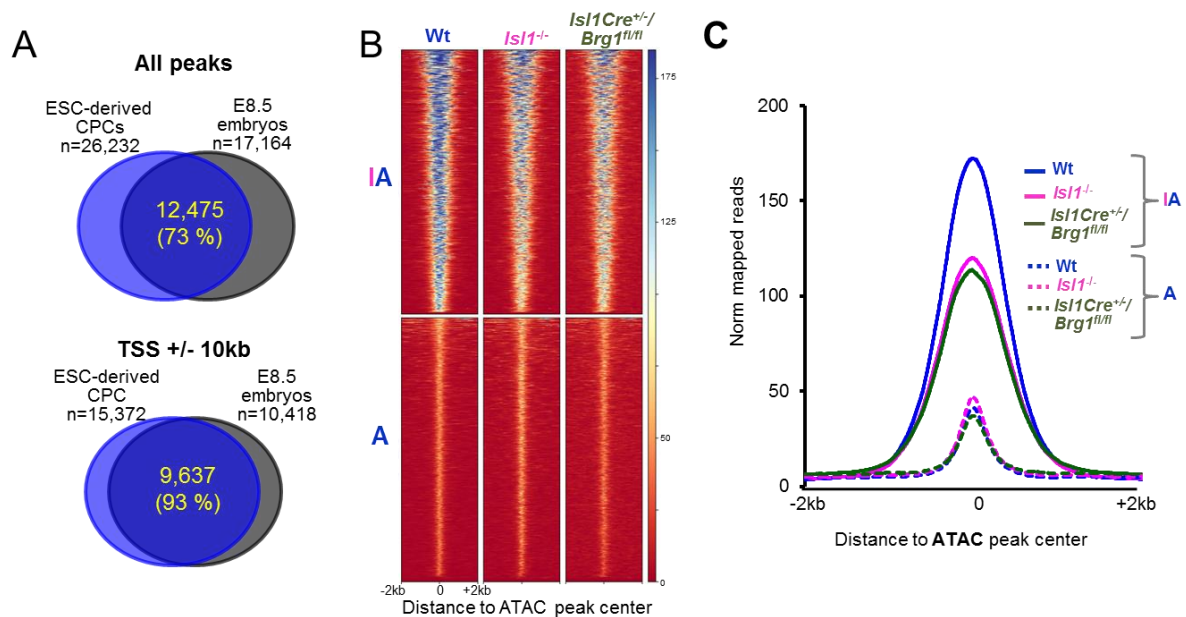


**Figure 40** *Isl1* and *Brg1*-Baf60c-based SWI/SNF complex shape the chromatin landscape at *Isl1* target sites in cardiac progenitors

(A) Overlap of all ATAC-Seq peaks (top) or peaks at Transcription Start Sites (TSS) +/- 10kb (bottom) in ESC-derived CPCs and E8.5 embryos. (B) Heat map of tag densities of ATAC-Seq in wild-type, *Isl1*<sup>-/-</sup> and *Isl1*-*Cre*<sup>+/+</sup>/*Brg1*<sup>fl/fl</sup> embryos at TOP1000 *Isl1*-ATAC (IA) or ATAC only (A) peaks. (C) Average ATAC-Seq tag intensities in wild-type, *Isl1*<sup>-/-</sup> and *Isl1*-*Cre*<sup>+/+</sup>/*Brg1*<sup>fl/fl</sup> embryos at *Isl1*-ATAC (IA) or ATAC only (A) peaks.

GO analysis of differential ATAC-Seq peaks in *Isl1* and/or *Brg1*-deficient embryos revealed that the *Isl1*/*Brg1* complex plays a key role in activating expression program essential for heart development, while repressing nervous system development (Figure 41A-B). Importantly, we observed significant overrepresentation of GO terms related to chromatin modification in ATAC-Seq peaks decreased in *Isl1* knockout embryos, including multiple components of the SWI/SNF chromatin remodeling complexes such as *Smarcd3* (*Baf60c*), *Arid1a* (*Baf250a*), *Smarcc2* (*Baf170*), *Dpf3* (*Baf45c*) as well as *Pbrm1* (*Baf180*) (Figure 41A and

41C). In addition, some target genes showed decreased chromatin accessibility only in *Isl1* knockout embryos (Figure 41C, e.g. *Dpf3* and *Tbx3*), suggesting that *Isl1* might work together with other chromatin modifiers in regulating these genes. In contrast, genes not bound by *Isl1* did not show changes in chromatin accessibility (Figure 41C, e.g. *Myh3*).

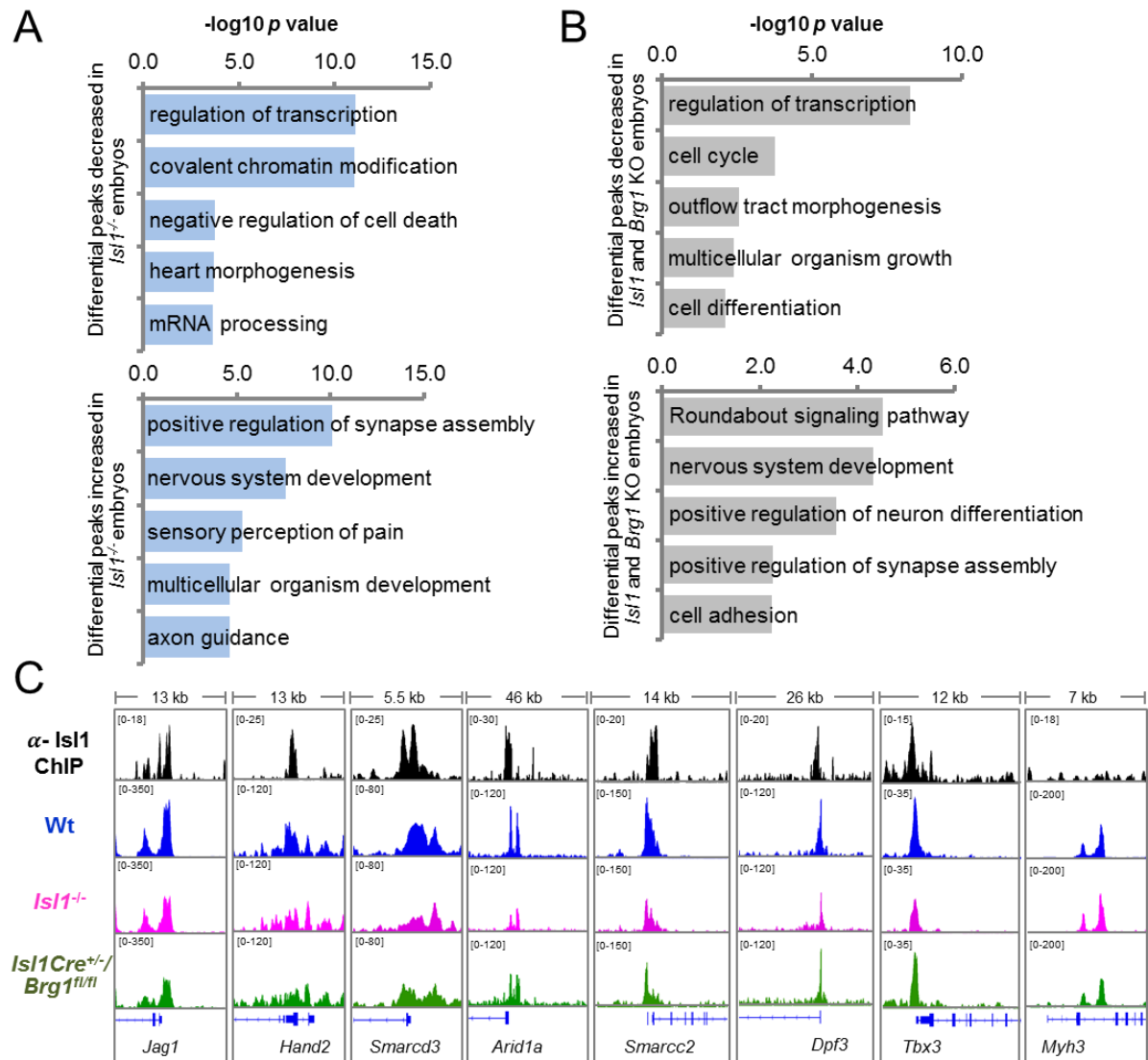


**Figure 41 *Isl1* and *Brg1*-Baf60c-based SWI/SNF complex induces chromatin reorganization in cardiac progenitors**

(A) GO terms enriched in ATAC-Seq peaks decreased (top panel) or increased (lower panel) more than 2 fold in *Isl1*<sup>-/-</sup> versus control embryos. (B) GO terms enriched in ATAC-Seq peaks decreased (top panel) or increased (lower panel) in both *Isl1*<sup>-/-</sup> and *Isl1*-*Cre*<sup>+/+</sup>/*Brg1*<sup>fl/fl</sup> embryos versus control embryos. (C) Examples of genes showing decreased ATAC-Seq signal at *Isl1* binding sites. Genome tracks of *Isl1* ChIP-Seq and ATAC-Seq of wild-type, *Isl1*<sup>-/-</sup> and *Isl1*-*Cre*<sup>+/+</sup>/*Brg1*<sup>fl/fl</sup> embryos are presented. *Myh3* was shown as a negative control.

### 3.6.3 *Isl1* plays a pioneering function in all three cardiovascular lineages

As described in the introduction, *Isl1*-positive cardiovascular progenitors are multipotent and can differentiate into all three cardiovascular lineages: cardiomyocytes, smooth muscle cells and endothelial cells (Moretti, Caron et al. 2006). Analysis of chromatin accessibility at promoters of cardiac, smooth muscle and endothelial development/differentiation genes revealed decrease in open chromatin at all cardiovascular lineage-related genes in *Isl1* and *Brg1*-deficient embryos (Figure 42A-D). Notably the ATAC-Seq signal was highly decreased at genes involved in cardiac contraction (Figure 42B). Nevertheless, these data suggest that *Isl1* might play a pioneering function for cardiac cell lineage settlement and requires the *Brg1*-based SWI/SNF chromatin remodeling complex.

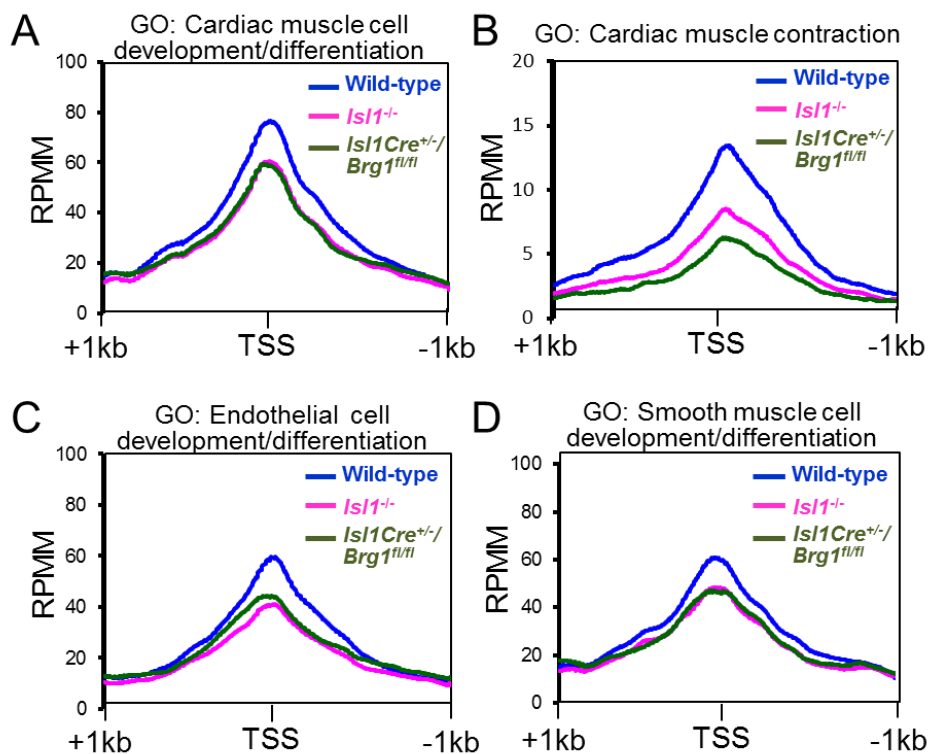


**Figure 42 *Isl1* and *Brg1*-Baf60c complex promote chromatin accessibility in all three cardiovascular lineages**

(A-D) Average ATAC-Seq tag intensities at TSS +/- 1kb of cardiac development and differentiation genes (A), cardiac contraction genes (B), as well as smooth muscle (C) and endothelial (D) development and differentiation genes in E8.5 wild-type, *Isl1*<sup>-/-</sup> and *Isl1*<sup>Cre<sup>+/+</sup></sup>/*Brg1*<sup>fl/fl</sup> embryos.

### 3.6.4 Isl1 acts as a pioneer factor independently of Gata4

The core cardiac transcription factor Gata4 represents a prototypical example of a pioneer factor, it binds efficiently to its target sequences on nucleosomal DNA (Cirillo and Zaret 1999) and induces chromatin reorganization driving heart development and disease (He, Gu et al. 2014). To address whether Gata4 binding might affect Isl1 binding or *vice versa*, we first compared the binding sites of Gata4 (Luna-Zurita, Stirnimann et al. 2016) and Isl1 in CPCs with ATAC-Seq peaks. Using the published Gata4 ChIP-exo data (Luna-Zurita, Stirnimann et al. 2016), we called peaks in each replicate and used high confidence peaks found in all three ChIP-Seq replicates for further analysis. This analysis identified 2,417 common Isl1-Gata4-ATAC peaks, showing that Isl1 and Gata4 often co-occupy at sites characterized with open chromatin (Figure 43). In addition, we identified accessible chromatin sites bound only by Isl1 or Gata4, supporting the notion that Isl1, similar to Gata4, might function as a pioneer transcription factor (Figure 43).

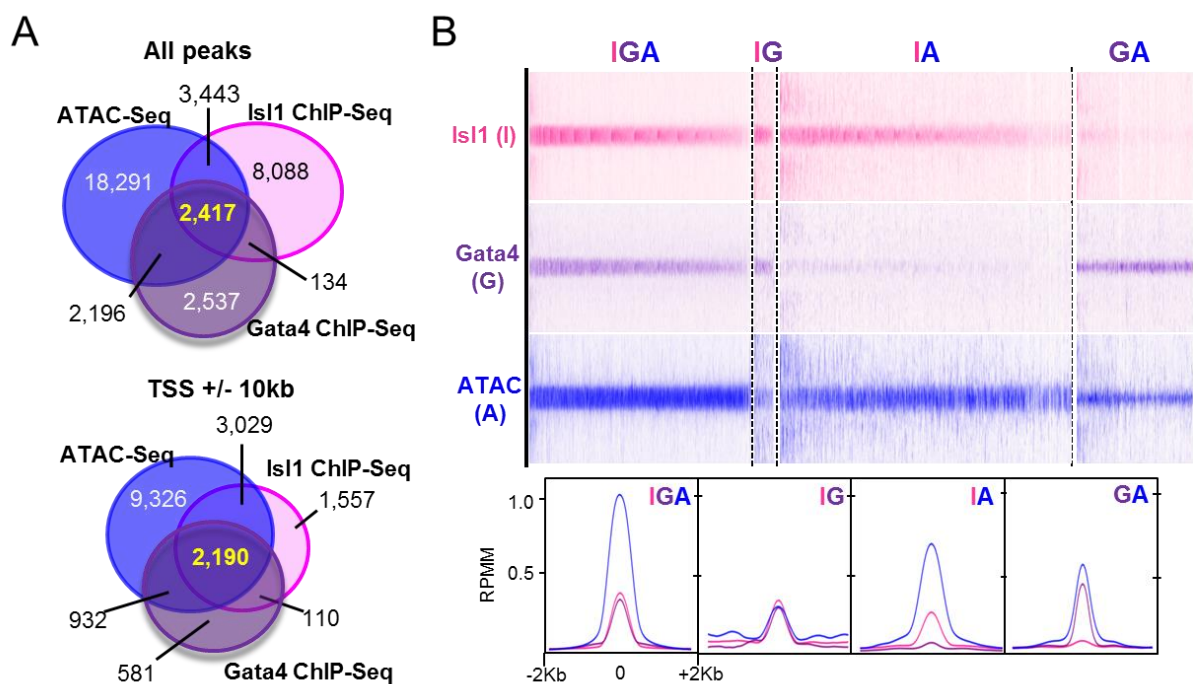


**Figure 43 Isl1 acts as a pioneer factor like Gata4**

**(A)** Overlap of all Isl1 ChIP-Seq, Gata4 ChIP-exo (Luna-Zurita, Stirnimann et al. 2016) and ATAC-Seq peaks (top) or peaks at Transcription Start Sites (TSS)  $\pm 10$ kb in CPCs. **(B)** Heatmap (top) and aggregation plot (bottom) of mapped reads of Isl1 ChIP-Seq, Gata4 ChIP-exo and ATAC-Seq at  $\pm 2$  kb around peak midpoints of Isl1, Gata4 and ATAC (IGA), Isl1 and Gata4 (IG), Isl1 and ATAC (IA), Gata4 and ATAC (GA) occupancy.

Moreover, ATAC-Seq analysis in E8.5 embryos with loss of *Isl1* or *Brg1* showed reduction in chromatin accessibility in both *Isl1*-ATAC sites bound or not bound by Gata4 (IGA or IA only), supporting the notion that *Isl1* acts as pioneer factor also independently of Gata4 (Figure 44).

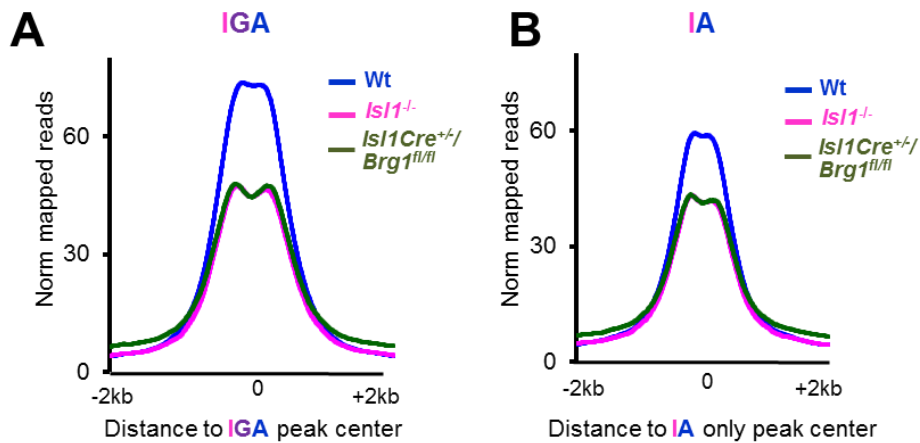


**Figure 44 *Isl1* acts as a pioneer factor independently of Gata4**

Average ATAC-Seq tag intensities at common peaks between *Isl1*, Gata4 and ATAC-Seq (IGA) in wild-type, *Isl1*<sup>-/-</sup> and *Isl1*-*Cre*<sup>+/+</sup>/*Brg1*<sup>fl/fl</sup> embryos (A) or at *Isl1* and ATAC-Seq only peaks (IA) (B).

In addition, Gata4 binding was decreased in *Isl1* depleted CPCs (Figure 45), however we cannot rule out whether *Isl1* is necessary for Gata4 association at *Isl1* target sites or that lower Gata4 occupancy could be due to the decreased levels of Gata4 in *Isl1*-deficient CPCs (Figure 20).

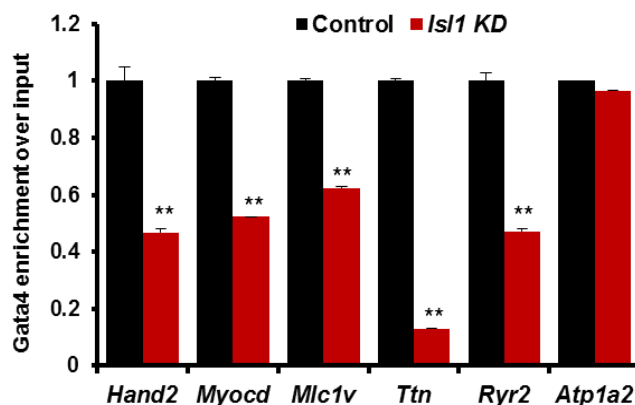


**Figure 45 Gata4 occupancy at *Isl1*- bound sequences is decreased in *Isl1* deficient CPCs**

ChIP-qPCR analysis of Gata4 binding at *Isl1* target sites in CPCs. *Atp1a2* was used as a negative control (n=2).

### 3.7 Working model

Taken together, these data suggest a pioneering function of *Isl1* in SHF development. *Isl1* acts as a pioneer transcription factor by binding to closed chromatin and then recruits the Brg1-Baf60c-based SWI/SNF complex to its target binding sites. *Isl1* works in concert with the Brg1-Baf60c-based SWI/SNF complex to confer permissive lineage-specific alterations in CPC chromatin landscape, which allow gene expression directly in CPCs or at a later time point in cardiomyocytes (Figure 46). Expression changes of *Isl1* target genes lead to cardiac development defects not only at the early embryonic stages, but also at the later stages when *Isl1* transcription is turned off.

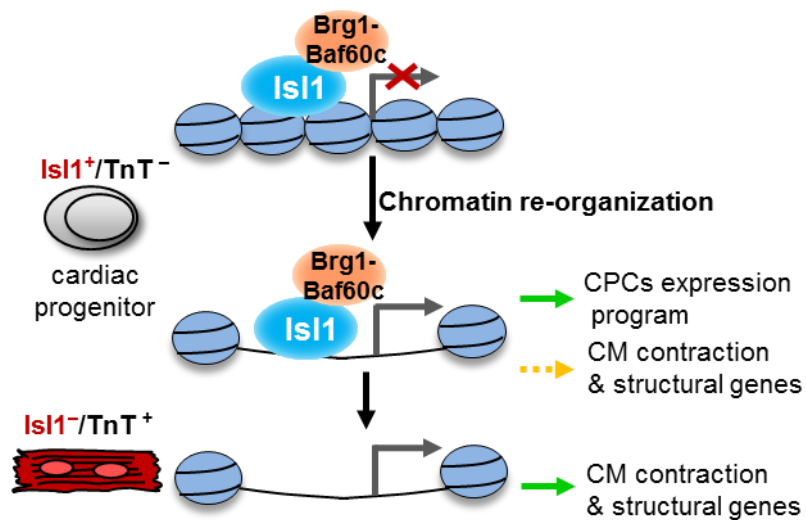


**Figure 46 Model of the role of *Isl1* in cardiogenesis by controlling epigenetic mechanisms and memory**

*Isl1* binds to compacted chromatin at genes involved in CPC function, as well as to genes involved in cardiomyocyte contraction and structural organization. *Isl1* then recruits Brg1-Baf60c complex to the binding sites and works cooperatively with the Brg1-Baf60c-based SWI/SNF complex to open up chromatin and allow gene expression directly in CPCs, or at a later time point in cardiomyocytes.

## 4. Discussion

The mammalian heart is the first functional organ to develop. Normal cardiac development is crucial for embryonic survival due to its critical nature in distributing blood through the vessels and the vital exchange of nutrients, oxygen, and wastes both to and from the developing baby. Heart development is controlled by a tight spatial and temporal regulation of gene networks, including signaling molecules, transcription factors and so on. Accurate knowledge of normal cardiac development is essential for proper understanding of congenital cardiac malformations that represent the most common congenital anomaly in newborns (Schleich, Abdulla et al. 2013), and might help to generate efficient therapies.

During cardiac development, heart tube elongation occurs by progressive addition of second heart field (SHF) progenitor cells to the poles of the heart. Unlike FHF cells, SHF cells show continued proliferation and delayed differentiation, and represent a reservoir of multipotent cardiac progenitor cells (CPCs) during cardiogenesis (Meilhac, Lescroart et al. 2014). Perturbation of SHF development results in congenital heart defects. As described in the introduction part, SHF derived cells are involved in most of the common CHDs, especially in the outflow tract (OFT) region. These include arterial pole defects resulting from OFT hypoplasia or failure of OFT remodeling, especially the OFT alignment and septation defects, such as persistent truncus arteriosus (PTA), transposition of the great arteries (TGA), overriding aorta (OA), which is usually associated with Tetralogy of Fallot (TOF) and double outlet right ventricle (DORV), in which the divided aorta and pulmonary trunks both exit the right ventricle (RV) only, as well as venous pole anomalies including atrial and atrioventricular septal defects (Kelly 2012, Neeb, Lajiness et al. 2013).

The SHF is marked by *Isl1* expression (Cai, Liang et al. 2003, Buckingham, Meilhac et al. 2005). *Isl1* plays critical roles in cardiac development which has been demonstrated by a lot of studies (Cai, Liang et al. 2003, Moretti, Caron et al. 2006, Moretti, Lam et al. 2007, Bu, Jiang et al. 2009, Wang, Li et al. 2016, Quaranta, Fell et al. 2018). However, detailed insights into its molecular mode of action underlying *Isl1* function in cardiac progenitor cells have not been fully elucidated, especially in epigenetic regulation during cardiogenesis.

In this study, using an *Isl1* knockout mouse line and an *Isl1* hypomorphic mouse line, we established directed cardiac differentiation method and genome-wide profiling of *Isl1*,

binding together with RNA- and ATAC-sequencing of cardiac progenitor cells and their derivatives, we uncover a regulatory network downstream of *Isl1* that orchestrates cardiogenesis. We show that *Isl1* binds to and regulates the expression of signaling molecules, transcription factors, epigenetic modifiers, and cardiomyocytes structural/contraction genes, with critical functions in cardiogenesis. We further identified *Isl1* as a novel pioneer factor which works in concert with Brg1-Baf60c-based SWI/SNF complex to open the “closed” chromatin and orchestrating gene expression programs during cardiogenesis.

#### **4.1 *Isl1* is critical for SHF development and depletion of *Isl1* leads to cardiac defects as seen in human CHD patients**

As the *Isl1* knockout mouse are lethal at early stage during embryonic development, we utilized an *Isl1* hypomorphic mouse line which can survive until birth, allowing us to analyze the role of *Isl1* in SHF derived structures that are dependent on *Isl1*, as well as the molecular regulation of *Isl1* during later stages of embryonic heart development. *Isl1* hypomorphic mouse embryos showed ventricular and atrial septal defects (VSDs and ASDs) and various degrees of OFT abnormalities, including partial outflow tract septation and misalignment or common arterial trunk (data done by our collaborators). Similarly, in human patients, genetic variations in *ISL1* have been associated with susceptibility to ventricular septal defect (Lang, Tian et al. 2013) and non-syndromic, complex congenital heart disease (Stevens, Hakonarson et al. 2010), whereas *ISL1* haploinsufficiency is associated with d-transposition of the great arteries (Osoegawa, Schultz et al. 2014).

Intersection of the RNA-Seq results from *Isl1* KO and *Isl1* hypomorphic embryos, together with *Isl1* ChIP-Seq data, identified many novel *Isl1* primary targets. Consistent with the phenotypes observed in the mouse models, we found an important group of *Isl1* target genes playing key roles in outflow tract morphogenesis, such as *Wnt5a/11*, *Tgfb2*, *Jag1*, *Smad6*, *Pbx3*, *Msx2*, *Fog2* (*Zfpm2*), *Tbx1/3/20*, *Plxna2* (Lin, Lin et al. 2012). In addition, many *Isl1* target genes are critical for development of the atrioventricular canal and atrial or ventricular septation, such as *Wnt2*, *Gata4/6*, *Tbx5*, *Nkx2.5* and *Hand1/2* (Lin, Lin et al. 2012, Bruneau 2013). Moreover, mutations in these genes have been found in human CHD cases. For example, *TBX20* loss-of-function mutations are present in patients with ToF, PTA and



DORV (Pan, Geng et al. 2015, Huang, Wang et al. 2017). Mechanistically, this loss-of-function mutation resulted in reduced synergistic activation between TBX20 and NKX2.5 as well as GATA4 (Huang, Wang et al. 2017). Multiple mutations in NKX2.5 and GATA4 have also been causally linked to various types of CHD, such as ASD, VSD and ToF (McElhinney, Geiger et al. 2003, Ding, Tong et al. 2015, Mattapally, Nizamuddin et al. 2015). GATA6 mutations are found in CHD cases with PTA, VSD or ToF (Kodo, Nishizawa et al. 2009, Meenakshi Maitra 2010, Wang, Luo et al. 2012). A heterozygous mutation in HAND2 (p.S65I), which significantly diminished its transcriptional activity, was identified in a patient with congenital ventricular septal defect (VSD) as well (Sun, Wang et al. 2016).

As described in the introduction, cardiac neural crest cells (CNCCs) migrate to the OFT region during cardiac development and play an essential role in OFT septation and alignment, which is a very important process and various common types of CHDs are caused by disruption of this process. Cells from SHF and CNCCs communicate with each other and work cooperatively to form different cardiovascular structures. Semaphorin 3c (Sema3c) is an important factor in this communication. During heart development, the OFT myocardium secretes Sema3c (ligand) to attract CNCCs, which express Plxna2 (receptor), and promotes them to migrate into the OFT (Lin, Lin et al. 2012). Knockout of Plxna2 or Sema3c in mice impairs the migration of neural crest cells, leading to PAA defects and PTA (Christopher B. Brown 2001, Leonard Feiner 2001). Interestingly, both Sema3c and Plxna2 are *Isl1* direct targets found in our study and showed decreased levels with *Isl1* loss-of-function. Besides, *Isl1* is also reported to be expressed in a subset of CNCCs (Engleka, Manderfield et al. 2012). So, *Isl1* may play a role in regulating CNCCs behaviors not only by the interactions between SHF and CNCCs, but could also function directly in CNCCs. The role of *Isl1* in regulating both SHF cells and CNCCs in the OFT may give a better explanation of various OFT defects observed in the *Isl1* hypomorphic embryos.

In addition, we also found many genes associated with epithelial to mesenchymal transition (EMT) to be downregulated in our *Isl1* hypomorphic data and bound by *Isl1*, such as *Wnt5a*, *Bmp4*, *Tgfb2*, *ErbB3*, *Snai1/2*, *Twist1/2*, *NFATc2/4* and *Msx1/2* (Lin, Lin et al. 2012, von Gise and Pu 2012, Bruneau 2013). EMT is an important process during cardiac development. Epicardial cells give rise to mesenchymal cells that migrate into the myocardium and differentiate into fibroblasts and coronary smooth muscle cells (von Gise and Pu 2012). The

atrioventricular cushion mesenchyme forms from an EMT of endocardial cells, further leading to the formation of mitral and tricuspid (atrioventricular) valves and cardiac chamber septation (Lin, Lin et al. 2012, von Gise and Pu 2012). The cushions in the OFT also arise from endocardium through EMT, in combined with CNCCs, contribute to aortic and pulmonic (semilunar) valves development and OFT septation (Lin, Lin et al. 2012, von Gise and Pu 2012). Errors of EMT lead to CHD (von Gise and Pu 2012, Rickert-Sperling, Kelly et al. 2015), especially cardiac septal defects and valve defects, as well as OFT defects. In the *Isl1* hypomorphic mice, in addition to ASDs and VSDs, we also observed aortic stenosis, which is a narrowing of the aortic valve opening. Thus, disruption of EMT process could be another reason for CHD caused by *Isl1*.

## **4.2 *Isl1* organizes a regulatory gene network driving second heart field development**

The analysis of our high-throughput sequencing datasets revealed a genome-wide transcriptional regulatory network orchestrated by *Isl1* during SHF development. We found that *Isl1* directly regulates large groups of genes during cardiogenesis. In addition to known *Isl1* targets, we identified a lot of novel primary downstream targets, many of which have been reported to be involved in heart development or are critical for SHF specification and expansion, especially signaling molecules and cardiac transcription factors. For example, *Fgf10*, a known *Isl1* target, acts as a marker of the anterior SHF (Golzio, Havis et al. 2012, Watanabe, Zaffran et al. 2012). Together with *Fgf8*, *Fgf10* promotes the proliferation of the cardiac progenitor cells that form the arterial pole of the heart (Watanabe, Zaffran et al. 2012). Interestingly, *Fgf8* was also found to be an *Isl1* direct downstream target in our study. It is required for SHF expansion, and thus for OFT elongation, septation and subsequent ventriculoarterial alignment through a cell autonomous mechanism (Hubert, Payan et al. 2018, Pérez-Pomares and Kelly 2018). Besides, *Wnt2* is a newly identified *Isl1* primary target in our data. Cell culture studies showed that *Wnt2*<sup>-/-</sup> ES cells exhibit impaired cardiomyocyte differentiation but enhanced hematopoietic differentiation (Wang, Gilner et al. 2007), which is consistent with our finding that *Isl1* controls cardiomyocyte lineage commitment, whereas inhibits hemopoiesis gene expression. In addition, the forkhead transcription factors *Foxc1* and *Foxc2*, which play key roles in cardiovascular development, are reported to act upstream

of *Isl1* in the SHF (Kang, Nathan et al. 2009). In this study, we found *Isl1* directly binds on both genes in CPCs. This mutual regulation is also seen between other cardiac transcription factors, such as *Gata4* and *Nkx2.5*, thus forms the complex transcriptional regulatory networks (Figure 6) in cardiogenesis.

Moreover, we did not observe any change in the expression of *Isl1* primary target genes in the left ventricle of *Isl1* hypomorphic embryos (data not shown), while they were significantly changed in dissected right ventricles (Figure 24), suggesting a specific role of *Isl1* in the second heart field. Interestingly, we also found some first heart field genes such as *Tbx5* and *Hand1*, also regulated by *Isl1* in the embryos (Figure 23 and 24). Since *Isl1* has been reported to be transiently expressed in CPCs of the first heart field (Laugwitz, Moretti et al. 2008), we cannot exclude a possibility that *Isl1* also plays a pioneer role in the first heart field. In addition, *Tbx5* was reported to play an essential role in the pSHF for atrial septation (Xie, Hoffmann et al. 2012) and *Hand1* was also reported to show expression in the SHF-derived myocardial cuff (Barnes, Firulli et al. 2010). Given the dynamic nature of cardiac gene expression, it cannot be ruled out that at some stages the FHF marker genes transiently expressed in the SHF and *vice versa*, even though they play a primary role in their own heart fields.

Importantly, in our cell culture studies and *in vivo* analysis, we found highly similar gene networks regulated by *Isl1*. For example, we found *Isl1* regulates cardiomyocyte structural genes and genes involved in cardiac contraction and sarcomerogenesis in both datasets (Figure 19 and 23), suggesting that *Isl1* directly controls cardiomyocyte identity, CPC differentiation and sarcomeric maturation. Moreover, consistent with our observation in *Isl1* hypomorphic cardiomyocytes with less prominent sarcomere structures, we also observed significant decrease of cardiomyocytes structural genes in the *Isl1* hypomorphic data at the later stages when *Isl1* is no longer expressed in the myocardium (Cai, Liang et al. 2003). We reason that *Isl1* binds to closed chromatin and spawns permissive cardiomyocyte lineage-specific alterations in the chromatin landscape of CPCs, which enables subsequent recruitment of additional regulatory factors activating these genes in cardiomyocytes when *Isl1* itself is switched off, thereby setting up a lasting regulatory network driving cardiogenesis.

In addition, data done by my colleague with *Isl1* loss-of-function at distinct stages of directed cardiac differentiation of mouse ESCs (Wamstad, Alexander et al. 2012) (data not shown) further confirm the transient requirement of *Isl1* in CPCs for the expression of cardiomyocyte structural and contraction genes. Briefly, cardiomyocyte marker genes and *Isl1* direct targets were significantly downregulated in day10 cardiomyocytes only when *Isl1* was knocked down at day3.7 during the differentiation of mesodermal precursors into cardiac progenitors but not at day8 after the appearance of beating cardiomyocytes. Taken together, our study supports the requirement of *Isl1* in CPCs in setting up a transcriptional program to ensure proper cardiomyocyte differentiation.

### **4.3 Baf60c is a key downstream target of *Isl1***

Among the targets of *Isl1* identified in our data, one of the targets, *Baf60c* (*Smarcd3*), a cardiac-specific component of the Brg1-based SWI/SNF chromatin remodeling complex, attracted our attention, since epigenetic mechanisms are central to establishment and maintenance of transcriptional memory (Jaenisch and Bird 2003, Bernstein, Mikkelsen et al. 2006, Reik 2007). *Baf60c* is expressed specifically in the heart and somites in the early mouse embryo and *Baf60c* knockdown embryos by RNAi showed shortened OFT, hypoplastic right ventricle and atria, causing lethality at E10.0-E11.0, suggesting a specific role of *baf60c* in the SHF (Lickert, Takeuchi et al. 2004, Lei, Liu et al. 2013). Myofibrillar defects and impaired contractile function are found in postnatal mice with *Baf60c* conditional deletion in cardiomyocytes (Sun, Hota et al. 2017). *Baf60c* was shown to be essential for cardiac growth and cardiomyocyte function at several stages of embryonic development, by regulating broad networks of genes encoding proteins essential for function of the contractile apparatus (Sun, Hota et al. 2017). Consistent with this, *Baf60c* was further shown to be an important modulator of the fundamental program of gene expression essential for cardiac structure and function (Sun, Hota et al. 2017). This is highly consistent with our RNA-Seq results which showed that *Baf60c*-activated genes are associated with cardiomyocytes structure (sarcomere organization) and function (cardiac muscle contraction), as well as ion transport (Figure 31) which is critical in controlling the contractile apparatus (Kuo and Ehrlich 2015). This is accordant with the reported data in *Baf60c*<sup>-/-</sup> embryonic hearts (E10.5 and

E12.5) and P7 *Baf60c*<sup>Myh6KO</sup> neonatal hearts (Sun, Hota et al. 2017), which identified Baf60c targets such as *Myf1/3/4/7*, *Tnni1/2*, *Casq1* and *Tcap*, that are also shown in our results.

As a downstream target of *Isl1*, Baf60c shares quite a lot of common targets with *Isl1* (up to 43%) in cardiac progenitor cells (Figure 32), including signaling molecules such as *Wnt2* and *Jag1*, transcription factors such as *Myocd* and *Hopx*, and especially cardiomyocytes structural genes such as *Myf2/3/4*, *Tnnt2*, *Actn2* and *Myh6*, and cardiac contraction associated genes such as *Atp1b1*, *Camk2d*, *Ryr2* and *Tnni1*. We found that Baf60c together with *Isl1* is required for the activation of genes involved in cardiomyocyte contraction, sarcomere organization and transcriptional regulation, whereas Baf60c alone activates genes participating in ion transport (Figure 31 and Figure 32). This is consistent with the gene expression changes observed in *Baf60c* knockout embryos (Sun, Hota et al. 2017).

#### **4.4 *Isl1* works together with Brg1-Baf60c-based SWI/SNF complex to regulate gene expression program during cardiogenesis**

Baf60c is a subunit of the Brg1-based SWI/SNF complex, which plays an important role in heart development (Hota and Bruneau 2016). Brg1, as the core catalytic subunit in this complex, was reported to be involved in cardiogenesis by more and more studies (Bultman, Gebuhr et al. 2000, Griffin, Curtis et al. 2010, Hang, Yang et al. 2010, Chang 2012, Wei Li, Yiqin Xiong et al. 2012, Alexander, Hota et al. 2015, Qian, Xiao et al. 2017, Hota, Johnson et al. 2019). *Mef2c-Cre Brg1*<sup>f/f</sup> embryos showed hypoplastic outflow tracts and right ventricles (Hang, Yang et al. 2010). Accordingly, in our study, using an *Isl1-Cre*, Brg1-deficient embryos showed a shortened outflow tract, a small right ventricle at E9.5 and died by E14.5. Consistent with severe SHF structure defects, we observed that the expression of *Isl1* target genes involved in outflow tract formation and SHF specification (*Mef2c*, *Tbx20*, *Hand2*, *Smarcd3*, and so on) was shown to be impaired in SHF derivatives of *Isl1/Brg1* double heterozygous embryos, and further decreased in *Isl1-Cre*<sup>+/-</sup>/*Brg1*<sup>f/f</sup> embryos (Figure 23 and 36). This is quite similar with the publication that the requirement of the balance between the dosage of Brg1 and disease-causing cardiac transcription factors, including *Tbx5*, *Tbx20* and *Nkx2.5* in heart development (Takeuchi, Lou et al. 2011). Thus, disruption of a delicate balance between *Isl1* and Brg1/BAF complex could also be a mechanistic cause of CHDs shown in *Isl1* haploinsufficiency patients (Osoegawa, Schultz et al. 2014).

Moreover, Brg1 interacts with cardiac transcription factors Tbx5, Nkx2.5 and Gata4, and this interaction is induced by Baf60c (Lickert, Takeuchi et al. 2004). In our study, we also found Brg1 and Baf60c interact with the transcription factor Isl1 in cardiac progenitor cells (Figure 33). In contrast, Baf60c does not seem to moderate Isl1 binding to the Brg1 complex, since we observed similar levels of Brg1 was co-immunoprecipitated by Isl1 in *Baf60c* KD CPCs compared with control (Figure 34). Considering Baf60c as a direct target of Isl1 (Figure 29), the loss of Baf60c upon Isl1 depletion may additionally affect the function of Tbx5, Nkx2.5 and Gata4, as an imbalance between their levels and the Brg1-Baf60c complex, was shown to result in impaired cardiac development and transcriptional activation of their targets (Takeuchi, Lou et al. 2011).

The interaction of Isl1 with Brg1/Baf60c led us to think that Isl1 may work cooperatively with Brg1 to induce chromatin reorganization and regulate target gene expression in cardiac progenitor cells. By comparing the ChIP-Seq data for Brg1 and Isl1, we noticed that they are highly co-occupied at Isl1 target sites in cardiac progenitors, especially near the TSS (Figure 35). Furthermore, they share a large group of common targets, such as *Wnt2*, *Smarcd3*, *Ryr2* and *Tbx20*. (Figure 36 and 37). A newly published study showed that Brg1-activated genes are enriched for sarcomere organization and assembly, heart morphogenesis and cardiac contraction, with a genome-wide transcriptome analysis in CPCs (Hota, Johnson et al. 2019). This is prominently consistent with what we found in our *Isl1* KO CPCs (Figure 19) and our in vivo data (Figure 23). Furthermore, we observed that Brg1 occupancy on Isl1 target sites was decreased with *Isl1* loss-of-function (Figure 38). Taken all together, we conclude that Isl1 might recruit the Brg1 complex to regulate nucleosome structure and expression of its target genes.

#### **4.5 Isl1 functions as a pioneer factor during cardiogenesis**

In this study, we showed that Isl1 recruits the Brg1-based SWI/SNF complex to its target sites to promote chromatin accessibility, which is the typical working pattern of pioneer factors (Figure 10) (Iwafuchi-Doi 2019). Furthermore, Brg1 was reported to initiate cardiac gene expression in cardiac precursor cells and maintain the cardiac program to facilitate cardiomyocyte differentiation by modulating temporal chromatin accessibility together with

Baf60c and Baf170 (Hota, Johnson et al. 2019). This suggests that Isl1 might work as a pioneer factor in organizing the transcription regulation in cardiac development. The classic characteristic of pioneer factors is capable of binding closed chromatin and open chromatin regions. A postdoc in our lab performed nucleosome assembly assays using *in vitro* assembled nucleosomes with recombinant human histones and a DNA fragment containing Isl1 motifs within the *Ttn* promoter, which is bound by Isl1 (Wang, Li et al. 2016) and downregulated in *Isl1* and *Baf60c* depleted CPCs (Figure 32), followed with electrophoretic mobility shift assays (EMSA), which have been used to identify many pioneer factors (Lai, Verhage et al. 2018). She found that Isl1 recognizes its DNA binding motif even when the DNA is wrapped around nucleosomes, which enables it to engage its target sites even in condensed chromatin. In combination with my data that Nkx2.5, which is supposed not to be a pioneer factor, only binds to the free *Ttn* probe but not to the assembled nucleosomes (data not shown), we further demonstrated that the binding of Isl1 to the nucleosomal DNA is specific.

We further performed ATAC-Seq, which is recently used to identify regions of open chromatin and assess genome-wide chromatin accessibility (Buenrostro, Giresi et al. 2013), in mESC-derived CPCs and in control versus *Isl1* and *Brg1* knockout embryos, to reveal that Isl1 acts as a pioneer factor to alter the chromatin accessibility in cardiac progenitor cells together with Brg1, thus modulate cardiomyocyte cell fate. ATAC-Seq analysis combined with genome-wide binding analysis of Isl1 revealed that open chromatin regions are centered on Isl1 binding sites in CPCs (Figure 39). Furthermore, ATAC-Seq analysis in *Isl1* and *Brg1*-deficient embryos together with control samples showed that loss of either *Isl1* or *Brg1* led to remarkable decrease of chromatin accessibility at ATAC/*Isl1* binding sites (IA), but no significant change in ATAC-Seq only sites (A, sites without *Isl1* binding) (Figure 40 and 41). In combination with the data showing *Isl1* recruits *Brg1* to its target sites (Figure 38), our data confirmed our hypothesis that *Isl1* acts as a pioneer factor and works in association with *Brg1* in shaping the chromatin landscape during cardiogenesis. Intriguingly, some target genes showed decreased chromatin accessibility only in *Isl1* knockout embryos, such as *Dpf3* and *Tbx3* (Figure 41), suggesting that *Isl1* might also work together with other chromatin remodelers to regulate their expression.

A large body of studies have demonstrated that the SWI/SNF complexes undergo progressive changes in subunit composition during developmental transitions and that the unique subunit composition at each developmental stage correlates with a gene expression program that is required for maintaining particular cell state (Wu, Lessard et al. 2009, Ho and Crabtree 2010, Toto, Puri et al. 2016). During cardiac differentiation, using immunoprecipitation with mass spectrometry, Hota et al. recently determined the dynamic composition of BAF complexes during mammalian cardiac differentiation, identifying several cell-type specific subunits (Hota, Johnson et al. 2019) (Figure 13) and there is a fine balance exists in the composition of the BAF complex (Hota, Johnson et al. 2019). Interestingly, we found significant decrease of chromatin accessibility at multiple components of the SWI/SNF chromatin remodeling complexes such as Smarcd3 (Baf60c), Arid1a (Baf250a), Smarcc2 (Baf170), Dpf3 (Baf45c), as well as Pbrm1 (Baf180) in *Isl1* knockout embryos, suggesting a mechanism by which *Isl1* reinforces its function in chromatin reorganization to drive cardiogenesis. Ablation of Baf250a, a critical regulatory subunit in SWI/SNF BAF complex, in the SHF using *Mef2c-Cre* leads to persistent truncus arteriosus, trabeculation defects, reduced cardiomyocyte proliferation and differentiation, and embryonic lethality around E13.0 (Lei, Gao et al. 2012). Baf180 deficiency in mouse embryos causes severe hypoplastic ventricle development and trophoblast placental defects, indicating a role of Baf180 in cardiac chamber maturation (Doerks, Copley et al. 2002). The cardiac-specific subunits of the complex, Baf45c and Baf60c, also play instrumental roles during cardiogenesis and cardiomyocyte differentiation (Lickert, Takeuchi et al. 2004, Lange, Kaynak et al. 2008, Sun, Hota et al. 2017). Baf170 was reported to facilitate cardiomyocyte differentiation, at least in part, via modulating chromatin accessibility (Hota, Johnson et al. 2019). Altogether, these data suggest that *Isl1* not only works in concert with Brg1-Baf60c-based SWI/SNF chromatin remodeling complex in shaping the chromatin landscape of its targets, but also functions in the reorganization of the chromatin structure of its subunits during cardiogenesis.

#### **4.6 *Isl1* plays a pioneering function independently of *Gata4***

During heart development, the complex morphogenetic and molecular events are regulated by many transcription factors, acting as a mechanistic link to the transcription apparatus for gene activation (Kathiriya, Nora et al. 2015). *Gata4* plays a key role in heart development



which was revealed by a lot of studies (Kuo, Morrisey et al. 1997{Lun Zhou, 2017 #3171, Watt, Battle et al. 2004, Rivera-Feliciano, Lee et al. 2006, Laforest and Nemer 2011}). It represents a prototypical example of a pioneer factor, which binds efficiently to its target sequences on nucleosomal DNA (Cirillo and Zaret 1999) and induces chromatin reorganization driving heart development and disease (He, Gu et al. 2014). Since *Isl1* and *Gata4* have overlapping expression in heart development (Heikinheimo, Scandrett et al. 1994), we analyzed whether *Gata4* binding affects the pioneering function of *Isl1* and *vice versa*. Comparison of *Gata4* and *Isl1* binding sites in CPCs with ATAC-Seq peaks, using the published *Gata4* ChIP-exo data (Luna-Zurita, Stirnimann et al. 2016), showed that 41% *Isl1* binding sites which characterized with open chromatin are co-bound by *Gata4* (Figure 43A), suggesting that *Isl1* and *Gata4* often co-occupy at target sites with accessible chromatin. This is consistent with the finding that *Gata4* and *Isl1* share common targets in the developing heart, such as *Hand2* (D.G. McFadden 2000). Furthermore, the ATAC-Seq signal at their co-occupied sites is higher than the ones they bind alone (Figure 43B bottom and Figure 44), suggesting that *Gata4* binding reinforces the pioneering function of *Isl1* or the pioneer functions of *Isl1* and *Gata4* lead to a synergistic effect on chromatin opening at their common target sites. Consistently, transcription of *Fgf10* mediated by *Isl1* is reported to be enhanced by the presence of *Gata4* (Golzio, Havis et al. 2012).

Moreover, we identified 59% of accessible chromatin sites with *Isl1* binding are not bound by *Gata4* (Figure 43), supporting the notion that *Isl1* functions as a pioneer transcription factor not depending on *Gata4* at these binding sites. In addition, the high average ATAC signal at *Isl1*-ATAC (IA) sites compared to ATAC only (A) sites further supports a role of *Isl1* in chromatin opening in CPCs (Figure 40). Importantly, reduction in chromatin accessibility was observed in both *Isl1*-ATAC sites bound or not bound by *Gata4* (IGA or IA) when *Isl1* is depleted in mouse embryos (Figure 44), supporting our conclusion that *Isl1* acts as pioneer factor independently of *Gata4*. Interestingly, we observed that *Gata4* binding at *Isl1* target sites was decreased in CPCs with *Isl1* loss-of-function in our study (Figure 45). Since *Gata4* is found to be a direct downstream target of *Isl1* in our study and knockout of *Isl1* leads to downregulation of *Gata4* in both mESC-derived CPCs and in embryonic tissues, the lower *Gata4* occupancy could be a result of reduced level of *Gata4* caused by *Isl1* loss-of-function.

## 4.7 Conclusions and perspectives

In our study, we found that *Isl1* is not only indispensable for early stage of cardiogenesis but also important for later stages of heart development. Reduced *Isl1* level caused various types of cardiac phenotype similar with what presented in human CHD patients. *Isl1* acts as a master transcription factor in SHF development by orchestrating a regulating network driving cardiogenesis and functions as a pioneer factor to reorganize the chromatin accessibility together with Brg1/Baf60c remodeling complex, to further regulate target gene expression and determine cardiac lineage cell fate.

In our work, we answered the questions we want to address in the objectives, but further studies need to be done to better understand the mechanisms underlying the role of *Isl1* in regulating SHF development. For example, we identified *Isl1* works jointly with Brg1 in the reorganization of chromatin landscape, but it is not clear how does Brg1 affect *Isl1* behavior. Studies on *Isl1* binding with *Brg1* depletion are necessary to prove whether Brg1 affects *Isl1* binding on its target sites or only affects the process of chromatin opening. Besides, we suspect that *Isl1* may work together with other chromatin remodeling complexes to shape the chromatin accessibility at some target genes, it is not clear which chromatin remodeler also participates in this process. In addition, to recruit cofactors (transcription factors, chromatin modifiers, repressors, and so on) and allow their binding to the open sites is one of the typical activities of a pioneer factor as described in the introduction (Figure 10). In this study, we identified quite a lot of new *Isl1* targets, but it is still not very clear which cofactors are recruited to the open sites to work cooperatively with *Isl1* in regulating these target genes after chromatin landscape reorganization. The identification of additional cofactors of *Isl1*, for example, using mass spectrometry, could help to clarify the clearer regulatory pattern.

During development, a fraction of transcription factors are retained on condensed mitotic chromosomes and “bookmark” specific loci, thus facilitating rapid gene reactivation post-mitosis and providing a transcriptional memory (Bellec, Radulescu et al. 2018, Mayran and Drouin 2018). Interestingly, the majority of the known mitotically retained TFs function as pioneer factors, such as FOXA1, GATA1 and SOX2 (Caravaca, Donahue et al. 2013, Bellec, Radulescu et al. 2018). In our study, we found *Isl1* binds a group of cardiomyocytes structural genes in CPCs which are supposed to be highly expressed at the later stages of

heart development when *Isl1* is no longer actively transcribed. As a pioneer factor, further studies are needed to address whether *Isl1* has a bookmarking function during cardiogenesis. To determine whether *Isl1* acts as a bookmarking factor in CPCs, mitotic and asynchronous subcellular fractionations (Liu, Pelham-Webb et al. 2017) in CPCs will be necessary. Expression of *Isl1* in both fractions could be detected by WB and performing *Isl1* CHIP-Seq in both fractions would be helpful to determine the binding of *Isl1* on specific target sites and regulation of *Isl1* on different subsets of genes at different cell states.

In addition, we firstly found *Isl1* acts as a pioneer factor in cardiogenesis in this study, it will be interesting to determine whether *Isl1* also functions as a pioneer factor in other tissues or developmental processes of other organs, for example, in the neural system, since *Isl1* is highly expressed in the neural system (Zhuang, Zhang et al. 2013) and was reported to be essential for sympathetic neuron proliferation, differentiation and diversification, as well as motor neuron development (Liang, Song et al. 2011, Zhang, Huang et al. 2018).

## 5. Materials and Methods

### 5.1 Chemicals used in this study

Chemicals	Source of supply	Reference number
2-Log DNA ladder (0.1-10.0 kb)	NEB	N3200L
Agarose	Carl Roth	3810.4
Ammonium persulfate (APS)	Sigma	A3678-25G
Ampicillin sodium salt	Sigma	A99518-25G
aqueous 30 % acrylamide and bisacrylamide stock solution (37.5:1)	Carl Roth	3029.1
BSA powder	Carl Roth	8076.2
BSA (used for ChIP)	NEB	B9000s
Bromophenol Blue	Sigma	B0126
Chloroform	Carl Roth	3313.4
Dimethyl Sulfoxide (DMSO)	Sigma	D-8779
Dithiothreitol (DTT)	Carl Roth	6908.3
Dry-milk, non-fat milk	BIO-RAD	170-6404
Ethylene glycol tetraacetic acid (EGTA )	Carl Roth	3054.2
Ethanol	Carl Roth	K928.3
Ethanol	Sigma	459844
Ethidium bromide solution	Sigma	E1510-10ML
Formaldehyde	Sigma	F8775
Glycerol	Carl Roth	3783.1
Glycine	Carl Roth	398.2
Herculase II Fusion Enzyme with dNTPs Combo	Agilent	600677
H2A/H2B dimers	NEB	M2508S
H3/H4 tetramers	NEB	M2509S
Igepal	Sigma	CA-630
Isopropanol	Carl Roth	6752.4
LB-agar (Lennox)	Carl Roth	X965.2
LB-medium (Lennox)	Carl Roth	X964.2
LiCl	Carl Roth	3739.1
Methanol	Carl Roth	4627.5

MgCl <sub>2</sub>	Sigma	M2393-500G
Nonidet P-40 (NP-40)	Fluka	74385
NaCl	Sigma	S3014
Na <sub>2</sub> EDTA	Sigma	E5134-250G
NaH <sub>2</sub> PO <sub>4</sub> · H <sub>2</sub> O	Sigma	53522-1KG
Na <sub>2</sub> HPO <sub>4</sub> · 12H <sub>2</sub> O	Sigma	04273
Phenol/Chloroform/Isoamyl alcohol	Carl Roth	A156.1
Protein A sepharose 6MB	GE Healthcare	17-0469-01
Protein G sepharose 4 fast flow	GE Healthcare	17-0618-01
Proteinase K	Sigma	P8044
Paraformaldehyde (PFA)	Sigma	15,812-7
Protease inhibitor cocktail set I	Calbiochem	535142
Phosphatase inhibitor Cocktail set V	Calbiochem	524632
Phenylmethylsulfonyl fluoride (PMSF)	Serva	32395
Potassium chloride (KCl)	Carl Roth	6781.3
PageRuler Plus Prestained Protein Ladder	Thermo Scientific	26619
Qiazol	Qiagen	79306
RedTaq PCR Reaction Mix	Sigma	R2523
Sodium dodecyl sulfate (SDS)	Sigma	L4390-100G
RNAse inhibitor	Applied biosystems	N8080119
Tetramethylethylenediamine (TEMED)	Carl Roth	2367.1
Triton X-100	Sigma	X100-500ML
Trizol	Invitrogen	15596026
Tris	Carl Roth	4855.2
Tween 20	Sigma	P1379
Urea	Carl Roth	2317.2
β-mercaptoethanol	Sigma	M3148

## 5.2 Kits used in this study

Kit	Source of supply	Reference number
Amersham ECL Prime Western Blotting Detection Reagent	GE Healthcare	RPN2232

GenElute™ gel extraction kit	Sigma	NA1111
GenElute™ HP plasmid midiprep kit	Sigma	NA0200
GenElute™ HP plasmid miniprep kit	Sigma	NA0160
GenElute™ PCR clean-up kit	Sigma	NA1020
High-Capacity cDNA Reverse Transcription Kit	Applied Biosystems	4368813
Nextera DNA Library Prep Kit	Illumina	15028211
Pierce™ BCA Protein Assay Kit	Thermo Scientific	23225
QIAquick PCR Purification Kit	Qiagen	28104
Quant-iT™ PicoGreen™ dsDNA Assay Kit	Invitrogen	P11496
RNeasy Microarray Tissue Mini Kit	Qiagen	73304
2x SYBR Green master mix	Applied Biosystems	4367659

### 5.3 Cell culture medium and supplements

Medium/supplements	Source of supply	Reference number
FBS	Gibco	10270-106
DMEM (1x)	Gibco	10938-025
DMEM + Glutamax	Gibco	61965-026
L-Glutamine	Gibco	25030-024
sodium pyruvate	Gibco	11360-039
Penicillin-Streptomycin	Gibco	15140-122
non-essential amino acids	Gibco	11140-035
leukemia inhibitory factor	Millipore	ESG1107
mitomycin	Sigma	M4287
KnockOut DMEM medium	Gibco	10829-018
KnockOut Serum Replacement	Gibco	10828-028
β-mercaptoethanol	Sigma	M3148
X-tremeGENE HP DNA Transfection Reagent	Roche	6366236001
Lipofectamine 2000	Invitrogen	11668019
Puromycin	Gibco	A11138-03
Neurobasal medium	Gibco	1103049
DMEM/F12	Gibco	21331020

IMDM	Gibco	12440053
Ham's F12 Nutrient Mix	Gibco	11765054
StemPro™-34 SFM	Gibco	10639011
N2 supplement	Gibco	17502-048
B27 supplement	Gibco	17504-044
B27 supplement without Vitamin A	Gibco	12587-010
Activin A	R&D systems	338-AC
BMP4	R&D systems	314-BP
VEGF	R&D systems	293-VE-010
bFGF	R&D systems	233-FB
FGF10	R&D systems	345-FG
7.5% BSA	Gibco	15260037
1-Thioglycerol	Sigma	M6145
L-Ascorbic Acid	Sigma	A4403
Trypsin-EDTA (1x) 0.05%	Gibco	25300-054
DPBS	Gibco	14190-094
gelatin	Sigma	G9391
Poly (2-hydroxyethyl methacrylate)	Sigma	P3932
DMSO	Sigma	D2650
POLYBRENE	Merck	TR-1003-G

## 5.4 Further materials

Further materials	Source of supply	Reference number
15ml Centrifuge Tubes	Greiner Bio-One	188271
50ml Centrifuge Tubes	Greiner Bio-One	227261
5ml Plastic pipet	Greiner Bio-One	606180
10ml Plastic pipet	Greiner Bio-One	607180
25ml Plastic pipet	Greiner Bio-One	760180
6-cm dish (cell culture)	Greiner Bio-One	628160
10-cm dish (cell culture)	Greiner Bio-One	664160
15-cm dish (cell culture)	Greiner Bio-One	639160

10-cm petri-dish	Greiner Bio-One	633180
6-well plates (cell culture)	Greiner Bio-One	657160
12-well plates (cell culture)	Greiner Bio-One	665180
24-well plates (cell culture)	Greiner Bio-One	662160
48-well plates (cell culture)	Greiner Bio-One	677180
96-well plate F bottom with lid	Greiner Bio-One	655180
96-well plate V bottom with lid	Greiner Bio-One	651180
Forceps (Dumont 5 antimagnetic e)	Carl Roth	LH66.1
MicroAMP fast optical 96-well reaction plate with barcode 0.1mL	Applied Biosystems	4346906
MicroAMP Optical adhesive film	Applied Biosystems	4311971
Reservoir	VWR	89094-664

## 5.5 Equipment used in this study

Equipment	Source of supply
Bacterial incubator 37°C	Thermo Scientific
Binocular microscope M165FC	Leica
Binocular microscope MZ16FA	Leica
Cell culture incubator	Thermo Scientific
Cell culture safety cabinet	Thermo Scientific
Centrifuge HERAEUS Fresco 17	Thermo Electron Corporation
Centrifuge HERAEUS Multifuge 1S-R	Thermo Electron Corporation
Centrifuge HERAEUS Pico 17	Thermo Electron Corporation
Cold light source KL2500 LCD	Zeiss
Confocal microscope LSM 700	Zeiss
Developing machine	GE Healthcare
Fluorescence microscope DM6000B	Leica
Heating block TH 21	HLC BioTech
Light microscope Wilovert S	Hund Wetzlar
Nanodrop 2000c Spectrophotometer	peQLab
Qubit™ Fluorometer	Thermo Scientific



Real-Time StepOne Plus Real-Time PCR System	Applied Biosystems
Rocking platform 444-0142	VWR
Rotator SB3	Stuart
Scale LC 4800 P	Sartorius
SDS-PAGE apparatus	Bio-Rad
Western Blotting Transfer apparatus	Bio-Rad
Sonifier Sonopuls GM 2070	Bandelin electronic
Thermal cycler C1000 Touch	BIO-RAD
Thermo block 5436	Eppendorf
Thermo block MHR 23	HLC BioTech
UV light source ebq100	Leistungselektronik Jena
UV light source EL 6000	Leica
UV-Crosslinker	Analytikjena
Vortexer VF2	IKA®-Labortechnik Staufen
Water bath cell culture WMB 22	Memmert
Water bath Julabo U3	Julabo Labortechnik GMBH

## 5.6 RNA extraction, cDNA synthesis and qPCR

### 5.6.1 RNA extraction

Total RNA from cell or tissue samples was extracted with TRIzol™ Reagent (Invitrogen, 15596026) for qPCR or with QIAzol Lysis Reagent and RNeasy Microarray Tissue Mini Kit (Qiagen, 73304) for RNA-Seq according to the user guides.

#### RNA extraction with TRIzol™ Reagent:

(1) Lyse and homogenize samples in TRIzol™ Reagent: for cells, pipet the lysate up and down several times to homogenize; for tissue, add 1 ml of TRIzol™ Reagent per sample and homogenize using a homogenizer. Incubate for 5 min at room temperature (RT, 15-25°C). Samples can be stored at -80°C for later manipulation or continued to step 2 immediately.

(2) Add 0.2 ml of chloroform per 1 ml of TRIzol™ Reagent used for lysis. Then securely cap the tube and vortex for 15 s.

(3) Incubate for 2-3 min at RT. Centrifuge the sample for 15 min at 12,000 × g at 4°C.

(4) The mixture separates into a lower red phenol-chloroform, and interphase, and a colorless upper aqueous phase. Transfer the aqueous phase containing the RNA to a new tube.

(5) Add 1 volume of isopropanol to the aqueous phase. Incubate for 10 min at RT.

(6) Centrifuge for 10 min at 12,000 × g at 4°C. Total RNA precipitate forms a white gel-like pellet at the bottom of the tube.

(7) Discard the supernatant with a micropipette.

(8) Wash the pellet in 1 ml of 75% ethanol.

(9) Vortex the sample briefly. Then centrifuge for 5 min at 7500 × g at 4°C.

(10) Discard the supernatant with a micropipette.

(11) Centrifuge the pellet for 5 min at 7500× g at 4°C. Then remove the supernatant completely.

(12) Air dry the RNA pellet for around 10 min.

(13) Dissolve the pellet in 20-50 µl of RNase-free water.

#### **RNA extraction with QIAzol Lysis Reagent and RNeasy Microarray Tissue Mini Kit:**

(1) Lyse and homogenize samples in QIAzol Reagent: for cells, pipet the lysate up and down several times to homogenize; for tissue, add 1 ml of QIAzol Reagent per sample and homogenize using a homogenizer. Incubate for 5 min at RT. Samples can be stored at -80°C for later manipulation or continued to step 2 immediately.

(2) Add 0.2 ml of chloroform per 1 ml of QIAzol Reagent used for lysis. Then securely cap the tube and vortex for 15 s.

(3) Incubate for 2-3 min at RT. Centrifuge the sample for 15 min at 12,000 × g at 4°C.

(4) The mixture separates into a lower red phenol-chloroform, and interphase, and a colorless upper aqueous phase. Transfer the upper phase containing the RNA to a new tube.

(5) Add 1 volume of 70% ethanol, and mix thoroughly by pipetting up and down. Transfer up to 700 µl of the sample to an RNeasy Mini spin column placed in a 2 ml collection tube. Close the lid gently, and centrifuge for 15 s at 13,000 rpm at RT. Discard the flow-through. If your

sample is more than 700  $\mu$ l, repeat this step using the remainder of the sample. Discard the flow-through.

(6) Add 700  $\mu$ l Buffer RW1 to the RNeasy spin column. Close the lid gently, and centrifuge for 15 s at 10,000 rpm to wash the membrane. Discard the flow-through.

(7) Add 500 $\mu$ l Buffer RPE to the RNeasy spin column. Close the lid gently, and centrifuge for 15 s at 13,000 rpm to wash the membrane. Discard the flow-through.

(8) Add 500  $\mu$ l Buffer RPE to the RNeasy spin column. Close the lid gently, and centrifuge for 2 min at 13,000 rpm to wash the membrane. Discard the flow-through.

(9) Place the RNeasy spin column in a new 2 ml collection tube, and discard the old collection tube with the flow-through. Close the lid gently, and centrifuge at full speed for 1 min.

(10) Place the RNeasy spin column in a new 1.5 ml collection tube. Add 30-50  $\mu$ l RNase-free water directly to the spin column membrane. Close the lid gently. To elute the RNA, centrifuge for 1 min at 13,000 rpm.

(11) Repeat step 10 using another volume of RNase-free water, or using the eluate from step 10 (if high RNA concentration is required). Reuse the collection tube from step 10.

Total RNA quality was checked by running an agarose gel in 1 $\times$  TBE buffer (0.089M Tris, 0.089M H<sub>3</sub>BO<sub>3</sub>, 2 mM Na<sub>2</sub>EDTA pH 8.0) with RNA mixed with 2 $\times$  RNA loading buffer (100  $\mu$ l formamide, 40  $\mu$ l formaldehyde, 20  $\mu$ l 10 $\times$  TBE and 2  $\mu$ l Ethidium bromide). RNA concentration was measured by NanoDrop2000/2000c or TECAN spectrophotometers.

### 5.6.2 cDNA synthesis

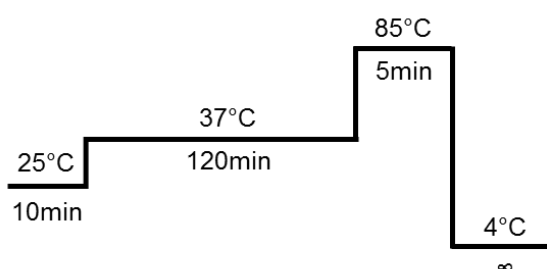
cDNA synthesis was done with the High-Capacity cDNA Reverse Transcription Kit (Applied Biosystems, 4368813) and PCR machine from BioRad (C1000 Touch™ Thermal Cycler). Generally, 1  $\mu$ g total RNA was mixed with 2 $\times$  RT master mix for each sample.

#### 2 $\times$ RT master mix:

Component	Volume
10 $\times$ RT Buffer	2 $\mu$ l
25 $\times$ dNTP Mix (100 mM)	0.8 $\mu$ l

10× RT Random Primers	2 µl
MultiScribe™ Reverse Transcriptase	1 µl
RNase Inhibitor	1 µl
Nuclease-free H <sub>2</sub> O	3.2 µl
Total per reaction	10 µl

**Program used in the thermal cycler for cDNA synthesis:**



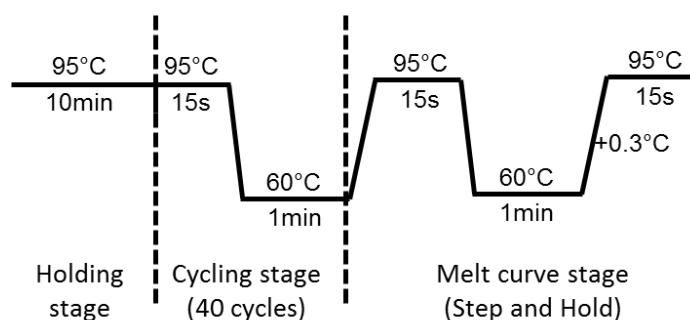
### 5.6.3 Quantitative real-time polymerase chain reaction (qPCR)

qPCR was done with Power SYBR Green PCR Master Mix (Applied Biosystems, 4367659) and the qPCR machine from Applied Biosystems (StepOne Plus System). cDNA synthesized from 1 µg RNA was diluted by 1 to 10 and 1 µl dilution was used for qPCR reaction.

**qPCR reactions were carried out in 10 µl volume:**

Component	Volume
2× SYBR® Green buffer	5 µl
5 µM primer F stock	0.5 µl
5 µM primer R stock	0.5 µl
Template (gDNA/cDNA)	1 µl
H <sub>2</sub> O	3 µl
Total per reaction	10 µl

**For qPCR, following thermal cycle condition was used:**



## 5.7 Mouse lines

*Is1* knockout mouse line is a kind gift from Sylvia Evans and the floxed Brg1 mouse line is kindly provided by Pierre Chambon and Daniel Metzger.

## 5.8 Genomic DNA extraction

Mice tails or ear tissues were incubated in 200-500  $\mu$ l lysis buffer with proteinase K over night at 55°C with 400 rpm shaking. Next day proteinase K was heat inactivated by incubating the samples at 95°C for 10 min. Then the tissue debris was pelleted for 5 min, 6,000 rpm and supernatant was transferred into new tubes and mixed with equal volume Isopropanol to precipitate genomic DNA (gDNA). The samples were centrifuged for 15 min (15,000 rpm, 4°C). Then supernatant was removed. Genomic DNA pellet was washed with 70% EtOH and centrifuged for 5 min with 15,000 rpm at 4°C. Discard the supernatant. The pellet was air-dried for 10 min at RT. Finally, dissolve the pellet in 100-300  $\mu$ l ddH<sub>2</sub>O.

### Lysis buffer for mouse tails or ear tissues:

Final concentration	Stock	Volume of stock for 200 ml solution
100 mM Tris pH 8.5	1 M Tris pH 8.5	20 ml
5 mM EDTA	0.5 M EDTA pH 8.0	2 ml
0.2% SDS	10% SDS	4 ml
200 mM NaCl	5 M NaCl	8 ml
H <sub>2</sub> O		166 ml
Total volume		200 ml

Freshly adding proteinase K (10  $\mu$ g/ $\mu$ l proteinase K stock is 100 $\times$  for adult tissues and 10 $\times$  for embryonic tails) before using.

## 5.9 Genotyping

1  $\mu$ l of gDNA was used in the genotyping PCR reaction (total reaction volume 10 or 20  $\mu$ l). REDTaq® ReadyMix™ PCR Reaction Mix (Sigma, R2523) was used for PCR reactions.

**PCR reaction** (take 20  $\mu$ l reaction system as an example):

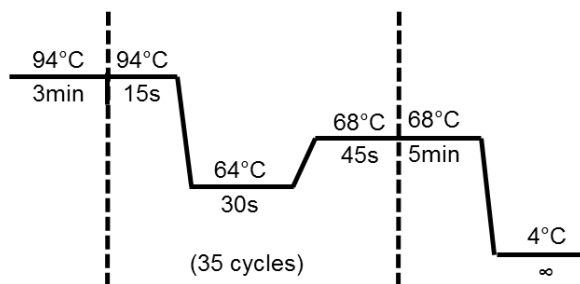
10  $\mu$ l 2xRedTaq

1  $\mu$ l primer1/2/3

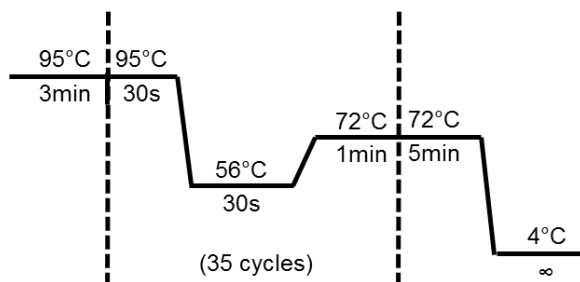
1  $\mu$ l gDNA

ddH<sub>2</sub>O to 20  $\mu$ l

**Program used in the thermal cycler for genotyping of Isl1 mice:**



**Program used in the thermal cycler for genotyping of Brg1 mice:**



**Primers used for genotyping:**

Isl1-F, ACTATTTGCCACCTAGCCACAGCA

Isl1-(384)-R, AATTCACACCAAACATGCAAGCTG

Isl1-Cre-Jes-R, CTAGAGCCTGTTTTGCACGTTT

Brg1\_P1 (TH185), GTCATACTTATGTCATAGCC

Brg1\_P2 (TG57), GCCTTGTCTCAAACGATAAG

Brg1\_P3 (TB82), GATCAGCTCATGCCCTAAGG

### **10× DNA loading buffer for agarose gel electrophoresis (protocol from Takara):**

0.9% SDS

50% Glycerol

0.05% Bromophenol Blue

### **DNA gel electrophoresis:**

Load the PCR products in 1% agarose gel and run at 145V for 30 min in parallel with DNA ladder. Then check the results and take images with a UV gel imaging system.

## **5.10 Protein extraction and co-immunoprecipitation (Co-IP)**

mESC-derived CPCs and homogenized embryo tissues were lysed in Co-IP buffer (50 mM Tris HCl pH 7.5, 10 mM EGTA, 100 mM NaCl, 0.1% Triton X-100, freshly adding protease inhibitor and phosphatase inhibitor) on ice for 15 min; then sonicate for 5-10 s with the tip sonifier. Then centrifugation was done at 4°C for 15 min with top speed. Transfer the supernatant to a new 1.5 ml tube. Protein concentration was determined with BCA method (Thermo scientific, 23225). Protein was then subjected to Co-IP or added with 2× SDS sample buffer (125 mM Tris-Cl pH 6.8, 4% SDS, 20% glycerol, 100 mM DTT, 0.02% Bromophenol blue) for Western Blot (WB).

For Co-IP done in mESC-derived CPCs, 5 million cells are used for each sample. For Co-IP done in embryos, 30 E8.25-E9.0 mouse embryos are used for each sample. The lysates were precleared with Protein-G-Sepharose beads (GE Healthcare, 17-0618) for 1-3 hours at 4°C; then incubated with the indicated antibodies overnight at 4°C followed by 1h incubation with Protein-G-Sepharose beads (GE Healthcare, 17-0618). Immunoprecipitates were washed 3-5 times with lysis buffer, then dissolved in 2× SDS sample buffer; incubated at 95°C for 10 min and subjected to standard WB analysis.

## **5.11 SDS-PAGE and Western Blot**

Proteins were mixed with 2× SDS sample buffer (125 mM Tris pH 6.8, 4% SDS, 20% glycerol, 100 mM DTT, 0.02% bromophenol blue) and incubated at 95°C for 10 min. Electrophoretical separation was performed with 10-15% SDS-PAGE gels (Bio-Rad). Proteins were transferred to nitrocellulose membrane using a wet-blot system (Bio-Rad) for 1-2 hours at 100V according to the molecular weight of the protein. Membranes were blocked for 1 hour at

room temperature (RT) with shaking in 5% milk (Bio-Rad) or BSA (Carl Roth) solved in 1× TBST buffer (0.242% Tris, 0.8% NaCl, 0.1% Tween-20). The primary antibodies were diluted in 5% milk or BSA in TBST and incubated with the membrane at 4°C overnight. Blots were washed 3 times (shaking for 10 min per washing) at RT with TBST. Secondary antibodies were diluted in TBST (1:10,000, HRP-conjugates). The incubation was followed by 3 times washing (shaking for 10 min per washing) at RT with TBST. After additional washing steps, the blots were developed by adding ECL reagent (GE Healthcare) and imaged with a developing system (GE Healthcare).

#### Separation gel (5 ml)

Component	Volume		
	10%	12%	15%
ddH <sub>2</sub> O	1.9 ml	1.6 ml	1.1 ml
30% aqueous acrylamide solution with 0.8% bisacrylamide (37.5:1)	1.7 ml	2.0 ml	2.5 ml
Buffer 1.5M Tris, pH8.8	1.3 ml	1.3 ml	1.3 ml
10% SDS	50 µl	50 µl	50 µl
10% APS	50 µl	50 µl	50 µl
TEMED	2 µl	2 µl	2 µl

#### 4% stacking gel (2 ml)

Component	Volume
ddH <sub>2</sub> O	1.4 ml
30% aqueous acrylamide solution with 0.8% bisacrylamide (37.5:1)	0.33 ml
Buffer 1.5 M Tris, pH 6.8	0.25 ml
10% SDS	20 µl
10% APS	20 µl
TEMED	2 µl



**1× SDS PAGE running buffer:**

0.125 M Tris base

0.96 mM Glycin

0.5% SDS

**1× Transfer buffer:**

25 mM Tris

0.2 mM Glycin

10% Methanol (freshly adding)

**10× TBS (pH 7.6):**

2.42% Tris

8% NaCl

**Primary antibodies used for Co-IP and WB:**

Antibody	Host	Usage	Company
Isl1	Mouse	WB (1 to 10) and Co-IP	DSHB, 39.4D5
Brg1	Rabbit	WB (1 to 1000) and Co-IP	Millipore, 07-478
Baf60c	Rabbit	WB (1 to 500)	a kind gift from Pier Lorenzo Puri
α-tubulin	Mouse	WB (1 to 3000)	Sigma, T5168
IgG	Mouse	Co-IP	CST, 2729
IgG	Rabbit	Co-IP	Santa Cruz, sc-2025

**Secondary antibodies used for WB:**

Antibody	Host	Dilution	Company
α-mouse HRP	donkey	1 to 10,000	Jackson ImmunoResearch, 715-035-150

$\alpha$ -rabbit HRP	donkey	1 to 10,000	Jackson ImmunoResearch, 111-035-003
----------------------	--------	-------------	--

## 5.12 Culturing of primary cells and cell lines

### 5.12.1 Mouse embryonic fibroblasts (MEFs)

MEFs are isolated from WT E13.5 mouse embryos. The isolation and culture processes are as follows:

- (1) Sacrifice the pregnant mouse.
- (2) Lie down the mouse on its back and swab with 70% ethanol. Using scissors make a cut across the belly and cut away the skin to expose the gut. With sterile forceps and scissors, dissect out the uterus and place it into a petri dish with sterile PBS.
- (3) Isolate the embryos from the uterus, and release the embryos from the embryonic sacs. Transfer embryos to a second petri dish with sterile PBS.
- (4) Remove the embryo heads and limbs and scoop out the liver, intestines and heart with a pair of forceps. Transfer the embryo carcass into a sterile 15mL tube with a sufficient volume of Trypsin/EDTA to cover the carcasses. Using scissors finely mince the tissue.
- (5) Incubate the tissue for 15 min at 37°C, then pipette the tissue a few times through a glass Pasteur pipette to dissociate the tissue. Allow the large pieces of cellular debris to settle. Remove the supernatant into a fresh tube and add 50 ml of MEF medium. Transfer to a 10-cm<sup>2</sup> dish. Seed cells from 2-3 embryos/dish. Incubate at 37°C with 5% CO<sub>2</sub>.
- (6) MEFs should attach and begin to divide in 1-3 days. After 2 days, change the medium. When the cells are confluent, usually in 3-4 days, the cultures are ready for freezing. Freeze them in MEF medium with 10% DMSO and 10% fetal bovine serum (FBS), at  $2 \times 10^6$  cells/vial (referred to as P0). Or continue culturing them by splitting them by 1:2 to 1:4 when they are very confluent. You can passage them up to P7.

#### MEF medium:

500 ml DMEM high glucose (4.5 g/l)

6 ml 100× Sodium pyruvate

6 ml 100× Penicillin-Streptomycin

6 ml 100× MEM NEAA

6 ml 100× L-Glutamine

50 ml fetal bovine serum

8 ul β-mercaptoethanol

#### **Preparing feeders:**

Mitomycin C powder (Sigma, M4287) was dissolved in sterilized ddH<sub>2</sub>O to get a concentration of 1 mg/ml and then filtered by 0.22 μm filter. Add newly prepared mitomycin C (10 μg/ml final concentration) to dishes with confluent MEFs. Treat the cells for 2 hours in the incubator. Then remove the medium and wash the treated cells for 3 times with PBS. Trypsin the cells and freeze them. Store the cells in liquid nitrogen for long term use. When you use, thaw the cells by 1 to 1 in MEF medium.

#### **5.12.2 Mouse embryonic stem cell lines (mESCs)**

E14 Tg(Nkx2.5-eGFP) ES cells (Hsiao, Yoshinaga et al. 2008) were maintained on mitomycin C treated mouse embryonic fibroblasts (feeders) in KnockOut ESC medium and cultured at 37°C with 5% CO<sub>2</sub>. Split regularly every second day.

KnockOut ESC medium: KnockOut DMEM medium (Gibco, 10829-018) containing 4.5 mg/ml D-glucose, supplemented with 10% KnockOut serum replacement (Gibco, 10828-028), 2 mM L-Glutamine (Gibco, 25030-024), 0.07 mM β-mercaptoethanol (Sigma, M3148), 0.1 mM non-essential amino acids (Gibco, 11140-035), 1 mM sodium pyruvate (Gibco, 11360-039), 100 U/ml Penicillin-Streptomycin (Gibco, 15140-122) and 1,000 U/ml of leukemia inhibitory factor (LIF ESGRO, Millipore).

#### **5.12.3 HEK293T cell line**

HEK293T cells (ATCC, CRL-11268) were cultured in DMEM medium containing 4.5 mg/ml D-glucose, plus 10% FBS (Gibco, 10270-106), 2 mM L-Glutamine (Gibco, 25030-024), 1 mM sodium pyruvate (Gibco, 11360-039), 100 U/ml Penicillin-Streptomycin (Gibco, 15140-122) at 37°C incubator with 5% CO<sub>2</sub> and split regularly at 80% confluency.

### 5.13 Generation of stable ES cell lines

HEK293T cells were plated one day before the transfection on 6-well plate. The cells were transfected with the following plasmids the next day when they reach around 50% confluency:

975 ng pCMV ΔR8.74 (addgene, 22036, lentiviral packaging plasmid)

525 ng pMD2.G (addgene, 12259, lentiviral envelope expressing plasmid)

1.5 μg shRNA/PLKO (lentiviral vectors)

**shRNA targeting sequences:** (From shRNA library kept in Max Planck institute for heart and lung research)

Isl1 shRNA-3: CTAACCCAGTAGAGGTGCAA

Isl1 shRNA-5: CGGCAATCAAATTCACGACCA

Baf60c shRNA-1: CGCCTAAAGTTCTCTGAGATT

Baf60c shRNA-2: GCTGCGCCTTTATATCTCCAA

Brg1 shRNA-1: GCTGCCAAATACAAACTCAAT

Brg1 shRNA-2: CCCACGATACAACCAGATGAA

Transfection was done according to the handbook of X-tremeGENE HP DNA Transfection Reagent (Roche, 6366236001). Plasmid: transfection reagent = 1:3. Change the medium to DMEM ESC medium (DMEM containing 4.5 mg/ml D-glucose, plus 15% FBS, 2 mM L-Glutamine, 1 mM sodium pyruvate, 100 U/ml Penicillin-Streptomycin, 0.1 mM non-essential amino acids, 0.1 mM β-mercaptoethanol) for the transfected HEK293T cells the next day. 72 hours after the transfection, virus was harvested by collecting the supernatant and centrifuging for 20 min at 4,200 rpm at RT. 0.1-0.2 million ES cells were infected with 2 ml virus in ESC medium plus 1,000 U/ml LIF and 8 μg/ml polybrene (Sigma, TR-1003-G) plating in one well of 5% Poly (2-hydroxyethyl methacrylate) (Sigma, P3932) coated 6-well plate. The next day, plate the infected cells on feeders. One day later, change the medium to KnockOut ESC medium. The next day, start the selection with 5 μg/ml puromycin. Two days later, change the medium. Now the cells can be harvested to check the knockdown efficiency and expanded for further experiments.

## 5.14 Generating *Isl1* KO mESC lines by CRISPR-Cas9 technique

Cas9 plasmid PX459 was obtained from Addgene (plasmid #62988). sgRNAs were synthesized and cloned into PX459. mESCs (E14:Nkx2.5-GFP line) were transfected with PX459-*Isl1* gRNA1 and PX459-*Isl1* gRNA2 transiently by using Lipofectamine 2000 (Invitrogen). After 24 hours of transfection, mESCs were selected with 4 µg/ml puromycin for 48 hours and plated on feeder cells with 5,000 cells per 6-cm dish. After culture for around 7 days, clones were picked and screened by PCR.

### gRNA sequences:

*Isl1*-gRNA1, CCGATTTAAGCCGGCGGAGT

*Isl1*-gRNA2, TCATGAGCGCATCTGGCCGA

### Primers used for screening *Isl1* knockout clones:

primer1, GGCTTAATCCTCTCCTGCGG

primer2, TTTTGGTGGATCGCCCATGTC

primer3, CTTGCCAAGAGTTGGGGTGA

## 5.15 Cardiac differentiation

### Directed cardiac differentiation:

ES cells were differentiated into cardiomyocytes by directed differentiation method described in (Wamstad, Alexander et al. 2012). Briefly, undifferentiated ES cells were grown on gelatin coated dishes in Neurobasal medium: DMEM/F12 (1:1; Gibco, 1103049 and 21331020) medium supplemented 2,000 U/ml LIF and 10 ng/ml BMP4 (R&D, 314-BP) for 2 days and differentiated by aggregation in low attachment petri dishes at a cell density of 75,000 cells/ml in IMDM: F12 medium (3:1; Gibco, 12440053 and 11765054). After 48h aggregates were dissociated and re-aggregated in the presence of Activin A (R&D, 338-AC; 5 ng/ml), VEGF (R&D, 293-VE-010; 5 ng/ml) and BMP4 (R&D, 314-BP; 0.1-0.8 ng/ml; Bmp4 concentration empirically determined depending on lot). 40h following the second aggregation, aggregates were dissociated and plated as a monolayer in Stempro-34 medium supplemented with Stempro34 nutrient supplement (Gibco, 10639011), L-Glutamine (2 mM, Gibco, 25030024), L-Ascorbic Acid (Sigma, A4403, 50 µg/ml), VEGF (R&D #293-VE-010; 5

ng/ml), bFGF (R&D, 233-FB; 10 ng/ml), and FGF10 (R&D, 345-FG; 25 ng/ml) growth factors. We usually obtain around 60-80% of Nkx2.5-GFP<sup>+</sup> CPCs using this protocol.

Nkx2.5-GFP<sup>+</sup> cells were FACS sorted at CPC stage for RNA extraction. FACS sorted was done by cell sorting core facility in medical faculty Mannheim of Heidelberg University.

**Neurobasal: DMEM/F-12 Growth medium composition for 50 ml**

50% Neurobasal	25 ml
50% DMEM-F12	25 ml
0.5× N2 supplement	0.25 ml
0.5× B27 supplement	0.5 ml
1× Penicillin-Streptomycin	0.5 ml
1× L-Glutamin	0.5 ml
0.05% BSA	0.33 ml (Stock 7.5% BSA)
1.5×10 <sup>4</sup> M monothioglycerol	0.5 µl
BMP4	10 ng/ml
LIF	2,000 U/ml

**Differentiation medium: 50 ml**

75% IMDM (with L-Gln)	37.5 ml
25% F12 (with L-Gln)	12.5 ml
0.5× N2 supplement	0.25 ml
0.5× B27 supplement without VA	0.5 ml
1× Penicillin-Streptomycin	0.5 ml
50 µg/ml L-Ascorbic acid	0.5 ml (100× Stock)
4.5×10 <sup>-4</sup> M monothioglycerol	2 µl

Add growth factors when necessary

**Hanging drops:**

ES cells from control and *Isl1* KO Nkx2.5-GFP ESC lines were cultured by hanging drops of 500 cells per drop in 15 µl ESC medium, in the absence of LIF. After 2 days in the hanging drop culture, the resulting embryoid bodies (EBs) were transferred to petri dishes in ESC medium. The following time points were used for analysis: day2/3 for mesoderm; day4/5 for CPCs and day9/10 for CMs.

## 5.16 Chromatin immunoprecipitation (ChIP)

Cells at different stages of differentiation and tissue from mouse embryos are dissociated to obtain single cells suspension. Then cells were fixed with 1% formaldehyde (Sigma, F8775) for 10 min at RT. Formaldehyde was quenched with glycine at final concentration of 125 mM and washed three times with precooled PBS on ice. Cells were lysed in L1 lysis buffer (50 mM Tris pH 8.0, 2 mM EDTA pH 8.0, 0.1% NP-40, 10% glycerol) for 5 min, and then nuclei were resuspended in L2 nuclear resuspension buffer (1% SDS, 5 mM EDTA pH 8.0, 50 mM Tris pH 8.0) after centrifuging 5 min at 3,000 rpm 4°C, followed by shearing. The samples then were diluted by 1:10 with DB-dilution buffer (0.5% NP-40, 200 mM NaCl, 5 mM EDTA, 50 mM Tris pH 8.0). After preclearing, chromatin was incubated with primary antibody overnight at 4°C followed by 1 hour incubation with Protein-A/G Sepharose beads (GE Healthcare). Immunoprecipitates were washed four times with NaCl-washing buffer (0.1% SDS, 1% NP-40, 2 mM EDTA, 500 mM NaCl, 20 mM Tris pH 8.0), followed by three washes with LiCl-washing buffer (0.1% SDS, 1% NP-40, 2 mM EDTA, 500 mM LiCl, 20 mM Tris pH 8.0) and three washes with TE buffer (Tris pH 8.0 20 mM; EDTA 2 mM), then eluted with EB-extraction buffer (TE pH 8.0, 2% SDS). Reverse cross-linking was done by incubation at 65°C overnight with shaking. DNA was purified with phenol/chloroform extraction and precipitation. Purified DNA was subjected to qPCR analysis or ChIP-Seq.

### Antibodies used for ChIP:

*Isl1*: Developmental Studies Hybridoma Bank, 39.4D5

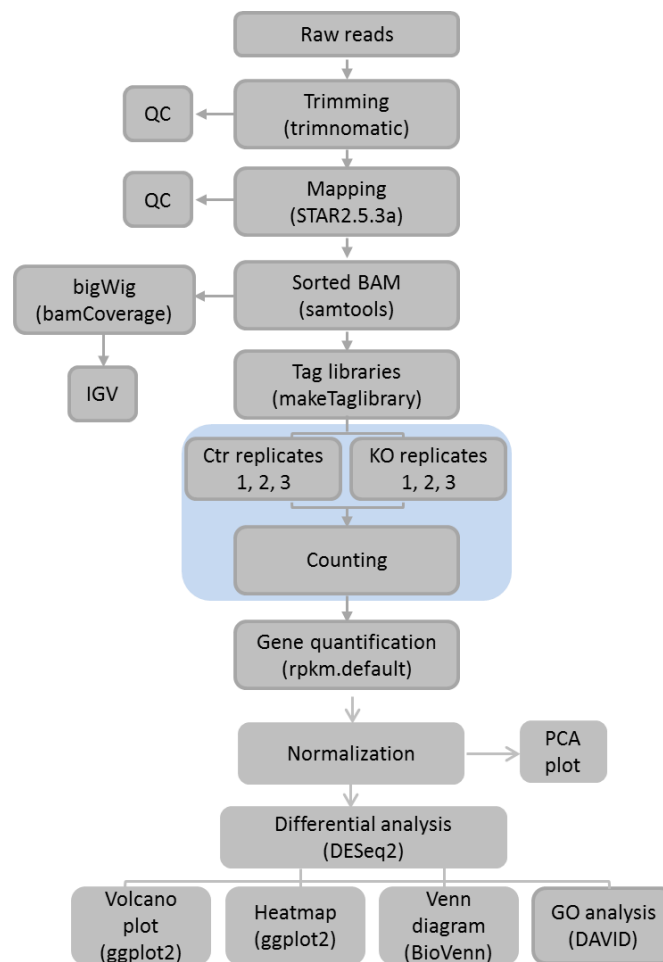
*Brg1*: Millipore, 07-478

*Gata4*: Santa Cruz, sc-1237

## 5.17 Bioinformatic analysis

### 5.17.1 RNA-Seq

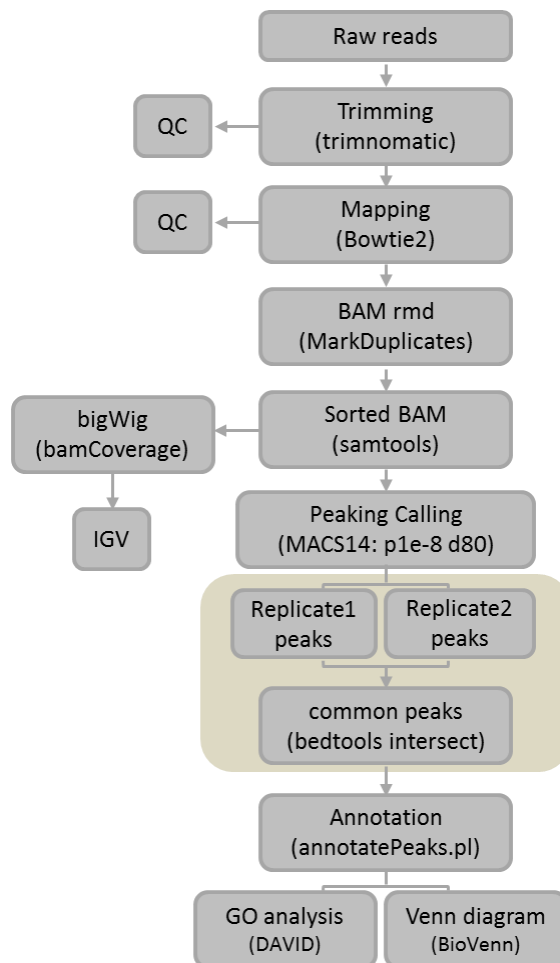
Sequencing was performed on the NextSeq500 instrument (Illumina) using v2 chemistry. All RNA libraries result in minimum of 30 million reads per library. All RNA-Seq reads were mapped to the mm9 reference genome using the STAR (PMID: 23104886) (-alignIntronMin 20 -alignIntronMax 500000). Samples were quantified by the use of analyzeRepeats.pl (PMID: 20513432) (mm9 -count exons -strand both -oadj). Differential gene expression and normalization was performed with DESeq2. Reads per kilobase per millions mapped (rpkm) for heatmap was obtained by the use of rpkm.default from EdgeR. The KNIME 2.9.1 platform (Konstanz, Germany) was used to filter differentially regulated genes. Heatmaps from the RNA-Seq were performed using heatmap.2 from ggplot2 in R. The PCA plots in each RNA-Seq set were obtained by the use of prcomp into a custom R-script. RNA-Seq data analysis workflow is shown below.





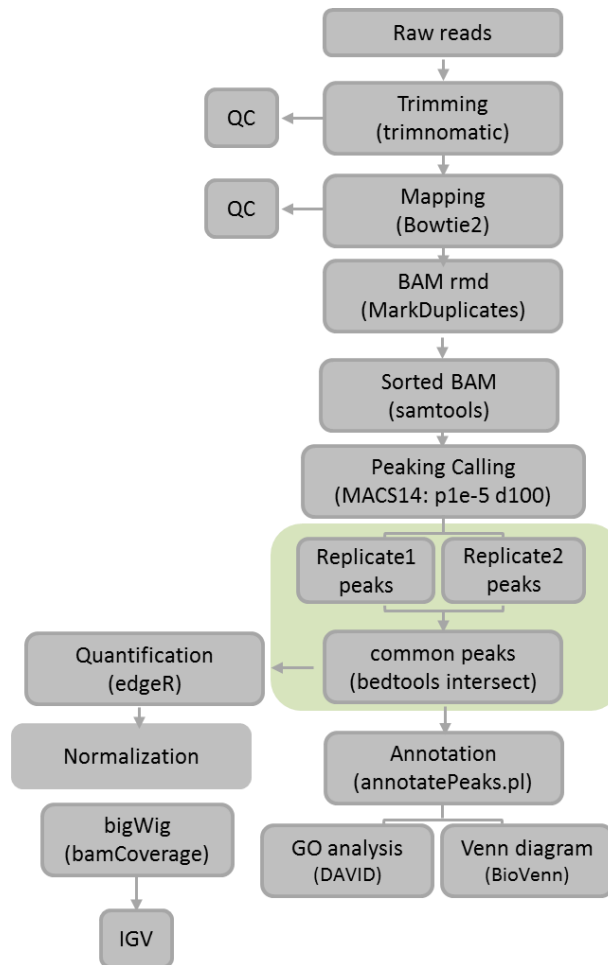
### 5.17.2 ChIP-Seq

ChIP-Seq reads were mapped to the mouse reference genome mm9 (UCSC assembly) using the default settings of bowtie2. Genome-wide distribution of the reads was performed using ngs.plot with mm9 Ensembl (version 67) as reference annotation. Peaks for Isl1-ChIP-Seq in Embryos and CPCs were called with the use of MACS14 PMID: 18798982 with the parameter (p1e8 d80 --nomodel --shiftsize 80). ChIP-Seq peak annotation was performed using annotatePeaks.pl (default settings). For data visualizing bam files were converted to BigWig files by the use of BamCoverage from deepTools2 (PMID: 24799436) (-b 20 -smooth 40 -e 150 --normalizeTo1x 2150570000). In Isl1 CPCs ChIP-Seq common peaks between both ChIP-Seq replicates, were obtained by the use of bedtools intersect (-wa). Venn diagrams were generated with BioVenn online tools (PMID: 18925949) and protein coding genes were used for all comparisons. ChIP-Seq data analysis workflow is shown below.



### 5.17.3 ATAC-Seq

Pharyngeal mesoderm and hearts of E8.5 embryos were dissected. Tissues or 50,000 CPCs were lysed in 50 µl cold lysis buffer (10 mM Tris-HCl pH 7.4, 10 mM NaCl, 3 mM MgCl<sub>2</sub>, 0.1% Igepal CA-630) and used for ATAC Library preparation using Tn5 Transposase from Nextera DNA Library Prep Kit (Illumina #15028211). After centrifugation (10 min, 500 g at 4°C), cell pellet was resuspended in the transposition reaction mix (25 µl TD-Buffer, 2.5 µl Tn5, 22.5 µl water) and incubated at 37°C for 30 min with gentle mixing. Immediately following the transposition reaction, purification was done using MinElute PCR Purification Kit (Qiagen, cat# 28004). Amplification of Library together with Indexing was performed as described in (Buenrostro, Giresi et al. 2013). Libraries were mixed in equimolar ratios and sequenced on NextSeq500 platform using V2 chemistry. The sequencing quality was assessed using FastQC (Anders and Huber 2010) (<http://www.bioinformatics.babraham.ac.uk/projects/fastqc>). Reads were mapped with bowtie2 to mm9 mouse genome. Samtools view (-F 1804 -f2) was used to remove reads unmapped, mate unmapped, not primary alignment. The MarkDuplicates.jar from Picard 1.136 was used to remove PCR artefacts. The mapped reads from two samples were merged using bam tools merge program (Barnett, Garrison et al. 2011). Peaks calling from each repetition was performed with by the use of MACS14 (PMID: 18798982) (p1e5 -nomodel and -shiftsize 100). Similar to Isl1-ChIP-Seq Bedtools v2.15 (intersect -wa) (PMID: 20110278) was used to obtain binding sites overlapping in at least 1bp each of the repetition. BamCoverage function of deepTools2 (PMID: 24799436) (-b 20 -smooth 40 -e 150) was used to create normalized bigwig files (reads per genome coverage, RPGC). Further bigWigAverageOverBed (<https://github.com/ENCODE-DCC/kentUtils>) was used to quantify the mapped reads on the peaks areas. The quantified matrix was normalized using edgeR (PMID: 19910308). Heatmaps and density plots were creating using computer matrix followed by plotHeatmap or plotProfile from deepTools2 (PMID: 24799436). ATAC-Seq data analysis workflow is shown below.



For ATAC-Seq analysis three wild-type, three *Isl1*<sup>-/-</sup> and three *Isl1-Cre*<sup>+/-</sup>/*Brg1*<sup>fl/fl</sup> E8.5 (6 somites) embryos and ESC-derived CPCs from two independent differentiations were used.

#### 5.17.4 Others

The *Isl1* regulated gene network presented in Results Figure 27 was built by submitting a curated list of *Isl1* primary downstream targets to the GeneMANIA web based software. The network was subdivided into transcription factors, signaling molecules, muscle structural and contractile genes and other genes involved in heart development and visualized using Cytoscape.

The taq heatmap was created using ngsplot PMID: 24735413 followed by the use of a home script. Bedtools v2.15 (intersect -wa) (PMID: 20110278) was used to find the common binding areas among *Isl1*-ChIP-Seq in CPCs, ATAC-Seq in CPCs and *Gata4*-ChIP-Seq in CPC (GSE72223). Similar settings were using to cross the common areas between *Isl1*- and *Brg1*-ChIP-Seq (GSE116281) and ATAC-Seq in CPCs vs ATAC-Seq in E8.5 embryos.

Gene ontology analysis was performed using DAVID Bioinformatics Resources 6.8. The other GO term related to cardiac muscle cell differentiation, endothelial cell differentiation and smooth muscle cell development/differentiation was obtained from (<http://amigo.geneontology.org/amigo/landing>). Computer matrix followed by plot profile from deepTools2 (PMID: 24799436) was used to plot the ATAC-Seq from E8.5 embryos on the TSS of the set of genes.

Brg1-ChIP-Seq (GSE116281) and Gata4-ChIP-Seq (GSE72223) were publically available data. Sequencing data (ChIP-Seq, RNA-Seq and ATAC-Seq) have been deposited in the Gene Expression Omnibus (GEO) under accession code GSE80383.

## 5.18 Primers used in this study

### 5.18.1 qPCR primers

Gene name	Sequence of qPCR primers
qGAPDH_F	AACTTTGGCATTGTGGAAGG
qGAPDH_R	GGATGCAGGGATGATGTTCT
qSox2_F	AGAACCCCAAGATGCACAAC
qSox2_R	TCTCGGTCTCGGACAAAAGT
qNanog_F	ACCTGAGCTATAAGCAGGTTAAGA
qNanog_R	GGGATACTCCACTGGTGCTG
qBry_F	AGGGAGACCCCAACGAACGC
qBry_R	CCGGGAACATCCTCCTGCCGTT
qMesp1_F	GTTTAAGCCCGGCCGTCTGCA
qMesp1_R	ATGTCGCTGCTGAAGAGCGGAGA
qMesp2_F	TAGAAAGAGCCGCTGACTCC
qMesp2_R	CTAGGCTCTGGGGACATCTG
qMef2c_F	TCCATCAGCCATTTCAACAA

qMef2c_R	AGTTACAGAGCCGAGGTGGA
qIsl1_F	ACGTGCTTTGTTAGGGATGG
qIsl1_R	CAAGAAGTCGTTCTTGCTGA
qHand2_F	CGGAGAGGCGGAGGCCTTCA
qHand2_R	CAGGGCCCAGACGTGCTGTG
qTbx5_F	ATGGTCCGTAAGTGGCAAAG
qTbx5_R	ACAAGTTGTCGCATCCAGTG
qTbx20_F	GCAGCAGAGAACACCATCAA
qTbx20_R	GTGAGCATCCAGACTCGTCA
qGata4_F	TCTCACTATGGGCACAGCAG
qGata4_R	GCGATGTCTGAGTGACAGGA
qTnnt2_F	ATCCCCGATGGAGAGAGAGT
qTnnt2_R	CTGTTCTCCTCCTCCTCACG
qMlc2a (Myl7)_F	CCCATCAACTTCACCGTCTT
qMlc2a (Myl7)_R	CGTGGGTGATGATGTAGCAG
qMlc2v (Myl2)_F	CTGCCCTAGGACGAGTGAAC
qMlc2v (Myl2)_R	CCTCTCTGCTTGTGTGGTCA
qTtn_F	ACCACCCAACCTTCAGTCAGC
qTtn_R	TCCCGGTAGAACTTCACCAC
qRyr2_F	TCTGCCAGGACTGTTTGTCC
qRyr2_R	GACTGAGGAAGGATCAGGGGA
qBaf60c (Smarcd3)_F	GAGATCAGTGCTCTGGACAGT
qBaf60c (Smarcd3)_R	GAGCAGGTCTTGGACGTAGC
qMyocd_F	GCTGAGACTCACCATGACAC

qMyocd_R	TGGACCTTTCAGTGGCGGTA
qBrg1_F	CACCTACCATGCCAACACTG
qBrg1_R	CGCTTGTCCCTTCTTCTGGTC
qPax7_F	CATGGTGGGCCATTTCCACT
qPax7_R	GGCCCGGGGCAGAACTAC
qTbx18_F	AATGAGCTGGATGACCAAGG
qTbx18_R	GGACAGATCATCTCCGCAAT
qSmyd3_F	CTCCGACCCCTTGGCTTAC
qSmyd3_R	TGGCAATTCGGCATTGAGAAC
qHdac3_F	CTCACGCCAGTATCTGGACC
qHdac3_R	CATACGTCAGGAGGTCTGCC
qMlc1v (MyI3)_F	ATCACATACGGGCAGTGTGG
qMlc1v (MyI3)_R	TTGAGCTCTTCTGTTTTGGC
qWnt2_F	CTGATGTAGACGCAAGGGGG
qWnt2_R	CCTGTAGCTCTCATGTACCACC
qTpm1_F	TCCAGCTGAAAGAGGCCAAG
qTpm1_R	CTTCTGAGAGCTCAGCCCG
qTmod1_F	GAGGATGAAATCCTGGGGGC
qTomd1_R	GGTGGTCTGATCCTTCTGCC

### 5.18.2 ChIP-qPCR primers

Gene name	Sequence of ChIP primers	ChIP
Hand2_F	AATTGCCGAGGTCCTTCT	Brg1/Gata4 ChIP
Hand2_R	CTCAGAGCCAGCCAACTACT	Brg1/ Gata4 ChIP

Ttn_F	CAGAATATGCAAATCCAGGTGC	Brg1/Gata4 ChIP
Ttn_R	CGAGGCATTGGTGAAGACTC	Brg1/ Gata4 ChIP
Ryr2_F	TAGGATGGATCTCACTGGATGGT	Brg1/Gata4 ChIP
Ryr2_R	AAAGTTAAGCCTTGCCCCACA	Brg1/ Gata4 ChIP
Myocd_F	CTGTCAGGCTAGCTGATGATGAA	Brg1/Gata4 ChIP
Myocd_R	ATACAACATCTTCCCCTTCACTTCC	Brg1/ Gata4 ChIP
Mlc1v_F	GTTCTCGACTCCTCCGGGAA	Brg1/Gata4 ChIP
Mlc1v_R	CTCCCCACGTGTCCTTGTC	Brg1/ Gata4 ChIP
Atp1a2_F	CGGAAAAGGCTGGGTAAAGT	Brg1/Gata4 ChIP
Atp1a2_R	GGGAGTGGGATTGTTTTCT	Brg1/ Gata4 ChIP
Mef2c_F	TCAGTGTCTGCTCCTGCTTC	Brg1 ChIP
Mef2c_R	TCCCTCCACACCTTACTGG	Brg1 ChIP

## 6. References

- Aalfs, J. D. and R. E. Kingston (2000). "What does 'chromatin remodeling' mean?" Trends in biochemical sciences **25**(11): 548-555.
- Abdul-Ghani, M., D. Dufort, R. Stiles, Y. De Repentigny, R. Kothary and L. A. Megeney (2011). "Wnt11 promotes cardiomyocyte development by caspase-mediated suppression of canonical Wnt signals." Mol Cell Biol **31**(1): 163-178.
- Abramzon, F., M. J. Bosaleh, P. Pollono, E. Levy Yeyati, J. Wolcan and G. A. Rodríguez-Granillo (2019). "Congenital Heart Disease." Clinical Atlas of Cardiac and Aortic CT and MRI **Chapter 6**: 201-285.
- Ahlgren, U., S. L. Pfaff, T. M. Jessell, T. Edlund and H. Edlund (1997). "Independent requirement for ISL1 in formation of pancreatic mesenchyme and islet cells." Nature **385**(6613): 257.
- Alexander, J. M., S. K. Hota, D. He, S. Thomas, L. Ho, L. A. Pennacchio and B. G. Bruneau (2015). "Brg1 modulates enhancer activation in mesoderm lineage commitment." Development **142**(8): 1418-1430.
- Almer, A., H. Rudolph, A. Hinnen and W. Hörz (1986). "Removal of positioned nucleosomes from the yeast PHO5 promoter upon PHO5 induction releases additional upstream activating DNA elements." The EMBO journal **5**(10): 2689-2696.
- Anders, S. and W. Huber (2010). "Differential expression analysis for sequence count data." Genome biology **11**(10): R106.
- Anderson, R. H., D. E. Spicer, N. A. Brown and T. J. Mohun (2014). "The development of septation in the four-chambered heart." Anat Rec (Hoboken) **297**(8): 1414-1429.
- Bach, I. (2000). "The LIM domain: regulation by association." Mechanisms of Development **91**(1-2): 5-17.
- Bakker, M. L., B. J. Boukens, M. T. Mommersteeg, J. F. Brons, V. Wakker, A. F. Moorman and V. M. Christoffels (2008). "Transcription factor Tbx3 is required for the specification of the atrioventricular conduction system." Circ Res **102**(11): 1340-1349.
- Barnes, R. M., B. A. Firulli, S. J. Conway, J. W. Vincentz and A. B. Firulli (2010). "Analysis of the Hand1 cell lineage reveals novel contributions to cardiovascular, neural crest, extra-embryonic, and lateral mesoderm derivatives." Developmental Dynamics **239**(11): 3086-3097.
- Barnes, R. M., I. S. Harris, E. J. Jaehnig, K. Sauls, T. Sinha, A. Rojas, W. Schachterle, D. J. McCulley, R. A. Norris and B. L. Black (2016). "MEF2C regulates outflow tract alignment and transcriptional control of TdGF1." Development **143**(5): 774-779.
- Barnett, D. W., E. K. Garrison, A. R. Quinlan, M. P. Strömberg and G. T. Marth (2011). "BamTools: a C++ API and toolkit for analyzing and managing BAM files." Bioinformatics **27**(12): 1691-1692.
- Basson, C. T., D. R. Bachinsky, R. C. Lin, T. Levi, J. A. Elkins, J. Soultz, D. Grayzel, E. Kroumpouzou, T. A. Traill, J. Leblanc-Straceski, B. Renault, R. Kucherlapati, S. J.G and C. E. Seidman (1997). "Mutations in human cause limb and cardiac malformation in Holt-Oram syndrome." Nature Genetics **15**: pages 30–35.



- Bellec, M., O. Radulescu and M. Lagha (2018). "Remembering the past: Mitotic bookmarking in a developing embryo." Curr Opin Syst Biol **11**: 41-49.
- Benoit G. Bruneau, Malcolm Logan, Nicole Davis, Tatjana Levia, Clifford J. Tabin, J.G. Seidman and C. E. Seidman (1999). "Chamber-Specific Cardiac Expression of Tbx5 and Heart Defects in Holt–Oram Syndrome." Developmental Biology **211**(1): 100-108.
- Bernstein, B. E., T. S. Mikkelsen, X. Xie, M. Kamal, D. J. Huebert, J. Cuff, B. Fry, A. Meissner, M. Wernig, K. Plath, R. Jaenisch, A. Wagschal, R. Feil, S. L. Schreiber and E. S. Lander (2006). "A bivalent chromatin structure marks key developmental genes in embryonic stem cells." Cell **125**(2): 315-326.
- Bhati, M., C. Lee, M. S. Gadd, C. M. Jeffries, A. Kwan, A. E. Whitten, J. Trewhella, J. P. Mackay and J. M. Matthews (2012). "Solution structure of the LIM-homeodomain transcription factor complex Lhx3/Ldb1 and the effects of a pituitary mutation on key Lhx3 interactions." PLoS One **7**(7): e40719.
- Bird, A. (2007). "Perceptions of epigenetics." Nature **447**(7143): 396-398.
- Birgit André'e, D. D., Britta Vorbusch, Hans-Henning Arnold, Thomas Brand (1998). "BMP-2 induces ectopic expression of cardiac lineage markers and interferes with somite formation in chicken embryos." Mechanisms of Development **70**: 119–131.
- Bisson, J. A., B. Mills, J. C. Paul Helt, T. P. Zwaka and E. D. Cohen (2015). "Wnt5a and Wnt11 inhibit the canonical Wnt pathway and promote cardiac progenitor development via the Caspase-dependent degradation of AKT." Dev Biol **398**(1): 80-96.
- Biswas, M., K. Voltz, J. C. Smith and J. Langowski (2011). "Role of histone tails in structural stability of the nucleosome." PLoS computational biology **7**(12): e1002279.
- Bondue, A., Lapouge, G., Paulissen, C., Semeraro, C., Iacovino, M., Kyba, M., Blanpain, C. (2008). "Mesp1 acts as a master regulator of multipotent cardiovascular progenitor specification." Cell Stem Cell **3**(1): 69-84.
- Bossard, P. and K. S. Zaret (1998). "GATA transcription factors as potentiators of gut endoderm differentiation." Development **125**(24): 4909-4917.
- Brade, T., S. Gessert, M. Kühl and P. Pandur (2007). "The amphibian second heart field: *Xenopus* islet-1 is required for cardiovascular development." Developmental biology **311**(2): 297-310.
- Bruneau, B. G. (2002). "Transcriptional Regulation of Vertebrate Cardiac Morphogenesis." Circulation Research **90**(5): 509-519.
- Bruneau, B. G. (2008). "The developmental genetics of congenital heart disease." Nature **451**(7181): 943-948.
- Bruneau, B. G. (2013). "Signaling and transcriptional networks in heart development and regeneration." Cold Spring Harb Perspect Biol **5**(3): a008292.
- Bu, L., X. Jiang, S. Martin-Puig, L. Caron, S. Zhu, Y. Shao, D. J. Roberts, P. L. Huang, I. J. Domian and K. R. Chien (2009). "Human ISL1 heart progenitors generate diverse multipotent cardiovascular cell lineages." Nature **460**(7251): 113-117.
- Buckingham, M. (2016). "First and Second Heart Field." 25-40.

Buckingham, M., S. Meilhac and S. Zaffran (2005). "Building the mammalian heart from two sources of myocardial cells." Nat Rev Genet **6**(11): 826-835.

Budry, L., A. Balsalobre, Y. Gauthier, K. Khetchoumian, A. L'Honoré, S. Vallette, T. Brue, D. Figarella-Branger, B. Meij and J. Drouin (2012). "The selector gene Pax7 dictates alternate pituitary cell fates through its pioneer action on chromatin remodeling." Genes & development **26**(20): 2299-2310.

Buenrostro, J. D., P. G. Giresi, L. C. Zaba, H. Y. Chang and W. J. Greenleaf (2013). "Transposition of native chromatin for fast and sensitive epigenomic profiling of open chromatin, DNA-binding proteins and nucleosome position." Nat Methods **10**(12): 1213-1218.

Buikema, J., P.-P. Zwetsloot, P. Doevendans, I. Domian and J. Sluiter (2014). "Wnt/ $\beta$ -Catenin Signaling during Cardiac Development and Repair." Journal of Cardiovascular Development and Disease **1**(1): 98-110.

Bultman, S., T. Gebuhr, D. Yee, C. La Mantia, J. Nicholson, A. Gilliam, F. Randazzo, D. Metzger, P. Chambon and G. Crabtree (2000). "A Brg1 null mutation in the mouse reveals functional differences among mammalian SWI/SNF complexes." Molecular cell **6**(6): 1287-1295.

Burrige, P. W., E. Matsa, P. Shukla, Z. C. Lin, J. M. Churko, A. D. Ebert, F. Lan, S. Diecke, B. Huber, N. M. Mordwinkin, J. R. Plews, O. J. Abilez, B. Cui, J. D. Gold and J. C. Wu (2014). "Chemically defined generation of human cardiomyocytes." Nat Methods **11**(8): 855-860.

Cai, C.-L., X. Liang, Y. Shi, P.-H. Chu, S. L. Pfaff, J. Chen and S. Evans (2003). "Isl1 Identifies a Cardiac Progenitor Population that Proliferates Prior to Differentiation and Contributes a Majority of Cells to the Heart." Developmental Cell **5**(6): 877-889.

Caputo, L., H. R. Witzel, P. Kolovos, S. Cheedipudi, M. Looso, A. Mylona, I. W. F. van, K. L. Laugwitz, S. M. Evans, T. Braun, E. Soler, F. Grosveld and G. Dobрева (2015). "The Isl1/Ldb1 Complex Orchestrates Genome-wide Chromatin Organization to Instruct Differentiation of Multipotent Cardiac Progenitors." Cell Stem Cell **17**(3): 287-299.

Caravaca, J. M., G. Donahue, J. S. Becker, X. He, C. Vinson and K. S. Zaret (2013). "Bookmarking by specific and nonspecific binding of FoxA1 pioneer factor to mitotic chromosomes." Genes Dev **27**(3): 251-260.

Chang, C. P., Bruneau, B. G. (2012). "Epigenetics and cardiovascular development." Annu Rev Physiol **74**: 41-68.

Chen, H., S. Shi, L. Acosta, W. Li, J. Lu, S. Bao, Z. Chen, Z. Yang, M. D. Schneider, K. R. Chien, S. J. Conway, M. C. Yoder, L. S. Haneline, D. Franco and W. Shou (2004). "BMP10 is essential for maintaining cardiac growth during murine cardiogenesis." Development **131**(9): 2219-2231.

Chi, T. H., M. Wan, P. P. Lee, K. Akashi, D. Metzger, P. Chambon, C. B. Wilson and G. R. Crabtree (2003). "Sequential roles of Brg, the ATPase subunit of BAF chromatin remodeling complexes, in thymocyte development." Immunity **19**(2): 169-182.

Ching, S. T., C. R. Infante, W. Du, A. Sharir, S. Park, D. B. Menke and O. D. Klein (2018). "Isl1 mediates mesenchymal expansion in the developing external genitalia via regulation of Bmp4, Fgf10 and Wnt5a." Hum Mol Genet **27**(1): 107-119.

Chong, J. J., E. Forte and R. P. Harvey (2014). "Developmental origins and lineage descendants of endogenous adult cardiac progenitor cells." Stem Cell Res **13**(3 Pt B): 592-614.

Christoffels, R. S. M. H. B. G. S. R. B. F. F. P. H. F. M. F. M. M. A. C. t. H. K. a. M. (2012). "Tbx2 and Tbx3 induce atrioventricular myocardial development and endocardial cushion formation." Cellular and Molecular Life Sciences **69**(8): 1377–1389.

Christoffels, V. M., J. B. Burch and A. F. Moorman (2004). "Architectural plan for the heart: early patterning and delineation of the chambers and the nodes." Trends Cardiovasc Med **14**(8): 301-307.

Christoffels, V. M., M. T. Mommersteeg, M. O. Trowe, O. W. Prall, C. de Gier-de Vries, A. T. Soufan, M. Bussen, K. Schuster-Gossler, R. P. Harvey, A. F. Moorman and A. Kispert (2006). "Formation of the venous pole of the heart from an Nkx2-5-negative precursor population requires Tbx18." Circ Res **98**(12): 1555-1563.

Christopher B. Brown, L. F., Min-Min Lu, Jun Li, Xiaokui Ma, Andrea L. Webber, Li Jia, Jonathan A. Raper, Jonathan A. Epstein (2001). "PlexinA2 and semaphorin signaling during cardiac neural crest development." Development **128**: 3071-3080.

Cirillo, L. A., F. R. Lin, I. Cuesta, D. Friedman, M. Jarnik and K. S. Zaret (2002). "Opening of compacted chromatin by early developmental transcription factors HNF3 (FoxA) and GATA-4." Molecular cell **9**(2): 279-289.

Cirillo, L. A., C. E. McPherson, P. Bossard, K. Stevens, S. Cherian, E. Y. Shim, K. L. Clark, S. K. Burley and K. S. Zaret (1998). "Binding of the winged-helix transcription factor HNF3 to a linker histone site on the nucleosome." The EMBO journal **17**(1): 244-254.

Cirillo, L. A. and K. S. Zaret (1999). "An early developmental transcription factor complex that is more stable on nucleosome core particles than on free DNA." Molecular cell **4**(6): 961-969.

Clapier, C. R., J. Iwasa, B. R. Cairns and C. L. Peterson (2017). "Mechanisms of action and regulation of ATP-dependent chromatin-remodelling complexes." Nature Reviews Molecular Cell Biology **18**(7): 407.

Clark, K. L., E. D. Halay, E. Lai and S. K. Burley (1993). "Co-crystal structure of the HNF-3/fork head DNA-recognition motif resembles histone H5." Nature **364**(6436): 412.

Cohen, E. D., M. F. Miller, Z. Wang, R. T. Moon and E. E. Morrisey (2012). "Wnt5a and Wnt11 are essential for second heart field progenitor development." Development **139**(11): 1931-1940.

Cohen, E. D., Y. Tian and E. E. Morrisey (2008). "Wnt signaling: an essential regulator of cardiovascular differentiation, morphogenesis and progenitor self-renewal." Development **135**(5): 789-798.

Colombo, S., C. de Sena-Tomas, V. George, A. A. Werdich, S. Kapur, C. A. MacRae and K. L. Targoff (2018). "Nkx genes establish second heart field cardiomyocyte progenitors at the arterial pole and pattern the venous pole through Isl1 repression." Development **145**(3).

D.G. McFadden, J. C., J.A. Richardson, D. Srivastava, A.B. Firulli, E.N. Olson (2000). "A GATA-dependent right ventricular enhancer controls dHAND transcription in the developing heart." Development **127**: 5331-5341.

de Pater, E., L. Clijsters, S. R. Marques, Y.-F. Lin, Z. V. Garavito-Aguilar, D. Yelon and J. Bakkers (2009). "Distinct phases of cardiomyocyte differentiation regulate growth of the zebrafish heart." Development **136**(10): 1633-1641.

Deepak Srivastava, T. T., Qing Lin, Margaret L. Kirby, Doris Brown & Eric N. Olson (1997). "Regulation of cardiac mesodermal and neural crest development by the bHLH transcription factor, dHAND." Nature Genetics **16**: pages154–160

DeLaughter, D. M., A. G. Bick, H. Wakimoto, D. McKean, J. M. Gorham, I. S. Kathiriya, J. T. Hinson, J. Homsy, J. Gray, W. Pu, B. G. Bruneau, J. G. Seidman and C. E. Seidman (2016). "Single-Cell Resolution of Temporal Gene Expression during Heart Development." Dev Cell **39**(4): 480-490.

Delmore, J. E., G. C. Issa, M. E. Lemieux, P. B. Rahl, J. Shi, H. M. Jacobs, E. Kastritis, T. Gilpatrick, R. M. Paranal and J. Qi (2011). "BET bromodomain inhibition as a therapeutic strategy to target c-Myc." Cell **146**(6): 904-917.

Denise van der Linde, D., E. E. Konings, M. A. Slager, M. Witsenburg, W. A. Helbing, J. J. Takkenberg and J. W. Roos-Hesselink (2011). "Birth prevalence of congenital heart disease worldwide: a systematic review and meta-analysis." J Am Coll Cardiol **58**(21): 2241-2247.

Ding, J.-d., J. Tong, K. Li, X. Fang, H. Li, X. Zhang, Y. Yao and G. Ma (2015). "The novel mutations of GATA4 gene in Chinese patients with sporadic congenital heart defects." Journal of Integrative Cardiology **1**(4).

Dirscherl, S. S. and J. E. Krebs (2004). "Functional diversity of ISWI complexes." Biochem Cell Biol **82**(4): 482-489.

Dodou, E., M. P. Verzi, J. P. Anderson, S. M. Xu and B. L. Black (2004). "Mef2c is a direct transcriptional target of ISL1 and GATA factors in the anterior heart field during mouse embryonic development." Development **131**(16): 3931-3942.

Doerks, T., R. R. Copley, J. Schultz, C. P. Ponting and P. Bork (2002). "Systematic identification of novel protein domain families associated with nuclear functions." Genome Res **12**(1): 47-56.

Doetschman, T. and M. Azhar (2012). "Cardiac-specific inducible and conditional gene targeting in mice." Circ Res **110**(11): 1498-1512.

Dorn, T., A. Goedel, J. T. Lam, J. Haas, Q. Tian, F. Herrmann, K. Bundschu, G. Dobрева, M. Schiemann, R. Dirschinger, Y. Guo, S. J. Kuhl, D. Sinnecker, P. Lipp, K. L. Laugwitz, M. Kuhl and A. Moretti (2015). "Direct nkx2-5 transcriptional repression of isl1 controls cardiomyocyte subtype identity." Stem Cells **33**(4): 1113-1129.

Drucker, M. W. a. D. J. (1995). "The LIM Domain Homeobox Gene isl-1 Is a Positive Regulator of Islet Cell-specific Proglucagon Gene Transcription." The Journal of Biological Chemistry **270**(21): 12646-12652.

Dupays, L., S. Kotecha, B. Angst and T. J. Mohun (2009). "Tbx2 misexpression impairs deployment of second heart field derived progenitor cells to the arterial pole of the embryonic heart." Dev Biol **333**(1): 121-131.

Durocher, D., F. Charron, R. Warren, R. J. Schwartz and M. Nemer (1997). "The cardiac transcription factors Nkx2-5 and GATA-4 are mutual cofactors." The EMBO journal **16**(18): 5687-5696.

Dyer, L. A. and M. L. Kirby (2009). "The role of secondary heart field in cardiac development." Dev Biol **336**(2): 137-144.

Dyer, L. A. and M. L. Kirby (2009). "Sonic hedgehog maintains proliferation in secondary heart field progenitors and is required for normal arterial pole formation." Dev Biol **330**(2): 305-317.

Elizabeth A. Lindsay, F. V., Hong Su, Masae Morishima, Tuong Huynh, Tiziano Pramparo, Vesna Jurecic, George Ogunrinu, Helen F. Sutherland, Peter J. Scambler, Allan Bradley & Antonio Baldini (2001). "Tbx1 haploinsufficiency in the DiGeorge syndrome region causes aortic arch defects in mice." Nature **410**: 97–101.

Elshatory, Y., D. Everhart, M. Deng, X. Xie, R. B. Barlow and L. Gan (2007). "Islet-1 controls the differentiation of retinal bipolar and cholinergic amacrine cells." J Neurosci **27**(46): 12707-12720.

Emma de Pater, M. C., Florian Priller, Justus Veerkamp, Ina Strate, Kelly Smith, Anne Karine Lagendijk, Thomas F. Schilling, Wiebke Herzog, Salim Abdelilah-Seyfried, Matthias Hammerschmidt, Jeroen Bakkers (2012). "Bmp Signaling Exerts Opposite Effects on Cardiac Differentiation." Circulation Research **110**(578-587).

Engleka, K. A., L. J. Manderfield, R. D. Brust, L. Li, A. Cohen, S. M. Dymecki and J. A. Epstein (2012). "Islet1 derivatives in the heart are of both neural crest and second heart field origin." Circ Res **110**(7): 922-926.

Fischer, A., C. Steidl, T. U. Wagner, E. Lang, P. M. Jakob, P. Friedl, K. P. Knobloch and M. Gessler (2007). "Combined loss of Hey1 and HeyL causes congenital heart defects because of impaired epithelial to mesenchymal transition." Circ Res **100**(6): 856-863.

Florian Kraus, B. H., Andreas Kispert (2001). "Cloning and expression analysis of the mouse T-box gene Tbx18." Mechanisms of Development **100**(1): 83-86.

Francou, A., E. Saint-Michel, K. Mesbah, M. Theveniau-Ruissy, M. S. Rana, V. M. Christoffels and R. G. Kelly (2013). "Second heart field cardiac progenitor cells in the early mouse embryo." Biochim Biophys Acta **1833**(4): 795-798.

Gadd, M. S., M. Bhati, C. M. Jeffries, D. B. Langley, J. Trehwella, J. M. Guss and J. M. Matthews (2011). "Structural basis for partial redundancy in a class of transcription factors, the LIM homeodomain proteins, in neural cell type specification." J Biol Chem **286**(50): 42971-42980.

Gadd, M. S., D. A. Jacques, I. Nisevic, V. J. Craig, A. H. Kwan, J. M. Guss and J. M. Matthews (2013). "A structural basis for the regulation of the LIM-homeodomain protein islet 1 (Isl1) by intra- and intermolecular interactions." J Biol Chem **288**(30): 21924-21935.

Galli, D., J. N. Dominguez, S. Zaffran, A. Munk, N. A. Brown and M. E. Buckingham (2008). "Atrial myocardium derives from the posterior region of the second heart field, which acquires left-right identity as Pitx2c is expressed." Development **135**(6): 1157-1167.

Garg, V. (2006). "Insights into the genetic basis of congenital heart disease." Cell Mol Life Sci **63**(10): 1141-1148.

Garg, V., I. S. Kathiriya, R. Barnes, M. K. Schluterman, I. N. King, C. A. Butler, C. R. Rothrock, R. S. Eapen, K. Hirayama-Yamada and K. Joo (2003). "GATA4 mutations cause human congenital heart defects and reveal an interaction with TBX5." Nature **424**(6947): 443.

Gessert, S. and M. Kuhl (2010). "The multiple phases and faces of wnt signaling during cardiac differentiation and development." Circ Res **107**(2): 186-199.

Ghosh, T. K., F. F. Song, E. A. Packham, S. Buxton, T. E. Robinson, J. Ronksley, T. Self, A. J. Bonser and J. D. Brook (2009). "Physical interaction between TBX5 and MEF2C is required for early heart development." Mol Cell Biol **29**(8): 2205-2218.

Gillette, T. G. and J. A. Hill (2015). "Readers, writers, and erasers: chromatin as the whiteboard of heart disease." Circ Res **116**(7): 1245-1253.

Goldberg, A. D., C. D. Allis and E. Bernstein (2007). "Epigenetics: a landscape takes shape." Cell **128**(4): 635-638.

Golzio, C., E. Havis, P. Daubas, G. Nuel, C. Babarit, A. Munnich, M. Vekemans, S. Zaffran, S. Lyonnet and H. C. Etchevers (2012). "ISL1 directly regulates FGF10 transcription during human cardiac outflow formation." PLoS One **7**(1): e30677.

Grego-Bessa, J., L. Luna-Zurita, G. del Monte, V. Bolos, P. Melgar, A. Arandilla, A. N. Garratt, H. Zang, Y. S. Mukoyama, H. Chen, W. Shou, E. Ballestar, M. Esteller, A. Rojas, J. M. Perez-Pomares and J. L. de la Pompa (2007). "Notch signaling is essential for ventricular chamber development." Dev Cell **12**(3): 415-429.

Griffin, C. T., C. D. Curtis, R. B. Davis, V. Muthukumar and T. Magnuson (2010). "The chromatin-remodeling enzyme BRG1 modulates vascular Wnt signaling at two levels." PNAS **108**(6): 2282-2287.

Gualdi, R., P. Bossard, M. Zheng, Y. Hamada, J. R. Coleman and K. S. Zaret (1996). "Hepatic specification of the gut endoderm in vitro: cell signaling and transcriptional control." Genes & development **10**(13): 1670-1682.

Hagey, D. W., C. Zaouter, G. Combeau, M. A. Lendahl, O. Andersson, M. Huss and J. Muhr (2016). "Distinct transcription factor complexes act on a permissive chromatin landscape to establish regionalized gene expression in CNS stem cells." Genome research.

Handy, D. E., R. Castro and J. Loscalzo (2011). "Epigenetic modifications: basic mechanisms and role in cardiovascular disease." Circulation **123**(19): 2145-2156.

Hang, C. T., J. Yang, P. Han, H. L. Cheng, C. Shang, E. Ashley, B. Zhou and C. P. Chang (2010). "Chromatin regulation by Brg1 underlies heart muscle development and disease." Nature **466**(7302): 62-67.

Harrelson, Z., R. G. Kelly, S. N. Goldin, J. J. Gibson-Brown, R. J. Bollag, L. M. Silver and V. E. Papaioannou (2004). "Tbx2 is essential for patterning the atrioventricular canal and for morphogenesis of the outflow tract during heart development." Development **131**(20): 5041-5052.

Harris, I. S. (2011). "Management of pregnancy in patients with congenital heart disease." Prog Cardiovasc Dis **53**(4): 305-311.

Harvey, C. B. a. R. P. (1997). "Homeodomain factor Nkx2-5 controls left/right asymmetric expression of bHLH gene eHand during murine heart development." Genes Dev. **11**: 1357-1369.

He, A., F. Gu, Y. Hu, Q. Ma, L. Y. Ye, J. A. Akiyama, A. Visel, L. A. Pennacchio and W. T. Pu (2014). "Dynamic GATA4 enhancers shape the chromatin landscape central to heart development and disease." Nature communications **5**: 4907.

He, A., S. W. Kong, Q. Ma and W. T. Pu (2011). "Co-occupancy by multiple cardiac transcription factors identifies transcriptional enhancers active in heart." Proceedings of the National Academy of Sciences **108**(14): 5632-5637.

Heikinheimo, M., J. M. Scandrett and D. B. Wilson (1994). "Localization of transcription factor GATA-4 to regions of the mouse embryo involved in cardiac development." Developmental biology **164**(2): 361-373.

Hemberger, M., W. Dean and W. Reik (2009). "Epigenetic dynamics of stem cells and cell lineage commitment: digging Waddington's canal." Nat Rev Mol Cell Biol **10**(8): 526-537.

High, F. A., R. Jain, J. Z. Stoller, N. B. Antonucci, M. M. Lu, K. M. Loomes, K. H. Kaestner, W. S. Pear and J. A. Epstein (2009). "Murine Jagged1/Notch signaling in the second heart field orchestrates Fgf8 expression and tissue-tissue interactions during outflow tract development." J Clin Invest **119**(7): 1986-1996.

Ho, L. and G. R. Crabtree (2010). "Chromatin remodelling during development." Nature **463**(7280): 474.

Ho, L. and G. R. Crabtree (2010). "Chromatin remodelling during development." Nature **463**(7280): 474-484.

Ho, L., R. Jothi, J. L. Ronan, K. Cui, K. Zhao and G. R. Crabtree (2009). "An embryonic stem cell chromatin remodeling complex, esBAF, is an essential component of the core pluripotency transcriptional network." Proc Natl Acad Sci U S A **106**(13): 5187-5191.

Ho, L., J. L. Ronan, J. Wu, B. T. Staahl, L. Chen, A. Kuo, J. Lessard, A. I. Nesvizhskii, J. Ranish and G. R. Crabtree (2009). "An embryonic stem cell chromatin remodeling complex, esBAF, is essential for embryonic stem cell self-renewal and pluripotency." Proc Natl Acad Sci U S A **106**(13): 5181-5186.

Hoffman, J. I. E. and S. Kaplan (2002). "The incidence of congenital heart disease." Journal of the American College of Cardiology **39**(12): 1890-1900.

Hofmann, J. J., A. Briot, J. Enciso, A. C. Zovein, S. Ren, Z. W. Zhang, F. Radtke, M. Simons, Y. Wang and M. L. Iruela-Arispe (2012). "Endothelial deletion of murine Jag1 leads to valve calcification and congenital heart defects associated with Alagille syndrome." Development **139**(23): 4449-4460.

Holtzinger, A. and T. Evans (2007). "Gata5 and Gata6 are functionally redundant in zebrafish for specification of cardiomyocytes." Developmental biology **312**(2): 613-622.

Hota, S. K. and B. G. Bruneau (2016). "ATP-dependent chromatin remodeling during mammalian development." Development **143**(16): 2882-2897.

Hota, S. K. and B. G. Bruneau (2016). "ATP-dependent chromatin remodeling during mammalian development." Development **143**(16): 2882-2897.

Hota, S. K., J. R. Johnson, E. Verschueren, R. Thomas, A. M. Blotnick, Y. Zhu, X. Sun, L. A. Pennacchio, N. J. Krogan and B. G. Bruneau (2019). "Dynamic BAF chromatin remodeling complex subunit inclusion promotes temporally distinct gene expression programs in cardiogenesis." Development: dev.174086.

Hsiao, E. C., Y. Yoshinaga, T. D. Nguyen, S. L. Musone, J. E. Kim, P. Swinton, I. Espineda, C. Manalac and B. R. Conklin (2008). "Marking embryonic stem cells with a 2A self-cleaving peptide: a NKX2-5 emerald GFP BAC reporter." PLoS one **3**(7): e2532.

Hsiao, E. C., Y. Yoshinaga, T. D. Nguyen, S. L. Musone, J. E. Kim, P. Swinton, I. Espineda, C. Manalac, P. J. deJong and B. R. Conklin (2008). "Marking embryonic stem cells with a 2A self-cleaving peptide: a NKX2-5 emerald GFP BAC reporter." *PLoS One* **3**(7): e2532.

Hu, T., H. Yamagishi, J. Maeda, J. McAnally, C. Yamagishi and D. Srivastava (2004). "Tbx1 regulates fibroblast growth factors in the anterior heart field through a reinforcing autoregulatory loop involving forkhead transcription factors." *Development* **131**(21): 5491-5502.

Huang, J., J. Elicker, N. Bowens, X. Liu, L. Cheng, T. P. Cappola, X. Zhu and M. S. Parmacek (2012). "Myocardin regulates BMP10 expression and is required for heart development." *J Clin Invest* **122**(10): 3678-3691.

Huang, R. T., J. Wang, S. Xue, X. B. Qiu, H. Y. Shi, R. G. Li, X. K. Qu, X. X. Yang, H. Liu, N. Li, Y. J. Li, Y. J. Xu and Y. Q. Yang (2017). "TBX20 loss-of-function mutation responsible for familial tetralogy of Fallot or sporadic persistent truncus arteriosus." *Int J Med Sci* **14**(4): 323-332.

Hubert, F., S. M. Payan and F. Rochais (2018). "FGF10 Signaling in Heart Development, Homeostasis, Disease and Repair." *Front Genet* **9**: 599.

Hutson, M. R., X. L. Zeng, A. J. Kim, E. Antoon, S. Harward and M. L. Kirby (2010). "Arterial pole progenitors interpret opposing FGF/BMP signals to proliferate or differentiate." *Development* **137**(18): 3001-3011.

I Lyons, L. M. P., L Hartley, R Li, J E Andrews, L Robb, and R P Harvey (1995). "Myogenic and morpho.genetic defects in the heart tubes of murlne embryos lacking the homeo box gene Nkx2-5." *Genes & Dev.* **9**: 1654-1666.

Ilagan, R., R. Abu-Issa, D. Brown, Y. P. Yang, K. Jiao, R. J. Schwartz, J. Klingensmith and E. N. Meyers (2006). "Fgf8 is required for anterior heart field development." *Development* **133**(12): 2435-2445.

Itoh, N., H. Ohta, Y. Nakayama and M. Konishi (2016). "Roles of FGF Signals in Heart Development, Health, and Disease." *Front Cell Dev Biol* **4**: 110.

Iwafuchi-Doi, M. (2019). "The mechanistic basis for chromatin regulation by pioneer transcription factors." *Wiley Interdiscip Rev Syst Biol Med* **11**(1): e1427.

Iwafuchi-Doi, M. and K. S. Zaret (2014). "Pioneer transcription factors in cell reprogramming." *Genes Dev* **28**(24): 2679-2692.

Iwafuchi-Doi, M. and K. S. Zaret (2016). "Cell fate control by pioneer transcription factors." *Development* **143**(11): 1833-1837.

Jaenisch, R. and A. Bird (2003). "Epigenetic regulation of gene expression: how the genome integrates intrinsic and environmental signals." *Nat Genet* **33 Suppl**: 245-254.

Jia, G., J. Preussner, X. Chen, S. Guenther, X. Yuan, M. Yekelchyk, C. Kuenne, M. Looso, Y. Zhou and S. Teichmann (2018). "Single cell RNA-seq and ATAC-seq analysis of cardiac progenitor cell transition states and lineage settlement." *Nature communications* **9**(1): 4877.

Jozwik, K. M. and J. S. Carroll (2012). "Pioneer factors in hormone-dependent cancers." *Nature Reviews Cancer* **12**(6): 381.

Jun Li, F. C., and Jonathan A. Epstein (2000). "Neural Crest Expression of Cre Recombinase Directed by the Proximal Pax3 Promoter in Transgenic Mice." *genesis* **26**: 162–164.



Kadam, S. and B. M. Emerson (2003). "Transcriptional specificity of human SWI/SNF BRG1 and BRM chromatin remodeling complexes." Molecular cell **11**(2): 377-389.

Kadoch, C. and G. R. Crabtree (2013). "Reversible disruption of mSWI/SNF (BAF) complexes by the SS18-SSX oncogenic fusion in synovial sarcoma." Cell **153**(1): 71-85.

Kang, J., E. Nathan, S. M. Xu, E. Tzahor and B. L. Black (2009). "Isl1 is a direct transcriptional target of Forkhead transcription factors in second-heart-field-derived mesoderm." Dev Biol **334**(2): 513-522.

Karen Waldo, S. M.-T., Donna Kumiski, and Margaret L. Kirby (1998). "Cardiac Neural Crest Cells Provide New Insight into Septation of the Cardiac Outflow Tract: Aortic Sac to Ventricular Septal Closure." Developmental biology **196**: 129–144.

Karin, M. (1990). "Too many transcription factors: positive and negative interactions." The New Biologist **2**(2): 126-131.

Karlsson, O., S. Thor, T. Norberg, H. Ohlsson and T. Edlund (1990). "Insulin gene enhancer binding protein Isl-1 is a member of a novel class of proteins containing both a homeo- and a Cys–His domain." Nature **344**(6269): 879.

Karlsson, O., S. Thor, T. Norberg, H. Ohlsson and T. Edlund (1990). "Insulin gene enhancer binding protein Isl-1 is a member of a novel class of proteins containing both a homeo- and a Cys–His domain." Nature **344**: 879–882.

Kathiriya, I. S., E. P. Nora and B. G. Bruneau (2015). "Investigating the transcriptional control of cardiovascular development." Circulation research **116**(4): 700-714.

Kattman, S. J., T. L. Huber and G. M. Keller (2006). "Multipotent flk-1+ cardiovascular progenitor cells give rise to the cardiomyocyte, endothelial, and vascular smooth muscle lineages." Dev Cell **11**(5): 723-732.

Kattman, S. J., A. D. Witty, M. Gagliardi, N. C. Dubois, M. Niapour, A. Hotta, J. Ellis and G. Keller (2011). "Stage-specific optimization of activin/nodal and BMP signaling promotes cardiac differentiation of mouse and human pluripotent stem cell lines." Cell Stem Cell **8**(2): 228-240.

Kelly, R. G. (2012). "The second heart field." Curr Top Dev Biol **100**: 33-65.

Kernell, K., G. Sydsjö, M. Bladh, N. E. Nielsen and A. Josefsson (2014). "Congenital heart disease in men – birth characteristics and reproduction: a national cohort study." BMC Pregnancy and Childbirth **14**(187): 1471-2393.

Kidder, B. L., S. Palmer and J. G. Knott (2009). "SWI/SNF-Brg1 regulates self-renewal and occupies core pluripotency-related genes in embryonic stem cells." Stem cells **27**(2): 317-328.

King, H. W. and R. J. Klose (2017). "The pioneer factor OCT4 requires the chromatin remodeller BRG1 to support gene regulatory element function in mouse embryonic stem cells." Elife **6**.

Kirby, M. L. and M. R. Hutson (2010). "Factors controlling cardiac neural crest cell migration." Cell Adh Migr **4**(4): 609-621.

Kirk, E. P., Sunde, M., Costa, M. W., Rankin, S. A., Wolstein, O., Castro, M. L., Butler, T. L., Hyun, C., Guo, G., Otway, R., Mackay, J. P., Waddell, L. B., Cole, A. D., Hayward, C., Keogh, A., Macdonald, P., Griffiths, L., Fatkin, D., Sholler, G. F., Zorn, A. M., Feneley, M. P., Winlaw, D.

S., Harvey, R. P. (2007). "Mutations in cardiac T-box factor gene TBX20 are associated with diverse cardiac pathologies, including defects of septation and valvulogenesis and cardiomyopathy." Am J Hum Genet **81**(2): 280-291.

Kloesel, B., J. A. DiNardo and S. C. Body (2016). "Cardiac Embryology and Molecular Mechanisms of Congenital Heart Disease: A Primer for Anesthesiologists." Anesth Analg **123**(3): 551-569.

Kodo, K., T. Nishizawa, M. Furutani, S. Arai, E. Yamamura, K. Joo, T. Takahashi, R. Matsuoka and H. Yamagishi (2009). "GATA6 mutations cause human cardiac outflow tract defects by disrupting semaphorin-plexin signaling." Proc Natl Acad Sci U S A **106**(33): 13933-13938.

Kokubo, H., S. Miyagawa-Tomita, M. Nakazawa, Y. Saga and R. L. Johnson (2005). "Mouse hesr1 and hesr2 genes are redundantly required to mediate Notch signaling in the developing cardiovascular system." Dev Biol **278**(2): 301-309.

Kokubo, H., S. Miyagawa-Tomita, H. Tomimatsu, Y. Nakashima, M. Nakazawa, Y. Saga and R. L. Johnson (2004). "Targeted disruption of hesr2 results in atrioventricular valve anomalies that lead to heart dysfunction." Circ Res **95**(5): 540-547.

Koshiba-Takeuchi, K., Y. Morita, R. Nakamura and J. K. Takeuchi (2016). "Etiology and Morphogenesis of Congenital Heart Disease." Springer Open: 295-303.

Kouzarides, T. (2007). "Chromatin modifications and their function." Cell **128**(4): 693-705.

Koyanagi, M., J. Haendeler, C. Badorff, R. P. Brandes, J. Hoffmann, P. Pandur, A. M. Zeiher, M. Kuhl and S. Dimmeler (2005). "Non-canonical Wnt signaling enhances differentiation of human circulating progenitor cells to cardiomyogenic cells." J Biol Chem **280**(17): 16838-16842.

Koyanagi, M., M. Iwasaki, J. Haendeler, M. Leitges, A. M. Zeiher and S. Dimmeler (2009). "Wnt5a increases cardiac gene expressions of cultured human circulating progenitor cells via a PKC delta activation." PLoS One **4**(6): e5765.

Kuo, C. T., E. E. Morrisey, R. Anandappa, K. Sigrist, M. M. Lu, M. S. Parmacek, C. Soudais and J. M. Leiden (1997). "GATA4 transcription factor is required for ventral morphogenesis and heart tube formation." Genes & development **11**(8): 1048-1060.

Kuo, I. Y. and B. E. Ehrlich (2015). "Signaling in muscle contraction." Cold Spring Harb Perspect Biol **7**(2): a006023.

Kwon, C., J. Arnold, E. C. Hsiao, M. M. Taketo, B. R. Conklin and D. Srivastava (2007). "Canonical Wnt signaling is a positive regulator of mammalian cardiac progenitors." Proc Natl Acad Sci U S A **104**(26): 10894-10899.

Kwon, C., K. R. Cordes and D. Srivastava (2008). "Wnt/beta-catenin signaling acts at multiple developmental stages to promote mammalian cardiogenesis." Cell Cycle **7**(24): 3815-3818.

Kwon, C., L. Qian, P. Cheng, V. Nigam, J. Arnold and D. Srivastava (2009). "A regulatory pathway involving Notch1/beta-catenin/Isl1 determines cardiac progenitor cell fate." Nat Cell Biol **11**(8): 951-957.

Laforest, B., G. Andelfinger and M. Nemer (2011). "Loss of Gata5 in mice leads to bicuspid aortic valve." The Journal of clinical investigation **121**(7): 2876-2887.

Laforest, B. and M. Nemer (2011). "GATA5 interacts with GATA4 and GATA6 in outflow tract development." Developmental biology **358**(2): 368-378.

- Lai, X., L. Verhage, V. Hugouvieux and C. Zubieta (2018). "Pioneer Factors in Animals and Plants-Colonizing Chromatin for Gene Regulation." Molecules **23**(8).
- Lang, J., W. Tian and X. Sun (2013). "Association between ISL1 variants and susceptibility to ventricular septal defect in a Chinese cohort." Molecular diagnosis & therapy **17**(2): 101-106.
- Lange, M., B. Kaynak, U. B. Forster, M. Tonjes, J. J. Fischer, C. Grimm, J. Schlesinger, S. Just, I. Dunkel, T. Krueger, S. Mebus, H. Lehrach, R. Lurz, J. Gobom, W. Rottbauer, S. Abdelilah-Seyfried and S. Sperling (2008). "Regulation of muscle development by DPF3, a novel histone acetylation and methylation reader of the BAF chromatin remodeling complex." Genes Dev **22**(17): 2370-2384.
- Längst, G. and L. Manelyte (2015). "Chromatin remodelers: from function to dysfunction." Genes **6**(2): 299-324.
- Latchman, D. S. (1997). "Transcription factors: an overview." The international journal of biochemistry & cell biology **29**(12): 1305-1312.
- Laugwitz, K. L., A. Moretti, L. Caron, A. Nakano and K. R. Chien (2008). "Islet1 cardiovascular progenitors: a single source for heart lineages?" Development **135**(2): 193-205.
- Lei, I., X. Gao, M. H. Sham and Z. Wang (2012). "SWI/SNF protein component BAF250a regulates cardiac progenitor cell differentiation by modulating chromatin accessibility during second heart field development." Journal of Biological Chemistry **287**(29): 24255-24262.
- Lei, I., L. Liu, M. H. Sham and Z. Wang (2013). "SWI/SNF in cardiac progenitor cell differentiation." Journal of cellular biochemistry **114**(11): 2437-2445.
- Leonard Feiner, A. L. W., Christopher B. Brown, Min Min Lu, Li Jia, Paul Feinstein, Peter Mombaerts, Jonathan A. Epstein, Jonathan A. Raper (2001). "Targeted disruption of semaphorin 3C leads to persistent truncus arteriosus and aortic arch interruption." Development **128**: 3061-3070.
- Lepore, J. J., P. A. Mericko, L. Cheng, M. M. Lu, E. E. Morrisey and M. S. Parmacek (2006). "GATA-6 regulates semaphorin 3C and is required in cardiac neural crest for cardiovascular morphogenesis." The Journal of clinical investigation **116**(4): 929-939.
- Lessard, J., J. I. Wu, J. A. Ranish, M. Wan, M. M. Winslow, B. T. Staahl, H. Wu, R. Aebersold, I. A. Graef and G. R. Crabtree (2007). "An essential switch in subunit composition of a chromatin remodeling complex during neural development." Neuron **55**(2): 201-215.
- Lessard, J., J. I. Wu, J. A. Ranish, M. Wan, M. M. Winslow, B. T. Staahl, H. Wu, R. Aebersold, I. A. Graef and G. R. Crabtree (2007). "An essential switch in subunit composition of a chromatin remodeling complex during neural development." neuron **55**(2): 201-215.
- Li, Q. Y., R. A. Newbury-Ecob, J. A. Terrett, D. I. Wilson, A. R. J. Curtis, C. H. Yi, T. Gebuhr, P. J. Bullen, S. C. Robson, T. Strachan, D. Bonnet, S. Lyonnet, I. D. Young, J. A. Raeburn, A. J. Buckler, D. J. Law and J. D. Brook (1997). "Holt-Oram syndrome is caused by mutations in TBX5, a member of the Brachyury (T) gene family." Nature Genetics volume **15**: 21-29.
- Liang, X., M. R. Song, Z. Xu, G. M. Lanuza, Y. Liu, T. Zhuang, Y. Chen, S. L. Pfaff, S. M. Evans and Y. Sun (2011). "Isl1 is required for multiple aspects of motor neuron development." Mol Cell Neurosci **47**(3): 215-222.
- Liang, X., Q. Zhang, P. Cattaneo, S. Zhuang, X. Gong, N. J. Spann, C. Jiang, X. Cao, X. Zhao, X. Zhang, L. Bu, G. Wang, H. S. Chen, T. Zhuang, J. Yan, P. Geng, L. Luo, I. Banerjee, Y. Chen, C. K.

Glass, A. C. Zambon, J. Chen, Y. Sun and S. M. Evans (2015). "Transcription factor ISL1 is essential for pacemaker development and function." J Clin Invest **125**(8): 3256-3268.

Liao, J., V. S. Aggarwal, S. Nowotschin, A. Bondarev, S. Lipner and B. E. Morrow (2008). "Identification of downstream genetic pathways of Tbx1 in the second heart field." Dev Biol **316**(2): 524-537.

Lickert, H., J. K. Takeuchi, I. v. Both, J. R. Walls, F. McAuliffe, S. L. Adamson, R. M. Henkelman, J. L. Wrana, J. Rossant and B. G. Bruneau (2004). "Baf60c is essential for function of BAF chromatin remodelling complexes in heart development." NATURE **432**.

Lickert, H., J. K. Takeuchi, I. Von Both, J. R. Walls, F. McAuliffe, S. L. Adamson, R. M. Henkelman, J. L. Wrana, J. Rossant and B. G. Bruneau (2004). "Baf60c is essential for function of BAF chromatin remodelling complexes in heart development." Nature **432**(7013): 107-112.

Lin, C. J., C. Y. Lin, C. H. Chen, B. Zhou and C. P. Chang (2012). "Partitioning the heart: mechanisms of cardiac septation and valve development." Development **139**(18): 3277-3299.

Lin, L., L. Bu, C. L. Cai, X. Zhang and S. Evans (2006). "Isl1 is upstream of sonic hedgehog in a pathway required for cardiac morphogenesis." Dev Biol **295**(2): 756-763.

Lin, Q., J. Schwarz, C. Bucana and E. N. Olson (1997). "Control of Mouse Cardiac Morphogenesis and Myogenesis by Transcription Factor MEF2C." Science **276**: 1404-1407.

Lindsley, R. C., J. G. Gill, M. Kyba, T. L. Murphy and K. M. Murphy (2006). "Canonical Wnt signaling is required for development of embryonic stem cell-derived mesoderm." Development **133**(19): 3787-3796.

Liu, J., M. Bressan, D. Hassel, J. Huisken, D. Staudt, K. Kikuchi, K. D. Poss, T. Mikawa and D. Y. Stainier (2010). "A dual role for ErbB2 signaling in cardiac trabeculation." Development **137**(22): 3867-3875.

Liu, W., J. Selever, D. Wang, M. F. Lu, K. A. Moses, R. J. Schwartz and J. F. Martin (2004). "Bmp4 signaling is required for outflow-tract septation and branchial-arch artery remodeling." Proc Natl Acad Sci U S A **101**(13): 4489-4494.

Liu, Y., B. Pelham-Webb, D. C. Di Giammartino, J. Li, D. Kim, K. Kita, N. Saiz, V. Garg, A. Doane, P. Giannakakou, A. K. Hadjantonakis, O. Elemento and E. Apostolou (2017). "Widespread Mitotic Bookmarking by Histone Marks and Transcription Factors in Pluripotent Stem Cells." Cell Rep **19**(7): 1283-1293.

Loh, K. M., A. Chen, P. W. Koh, T. Z. Deng, R. Sinha, J. M. Tsai, A. A. Barkal, K. Y. Shen, R. Jain, R. M. Morganti, N. Shyh-Chang, N. B. Fernhoff, B. M. George, G. Wernig, R. E. A. Salomon, Z. Chen, H. Vogel, J. A. Epstein, A. Kundaje, W. S. Talbot, P. A. Beachy, L. T. Ang and I. L. Weissman (2016). "Mapping the Pairwise Choices Leading from Pluripotency to Human Bone, Heart, and Other Mesoderm Cell Types." Cell **166**(2): 451-467.

Lorenzen, J. M., F. Martino and T. Thum (2012). "Epigenetic modifications in cardiovascular disease." Basic Res Cardiol **107**(2): 245.

Lu, C. X., W. Wang, Q. Wang, X. Y. Liu and Y. Q. Yang (2018). "A Novel MEF2C Loss-of-Function Mutation Associated with Congenital Double Outlet Right Ventricle." Pediatr Cardiol **39**(4): 794-804.

Luna-Zurita, L., C. U. Stirnimann, S. Glatt, B. L. Kaynak, S. Thomas, F. Baudin, M. A. Samee, D. He, E. M. Small, M. Mileikovsky, A. Nagy, A. K. Holloway, K. S. Pollard, C. W. Muller and B. G. Bruneau (2016). "Complex Interdependence Regulates Heterotypic Transcription Factor Distribution and Coordinates Cardiogenesis." Cell **164**(5): 999-1014.

Lunyak, V. V. and M. G. Rosenfeld (2008). "Epigenetic regulation of stem cell fate." Hum Mol Genet **17**(R1): R28-36.

Luo, Z., H. Sun, Z. Yang, Y. Ma, Y. Gu, Y. He, D. Wei, L. Xia, B. Yang and T. Guo (2014). "Genetic variations of ISL1 associated with human congenital heart disease in Chinese Han people." Genet Mol Res **13**: 1329-1338.

M Wang, a. D. J. D. (1994). "The LIM domain homeobox gene isl-1: conservation of human, hamster, and rat complementary deoxyribonucleic acid sequences and expression in cell types of nonneuroendocrine lineage." Endocrinology **134**(3): 1416-1422.

M. Tanaka, Z. C., S. Bartunkova, N. Yamasaki, S. Izumo (1999). "The cardiac homeobox gene Csx/Nkx2.5 lies genetically upstream of multiple genes essential for heart development." Development **126**: 1269-1280.

Ma, L., J. Wang, L. Li, Q. Qiao, R.-M. Di, X.-M. Li, Y.-J. Xu, M. Zhang, R.-G. Li and X.-B. Qiu (2018). "ISL1 loss-of-function mutation contributes to congenital heart defects." Heart and vessels: 1-11.

Ma, Q., B. Zhou and W. T. Pu (2008). "Reassessment of Isl1 and Nkx2-5 cardiac fate maps using a Gata4-based reporter of Cre activity." Dev Biol **323**(1): 98-104.

MacGrogan, D., M. Nus and J. L. d. I. Pompa (2010). "Notch Signaling in Cardiac Development and Disease." **92**: 333-365.

Maeda, J., H. Yamagishi, J. McAnally, C. Yamagishi and D. Srivastava (2006). "Tbx1 is regulated by forkhead proteins in the secondary heart field." Dev Dyn **235**(3): 701-710.

Manelyte, L. and G. Langst (2013). "Chromatin Remodelers and Their Way of Action."

Marroncelli, N., M. Bianchi, M. Bertin, S. Consalvi, V. Saccone, M. Bardi, P. L. Puri, D. Palacios, S. Adamo and V. Moresi (2018). "HDAC4 regulates satellite cell proliferation and differentiation by targeting P21 and Sharp1 genes." Scientific reports **8**(1): 3448.

Martins, P. and E. Castela (2008). "Transposition of the great arteries." Orphanet J Rare Dis **3**: 27.

Marvin MJ, D. R. G., Gardiner A, Bush SM, Lassar AB. (2001). "Inhibition of Wnt activity induces heart formation from posterior mesoderm." Genes & Dev. **15**: 316-327.

Materna, S. C., T. Sinha, R. M. Barnes, K. Lammerts van Bueren and B. L. Black (2019). "Cardiovascular development and survival require Mef2c function in the myocardial but not the endothelial lineage." Dev Biol **445**(2): 170-177.

Mattapally, S., S. Nizamuddin, K. S. Murthy, K. Thangaraj and S. K. Banerjee (2015). "c.620C>T mutation in GATA4 is associated with congenital heart disease in South India." BMC Med Genet **16**: 7.

Mavroudis, C. (2015). "Truncus Arteriosus." 131-143.

May, G., S. Soneji, A. J. Tipping, J. Teles, S. J. McGowan, M. Wu, Y. Guo, C. Fugazza, J. Brown, G. Karlsson, C. Pina, V. Olariu, S. Taylor, D. G. Tenen, C. Peterson and T. Enver (2013).

"Dynamic analysis of gene expression and genome-wide transcription factor binding during lineage specification of multipotent progenitors." Cell Stem Cell **13**(6): 754-768.

Maya-Ramos, L., J. Cleland, M. Bressan and T. Mikawa (2013). "Induction of the Proepicardium." J Dev Biol **1**(2): 82-91.

Mayran, A. and J. Drouin (2018). "Pioneer transcription factors shape the epigenetic landscape." J Biol Chem **293**(36): 13795-13804.

Mayran, A., K. Khetchoumian, F. Hariri, T. Pastinen, Y. Gauthier, A. Balsalobre and J. Drouin (2018). "Pioneer factor Pax7 deploys a stable enhancer repertoire for specification of cell fate." Nature genetics **50**(2): 259.

Mazina, M. Y. and N. Vorobyeva (2016). "The role of ATP-dependent chromatin remodeling complexes in regulation of genetic processes." Russian Journal of Genetics **52**(5): 463-472.

McElhinney, D. B., E. Geiger, J. Blinder, D. Woodrow Benson and E. Goldmuntz (2003). "NKX2.5 mutations in patients with congenital heart disease." Journal of the American College of Cardiology **42**(9): 1650-1655.

McFadden, D. G., A. C. Barbosa, J. A. Richardson, M. D. Schneider, D. Srivastava and E. N. Olson (2005). "The Hand1 and Hand2 transcription factors regulate expansion of the embryonic cardiac ventricles in a gene dosage-dependent manner." Development **132**(1): 189-201.

Meenakshi Maitra, S. N. K., Deepak Srivastava & Vidu Garg (2010). "Identification of GATA6 Sequence Variants in Patients With Congenital Heart Defects." Pediatric Research **68**: 281–285.

Meilhac, F. L. a. S. n. M. (2012). "Cell Lineages, Growth and Repair of the Mouse Heart." Mouse Development Results and Problems in Cell Differentiation **55**(chapter 15): 263-289.

Meilhac, S. M. and M. E. Buckingham (2018). "The deployment of cell lineages that form the mammalian heart." Nat Rev Cardiol **15**(11): 705-724.

Meilhac, S. M., F. Lescroart, C. Blanpain and M. E. Buckingham (2014). "Cardiac cell lineages that form the heart." Cold Spring Harb Perspect Med **4**(9): a013888.

Mesbah, K., Z. Harrelson, M. Theveniau-Ruissy, V. E. Papaioannou and R. G. Kelly (2008). "Tbx3 is required for outflow tract development." Circ Res **103**(7): 743-750.

Midgett, M. and S. Rugonyi (2014). "Congenital heart malformations induced by hemodynamic altering surgical interventions." Front Physiol **5**: 287.

Mikawa and Takashi (1999). Cardiac lineages. Heart development, Elsevier: 19-33.

Mitsiadis, T. A. (2003). "Role of Islet1 in the patterning of murine dentition." Development **130**(18): 4451-4460.

Molkentin, J. D., Q. Lin, S. A. Duncan and E. N. Olson (1997). "Requirement of the transcription factor GATA4 for heart tube formation and ventral morphogenesis." Genes & development **11**(8): 1061-1072.

Moretti, A., L. Caron, A. Nakano, J. T. Lam, A. Bernshausen, Y. Chen, Y. Qyang, L. Bu, M. Sasaki, S. Martin-Puig, Y. Sun, S. M. Evans, K. L. Laugwitz and K. R. Chien (2006). "Multipotent embryonic isl1+ progenitor cells lead to cardiac, smooth muscle, and endothelial cell diversification." Cell **127**(6): 1151-1165.

Moretti, A., J. Lam, S. Evans and K. Laugwitz (2007). "Biology of Isl1+ cardiac progenitor cells in development and disease." Cellular and molecular life sciences: CMLS **64**(6): 674-682.

Morris, J. (2001). "Genes, genetics, and epigenetics: a correspondence." Science **293**(5532): 1103-1105.

Mugdha Bhati, C. L., Amy L Nancarrow, Mihwa Lee, Vanessa J Craig, Ingolf Bach, J Mitchell Guss, Joel P Mackay, Jacqueline M Matthews (2008). "Implementing the LIM code: the structural basis for cell type-specific assembly of LIM-homeodomain complexes." The EMBO Journal **27**: 2018-2029.

Munshi, N. V., J. McAnally, S. Bezprozvannaya, J. M. Berry, J. A. Richardson, J. A. Hill and E. N. Olson (2009). "Cx30.2 enhancer analysis identifies Gata4 as a novel regulator of atrioventricular delay." Development **136**(15): 2665-2674.

Naito, A. T., I. Shiojima, H. Akazawa, K. Hidaka, T. Morisaki, A. Kikuchi and I. Komuro (2006). "Developmental stage-specific biphasic roles of Wnt/beta-catenin signaling in cardiomyogenesis and hematopoiesis." Proc Natl Acad Sci U S A **103**(52): 19812-19817.

Nakamura, R., K. Koshiba-Takeuchi, M. Tsuchiya, M. Kojima, A. Miyazawa, K. Ito, H. Ogawa and J. K. Takeuchi (2016). "Expression analysis of Baf60c during heart regeneration in axolotls and neonatal mice." Dev Growth Differ **58**(4): 367-382.

Narita, N., M. Bielinska and D. B. Wilson (1997). "Wild-type endoderm abrogates the ventral developmental defects associated with GATA-4 deficiency in the mouse." Developmental biology **189**(2): 270-274.

Neeb, Z., J. D. Lajiness, E. Bolanis and S. J. Conway (2013). "Cardiac outflow tract anomalies." Wiley Interdiscip Rev Dev Biol **2**(4): 499-530.

Nemer, S. M. F. C. L. R. M. (2000). "GATA-dependent recruitment of MEF2 proteins to target promoters." The EMBO journal **19**(9): 2046-2055.

Nili, E. L., Y. Field, Y. Lubling, J. Widom, M. Oren and E. Segal (2010). "p53 binds preferentially to genomic regions with high DNA-encoded nucleosome occupancy." Genome research.

Onizuka, T., S. Yuasa, D. Kusumoto, K. Shimoji, T. Egashira, Y. Ohno, T. Kageyama, T. Tanaka, F. Hattori, J. Fujita, M. Ieda, K. Kimura, S. Makino, M. Sano, A. Kudo and K. Fukuda (2012). "Wnt2 accelerates cardiac myocyte differentiation from ES-cell derived mesodermal cells via non-canonical pathway." J Mol Cell Cardiol **52**(3): 650-659.

Osoegawa, K., K. Schultz, K. Yun, N. Mohammed, G. M. Shaw and E. J. Lammer (2014). "Haploinsufficiency of insulin gene enhancer protein 1 (ISL1) is associated with d-transposition of the great arteries." Mol Genet Genomic Med **2**(4): 341-351.

Pacheco-Leyva, I., A. C. Matias, D. V. Oliveira, J. M. Santos, R. Nascimento, E. Guerreiro, A. C. Michell, A. M. van De Vrugt, G. Machado-Oliveira, G. Ferreira, I. Domian and J. Braganca (2016). "CITED2 Cooperates with ISL1 and Promotes Cardiac Differentiation of Mouse Embryonic Stem Cells." Stem Cell Reports **7**(6): 1037-1049.

Paige, S. L., K. Plonowska, A. Xu and S. M. Wu (2015). "Molecular regulation of cardiomyocyte differentiation." Circ Res **116**(2): 341-353.

Pan, Y., R. Geng, N. Zhou, G. F. Zheng, H. Zhao, J. Wang, C. M. Zhao, X. B. Qiu, Y. Q. Yang and X. Y. Liu (2015). "TBX20 loss-of-function mutation contributes to double outlet right ventricle." Int J Mol Med **35**(4): 1058-1066.

Park, E. J., L. A. Ogden, A. Talbot, S. Evans, C. L. Cai, B. L. Black, D. U. Frank and A. M. Moon (2006). "Required, tissue-specific roles for Fgf8 in outflow tract formation and remodeling." Development **133**(12): 2419-2433.

Park, N. I., P. Guilhamon, K. Desai, R. F. McAdam, E. Langille, M. O'Connor, X. Lan, H. Whetstone, F. J. Coutinho and R. J. Vanner (2017). "ASCL1 reorganizes chromatin to direct neuronal fate and suppress tumorigenicity of glioblastoma stem cells." Cell stem cell **21**(2): 209-224. e207.

Pataskar, A., J. Jung, P. Smialowski, F. Noack, F. Calegari, T. Straub and V. K. Tiwari (2016). "NeuroD1 reprograms chromatin and transcription factor landscapes to induce the neuronal program." The EMBO journal **35**(1): 24-45.

Pérez-Pomares, J. M. and R. Kelly (2018). The ESC Textbook of Cardiovascular Development, Oxford University Press.

Peterkin, T., A. Gibson and R. Patient (2007). "Redundancy and evolution of GATA factor requirements in development of the myocardium." Developmental biology **311**(2): 623-635.

Pfaff, S. L., M. Mendelsohn, C. L. Stewart, T. Edlund and T. M. Jessell (1996). "Requirement for LIM Homeobox Gene Isl1 in Motor Neuron Generation Reveals a Motor Neuron Dependent Step in Interneuron Differentiation." Cell **84**: 309–320.

Plageman, T. F., Jr. and K. E. Yutzey (2004). "Differential expression and function of Tbx5 and Tbx20 in cardiac development." J Biol Chem **279**(18): 19026-19034.

Ponchel, F. and A. N. Burska (2016). "Epigenetic Modifications: Are we Closer to Clinical Applicability?" Journal of Pharmacogenomics & Pharmacoproteomics **07**(02).

Portela, A. and M. Esteller (2010). "Epigenetic modifications and human disease." Nat Biotechnol **28**(10): 1057-1068.

Posch, M. G., Gramlich, M., Sunde, M., Schmitt, K. R., Lee, S. H., Richter, S., Kersten, A., Perrot, A., Panek, A. N., Al Khatib, I. H., Nemer, G., Megarbane, A., Dietz, R., Stiller, B., Berger, F., Harvey, R. P., Ozelik, C. (2010). "A gain-of-function TBX20 mutation causes congenital atrial septal defects, patent foramen ovale and cardiac valve defects." J Med Genet **47**(4): 230-235.

Qian, Y., D. Xiao, X. Guo, H. Chen, L. Hao, X. Ma, G. Huang, D. Ma and H. Wang (2017). "Hypomethylation and decreased expression of BRG1 in the myocardium of patients with congenital heart disease." Birth defects research **109**(15): 1183-1195.

Qiao, X. H., F. Wang, X. L. Zhang, R. T. Huang, S. Xue, J. Wang, X. B. Qiu, X. Y. Liu and Y. Q. Yang (2017). "MEF2C loss-of-function mutation contributes to congenital heart defects." Int J Med Sci **14**(11): 1143-1153.

Qing Lin, J. S., Corazon Bucana, Eric N. Olson (1997). "Control of Mouse Cardiac Morphogenesis and Myogenesis by Transcription Factor MEF2C." Science **276**: 1404-1407.

Quaranta, R., J. Fell, F. Ruhle, J. Rao, I. Piccini, M. J. Arauzo-Bravo, A. O. Verkerk, M. Stoll and B. Greber (2018). "Revised roles of ISL1 in a hES cell-based model of human heart chamber specification." Elife **7**.

Qyang, Y., S. Martin-Puig, M. Chiravuri, S. Chen, H. Xu, L. Bu, X. Jiang, L. Lin, A. Granger, A. Moretti, L. Caron, X. Wu, J. Clarke, M. M. Taketo, K. L. Laugwitz, R. T. Moon, P. Gruber, S. M.



Evans, S. Ding and K. R. Chien (2007). "The renewal and differentiation of Isl1+ cardiovascular progenitors are controlled by a Wnt/beta-catenin pathway." Cell Stem Cell **1**(2): 165-179.

R.J. Schwartz, E. N. O. (1999). "Building the heart piece by piece: modularity of cis-elements regulating Nkx2-5 transcription." Development **126**: 4187-4192.

Radde-Gallwitz, K., L. Pan, L. Gan, X. Lin, N. Segil and P. Chen (2004). "Expression of Islet1 marks the sensory and neuronal lineages in the mammalian inner ear." J Comp Neurol **477**(4): 412-421.

Ramón Muñoz-Chápuli, D. M., Mauricio González-Iriarte, Rita Carmona, Gerardo Atencia and José María Pérez-Pomares (2002). "The Epicardium and Epicardial-Derived Cells: Multiple Functions in Cardiac Development." Rev Esp Cardiol **55**(10): 1070-1082.

Rana, M. S., M. Theveniau-Ruissy, C. De Bono, K. Mesbah, A. Francou, M. Rammah, J. N. Dominguez, M. Roux, B. Laforest, R. H. Anderson, T. Mohun, S. Zaffran, V. M. Christoffels and R. G. Kelly (2014). "Tbx1 coordinates addition of posterior second heart field progenitor cells to the arterial and venous poles of the heart." Circ Res **115**(9): 790-799.

Reik, W. (2007). "Stability and flexibility of epigenetic gene regulation in mammalian development." Nature **447**(7143): 425-432.

Rickert-Sperling, S., R. Kelly and D. J. Driscoll (2015). Congenital Heart Diseases: The Broken Heart, Springer.

Rivera-Feliciano, J., K.-H. Lee, S. W. Kong, S. Rajagopal, Q. Ma, Z. Springer, S. Izumo, C. J. Tabin and W. T. Pu (2006). "Development of heart valves requires Gata4 expression in endothelial-derived cells." Development **133**(18): 3607-3618.

Rivera-Feliciano, J., K. H. Lee, S. W. Kong, S. Rajagopal, Q. Ma, Z. Springer, S. Izumo, C. J. Tabin and W. T. Pu (2006). "Development of heart valves requires Gata4 expression in endothelial-derived cells." Development **133**(18): 3607-3618.

Robert G.Kelly, N. A. B., Margaret E.Buckingham (2001). "The Arterial Pole of the Mouse Heart Forms from Fgf10-Expressing Cells in Pharyngeal Mesoderm." Developmental Cell **1**(3): Pages 435-440.

Robert H Anderson, S. W., Nigel A Brown, Wouter Lamers, Antoon Moorman (2003). "DEVELOPMENT OF THE HEART: (2) SEPTATION OF THE ATRIUMS AND VENTRICLES." Heart **89**: 949-958.

Rochais, F., K. Mesbah and R. G. Kelly (2009). "Signaling pathways controlling second heart field development." Circ Res **104**(8): 933-942.

S.J. Conway, D. J. H., A.J. Copp (1997). "Pax3 is required for cardiac neural crest migration in the mouse: evidence from the splotch (Sp2H) mutant." Development **124**: 505-514.

Sadahiro, T., M. Isomi, N. Muraoka, H. Kojima, S. Haginiwa, S. Kurotsu, F. Tamura, H. Tani, S. Tohyama, J. Fujita, H. Miyoshi, Y. Kawamura, N. Goshima, Y. W. Iwasaki, K. Murano, K. Saito, M. Oda, P. Andersen, C. Kwon, H. Uosaki, H. Nishizono, K. Fukuda and M. Ieda (2018). "Tbx6 Induces Nascent Mesoderm from Pluripotent Stem Cells and Temporally Controls Cardiac versus Somite Lineage Diversification." Cell Stem Cell **23**(3): 382-395 e385.

Samsa, L. A., B. Yang and J. Liu (2013). Embryonic cardiac chamber maturation: Trabeculation, conduction, and cardiomyocyte proliferation. American Journal of Medical Genetics Part C: Seminars in Medical Genetics, Wiley Online Library.

Samuel L. Pfaff, M. M., \*Colin L. Stewart,† Thomas Edlund,‡and Thomas M. Jessell\* (1996). "Requirement for LIM Homeobox Gene Isl1 in Motor Neuron Generation Reveals a Motor Neuron–Dependent Step in Interneuron Differentiation." Cell **84**: 309–320.

Santini, M. P., E. Forte, R. P. Harvey and J. C. Kovacic (2016). "Developmental origin and lineage plasticity of endogenous cardiac stem cells." Development **143**(8): 1242-1258.

Scheuermann, J. C. and L. A. Boyer (2013). "Getting to the heart of the matter: long non-coding RNAs in cardiac development and disease." EMBO J **32**(13): 1805-1816.

Schleich, J. M., T. Abdulla, R. Summers and L. Houyel (2013). "An overview of cardiac morphogenesis." Arch Cardiovasc Dis **106**(11): 612-623.

Schlesinger, J., M. Schueler, M. Grunert, J. J. Fischer, Q. Zhang, T. Krueger, M. Lange, M. Tönjes, I. Dunkel and S. R. Sperling (2011). "The cardiac transcription network modulated by Gata4, Mef2a, Nkx2. 5, Srf, histone modifications, and microRNAs." PLoS genetics **7**(2): e1001313.

Schoenwolf, S. Y. a. G. C. (2000). "Islet-1 Marks the Early Heart Rudiments and is Asymmetrically Expressed During Early Rotation of the Foregut in the Chick Embryo." The anatomical record **260**: 204–207.

Seo, S. and T. Kume (2006). "Forkhead transcription factors, Foxc1 and Foxc2, are required for the morphogenesis of the cardiac outflow tract." Dev Biol **296**(2): 421-436.

Shi, Y., S. Katsev, C. Cai and S. Evans (2000). "BMP signaling is required for heart formation in vertebrates." Dev Biol **224**(2): 226-237.

Singh, A. P., J. Foley, A. Tandon, D. Phadke, H. K. Kinyamu and T. K. Archer (2017). "A role for BRG1 in the regulation of genes required for development of the lymphatic system." Oncotarget **8**(33): 54925.

Sinha, T., D. Li, M. Theveniau-Ruissy, M. R. Hutson, R. G. Kelly and J. Wang (2015). "Loss of Wnt5a disrupts second heart field cell deployment and may contribute to OFT malformations in DiGeorge syndrome." Hum Mol Genet **24**(6): 1704-1716.

Sokpor, G., R. Castro-Hernandez, J. Rosenbusch, J. F. Staiger and T. Tuoc (2018). "ATP-Dependent Chromatin Remodeling During Cortical Neurogenesis." Front Neurosci **12**: 226.

Soufi, A., G. Donahue and K. S. Zaret (2012). "Facilitators and impediments of the pluripotency reprogramming factors' initial engagement with the genome." Cell **151**(5): 994-1004.

Soufi, A., M. F. Garcia, A. Jaroszewicz, N. Osman, M. Pellegrini and K. S. Zaret (2015). "Pioneer transcription factors target partial DNA motifs on nucleosomes to initiate reprogramming." Cell **161**(3): 555-568.

Spitz, F. and E. E. Furlong (2012). "Transcription factors: from enhancer binding to developmental control." Nature reviews genetics **13**(9): 613.

Srinageshwar, B., P. Maiti, G. L. Dunbar and J. Rossignol (2016). "Role of Epigenetics in Stem Cell Proliferation and Differentiation: Implications for Treating Neurodegenerative Diseases." Int J Mol Sci **17**(2).

Stankunas, K., C. T. Hang, Z.-Y. Tsun, H. Chen, N. V. Lee, J. I. Wu, C. Shang, J. H. Bayle, W. Shou and M. L. Iruela-Arispe (2008). "Endocardial Brg1 represses ADAMTS1 to maintain the microenvironment for myocardial morphogenesis." Developmental cell **14**(2): 298-311.

Stennard, F. A., M. W. Costa, D. A. Elliott, S. Rankin, S. J. Haast, D. Lai, L. P. McDonald, K. Niederreither, P. Dolle and B. G. Bruneau (2003). "Cardiac T-box factor Tbx20 directly interacts with Nkx2-5, GATA4, and GATA5 in regulation of gene expression in the developing heart." Developmental biology **262**(2): 206-224.

Stevens, K. N., H. Hakonarson, C. E. Kim, P. A. Doevendans, B. P. Koeleman, S. Mital, J. Raue, J. T. Glessner, J. G. Coles and V. Moreno (2010). "Common variation in ISL1 confers genetic susceptibility for human congenital heart disease." PLoS one **5**(5): e10855.

Sun, X., S. K. Hota, Y. Q. Zhou, S. Novak, D. Miguel-Perez, D. Christodoulou, C. E. Seidman, J. G. Seidman, C. C. Gregorio, R. M. Henkelman, J. Rossant and B. G. Bruneau (2017). "Cardiac-enriched BAF chromatin-remodeling complex subunit Baf60c regulates gene expression programs essential for heart development and function." Biol Open **7**(1).

Sun, X., S. K. Hota, Y. Q. Zhou, S. Novak, D. Miguel-Perez, D. Christodoulou, C. E. Seidman, J. G. Seidman, C. C. Gregorio, R. M. Henkelman, J. Rossant and B. G. Bruneau (2017). "Cardiac-enriched BAF chromatin-remodeling complex subunit Baf60c regulates gene expression programs essential for heart development and function." Biol Open.

Sun, Y., I. M. Dykes, X. Liang, S. R. Eng, S. M. Evans and E. E. Turner (2008). "A central role for Islet1 in sensory neuron development linking sensory and spinal gene regulatory programs." Nat Neurosci **11**(11): 1283-1293.

Sun, Y., X. Liang, N. Najafi, M. Cass, L. Lin, C. L. Cai, J. Chen and S. M. Evans (2007). "Islet 1 is expressed in distinct cardiovascular lineages, including pacemaker and coronary vascular cells." Dev Biol **304**(1): 286-296.

Sun, Y. M., J. Wang, X. B. Qiu, F. Yuan, R. G. Li, Y. J. Xu, X. K. Qu, H. Y. Shi, X. M. Hou, R. T. Huang, S. Xue and Y. Q. Yang (2016). "A HAND2 Loss-of-Function Mutation Causes Familial Ventricular Septal Defect and Pulmonary Stenosis." G3 (Bethesda) **6**(4): 987-992.

Takeuchi, J. K. and B. G. Bruneau (2009). "Directed transdifferentiation of mouse mesoderm to heart tissue by defined factors." Nature **459**(7247): 708.

Takeuchi, J. K., X. Lou, J. M. Alexander, H. Sugizaki, P. Delgado-Olguin, A. K. Holloway, A. D. Mori, J. N. Wylie, C. Munson, Y. Zhu, Y. Q. Zhou, R. F. Yeh, R. M. Henkelman, R. P. Harvey, D. Metzger, P. Chambon, D. Y. Stainier, K. S. Pollard, I. C. Scott and B. G. Bruneau (2011). "Chromatin remodelling complex dosage modulates transcription factor function in heart development." Nat Commun **2**: 187.

Takeuchi, J. K., M. Mileikovskaia, K. Koshiba-Takeuchi, A. B. Heidt, A. D. Mori, E. P. Arruda, M. Gertsenstein, R. Georges, L. Davidson, R. Mo, C. C. Hui, R. M. Henkelman, M. Nemer, B. L. Black, A. Nagy and B. G. Bruneau (2005). "Tbx20 dose-dependently regulates transcription factor networks required for mouse heart and motoneuron development." Development **132**(10): 2463-2474.

Takeuchi, J. K., Ohgi, M., Koshiba-Takeuchi, K., Shiratori, H., Sakaki, I., Ogura, K., Saijoh, Y., Ogura, T. (2003). "Tbx5 specifies the left/right ventricles and ventricular septum position during cardiogenesis." Development **130**(24): 5953-5964.

Tanaka, Y., M. Tawaramoto-Sasanuma, S. Kawaguchi, T. Ohta, K. Yoda, H. Kurumizaka and S. Yokoyama (2004). "Expression and purification of recombinant human histones." Methods **33**(1): 3-11.

Terami, H., K. Hidaka, T. Katsumata, A. Iio and T. Morisaki (2004). "Wnt11 facilitates embryonic stem cell differentiation to Nkx2.5-positive cardiomyocytes." Biochem Biophys Res Commun **325**(3): 968-975.

Tian, Y., E. D. Cohen and E. E. Morrisey (2010). "The importance of Wnt signaling in cardiovascular development." Pediatr Cardiol **31**(3): 342-348.

Tian, Y., L. Yuan, A. M. Goss, T. Wang, J. Yang, J. J. Lepore, D. Zhou, R. J. Schwartz, V. Patel, E. D. Cohen and E. E. Morrisey (2010). "Characterization and in vivo pharmacological rescue of a Wnt2-Gata6 pathway required for cardiac inflow tract development." Dev Cell **18**(2): 275-287.

Tiffani Thomas, H. Y., Paul A. Overbeek, Eric N. Olson, Deepak Srivastava (1998). "The bHLH Factors, dHAND and eHAND, Specify Pulmonary and Systemic Cardiac Ventricles Independent of Left-Right Sidedness." Developmental Biology **196**(2): 228-236.

Toto, P. C., P. L. Puri and S. Albin (2016). "SWI/SNF-directed stem cell lineage specification: dynamic composition regulates specific stages of skeletal myogenesis." Cell Mol Life Sci **73**(20): 3887-3896.

Tremblay, M., O. Sanchez-Ferras and M. Bouchard (2018). "GATA transcription factors in development and disease." Development **145**(20): dev164384.

Triedman, J. K. and J. W. Newburger (2016). "Trends in Congenital Heart Disease: The Next Decade." Circulation **133**(25): 2716-2733.

Tsuchihashi, T., J. Maeda, C. H. Shin, K. N. Ivey, B. L. Black, E. N. Olson, H. Yamagishi and D. Srivastava (2011). "Hand2 function in second heart field progenitors is essential for cardiogenesis." Dev Biol **351**(1): 62-69.

Tsukui T, C. J., Tamura K, Ruiz-Lozano P, Rodriguez-Esteban C, Yonei-Tamura S, Magallón J, Chandraratna RA, Chien K, Blumberg B, Evans RM, Belmonte JC. (1999). "Multiple left-right asymmetry defects in Shh-/- mutant mice unveil a convergence of the Shh and retinoic acid pathways in the control of Lefty-1." Proc. Natl. Acad. Sci. **96**: 11376–11381.

Ueyama, T., H. Kasahara, T. Ishiwata, Q. Nie and S. Izumo (2003). "Myocardin expression is regulated by Nkx2.5, and its function is required for cardiomyogenesis." Mol Cell Biol **23**(24): 9222-9232.

Urness, L. D., S. B. Bleyl, T. J. Wright, A. M. Moon and S. L. Mansour (2011). "Redundant and dosage sensitive requirements for Fgf3 and Fgf10 in cardiovascular development." Dev Biol **356**(2): 383-397.

Valerie A. Schneider, M. M. (2002). "Wnt antagonism initiates cardiogenesis in *Xenopus laevis*." GENES & DEVELOPMENT **15**: 304-315.

Vallaster, M., C. D. Vallaster and S. M. Wu (2012). "Epigenetic mechanisms in cardiac development and disease." Acta Biochim Biophys Sin (Shanghai) **44**(1): 92-102.

van der Bom, T., A. C. Zomer, A. H. Zwinderman, F. J. Meijboom, B. J. Bouma and B. J. Mulder (2011). "The changing epidemiology of congenital heart disease." Nat Rev Cardiol **8**(1): 50-60.

Van Handel, B., A. Montel-Hagen, R. Sasidharan, H. Nakano, R. Ferrari, C. J. Boogerd, J. Schredelseker, Y. Wang, S. Hunter and T. Org (2012). "Scl represses cardiomyogenesis in prospective hemogenic endothelium and endocardium." Cell **150**(3): 590-605.

van Vliet, P. P., L. Lin, C. J. Boogerd, J. F. Martin, G. Andelfinger, P. D. Grossfeld and S. M. Evans (2017). "Tissue specific requirements for WNT11 in developing outflow tract and dorsal mesenchymal protrusion." Dev Biol **429**(1): 249-259.

Vincent, S. D. and M. E. Buckingham (2010). How to make a heart: the origin and regulation of cardiac progenitor cells. Current topics in developmental biology, Elsevier. **90**: 1-41.

Vincenz, J. W., R. M. Barnes, B. A. Firulli, S. J. Conway and A. B. Firulli (2008). "Cooperative interaction of Nkx2.5 and Mef2c transcription factors during heart development." Dev Dyn **237**(12): 3809-3819.

Vincenz, J. W., J. R. McWhirter, C. Murre, A. Baldini and Y. Furuta (2005). "Fgf15 is required for proper morphogenesis of the mouse cardiac outflow tract." Genesis **41**(4): 192-201.

Vissers, L. E., C. M. van Ravenswaaij, R. Admiraal, J. A. Hurst, B. B. de Vries, I. M. Janssen, W. A. van der Vliet, E. H. Huys, P. J. de Jong, B. C. Hamel, E. F. Schoenmakers, H. G. Brunner, J. A. Veltman and A. G. van Kessel (2004). "Mutations in a new member of the chromodomain gene family cause CHARGE syndrome." Nat Genet **36**(9): 955-957.

von Gise, A. and W. T. Pu (2012). "Endocardial and epicardial epithelial to mesenchymal transitions in heart development and disease." Circ Res **110**(12): 1628-1645.

Waldo, K. L., D. H. Kumiski, K. T. Wallis, H. A. Stadt, M. R. Hutson, D. H. Platt and M. L. Kirby (2001). "Conotruncal myocardium arises from a secondary heart field." Development **128**: 3179-3188.

Wamstad, J. A., J. M. Alexander, R. M. Truty, A. Shrikumar, F. Li, K. E. Eilertson, H. Ding, J. N. Wylie, A. R. Pico, J. A. Capra, G. Erwin, S. J. Kattman, G. M. Keller, D. Srivastava, S. S. Levine, K. S. Pollard, A. K. Holloway, L. A. Boyer and B. G. Bruneau (2012). "Dynamic and coordinated epigenetic regulation of developmental transitions in the cardiac lineage." Cell **151**(1): 206-220.

Wang, H., J. B. Gilner, V. L. Bautch, D. Z. Wang, B. J. Wainwright, S. L. Kirby and C. Patterson (2007). "Wnt2 coordinates the commitment of mesoderm to hematopoietic, endothelial, and cardiac lineages in embryoid bodies." J Biol Chem **282**(1): 782-791.

Wang, J., S. B. Greene, M. Bonilla-Claudio, Y. Tao, J. Zhang, Y. Bai, Z. Huang, B. L. Black, F. Wang and J. F. Martin (2010). "Bmp signaling regulates myocardial differentiation from cardiac progenitors through a MicroRNA-mediated mechanism." Dev Cell **19**(6): 903-912.

Wang, J., X. J. Luo, Y. F. Xin, Y. Liu, Z. M. Liu, Q. Wang, R. G. Li, W. Y. Fang, X. Z. Wang and Y. Q. Yang (2012). "Novel GATA6 mutations associated with congenital ventricular septal defect or tetralogy of fallot." DNA Cell Biol **31**(11): 1610-1617.

Wang, Q. T. (2012). "Epigenetic regulation of cardiac development and function by polycomb group and trithorax group proteins." Developmental Dynamics **241**(6): 1021-1033.

Wang, R. N., J. Green, Z. Wang, Y. Deng, M. Qiao, M. Peabody, Q. Zhang, J. Ye, Z. Yan, S. Denduluri, O. Idowu, M. Li, C. Shen, A. Hu, R. C. Haydon, R. Kang, J. Mok, M. J. Lee, H. L. Luu and L. L. Shi (2014). "Bone Morphogenetic Protein (BMP) signaling in development and human diseases." Genes Dis **1**(1): 87-105.

Wang, W., Y. Xue, S. Zhou, A. Kuo, B. R. Cairns and G. R. Crabtree (1996). "Diversity and specialization of mammalian SWI/SNF complexes." Genes & development **10**(17): 2117-2130.

Wang, Y., Y. Li, C. Guo, Q. Lu, W. Wang, Z. Jia, P. Chen, K. Ma, D. Reinberg and C. Zhou (2016). "ISL1 and JMJD3 synergistically control cardiac differentiation of embryonic stem cells." Nucleic Acids Res **44**(14): 6741-6755.

Wapinski, O. L., T. Vierbuchen, K. Qu, Q. Y. Lee, S. Chanda, D. R. Fuentes, P. G. Giresi, Y. H. Ng, S. Marro and N. F. Neff (2013). "Hierarchical mechanisms for direct reprogramming of fibroblasts to neurons." Cell **155**(3): 621-635.

Washington Smoak, I., N. A. Byrd, R. Abu-Issa, M. M. Goddeeris, R. Anderson, J. Morris, K. Yamamura, J. Klingensmith and E. N. Meyers (2005). "Sonic hedgehog is required for cardiac outflow tract and neural crest cell development." Dev Biol **283**(2): 357-372.

Watanabe, Y., S. Miyagawa-Tomita, S. D. Vincent, R. G. Kelly, A. M. Moon and M. E. Buckingham (2010). "Role of mesodermal FGF8 and FGF10 overlaps in the development of the arterial pole of the heart and pharyngeal arch arteries." Circ Res **106**(3): 495-503.

Watanabe, Y., S. Zaffran, A. Kuroiwa, H. Higuchi, T. Ogura, R. P. Harvey, R. G. Kelly and M. Buckingham (2012). "Fibroblast growth factor 10 gene regulation in the second heart field by Tbx1, Nkx2-5, and Islet1 reveals a genetic switch for down-regulation in the myocardium." Proceedings of the National Academy of Sciences: 201215360.

Watt, A. J., M. A. Battle, J. Li and S. A. Duncan (2004). "GATA4 is essential for formation of the proepicardium and regulates cardiogenesis." Proceedings of the National Academy of Sciences **101**(34): 12573-12578.

Wei, D., H. Bao, N. Zhou, G. F. Zheng, X. Y. Liu and Y. Q. Yang (2013). "GATA5 loss-of-function mutation responsible for the congenital ventriculoseptal defect." Pediatr Cardiol **34**(3): 504-511.

Wei Li, Yiqin Xiong, Ching Shang, Karen Y. Twu, Calvin T. Hang, Jin Yang, Pei Han, Chieh-Yu Lin, Chien-Jung Lin, Feng-Chiao Tsai, Kryn Stankunas, Tobias Meyer, Daniel Bernstein, Minggui Pan and C.-P. Chang (2012). "Brg1 governs distinct pathways to direct multiple aspects of mammalian neural crest cell development." PNAS **110**(5): 1738-1743.

Westerlund, J., L. Andersson, T. Carlsson, P. Zoppoli, H. Fagman and M. Nilsson (2008). "Expression of Islet1 in thyroid development related to budding, migration, and fusion of primordia." Dev Dyn **237**(12): 3820-3829.

Witzel, H. R., B. Jungblut, C. P. Choe, J. G. Crump, T. Braun and G. Dobрева (2012). "The LIM protein Ajuba restricts the second heart field progenitor pool by regulating Isl1 activity." Dev Cell **23**(1): 58-70.

Wu, J. I., J. Lessard and G. R. Crabtree (2009). "Understanding the words of chromatin regulation." Cell **136**(2): 200-206.

Wu, S. M., Y. Fujiwara, S. M. Cibulsky, D. E. Clapham, C. L. Lien, T. M. Schultheiss and S. H. Orkin (2006). "Developmental origin of a bipotential myocardial and smooth muscle cell precursor in the mammalian heart." Cell **127**(6): 1137-1150.

Xiaobing Jiang, D. H. R., Philippe Soriano, Andrew P. McMahon and Henry M. Sucov (2000). "Fate of the mammalian cardiac neural crest." Development: 1607-1616.

Xiaojun Lian, C. H., Gisela Wilson, Kexian Zhu, Laurie B. Hazeltine, Samira M. Azarin, Kunil K. Raval, Jianhua Zhang, Timothy J. Kamp, and Sean P. Palecek (2012). "Robust cardiomyocyte

differentiation from human pluripotent stem cells via temporal modulation of canonical Wnt signaling." PNAS **109**(27): E1848-E1857.

Xie, L., A. D. Hoffmann, O. Burnicka-Turek, J. M. Friedland-Little, K. Zhang and I. P. Moskowitz (2012). "Tbx5-hedgehog molecular networks are essential in the second heart field for atrial septation." Developmental cell **23**(2): 280-291.

Xin, M., E. N. Olson and R. Bassel-Duby (2013). "Mending broken hearts: cardiac development as a basis for adult heart regeneration and repair." Nature Reviews Molecular Cell Biology **14**(8): 529-541.

Xu, H., M. Morishima, J. N. Wylie, R. J. Schwartz, B. G. Bruneau, E. A. Lindsay and A. Baldini (2004). "Tbx1 has a dual role in the morphogenesis of the cardiac outflow tract." Development **131**(13): 3217-3227.

Y. Saga, N. H., S. Kobayashi, T. Magnuson, M.F. Seldin, M.M. Taketo (1996). "MesP1: a novel basic helix-loop-helix protein expressed in the nascent mesodermal cells during mouse gastrulation." Development **122**: 2769-2778.

Yamagishi, H., E. N. Olson and D. Srivastava (2000). "The basic helix-loop-helix transcription factor, dHAND, is required for vascular development." J Clin Invest **105**(3): 261-270.

Yan, M. S., C. C. Matouk and P. A. Marsden (2010). "Epigenetics of the vascular endothelium." J Appl Physiol (1985) **109**(3): 916-926.

Yang, L., C. L. Cai, L. Lin, Y. Qyang, C. Chung, R. M. Monteiro, C. L. Mummery, G. I. Fishman, A. Cogen and S. Evans (2006). "Isl1Cre reveals a common Bmp pathway in heart and limb development." Development **133**(8): 1575-1585.

Yuan, X., H. Qi, X. Li, F. Wu, J. Fang, E. Bober, G. Dobрева, Y. Zhou and T. Braun (2017). "Disruption of spatiotemporal hypoxic signaling causes congenital heart disease in mice." The Journal of clinical investigation **127**(6): 2235-2248.

Yumiko Saga, S. K., and Sachiko Miyagawa-Tomita (2000). "Mesp1 Expression Is the Earliest Sign of Cardiovascular Development." Trends in Cardiovascular Medicine **10**(8): 345-352.

Zaffran, S., N. Robrini and N. Bertrand (2014). "Retinoids and Cardiac Development." Journal of Developmental Biology **2**(1): 50.

Zaret, K., J. Caravaca, A. Tulin and T. Sekiya (2010). Nuclear mobility and mitotic chromosome binding similarities between pioneer transcription factor FoxA and linker histone H1. Cold Spring Harbor symposia on quantitative biology, Cold Spring Harbor Laboratory Press.

Zaret, K. S. and J. S. Carroll (2011). "Pioneer transcription factors: establishing competence for gene expression." Genes Dev **25**(21): 2227-2241.

Zaret, K. S., J. Lerner and M. Iwafuchi-Doi (2016). "Chromatin Scanning by Dynamic Binding of Pioneer Factors." Mol Cell **62**(5): 665-667.

Zaret, K. S. and S. E. Mango (2016). "Pioneer transcription factors, chromatin dynamics, and cell fate control." Current opinion in genetics & development **37**: 76-81.

Zeisberg, E. M., Q. Ma, A. L. Juraszek, K. Moses, R. J. Schwartz, S. Izumo and W. T. Pu (2005). "Morphogenesis of the right ventricle requires myocardial expression of Gata4." The Journal of clinical investigation **115**(6): 1522-1531.

Zhang, L., A. Nomura-Kitabayashi, N. Sultana, W. Cai, X. Cai, A. M. Moon and C. L. Cai (2014). "Mesodermal Nkx2.5 is necessary and sufficient for early second heart field development." Dev Biol **390**(1): 68-79.

Zhang, Q., R. Huang, Y. Ye, X. Guo, J. Lu, F. Zhu, X. Gong, Q. Zhang, J. Yan, L. Luo, S. Zhuang, Y. Chen, X. Zhao, S. M. Evans, C. Jiang, X. Liang and Y. Sun (2018). "Temporal requirements for ISL1 in sympathetic neuron proliferation, differentiation, and diversification." Cell Death Dis **9**(2): 247.

Zhuang, S., Q. Zhang, T. Zhuang, S. M. Evans, X. Liang and Y. Sun (2013). "Expression of Isl1 during mouse development." Gene Expr Patterns **13**(8): 407-412.



## 7. Acknowledgements

Firstly I would like to thank my supervisor Prof. Dr. Gergana Dobрева who provides me the position and interesting project. During my PHD period she taught me not only the knowledge of my project but also the rigorous scientific attitude.

I thank Prof. Dr. Katja Sträßer to be my supervisor for the registration in Justus-Liebig-Universität Gießen. I thank all the members of my thesis committee for reviewing my thesis.

I thank my colleagues Yanhan, Yonggang and Yanyan who helped me a lot not only on working but also on life.

I thank my colleague Julio for bioinformatic analysis in this project. I thank the mice facility in MPI-HLR and Alex for taking care of the mice. I thank our collaborators in Shanghai for providing the *Isl1* hypomorph data. I thank Yonggang for sharing his *Isl1* KO ESC lines. Thanks to all the colleagues in the lab for nice data discussion and nice time spent together.

We are grateful to Sylvia Evans to provide us with the *Isl1* knockout mice and Pierre Chambon and Daniel Metzger for providing us with the floxed Brg1 mice and Pier Lorenzo Puri for the Baf60c antibody. I would like to thank Stefanie Uhlig for the FACS in the Flow Core Mannheim of Heidelberg University.

I am grateful to my family members who give me support all the time.

Last but not least, I would like to thank Max Planck Institute for heart and lung research (Bad Nauheim) and Mannheim medical faculty of Heidelberg University (Mannheim) for providing me the stimulating working environment and nice research atmosphere.

**Der Lebenslauf wurde aus der elektronischen  
Version der Arbeit entfernt.**

**The curriculum vitae was removed from the  
electronic version of the paper.**